Interactions of *Medicago truncatula* with soil-borne microbes – Role of *MtTPS10* in defense against the root pathogen *Aphanomyces euteiches*

Dissertation

zur Erlangung des
Doktorgrades der Naturwissenschaften (Dr. rer. nat.)

der

Naturwissenschaftlichen Fakultät I – Biowissenschaften

der Martin-Luther-Universität
Halle-Wittenberg,

vorgelegt

von Frau Heena Yadav

geboren am 04.04.1990 in Kota, Indien

Gutachter

1. Prof. Dr. Bettina Hause

2. Prof. Dr. Edgar Peiter

3. Prof. Dr. Franziska Krajinski-Barth

Defense date: 04.06.2019, Halle (Saale)

"Somewhere, something incredible is waiting to be known."
— *Carl Sagan*

Table of contents

List of tables

List of figures

List of abbreviations

amiRNA	Artificial microRNA
ATP	Adenosine triphosphate
bp	Base pair
BLAST	Basic local alignment search tool
Bt	*Bacillus thuringiensis*
Ca^{2+}	Calcium
cDNA	Complimentary DNA
CDS	Coding sequence
CRISPR	Clustered Regularly Interspaced Short Palindromic Repeats
DsRed	Discosoma sp. red fluorescent protein
DMI	Do not make infection
DMSO	Dimethyl sulfoxide
fig	Figure
g	gravity; unit for relative centrifugal force
g	grams
GC-MS	Gas chromatography-mass spectrometry
h	Hour
hpi	Harvest post treatment
IPD3	Interacting protein DMI3
kDa	Kilodalton
L	Liter
LC-MS	Liquid chromatography mass spectrometry
Lj	*Lotus japonicus*
Lys-M	Lysin motif
LYK	LysM domain containing receptor-like kinases
MeJA	Methyl jasmonate
min	Minute
ml	milliliter
MSR	Modified Strullu Romand medium
MtGEA	*Medicago truncatula* gene expression atlas
N	Nitrogen
NCBI	National Center for Biotechnology Information
NFP	Nod factor perception

NFR	Nod factor receptor
NIN	Nodule inception
OD	Optical density
Pi	Inorganic phosphate
RAM	Required for arbuscular mycorrhization
ROS	Reactive oxygen species
rpm	Revolutions per minute
rRNA	Ribosomal RNA
s	seconds
SARDI	South Australian Research and Development Institute
SYMRK	Symbiosis receptor kinase
tab	table
WGA	Wheat germ agglutinin

I. Introduction

With an increasing world population, the food demand is expected to increase by 60 % (Alexandratos and Bruinsama, 2012). This challenge can only be met by a combination of reduction in food wastage and increase in crop yield and productivity (Godfray et al., 2010). Despite the use of chemicals and pesticides, a large number of crops fall victim to various pathogens, ultimately leading to a loss of ~ 15 % of global crop production (Pinstrup-Anderson, 2001; Oerke, 2005). The use of chemical control for crop diseases is not only an expensive option but may have also negative effects on the environment. Therefore, exploitation of plant's immune system for the identification of resistance (R) genes can provide an economical and environmentally safe way to control plant diseases (Ning et al., 2017).

I.1 Plant-microbe interactions

Since the establishment of plants about 480 million years ago, they are continuously challenged by their surrounding environment and interacts with a large multitude of animals, viruses, bacteria, and fungi, above ground and below-ground. Some of these interactions can protect the host plants against microbial and non-microbial invaders, while other interactions can negatively affect the plants. Therefore, for a sustainable agriculture, research on plant-microbial interaction in the rhizosphere and the phyllosphere is critical for farming practices that would be less dependent on chemical fertilizers and would rely more on harnessing plant's microbiota (Igiehon and Babalola, 2018). Globally, enormous research efforts are being laid to better understand the plant immune system in order to develop pathogen resilient and high yielding crops for a food secure future.

The establishment of the first land plants was facilitated by symbiotic fungal associations, suggesting that the plants and microbes have co-evolved since their arrival on land (Gehrig et al., 1996). This co-existence of plants and microbes had resulted in many beneficial plant-microbe associations. The research over the past 150 years showed that these bacterial and fungal interactions with the host plants, promote plant growth as well as suppress pathogens (Whipps, 2001; Thakore, 2006). The beneficial microbe-plant interaction can affect the plant growth either directly or indirectly through antagonistic activity against the pathogens. For all kinds of plant-microbe interaction, the first step is colonization of the host plant. The first steps of colonization are recognition, adherence, invasion (endophytes and pathogens), colonization and growth. A common feature of symbiotic interactions is the ability of microbes to capture and trade off plant growth limiting nutrients in exchange of photosynthetic derivatives (Oldroyd, 2013). The best studied

symbiotic associations are those between plants and the arbuscular mycorrhizal fungi (AMF), and legumes and nitrogen-fixing bacteria, rhizobia bacteria.

I.1.1 Arbuscular Mycorrhizal Fungus (AMF)

The arbuscular mycorrhiza symbiosis between plant roots and fungi of Glomeromycota phylum (Tisserant et al., 2013) occur in different forms and is referred to as mycorrhiza (Greek 'mycos'- fungus, 'rhiza'- root). The ectomycorrhizal symbiotic association is prominent on temperate forest trees, here the fungi live outside of the plant cells, whereas in endomycorrhiza, fungal hyphae reside in the plant root cells. Arbuscular mycorrhiza is considered to be a successful and widespread symbiosis partner, as ~ 70-90 % of land plant species can form mycorrhizal associations. Among the AMF species, *Rhizophagus irregularis* belonging to the division Mucoromycota (Tab.I.1) is one of the most widely studied AMF, as it can colonize the host plant easily and rapidly. In particular, *R. irregularis* can be cultured *in vitro* monoaxenic culture together with *Agrobacterium rhizogenes* transformed carrot roots (Becárd and Fortin, 1988; Spatafora et al., 2016).

Tab.I.1: Scientific classification of *R. irregularis*

Kingdom	Fungi
Division	Mucoromycota
Phylum	Glomeromycota
Class	Glomeromycetes
Order	Glomerales
Family	Glomeraceae
Genus	Rhizophagus
Species	*R. irregularis*

The symbiotic developments lead to the formation of the tree-shaped structures, known as arbuscles within the plant root cells. These arbuscles serve as the primary site for nutrient exchange between the fungal and the plant partner. In exchange for nutrients, plants provide photosynthetic products (up to 5 billion tonnes of carbon/year) to AMF. In this way, AMF also contributes to the terrestrial ecosystem productivity by cycling phosphate and carbon (Parniske, 2008).

AMF is obligate biotroph and, therefore, dependent on a living phototrophic partner to complete its life cycle and produce next generation of spores. In the pre-symbiotic stage, a mature spore residing in the soil germinate after a period of dormancy. The fungal hyphae grow towards the roots which release strigolactones (Akiyama et al., 2005). Strigolactones are short-lived molecules in the rhizosphere, due to hydrolysis of their ether bond in water. These compounds form a concentration gradient and has been suggested to be an indicator of the host root proximity (Parniske, 2005). If the AMF is not able to find and colonize the host roots within ~ 4 weeks, another round of dormancy may start. This includes retraction of nuclei and cytoplasm followed by the successive septation of the empty hyphal compartments. This way, a single spore can germinate up to 10 times and can remain viable for months (Koske, 1981). The strigolactone, when perceived by the fungus leads to continued hyphal growth, increased physiological activity and profuse branching of the hyphae (Parniske, 2008). The contact of the hyphae with the root surface marks the initiation of the symbiotic phase. AMF invasion involves the formation of a thickened hyphae, hyphopodium or, appressorium. This infection peg allows the fungal hyphae growth into the root epidermal cells. The plant cell prepares an intracellular environment for AMF by forming a pre-penetration apparatus (PPA) that leads the hyphae through the cytoplasm (Genre et al., 2005). The plant nuclei guide the developing PPA into the cell. After the completion of PPA, the fungal hyphae spread with the help of intraradical hyphae and colonize the root cortex (Fig.I.1).
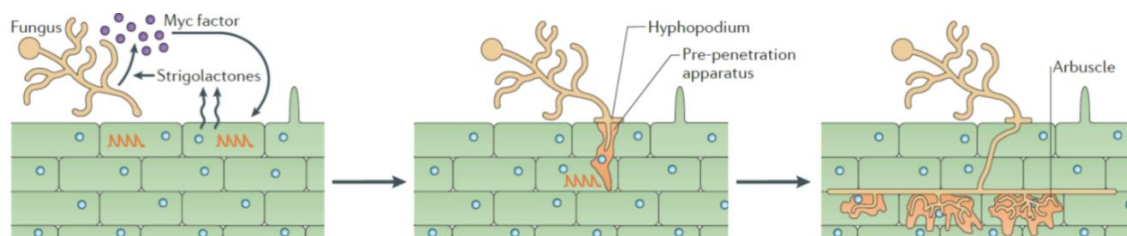
Fig.I.1: Lifecycle of AMF (from Oldroyd, 2013): The mature spores germinate and lead to hyphal branching after perception of plant strigolactones in the rhizosphere of host plants. On the surface of the root, the hyphae forms thicken hyphopodia-like appressorium. The epidermis root cells facilitate the entry of the fungus via formation of a pre-penetration apparatus (PPA). After entrance into the host root, the fungus spreads in the apoplast via growth of intraradical hyphae. They build tree-like structures named arbuscules by dichotomous branching, which are thought to be the main organs of nutrition exchange in the symbiosis.

The symbiosis pathway

The rhizobia mediated nitrogen-fixing symbiosis and AM symbiosis share a common signaling pathway, the so-called SYM pathway (Fig.I.2; Parniske, 2008). The Myc factor (a mixture of lipochitooligosaccharides, Myc-LCO), are similar to rhizobia signaling Nod factors and are secreted by AMF to communicate with its host (Maillet et al., 2011). The

Nod factors are perceived by LysM-motif containing receptors- MtLYK3/LjNFR1 and MtNFP/LjNFR5 (Radutoiu et al., 2007), whereas no receptor for Myc factor perception has been identified to date. After perception of the fungal-based factors, signal transmission from the plasma membrane to the cell nucleus takes place. DMI2/SYMRK is involved in endosymbiosis signal perception (Endre et al., 2002; Stracke et al., 2002) and is also believed to act as co-receptor to the unidentified Myc factor receptor. Recently, the role of mevalonate as a secondary messenger that transmits symbiotic factor perception from the plasma membrane to the nucleus via direct interaction with DMI1 has been discovered (Venkateshwaran et al., 2015).
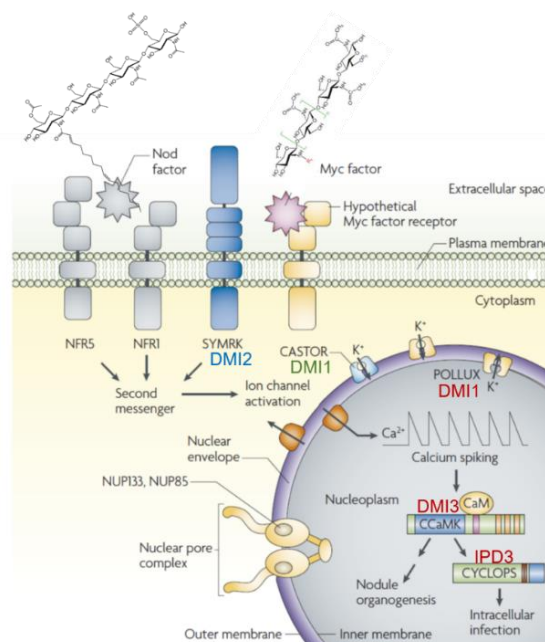
Fig.I.2: The SYM pathway common for AM and root nodule symbiosis (modified after Parniske, 2008): The AM fungal or rhizobia-derived signals are perceived by specific receptors. The receptor kinase DMI2 and the potassium channel DMI1 act upstream of the Nod- and Myc factor-induced calcium signatures. The CCaMK, DMI3 interacts with IPD3 in the nucleus and mediates the transcription required for symbiosis.

The enzyme 3-hydroxy-3-methylglutaryl-CoA (HMG-CoA) reductase of mevalonate pathway interacts with DMI2 and transmits the Myc and Nod factor perception to the nucleus, eventually generating symbiotic nuclear Ca^{2+} oscillations (Kevei et al., 2007; Venkateshwaran et al., 2015). These nuclear Ca^{2+} oscillations are deciphered by a master decoder and regulatory kinase, calcium, and calmodulin-dependent kinase (CCaMK), which further initiates the transcriptional response (Miller et al., 2013). The Ca^{2+} oscillations induce the interaction of Ca^{2+} calmodulin (CaM) with CCaMK leading to a conformation change in the kinase that initiates phosphorylation of target proteins, such

as, CYCLOPS (encoded by *CYCLOPS* in *L. japonicus* and IPD3 in *M. truncatula*) (Yano et al., 2008; Miller et al., 2013). In rhizobial interaction, GRAS domain containing transcription factors such as NSP1 and NSP2 act downstream of CCaMK and control nodule formation (Hirsch et al., 2009). NSP1 and NSP2 form a heterocomplex and promotes the expression of nodulation inception proteins, such as NIN1 and ERN1 (Stracke et al., 2002; Marsch et al., 2007; Oldroyd, 2013; Cerri et al., 2016). In mycorrhizal colonization, another GRAS transcription factor, RAM1, has been shown to act downstream of the symbiosis signaling pathway (Gobbato et al., 2012). Mutants in RAM1 have defects in the formation of hyphopodia and regulates RAM2, a gene involved in the production of cutin, which promotes hyphopodia formation (Gobbato et al., 2013; Wang et al., 2012; Oldroyd, 2013).

I.1.2 Oomycetes as plant pathogens

Plant diseases pose threats to crop production causing yield loss and reduced product quality in horticulture, agriculture, and forestry. The two most important groups of eukaryotic plant pathogens that cause a worldwide threat to food security are fungi and oomycetes (Fisher et al., 2012). These microbes cause Emerging infectious diseases (EIDs) that are increasing in their incidence, geographic or host range, and virulence (Jones et al., 2008).

Oomycetes or the 'water molds', consists of several organisms, of which more than 60 % are plant parasites (Thines and Kamoun, 2010). Plant pathologists considered oomycete as lower fungi for a long time, due to their filamentous growth habit, nutrient absorption and reproduction via spores (Fry and Grünwald, 2010). But phylogenetic analysis revealed that fungi share a common ancestry with animals, whereas, the oomycetes are closest relatives of the heterokont golden-brown algae (Baldauf et al., 2000). Oomycetes are divided into two orders Saprolegniales, which consists of about 500 species and Peronosporales, which consists of 1300 species (Thines & Kamoun, 2010). Oomycetes can be distinguished from fungi based on various characteristics. The cell wall of oomycetes is composed of β-1,3 and β-1,6 glucans, whereas fungi cell wall comprises of chitin. The oomycetes also produce motile bi-flagellated zoospores from the sporangia, which can swim in water films, on leaf surfaces, in soil, and in natural water bodies. After some time of free swimming, the zoospores settle on a surface, retract their flagella and secrete a mucilaginous matrix that helps them adhere to the surface (Fry and Grünwald, 2010).

I.1.3 *Aphanomyces euteiches*

Among Saprolegniales, the genus *Aphanomyces* includes destructive pathogens on plants and animals in terrestrial and aquatic habitats (Gaulin et al., 2008; Blazer et al., 2002). The plant pathogenic species *Aphanomyces euteiches* (Jones & Drechsler, 1925) causes root rot disease in both annual and perennial legume species such as alfalfa, peas, faba beans and lentils (Gaulin et al., 2007; Levenfors et al., 2003; Wicker et al., 2001) The *Aphanomyces* root rot (ARR) in field pea (*Pisum sativum*) is a major limitation to pea production worldwide, accounting for 80 % losses each year (Gaulin et al., 2007). This soil-borne pathogen can survive in soil for many years and until now no chemical control is available (Gaulin et al., 2007, Hughes et al., 2013). The only possible measure is to abandon the infested fields for at least 10 years or the use of resistant cultivars (Hughes et al., 2013). The primary symptoms of *A. euteiches* infestation include soft, water-soaked, honey-brown or blackish-brown roots and eventually leads to a reduction in root volume and function. The secondary symptoms can be visible in stems, characterized by chlorosis of the cotyledons and necrosis of epicotyls or hypocotyls (Hughes et al., 2013).

The sexual reproduction of *A. euteiches* occurs via the production of gametogonia: oogonia and antheridia. They are homothallic species, which means that each individual can produce oogonia and antheridia and are self-compatible. The fertilized oogonium transforms in a thick-walled oospore and these oospores can remain dormant in the soil for many years. The oospore germinates as a response to unknown chemical signals exuded by the host roots. The oospores form a germ tube that either proliferates as hyphae or sporangia. The sporangia from the germinating oospore can reach up to 8-10 times the diameter of the oospore and the nuclei (2N) migrate through the sporangia to develop a cell wall and forms a primary spore. The primary spores aggregate at the apex of sporangium and releases zoospores through a pore in the cell wall of primary spore. These motile zoospores can swim towards the host root, loses its flagella and forms a germ tube. Hyphae, derived from the germ tube, penetrates the host epidermal cells and colonize the roots and subterranean stem tissues (Fig.I.3; Hughes et al., 2013).
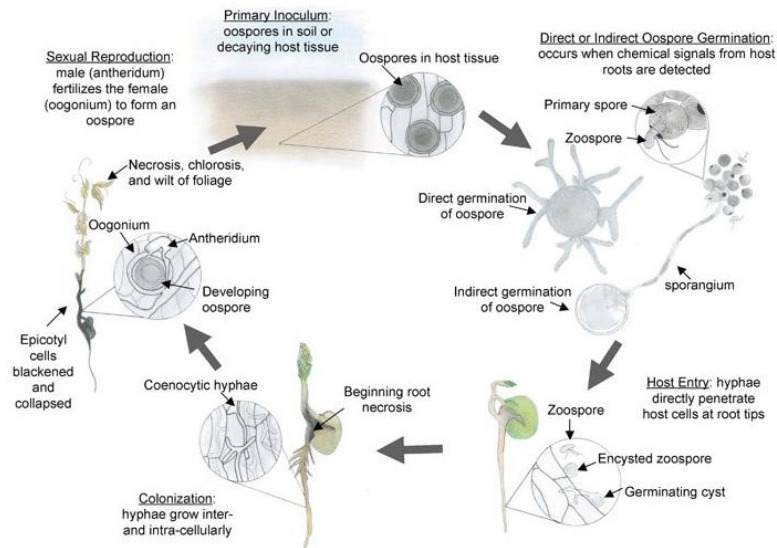
Fig.I.3: Life cycle of _A. euteiches_ (from Hughes et al., 2013)

Recent developments in _A. euteiches_ research field revealed effectors that might induce PAMP-triggered immunity (PTI) responses. The branched glucan chitosaccharide from _A. euteiches_ cell wall fractions induce defense gene expression and nuclear calcium oscillation in root epidermis of _M. truncatula_ (Nars et al., 2013). To overcome PTI, oomycete pathogens have also developed many effectors. The _A. euteiches_ secretome contains two kinds of effectors- RXLR effectors and the Crinklers (CRNs). A transcriptome analysis of _A. euteiches_ revealed two unigenes containing RxLR-dEER motif and showed homology to _Phytophthora sojae_ and _P. ramorum_ genes. Another effector containing RxLx [EDQ]-dEER motif encodes a putative lysine-rich protein (Gaulin et al., 2008). These RXLR type unigenes were either incomplete or showed no homology to known protein sequences, therefore, no RXLR effectors are identified in _A. euteiches_ up to date. The Crinkling and Necrosis (CRN) family was first discovered in _P. infestans_ (Torto et al., 2003). Recently, 160 CRNs were detected in _A. euteiches_ genome and the majority of them harbor LYLAK motif at the N terminal rather than canonical _Phytophthora_ LxLFLAK motif (Gaulin et al., 2018).

I.2 Plant immunity

The co-evolutionary arms race between the plant and the pathogen species have led to various pathogen virulence strategies and plants have also developed a plethora of defense mechanisms against these organisms (Pieterse et al., 2009). The plant immune system is an elaborate and multilayered system which involves several lines of defense. Plant pathogens invade the host species to attain nutrients to sustain their growth and in order to do so, the pathogen must pass plant's physical structural barrier of the cuticle, cell

wall and preformed antimicrobial compounds (Pieterse et al., 2009, Hückelhoven, 2007, Miedes et al., 2014). But many microbes are able to break through this pre-invasive layer of defense, thereby, plants have developed a post-invasive line of defense, whereby, plants recruit sophisticated strategies to perceive the microbe and translate the perception into an effective immune system (Jones and Dangl, 2006; Pieterse et al., 2009).

I.2.1 PAMP-triggered immunity (PTI)

The primary plant immune response includes recognition of common features of microbes (Microbe-associated molecular patterns, MAMPs) or pathogens (Pathogen-associated molecular patterns, PAMPs). These conserved microbial signatures are perceived by plant-encoded PAMP receptors, or pattern recognition receptors, PRRs (Zipfel, 2009). The PAMPs are general elicitors of plant defense and are characteristic of microbial organisms but are absent in host plant species. Many PAMPs that trigger innate plant defense have been characterized over the years, which includes lipopolysaccharide (LPS) fraction of gram-negative bacteria, peptidoglycans of gram-positive bacteria, eubacterial flagellin, methylated bacterial DNA fragments and fungal cell-derived glucans, chitins, mannans and proteins (Nürnberger et al., 2004; Aderem et al., 2000; Medzhitov and Janeway, 2002; Girardin et al., 2002).

Flg22, a 22 amino acid highly conserved N terminal fragment of flagellin and the main building block of the eubacterial flagella is the most well studied PAMP. Flg22 have been shown to trigger plant defense response in plants like *Arabidopsis* and tomato (Felix et al., 1999), suggesting that plants have maintained the ability to recognize this PAMP over the evolution. The *Arabidopsis* Flagellin sensing 2 (FLS2), which consists of an extracellular leucine-rich repeat (LRRs) and an intracellular serine/threonine kinase domain (Gomez-Gomez and Boller, 2000) binds flg22 and confers recognition specificity. Plants mutated in FLS2 are not able to recognize flagellin and are more susceptible to bacterial pathogens (Gomez-Gomez and Boller, 2000; Zipfel et al., 2004).

Many signature PAMPs have also been characterized from fungi and oomycetes, such as ergosterol, glycosylated proteins, cell wall components like chitin and ß-glucan (Zipfel and Felix, 2005). For instance, the elicitor Pep 13, isolated from *P. sojae* is a surface exposed domain of pathogen's cell wall transglutaminase, which activates plant defense in parsley and potato during *Phytophthora* infection (Brunner et al., 2002).

The PAMPs are recognized by LRR-RK, which in turn initiate diverse downstream signaling, the earliest response being oxidative burst produced by NADPH oxidase (Torres et al., 2006), followed by activation of MAP kinase cascade and WRKY transcription factors. Late responses (hours to days) includes callose deposition at the site of infection

and production of salicylic acid and ethylene (Pieterse et al., 2009; Nürnberger et al., 2004; Chrisholm et al., 2006). In most cases, the PTI is sufficient to avoid microbial growth and proliferation in the apoplast and ensures host survival. Very few macroscopic disease symptoms are visible at this stage, suggesting that PTI might underlie non-host resistance (Göhre and Robatzek, 2008).

I.2.2 Effector-triggered immunity (ETI)

A successful pathogen is able to manipulate the cellular environment of the host plant, by suppressing the natural defense response of the host and making the host cellular environment suitable for the pathogen to grow and reproduce (Boyd et al., 2013). The pathogens accomplish this by secretion of an arsenal of proteins, termed as effector proteins or avirulence (Avr) proteins, that targets host defense pathways (Koeck et al., 2011).

Plant pathogens can deliver about 20-100 effectors in the host cells via various mechanisms (Cunnac et al., 2004; Lindeberg et al., 2006). For example, bacterial pathogens are known to deliver the effectors into host cells using type III secretion system (TTSS) and fungi can deliver them through their infection structures (appresoria or hyphopodium) (Presti et al., 2015). These effector molecules can initiate an effector-triggered susceptibility (ETS) in the host plant and to counteract these effector molecules, plants have developed a second layer of defense mediated by R (resistance) genes. Most of the R genes encode NB-LRR (nucleotide binding leucine-rich repeat) proteins and can initiate an effector-triggered immunity (ETI). ETI is a faster and stronger response, compared to PTI, and is associated with hypersensitive response followed by programmed cell death, to prevent the spread of the pathogen (Fig.I.4). Therefore, NB-LRR mediated disease resistance is found to be effective against obligate biotrophs and hemibiotrophs, but not against necrotrophs (Glazebrook et al., 2005). In many studies, R proteins have been shown to interact directly with the intracellular effectors (Deslandes et al., 2003; Dodds et al., 2006), but in many cases, direct interaction does not explain effector detection (Bent and Mackey, 2007). This indirect interaction of R proteins and the effectors could be explained by "guard theory" (Van der Biezen and Jones, 1998). This theory postulates that pathogen effector proteins target host proteins (other than R proteins), and the perturbation of those target proteins, eventually leads to R protein activation (Bent and Mackey, 2007). Thus, the role of R proteins is to "guard" the Avr mediated perturbance (Nürnberger et al., 2004). A well-understood example of this model is the *Pseudomonas syringae* effector AvrRpm1 or AvrB that phosphorylates RIN4 and resistance is conferred by activation of RPM1 (Mackey et al., 2002). However, *P. syringae* pv. tomato-derived Avr

protein, AvrRpt2 cleaves RIN4 and the resistance is conferred by cognate R protein RPS2 (Axtell and Staskawicz, 2003).

Although, some pathogens can conquer the ETI defense by evolving their effectors, and in return, these effectors can be recognized by the cognate R proteins leading to a dynamic evolutionary arms race between the pathogen and the plant (Fig.I.4).
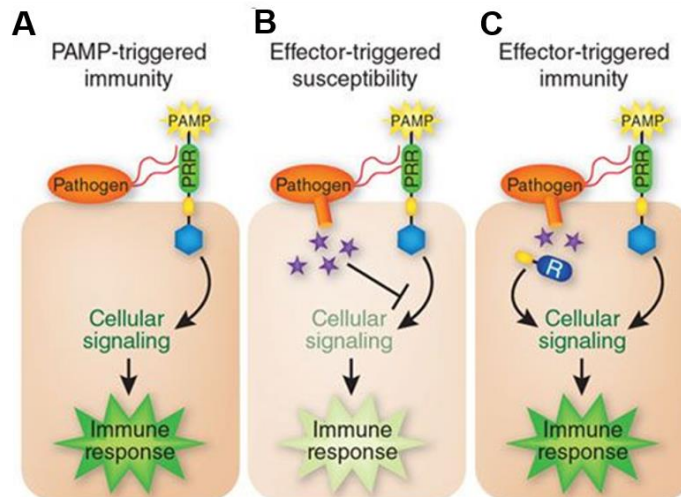
Fig.I.4: Schematic representation of the plant immune system (from Pieterse et al., 2009): (A) when a pathogen attack, PAMP signals perception by PRRs initiates PAMP-triggered immunity (PTI); (B) over the course of evolution, pathogens have developed effectors (purple stars) against plant defense system, which leads to effector-triggered susceptibility (ETS); (C) As a response to the pathogen effectors, plants have developed R genes, which can initiate effector-triggered immunity (ETI).

I.2.3 *Medicago truncatula* as a model plant

Legumes (Fabaceae) are an important source of proteins for human food and animal forage, after grasses (Gramineae). Soybean (*Glycine max*) accounts for 50 % of the world's oilseed production and alfalfa (*Medicago sativa*) is a major forage and cover crop (Cook, 1999). Apart from being a rich source of proteins for humans, legumes also improve the soil fertility and decrease the need for N fertilizers via symbiotic interaction with nitrogen-fixing bacteria, and thus contribute to the sustainability of agriculture (Sugiyama & Yazaki, 2012). About 40-60 million tonnes of N are fixed annually by cultivated legumes (Smil, 1999), saving about 10 billion dollars on N fertilizers (Graham and Vance, 2003). Moreover, legumes provide a unique research opportunity in the area of plant-microbe interaction for symbiotic nitrogen fixations, mycorrhizal interactions and legume-pathogens interactions (Cook, 1999). Due to the genome size and complexity of *Glycine max* (2n = 20, ~ 1100 Mbp) and *Medicago sativa* (auto tetraploid, 2n = 4x = 32, 800-1000 Mbp), *Medicago truncatula* have emerged as a valuable model plant.

M. truncatula is an annual medic from the Trifolieae tribe and a close relative of *M. sativa*. The genus *Medicago* originates from the Fertile Crescent and its species cover the Mediterranean basin. During the 19th century, *Medicago* species spread to parts of the American and Australian continent. The natural attributes of *M. truncatula* such as rapid life cycle, diploid genome (2n = 16), autogamous, prolific seed production and the small genome of around 550 Mbp, make it a valuable genetic resource for the scientific community (Ané et al., 2008). Recently, a newer version of *M. truncatula* genome (version Mt.4) had been released and a total of 50,894 genes (31,661 high confidence and 19,233 low confidence) are included in the latest release (Tang et al., 2014). *M. truncatula* is native of Mediterranean region and various ecotypes have been collected throughout the basin, these ecotypes exhibit variations in growth habitat, flowering time, symbiotic specificity and disease resistance (Cook, 1999). Being a member of the legume family, *M. truncatula* can form symbiotic associations with a wide array of arbuscular mycorrhiza fungus and can develop N fixing root nodules in association with *Sinorhizobium meliloti*. Jemalong A17 derived from the commercial cultivar serves as the reference line for most of the genomic approaches, due to its transformability and *in vitro* regeneration capacity (Barker et al., 1990; Nolan et al., 1989; Thomas et al., 1992). Several protocols have been developed and optimized over the years for *M. truncatula* transformation using *Agrobacterium tumefaciens*. Although, R108 and Jemalong 2HA are considered to have higher regeneration capacity, compared to A17 (Hoffmann et al., 1997; Rose et al., 1999). R108 was identified from an *in vitro* screen of *M. truncatula* ecotypes Ghor-1, 108-1, 131-1, 139-2 and E4258. Hoffmann et al. (1997) isolated a derivative of 108-1, R108-1 which showed enhanced capacity to form somatic embryos and efficient regeneration in diploid plants. Jemalong 2HA is a super embryogenic line and was developed from Jemalong A17. Due to its high regeneration capacity, Jemalong 2HA is considered valuable for dissection of totipotency and somatic embryogenesis (Rose 2008, Rose et al., 1999).

The time-consuming regeneration steps in *M. truncatula* prompted the scientists towards *Tnt1* insertion mutants and hairy root transformation using *Agrobacterium rhizogenes* (Tadege et al., 2005, Boisson-Dernier et al., 2001). Considering the valuable genetic resources and databases available in *M. truncatula*, we chose it as the model plant for our studies.

I.3 *Medicago- Aphanomyces* interaction

Plants defend themselves against oomycete pathogens by inducing various responses such as the production of reactive oxygen species (ROS), hypersensitive response, cell wall reinforcement, synthesis of pathogen-related (PR) proteins and phytoalexin formation.

The PR proteins are plant-specific proteins that are classified into 17 functional families and possess hydrolytic activities against pathogens. ß-1, 3 glucanases, and chitinases are well-studied PR proteins as they are involved in the degradation of pathogen cell walls (Mauch et al., 1988). Several subclasses of PR-10 proteins, some having ribonuclease and antifungal activity, are found in legume plants (Samac and Graham, 2007). A group of PR-10 like proteins, annotated as abscisic acid responsive proteins (ABR17s) were induced in the *M. truncatula* root proteome after *A. euteiches* infection (Colditz et al., 2004, 2005). However, another study by Colditz et al. (2007), showed that the silencing of PR10-1 in *M. truncatula* increased tolerance to *A. euteiches*. This study suggests that a new set of PR-proteins are induced, which are normally repressed by PR-10 gene expression (Colditz et al., 2007). Thin transverse cross-sections of roots inoculated with *A. euteiches* demonstrated higher accumulation of phenols and lignin in resistant line, compared to the susceptible line (Djébali et al., 2009). Moreover, microscopy observations revealed the formation of an additional pericycle cell layer in the resistant line, for the protection of the root central cylinder against pathogen invasion (Djébali et al., 2009).

Many preformed or pathogen inducible secondary metabolites belonging to the phenylpropanoid pathway can function as either antimicrobial compounds or signaling molecules in local and systemic plant immunity (Naoumkina et al., 2010). The phenylpropanoids are natural products derived from the amino acid L-phenylalanine and are involved in many plant physiological processes ranging from flower and fruit pigmentation, use as phytoalexins to signaling molecules for symbiotic associations (Tanaka et al., 2008; Dixon et al., 2002). Many genes involved in the flavonoid biosynthesis pathway are highly upregulated in the partially resistant line (Badis et al., 2015). This demonstrates a clear role of the phenylpropanoids in *A. euteiches* infection.

I.4 Plant communication through volatiles

Another way of chemical defense in plants is the emission of volatile compounds. Volatile organic compounds (VOC) are lipophilic liquids having a high vapor pressure that can cross-membranes and are released into the atmosphere or soil (Pischersky et al., 2006). Plants use volatiles as a language for communicating with their surrounding environment. To date, more than 1700 plant volatiles has been identified from ~ 90 plant families (Dudareva et al., 2006).

Plant volatiles constitutes about 1 % of plant secondary metabolites, mainly represented by terpenoids, phenylpropanoids/benzenoids, fatty acid derivatives, and amino acid derivatives (Dudareva et al., 2006). The plant volatiles can be exudated constitutively or can be stress-induced (Kessler and Baldwin, 2002). The plant exudes volatiles from

various tissues, either to defend against herbivores and pathogens or as a reproductive advantage by attracting pollinators and seed dispersers (Dudareva et al., 2006). Enzymatic modifications of volatile compounds such as hydroxylation, acetylation, and methylation lead to their diversity (Dudareva et al., 2004; Gang, 2005). Plants employ volatiles for two types of defense: 1) direct defense, where plants can directly influence the attacker's physiology or behavior through volatiles (Mithöfer and Boland; 2012, Pierik et al., 2014) and 2) indirect defense, by initiating tripartite associations, where plants release volatiles to attract natural enemies of the attacker (Fig.I.5) (Pierik et al., 2014).
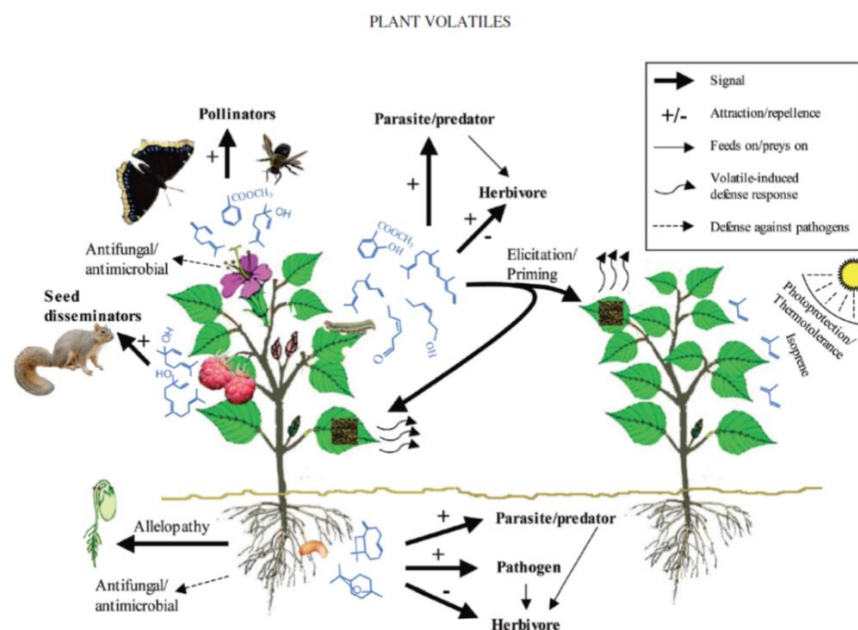
Fig.I.5: Pictorial representation of volatile-mediated plant interactions with the surrounding environment (from Dudareva et al., 2006).

I.4.1 Volatiles for direct plant defense

Many plant species are known to produce and store volatile compounds in specialized organs, such as trichomes (Schilmiller et al., 2008). These glandular organs are known to store specialized metabolites from various classes, like terpenes (Gershenzon et al., 1992), phenylpropanoid derivatives (Gang et al., 2002), acyl sugars (Kroumova and Wagner, 2003; Li and Steffens, 2000), methyl ketones (Fridman et al., 2005) and flavonoids (Voirin et al., 1993). The specialized metabolites stored in trichomes have direct toxic effects on herbivores (Kennedy, 2003; Gassmann et al., 2005). In angiosperms, these specialized structures reduce the risk of auto toxicity in the emitter plants, maintaining high concentrations of these defensive metabolites at crucial infection sites and often serve as the first line of defense against herbivores and pathogens (Theis and Lerdau, 2003). Conifers have different strategies for the storage and release of their

defensive oleoresin (a complex mixture of mono-, sesqui- and diterpenes) blends (Langenheim, 1994). On the one hand, *Pinus* plants can store the defense blends in a resin canal system and on herbivory attack, the terpenes travel through the canals (often several meters) to the site of attack, on the other hand, *Thuja* (cedar) plants store their defense terpenes in simple resin cells, whereas *Abies* (true firs) plants store them in multicellular resin blisters (Theis and Lerdau, 2003).

Various plant species store and synthesize volatile terpenoids in the roots and rhizomes as a direct defense against soil-borne microbes (Bos et al., 2002; Kovacevic et al., 2002). For instance, *Arabidopsis* roots have been shown to synthesize volatile monoterpene 1,8-cineole, known to have anti-microbial activity (Hammer et al., 2003; Pina-vaz et al., 2004; Chen et al., 2004). Also, *P. syringae* or *Alternaria brassicola* infection of *Arabidopsis* root cultures induces emission of 1,8-cineole (Steeghs et al., 2004).

Green leaf volatiles (GLVs), are mainly C6 molecules and are exudated after herbivory or pathogen attack by almost all green plants (Scala et al., 2013). GLVs have also been shown to have direct antimicrobial activity against fungi and bacteria (Hamilton-kemp et al., 1992; Nakamura and Hatanaka, 2002). For example, after *P. syringae* attack, Lima bean plants release (E)-2- hexenal and (Z)-3-hexenol (Croft et al., 1993) and *Nicotiana tabaccum* plants release (E)-2-hexenal (Heiden et al., 2003).

In general, flowers lack the physical barrier of the lignified cell wall and impermeable cuticle, which makes them susceptible to pathogens and florivores (Muhlemann et al., 2014). Many flowering species are known to emit toxic floral volatiles to directly defend the reproductive organs of the plant (Chen et al., 2003). Huang et al. (2012) have shown that (E)-ß caryophyllene mutant *Arabidopsis* plants harbored denser bacterial population on their stigmas and reduced seed weight, suggesting a direct defensive role of this compound against the pathogenic bacterium, *P. syringae*.

I.4.2 Volatiles for indirect plant defense

Plants live in a co-operative and mutual relationship with many organisms and when the plants have a weak defense against some herbivore, they release volatiles to attract the natural enemies of the herbivores as 'bodyguards' (Mumm and Dicke, 2010). This tri-trophic interaction can benefit the plant in terms of reduction in herbivory and increased reproductive fitness (De Moraes et al., 1998; Kessler and Baldwin, 2001; Degenhardt, 2009). In indirect defense, plants emit a unique blend of volatile compounds, also known as herbivore-induced plant volatiles (HIPV) to attract the herbivore enemies (Clavijo McCormick et al., 2012). These HIPVs are used by many parasitoids and predators as a cue to the site of the attack. The very first example of indirect defense was demonstrated

by Turlings et al. (1990) in maize leaves attacked by *Spodoptera littoralis* (lepidoptera). As a consequence of herbivore attack, maize leaves emitted volatiles that attracted the parasitic braconid wasp *Cotesia marginventris* (Hymenoptera), which oviposit into the lepidoptera. The larvae of *C. marginventris* develops inside the lepidopteran host and eventually kills the host on emergence (Degenhardt, 2009). The indirect plant defense has been shown for several plant species (Van den Boom et al., 2004) and depending on the herbivore, the amount and composition of plant volatiles can vary (Takabayaschi and Dicke, 1996; Turlings et al., 1998). Plants can also activate their indirect response upon egg deposition by herbivores. The induced signals can attract predators and parasitoids of the eggs (Turlings and Benrey, 1998; Kessler and Baldwin, 2002).

Indirect plant defense is also crucial for below ground interactions. Although more research had been done in above ground interactions, recent research developments in this field have also gained attention. Rasmann et al. (2005) demonstrated that the maize roots upon feeding by *Diabrotica virgifera* (western corn rootworm) emit volatile (E)-ß-caryophyllene signals to attract entomopathogenic nematode (*Heterorhabditis megidis*).

Plants are also known to protect themselves by secreting sweet components termed as extra floral nectar (EFN). EFNs are also involved in indirect plant defense as they can attract mutualistic ants that feed on plant damaging herbivores (Kost and Heil, 2008).

I.4.3 Volatile mediated signaling between and within plants

Over the years, plants have evolved the capacity to emit as well as perceive volatile signals (Heil and Karban, 2010). Plant emitted volatiles play a role in plant-plant interactions and can induce expression of defense-related genes and volatile emission from healthy parts of the same plant or the neighboring undamaged plants (Dudareva et al., 2006), this way damaged plants send 'warning' signals and eventually can decrease the damage caused by herbivores (Arimura et al., 2002, 2004; Ruther and Kleier, 2005). VOCs had been proposed to serve as internal signals for within plant signaling (Farmer, 2001; Orians, 2005). VOCs signaling is considered faster than vascular signaling, as the green leaf volatiles are released immediately after the cell damage, and can provide rapid, reliable and mobile signals of the 'damaged self' for preparing the systemic organs of the future attack (Heil and Karban, 2010; Heil, 2009). VOCs are also involved in priming the neighboring tissue or plant for a faster and stronger response upon attack. For example, Engelberth et al. (2004) demonstrate that the maize seedlings when pre-exposed to GLV compounds such as (Z)-3 hexenal, (Z)-3-hexen-1-ol and (Z)-3-hexenyl acetate responded to wounding and caterpillar treatment with higher production of jasmonic acid and release of sesquiterpenes, compared to plant that was not pre-exposed to the volatile blend.

Therefore, VOCs mediated self-priming helps the plant to prepare for systemic defense against the future attack (Heil and Bueno, 2007; Frost et al., 2007; Rodriguez- Saona et al., 2009).

VOCs can also mediate priming in non-related plants, for instance, when *Nicotiana attenuata* plants were exposed to volatiles from clipped sagebrush, they showed lower damage by herbivore and high mortality rate of young *Manduca sexta* caterpillars (Kessler et al., 2006). Apart from perceiving signals from damaged hosts, plants can also perceive signals from undamaged hosts. For instance, seedlings of parasitic plants *Cuscuta pentagona* grew towards the volatile produced from their preferred host species and away from their non-host species (Runyon et al., 2006). These reports support the idea that damaged and undamaged plants can benefit their neighbors by emitting volatiles, but the emitter plants do not benefit from these cues. These cues benefit emitter plants only in the case of allelopathy.

But it's still an open question, whether these cues should be considered as communication or eavesdropping (Heil and Karban, 2009). A proper understanding of the volatile mediated defense signaling, identifying the functional as well as regulatory genes for the biosynthesis of these cues, could be beneficial for the breeding program (Pickett and Khan, 2016).

I.5 Terpenoids

Terpenoids represent the largest and structurally most diverse chemical compounds produced by plants. Terpenoid metabolites are employed for a variety of functions in growth and development and also for chemical interactions and plant protection from biotic and abiotic stresses (Tholl, 2015). The plant-based terpenes have also been used in the food and cosmetic industry, pharmaceutical industry, chemical industry and recently have also been exploited in the development of biofuel products (Tholl, 2015; Mewalal et al., 2017). The terpenoids Taxol, a diterpene from *Taxus buccata* and artemisinin, a sesquiterpene lactone from *Artemisia annua* are well known for their antineoplastic and antimalarial effects (Croteau et al., 2006; Pollier et al., 2011). The structurally diverse terpenoids share a common biosynthetic pathway and can be divided into three phases: i) formation of basic C_5 precursor unit - the C_5 molecule, isopentenyl pyrophosphate (IPP) and its allylic isomer, dimethylallyl pyrophosphate (DMAPP) are synthesized by two independent pathways, mevalonate (MVA) pathway located in the cytosol and 2-methyl-erythritol 4-phosphate/1-deoxy-xylulose 5-phosphate (MEP/DOXP) pathway located in the plastids (Dudareva et al., 2004).
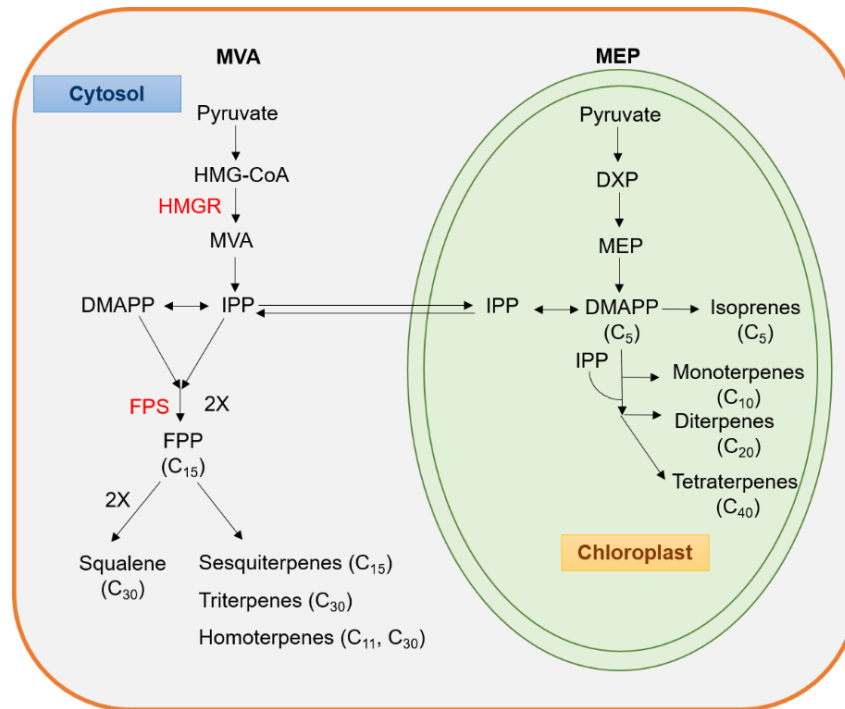
Fig.I.6: Schematic representation of isoprenoid biosynthetic pathway: In plant cells, two isoprenoid biosynthetic pathways are found, the cytosolic MVA pathway and the plastid MEP pathway. The cytosolic MVA pathway produces sesquiterpenes, triterpenes, and homoterpenes, whereas the MEP pathway produces monoterpenes, diterpenes, and tetraterpenes.

ii) In the second phase, three molecules of IPP condense with DMAPP to form the precursor molecule geranylgeranyl pyrophosphate (GGPP; C_{20}) in the plastids, whereas in the cytosol, two molecules of IPP condense with DMAPP to form farnesyl pyrophosphate (FPP; C_{15}). These LEGO-like building blocks serve as the substrates for an important family of enzymes, the terpene synthases (TPS) (Baldwin, 2010; Dudareva et al., 2004). iii) The third phase of terpene biosynthesis includes the terpene synthases catalyzed conversion of 'LEGO' blocks to various types of terpenes: hemiterpenes (C_5), monoterpenes (C_{10}), diterpenes (C_{20}) and tetraterpenes (C_{40}) are mainly synthesized in the plastid, whereas sesquiterpenes (C_{15}) and triterpenes (C_{30}) are synthesized in the cytosol (Fig.I.6) (Martin, 2003). The removal of the pyrophosphate from C_5-C_{20} substrates to form an unstable carbocation is considered as the first committed step of TPS-catalyzed reaction (Baldwin, 2010). These terpene synthases have the unique ability to make multiple products from one substrate. A single TPS can catalyze the formation of as many as 52 products or as few as 1 (Baldwin, 2010). Many terpene volatiles products are either direct products of TPSs or modification of initial products by reactions such as oxidation, dehydrogenases, acylation or methylation (Dudareva et al., 2004).

TPSs can be sub-divided into 7 different clades, based on their phylogenetic data. TPS-A consists of sesquiterpene producing, TPS-B and TPS-G consist of monoterpene producing, and TPS-C and TPS-E/F consists of diterpene producing. Additionally, TPS-D is a gymnosperm specific clade and consists of mono-, sesqui- and diterpene synthases, TPS-H is specific to lycopod and consists of diterpene synthases (Irmisch et al., 2014). A new class of terpene synthases is found in *Selaginella moellendorffii* that shows similarity to microbial terpene synthases and is termed as microbial terpene synthase-like (MTPSL) (Jia et al., 2012). The TPS proteins usually comprise of 500-900 amino acids, masses of about 60-100 kDa and require cofactors such as Mg^{2+} or Mn^{2+}.

In general, the role of terpenes in gymnosperms and angiosperms have been very well studied. In gymnosperms, a large number of Terpene synthases (TPS) have been functionally characterized from species of spruce, grand fir and other medicinally useful species such as *Ginkgo biloba* and *Taxus* (Keeling and Bohlmann, 2006; Keeling et al., 2011). Among angiosperms, terpene metabolism and regulation has been very well studied in the model plant, *Arabidopsis thaliana*, the availability of molecular and genetic resources in this species makes an in-depth study of the biological role of TPS possible. *A. thaliana* has a total of 32 TPS, of which 14 have been functionally characterized and are shown to be involved in defense functions (Tholl et al., 2011; Chen et al, 2004; Birnhaum et al., 2003; Brady et al., 2007).

I.6 Aim of the study

Plants interact with a variety of organisms in the rhizosphere. These interactions can be beneficial, harmful or neutral. A detailed understanding of such interactions could be beneficial for sustainable agricultural practices, but the study of rhizosphere interactions can be challenging, due to the complex nature of these interactions. Therefore, this thesis aimed to understand the early interaction of a host plant, *M. truncatula* with a beneficial fungus, *R. irregularis* and an oomycete pathogen, *A. euteiches*. These interactions should be studied using two different approaches.

i) In the first approach, the genetic variability in the SARDI core collection of 32 *M. truncatula* accession lines should be analyzed in terms of mycorhization intensities and response to the pathogen. This approach should give an insight into loci responsible for mycorrhization and pathogen resistance.

ii) The second approach was to investigate the early responses of *M. truncatula* roots to the incoming microbes, these early reactions might aid in the recognition of these microbes as beneficial or pathogenic. Additionally, use of plants at two developmental stages, six-day-old seedlings grown in sterile conditions and 6-week old plants grown in an aeroponic system, might be useful for the identification of microbe responsive genes, independent of the plant developmental stage. A transcriptional level study might be helpful for the understanding of early events occurring in plants after contact to a good or a bad microbe. The outcome from the transcriptomics might consist of genes that are differentially regulated after treatment in either of the development stage but should also consist of genes that are either similarly regulated or are regulated in an inverse manner. The genes commonly regulated in the two developmental stages of the plant might hint towards the gene regulatory network induced in response to either of the microbe. In particular, genes belonging to secondary metabolite class would be of interest, as the compounds encoded by this class of genes might be involved in the microbe recognition and/or defense. Analysis and characterization of such genes would add valuable information to the plant-microbe field and uncover their role in plant fitness and survival.

II. Results

II.1 To study mycorrhization diversity in *M. truncatula* accession lines

Sustainable agriculture demands healthy, high yielding and pathogen resistant plants with minimal nutrient input. This can be achieved by employing micro-organisms that help plants with the uptake of nutrients, for example arbuscular mycorrhiza (AM) can not only increase uptake of nutrients like P, N, Zn and Cu (Cavagnaro et al., 2008; Tarkalson et al., 1998; Liu et al., 2000) but is also known to have bio-protective effect against many pathogens (Whipps et al., 2004; Jung et al., 2012). This protective effect is known as Mycorrhiza Induced Resistance (MIR).

An inbred core collection of 32 lines from SARDI, which represent the bulk of diversity segregating in *M. truncatula* collection was used for this study (Ronfort et al., 2006). The South Australian Research and Development Institute (SARDI), houses the world's largest and oldest *Medicago* species collections. Previously, Ellwood et al. (2006) used the SARDI collection for mapping the genetic diversity in *M. truncatula*.

For this study, the 32 accession lines were analyzed, in terms of their symbiotic interaction with *R. irregularis*, using either a highly active inoculum or native sandy soil. The outcome from these experiments showed varied results and no conclusions could be drawn (Ph.D. thesis Dorothée Klemann, 2016). Therefore, in order to have a deeper and clear insight into the mycorrhization capability of these accession lines, the number of lines were narrowed down according to their root system architecture (RSA) in two different phosphates (Pi) conditions. The RSA was measured in terms of primary root length and number of lateral roots. Phosphate was chosen for RSA studies as it is an important micronutrient for plant growth and is also a crucial factor for the establishment of AM symbiosis. Additionally, Pi depriving conditions have been known to reprogram the root development (Vance et al., 2003), depending on the plant species and the genotype under study. Moreover, previous studies have reported that mycorrhization leads to altered RSA by increasing the lateral root (LR) development, probably in order to increase the mycorrhiza colonization sites (Harrison et al., 2005; Paszkowski and Boller, 2002; Oláh et al., 2005). Another study by Schultz et al. (2010) demonstrated the differences in eight *M. truncatula* ecotypes in terms of RSA (with limiting Zn) and uptake of nutrients like Zn, Mg, Fe, Mo under mycorrhizal and non-mycorrhizal conditions. Although, Schultz et al. (2010) used a different set of ecotypes than this study two lines were common in both the studies (line 530 and line 736, which are denoted by F83005 and DZA045 in Schultz et al., respectively). None of the lines showed significant differences

in root length and lateral roots under Pi abundant (13 mM) and Pi depriving (3 mM) conditions. However, few lines showed differences in either of the studied trait, lines 368 and 542 with increased root length under Pi depriving conditions, line 213 with increased lateral root numbers under low Pi and line 163 with increased root length under high Pi were selected for further mycorrhization and *A. euteiches* infection studies, together with the reference line A17.

For mycorrhizal studies, the five selected lines were inoculated with *R. irregularis* for two weeks and the mycorrhization in harvested roots was analyzed using ink staining, molecular markers such as *R. irregularis* fungal marker gene (*RiTUB*) and mycorrhiza induced plant marker gene (*MtPT4*). The ink staining did not show any significant differences among the studied lines. However, the qPCR data revealed that in higher Pi conditions, line 368 and line 555 were significantly different in terms of *MtPT4* and *RiTUB* transcript levels, respectively. To further investigate the correlation of mycorrhization to other micro-organisms, selected lines were also analyzed for infection with *A. euteiches*. Two different approaches were undertaken for studying plant's response to *A. euteiches*, one was performed in plates under sterile conditions and another one was in a climate chamber. Plants were infected with two different strains of *A. euteiches* and the infection was assayed by fresh weight measurements and *A. euteiches* biomass quantification using *5.8s rRNA* marker gene. The qPCR data analysis demonstrated that line 368 and 542 were partially resistant to *A. euteiches*, whereas, line 555 was more susceptible, compared to A17. An interesting observation was that line 368 expressed significant *PT4* transcript levels and lower levels *A. euteiches 5.8s rRNA* transcript. This suggests that a locus in the genome might be responsible for a greater number of active arbuscle formation and some locus might be responsible for restricting the *A. euteiches* growth. Further studies on line 368 might help to identify QTLs responsible for a higher number of active arbuscles and low pathogenic biomass. A cross between lines 368 x A17, line 368 and *A. euteiches* susceptible line 535 (Djébali et al., 2009; Bonhome et al., 2014; Badis et al., 2015) and the analysis of the resulting daughter generations might give hints for the low pathogenicity and high arbuscle numbers in line 368.

The results of this part have been published and the complete publication is attached in the Appendix section.

II.2 Early communication between host plant, beneficial fungus and pathogenic oomycete

To understand how the host plant recognizes the incoming microbe as friend or foe, the study of early responses between the host plant and the microbes will deliver the first insights in the plant disease resistance research. Therefore, we studied early responses of the host plant, *M. truncatula* to symbiotic fungus – *R. irregularis* and pathogenic oomycete – *A. euteiches*. In a previous study, the early responses of *M. truncatula* after contact with the microbes were studied in seedlings stage via a transcriptomics approach (Ph.D. thesis Dorothée Klemann, 2016). Here, the time point of two hours after contact with the microbes was selected because a high number of genes were shown to be differentially regulated after contact with *R. irregularis* spores at this time point (Ph.D. thesis Dorothée Klemann, 2016).

II.2.1 Identification of early responses to microbes using transcriptomic approach

As a follow-up approach for the identification of early responses of the host plant irrespective of their developmental stage, a transcriptomics approach with adult plants was performed. For this, six-week-old plants grown in an aeroponic system were used and the whole root system of these plants was either treated with *R. irregularis* spores or *A. euteiches* zoospores or remained non-treated for two hours. The roots were harvested for RNA analysis followed by hybridization, three replicates were taken for each treatment. The raw data were normalized by robust multiarray normalization and differentially regulated genes were identified by at least a two-fold change between the control and treated samples. The p-values were adjusted by the false discovery rate procedure (Benjamini and Hochberg, 1995). The transcriptomic data was analyzed by Dr. Benedikt Athmer, IPB and is provided in a CD attached along with this thesis.

According to the mentioned criteria, no genes were differentially regulated after inoculation with *R. irregularis* treatment. However, treatment with *A. euteiches* zoospores revealed ~ 200 genes that were differentially regulated, of which 138 genes were upregulated and 60 were downregulated (Fig.II.1.A). The commonly regulated genes in seedlings and adult plants after treatment with beneficial and pathogenic microbes were of interest. Unfortunately, as there were no differential regulated genes after treatment with *R. irregularis* in adult plants, the study was focused more on plant response after treatment with the pathogen. A comparison between seedlings and adult plants differentially expressed genes, revealed commonly regulated genes in both the developmental stages of the plant and genes that were specific to either of the developmental stage (Fig.II.1.B). The set of commonly regulated genes were

of prime importance, as these might help to understand the early plant responses to the pathogen.
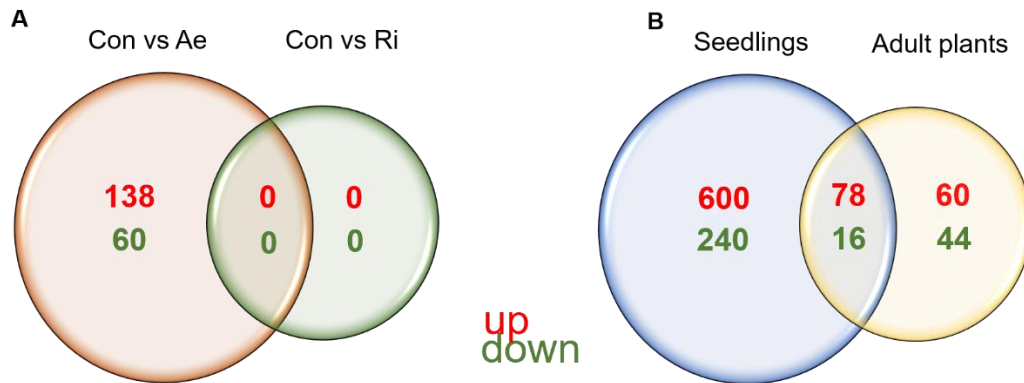
Fig.II.1: Transcriptomics analysis after inoculation with *R. irregularis* spores and *A. euteiches* zoospores: Venn diagram showing numbers of differentially regulated genes. (A) RNA isolated from six-week-old plants treated for two hours with *R. irregularis* spores or *A. euteiches* zoospores were subjected to transcript profiling using Affymetrix Medicago GeneChip array. (B) Venn diagram showing commonly regulated genes in seedlings and adult plants. The significantly up-regulated (red) and down-regulated (green) genes, compared to non-treated plants are shown. (p ≤ 0.01, n=3), *A. euteiches* treated (Ae), *R. irregularis* treated (Ri) and Control (con).

However, genes belonging to either of the developmental stages were also appealing, among them a *WRKY1b* transcription factor (*Medtr2g088000.1*) was found to be upregulated only in adult plants after *A. euteiches* treatment. Interestingly, this gene is not yet characterized in *M. truncatula*, therefore an *in silico* search was performed using MtGEA web database and Medicago eFP browser. The outcome of expression data analysis shows that *MtWRKY1b* is induced after 1 day of *A. euteiches* treatment (Fig.II.2.A) and has an enhanced expression only in roots (Fig.II.2.B). Here, it can be speculated that this transcription factor might be involved in the regulation of defense functions against *A. euteiches.*
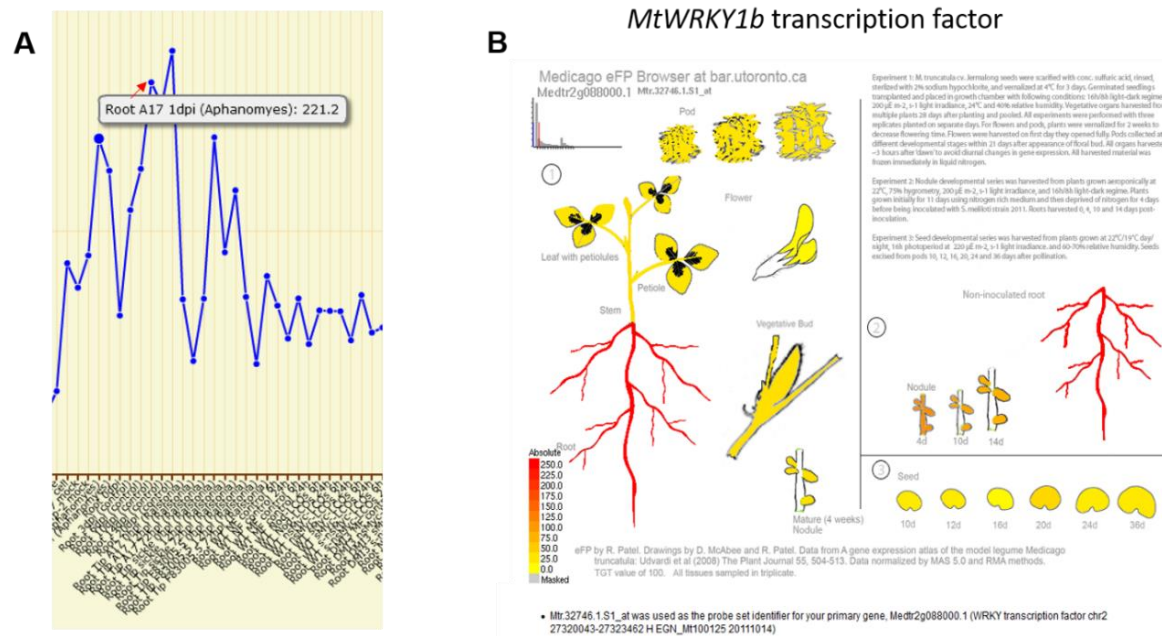
Fig.II.2: Expression data analysis of *MtWRKY1b*: (A). MtGEA database was searched for the probeset id of *MtWRKY1b*. The transcript of *MtWRKY1b* was abundant after 1-day infection with *A. euteiches*. (B). Organ-specific expression of *MtWRKY1b* was analyzed using Medicago eFP browser.

Among the commonly regulated genes, a terpene synthase *Medtr2g089120* was upregulated in adult plants and in seedlings after 2 hours pathogen treatment. *Medtr2g089120* is annotated as *MtTPS6* (Parker et al., 2014) and belongs to the TPS-G monoterpene producing family (Fig.II.5). The gene expression analysis was performed using *M. truncatula* gene expression atlas which shows upregulation of *Medtr2g089120* also after 1 day *A. euteiches* treatment (Fig.II.3.A). The tissue specificity was analyzed using eFP browser, showing that *MtTPS6* is expressed specifically in roots, similar to *MtWRKY1b* expression (Fig.II.3.B). *MtTPS6* and *MtWRKY1b* were only analyzed *in silico*, although their functional and molecular characterization was not performed in this study.
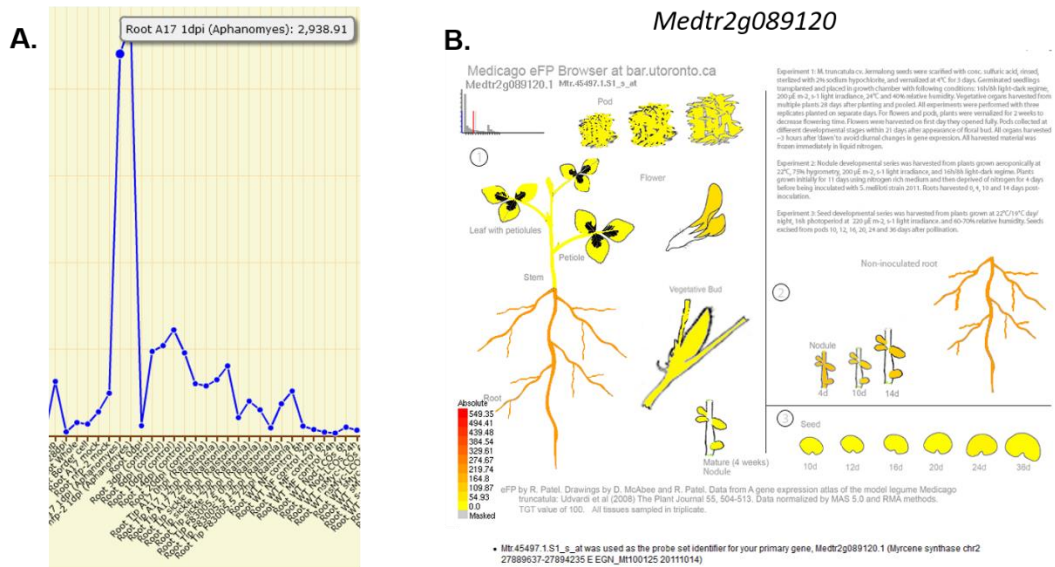
Fig.II.3: Expression analysis of *MtTPS6*: (A). MtGEA database was searched for the probeset id of *MtTPS6*. The transcript of *MtTPS6* was highly abundant after 1-day infection with *A. euteiches*. (B). Organ-specific expression of *MtTPS6* was analyzed using Medicago eFP browser.

II.2.2 Identification and characterization of *MtTPS10*

In the common set of genes, another gene that caught our attention also belonged to the terpene synthase class (*Medtr5g073200)* and is annotated as *MtTPS10* (Parker et al., 2014). From the transcriptomics data, this gene was found to be 22-fold up-regulated in seedlings and 2-fold up-regulated in adult plants compared to non- treated plants. As a first step, to circumvent that the gene might be a false positive pick from transcriptomics, expression of this gene was validated using qPCR from both the plant developmental stages in independent experiments, with three biological replicates each (Fig.II.4.A & B).

In both the developmental stages, *TPS10* was highly induced after *A. euteiches* treatment, compared to non-treated samples. The *TPS10* relative transcript levels in the adult plants were 75 times induced compared to the mock-treated, whereas, in seedlings, the transcript levels were 140 times higher compared to the mock treated. The less transcript induction can be attributed to the different developmental stages of the plants. However, despite the differences in the level of transcript induction, *TPS10* was successfully validated as an early *A. euteiches* inducible gene in seedlings and adult plants.
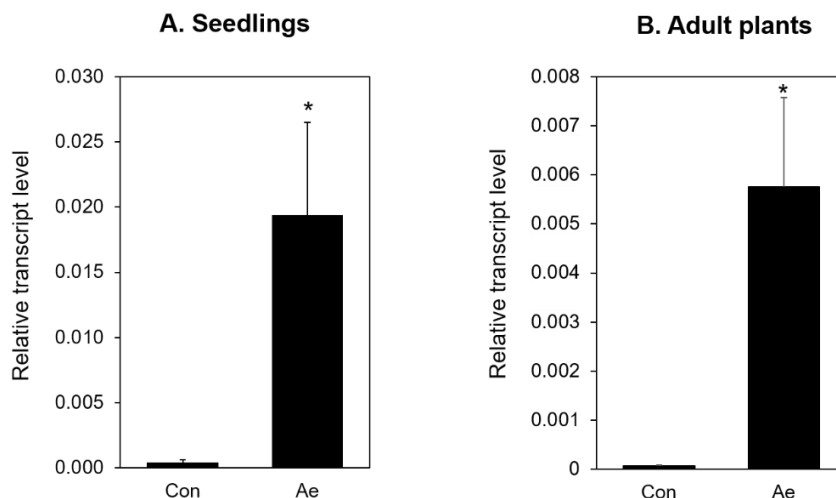
Fig.II.4: *TPS10* **transcript accumulation after treatment with** *A. euteiches***:** (A) Roots of one-week-old seedlings, (B) and six-week-old adult plants were treated either with *A. euteiches* zoospores or mock inoculated with swamp water for two hours. The transcript levels were determined by qPCR and normalized against the housekeeping gene *MtHIS3like*. Data shown is with 3 replicates, error bars represent standard error (SE), and statistical analysis was performed using one factorial ANOVA followed by Tukey HSD, * = $p \leq 0.05$, n=3, where *A. euteiches* treated (Ae) roots were compared to control (con) roots.

After successful validation of the *TPS10* expression in seedlings as well as in adult plants, literature and *in silico* search was performed to gain more knowledge about the gene and its encoded enzyme. The enzyme should belong to the class A of terpene synthase family, which consists of sesquiterpene producing terpene synthases. To gain an insight into the similarity pattern of MtTPS10 protein to other *M. truncatula* terpene synthase family members, a phylogenetic tree was constructed using the protein sequences of all 23 *M. truncatula* terpene synthases. The phylogenetic tree revealed a high similarity of MtTPS10 to Medtr5g094620 and Medtr5g073260. However, these terpene synthases are also not characterized in *M. truncatula*. Interestingly, MtTPS10 was found to be similar to Medtr5g062230 (Fig.II.5), which is a well-characterized herbivore-induced terpene synthase in *M. truncatula* (Vattekatte et al., 2017; Arimura et al., 2008).
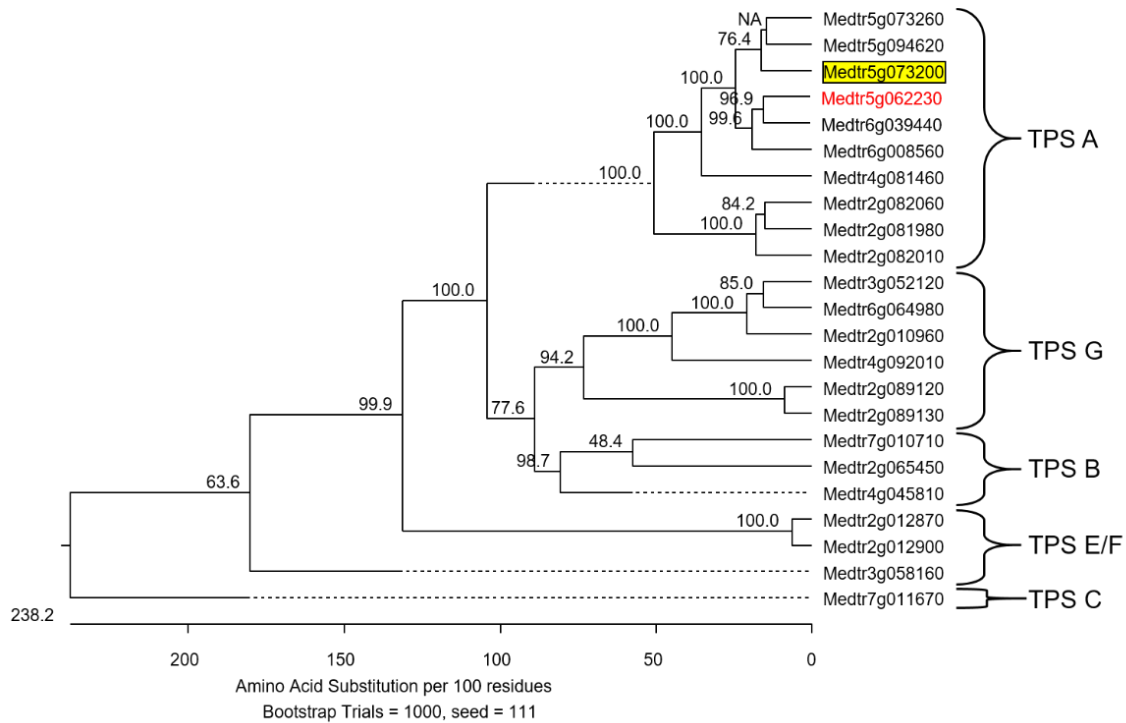
Fig.II.5: Phylogenetic tree of *M. truncatula* terpene synthases*:* The phylogenetic tree was constructed using MegAlign software from 23 annotated terpene synthases. The bootstrap values are indicated on each branch of the tree.

II.2.2.1 Expression kinetics of *TPS10* after *A. euteiches* infection

The induction of *TPS10* by *A. euteiches* inoculation was analyzed by performing a time course experiment ranging from early time points to the late infection stage. One-week-old A17 seedlings were treated either with swamp water or with *A. euteiches* zoospores for the indicated time points and the transcript levels were quantified at those time points using qPCR. The qPCR data showed that the *TPS10* transcripts were significantly accumulated after early *A. euteiches* contact, particularly after 2 hpi. But, soon after that, the transcript accumulation reduced already after 6 hpi *A. euteiches* inoculation and was no more differentially expressed to mock-treated plants (Fig.II.6). The *TPS10* transcript accumulation in *A. euteiches* treated seedlings was compared to the mock-treated seedlings for each time points. This data suggests that the *TPS10* is an early induced gene in response to *A. euteiches* treatment.
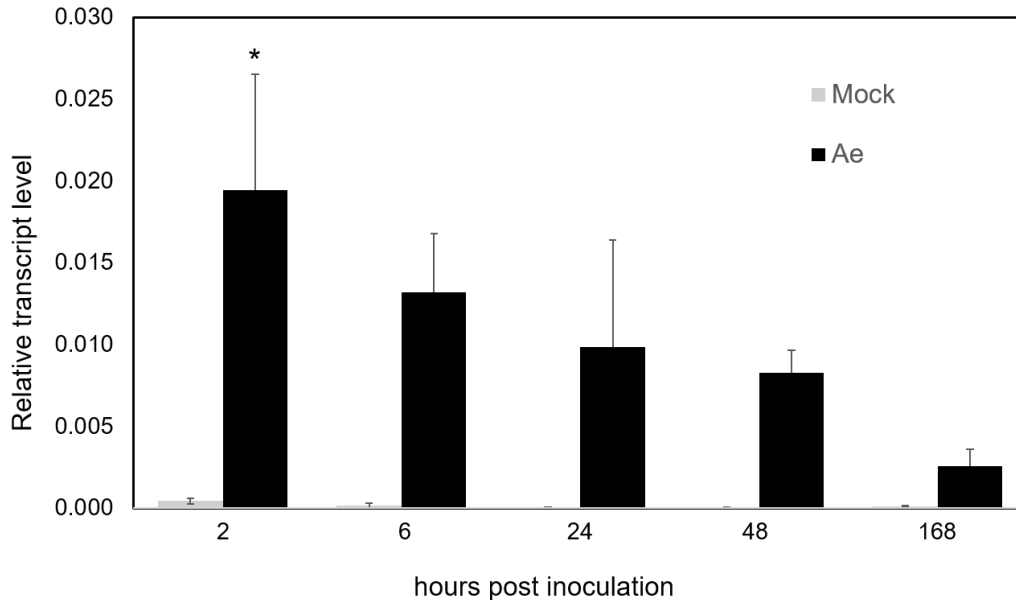
Fig.II.6: Transcript accumulation of *TPS10* transcripts after *A. euteiches* treatment of roots*: One-week-old seedlings were either treated with *A. euteiches* zoospores or mock treated with swamp water for the indicated time points and data analyzed using qPCR and normalized against the housekeeping gene *MtHIS3like*. The data shown is with 3 replicates, error bars represent standard error (SE). The *A. euteiches* treated seedlings (Ae) from a time point were compared to the mock-treated seedlings of the respective time point, significance tested using one factorial ANOVA followed by Tukey HSD, * = $p \leq 0.05$.

II.2.2.2 Effect of various treatments on *TPS10* transcript accumulation

To investigate whether *TPS10* is a pathogen-specific gene or can it also be induced by other treatments, one-week-old A17 seedlings were either treated with *A. euteiches* zoospores, *A. euteiches* zoospores boiled at 95 °C for 10 min (dead *A. euteiches* zoospores), *R. irregularis* spores, *R. irregularis* spores boiled at 95 °C for 10 min (dead *R. irregularis* spores), spores of pathogenic fungus *Colletotrichum trifolii* (*C.trifolii*) and another pathogenic oomycete *Phytophthora palmivora* (*P. palmivora*). The *P. palmivora* treated seedlings were kindly provided by Dr. Aleksandr Gavrin, The Sainsbury Laboratory, Cambridge. All treatments were performed for 2 h and control plants were either mock treated with swamp water, Tween20, citrate buffer or non- treated. To test the induction of *TPS10* transcript accumulation by abiotic stress treatments, seedlings grown in M-medium plates for one week were transferred to new M-medium plates containing either 100 mM NaCl or 50 µM MeJA for 2 h. The mock controls were transferred to new M-medium plates with no additions. For the wounding experiments, one-week-old seedling roots were squeezed with tweezers at three different positions on the root and the controls remained unwounded for 2 h. The data revealed that the *TPS10*

transcripts were significantly and specifically induced only by vital zoospores of oomycetes (*A. euteiches* and *P. palmivora*) but were neither induced by a pathogenic fungus (*C. trifolii*) nor by a beneficial fungus (*R. irregularis*) (Fig.II.7). Additionally, NaCl, MeJA, and wounding also did not induce the transcript levels. The transcripts levels could also be induced by dead *A. euteiches* zoospores but the induction was not statistically significant. The transcript quantifications were compared to the respective mock treated seedlings. This hints that *TPS10* is exclusively an oomycete response plant gene.
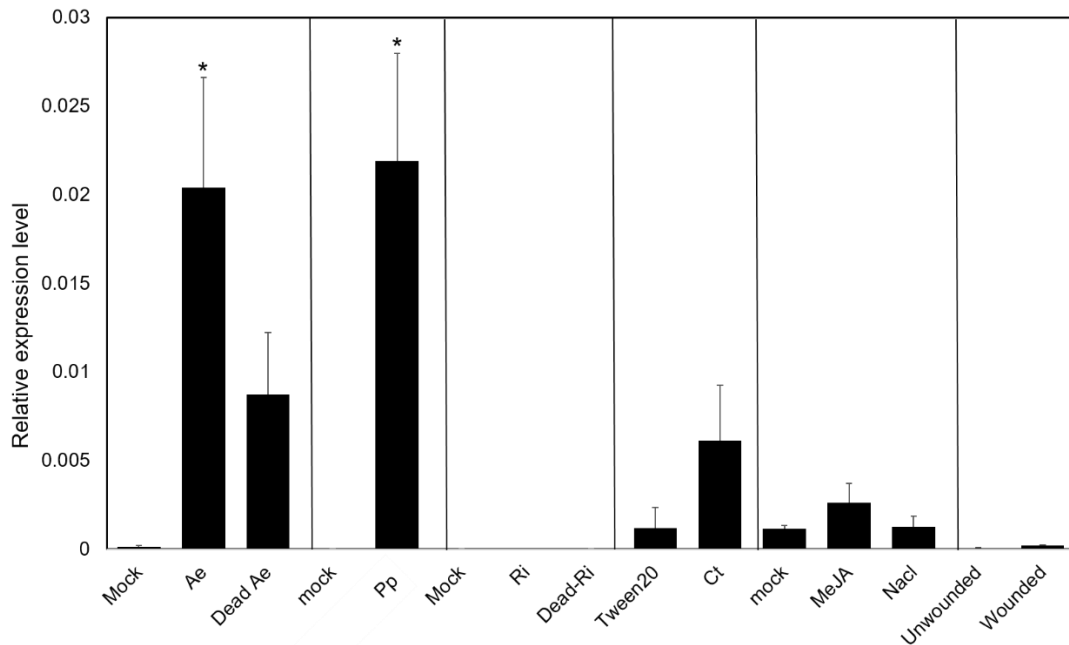
Fig.II.7: *TPS10* **transcript accumulation in response to various biotic and abiotic treatments***:* One-week-old seedlings were treated with zoospores of *A. euteiches* (Ae), boiled *A. euteiches* (dead Ae) and *P. palmivora* (Pp), spores of *C. trifolii* (Ct) fungus, *R. irregularis* (Ri), and boiled *R. irregularis* (dead Ri). The stress treatments were performed using 50 µM MeJA, 100 mM NaCl and wounded for 2 hours. The transcript accumulation of *TPS10* was quantified using qPCR and normalized against the housekeeping gene *MtHIS3like*. The data shown is with 3 replicates, error bars represent standard error (SE), and statistical analysis was done using ANOVA followed by Tukey HSD, * = p ≤ 0.05, where significance was tested between the mock controls and the treatment. The black lines separate different experiments.

II.2.2.3 Organ specificity of *TPS10*

In silico analysis revealed no expression and functional data on *TPS10*, thereby, an experiment was performed to acquire information about its organ specificity. One-week-old A17 plants were either not infected or infected with *A. euteiches* zoospores for four weeks,

the roots and leaves were separately harvested and *TPS10* transcript accumulation was analyzed using qPCR. The data demonstrated low transcript levels in leaves before and after *A. euteiches* infection. The *A. euteiches* infection did not lead to any *TPS10* transcript induction in leaves. In the case of non-infected root samples also, only basal transcript levels were detected. However, in *A. euteiches* infected roots, the transcript levels were significantly enhanced, compared to non-infected roots. This dataset showed that the *TPS10* is a root-specific gene and is induced specifically after *A. euteiches* infection.
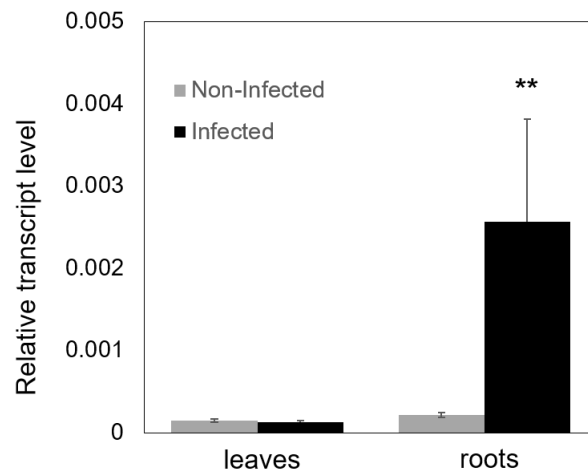
Fig.II.8: Organ specificity of *TPS10* expression after *A. euteiches* infection: One-week-old plants were infected with *A. euteiches* for 4 weeks and the transcript accumulation was analyzed in roots and leaves of infected and non-infected plants using qPCR and normalized against the housekeeping gene *MtHIS3like*. The data shown is with 3 replicates, error bars represent standard error (SE), and significance was tested between non-infected leaves and infected leaves, non-infected roots and infected roots using one factorial ANOVA followed by Tukey HSD, ** = p ≤ 0.01.

II.2.2.4 Promoter-*GUS* fusion of *TPS10*

The cell specificity of *TPS10* expression was studied in detail by cloning a 2 kb region upstream of the start codon to drive the *GUS* reporter gene. A DsRed module was also cloned in the final vector for the selection of positive transformed roots (Fig.II.9.A). The final construct was then transiently transformed in *M. truncatula* c.v. A17 via hairy root transformation. The transformed roots were selected by DsRed fluorescence and were either infected with *A. euteiches* zoospores for 2 h and 24 h or not treated, followed by staining with X-Gluc. In addition, the stained root fragments were embedded and sectioned into 10 μm thick cross sections and analyzed using bright field microscopy. The micrographs revealed that the 2 kb

region behaves as a strong promoter (Fig.II.9.B, C, and D). Even without infection, a basal level of staining in root segments and root sections could be observed. This basal level staining, however, could be drastically enhanced by *A. euteiches* infection for 2 hours and 24 hours indicating that the promoter is activated upon *A. euteiches* treatment. There was no cell-specific expression observed since the staining was observed in all root cells.
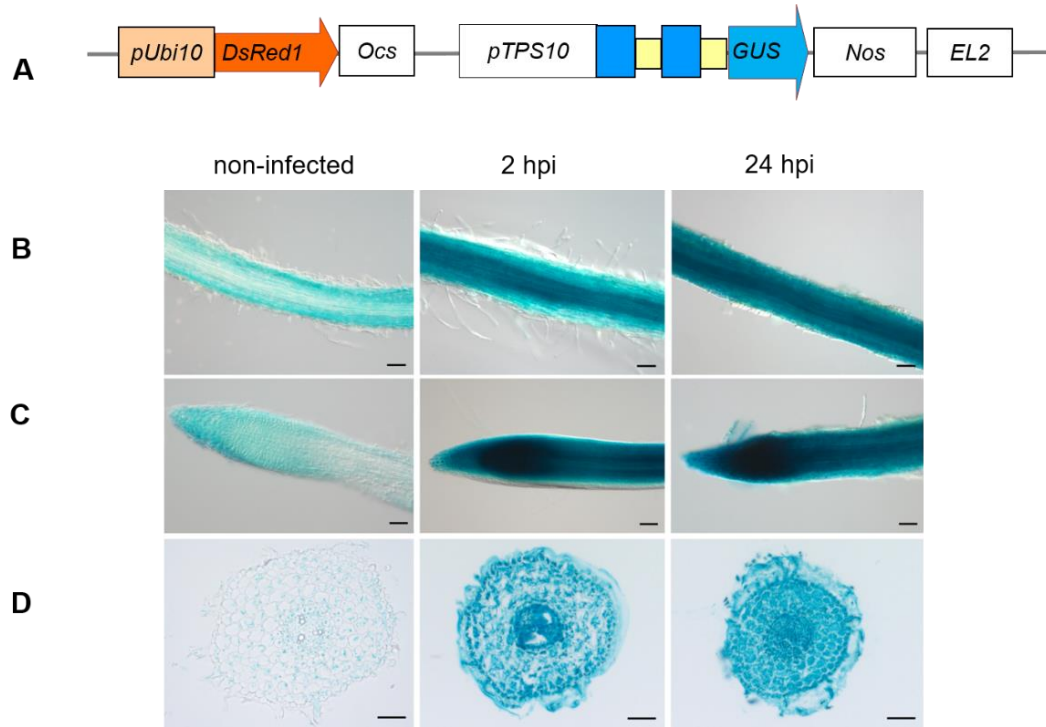
Fig.II.9: *pTPS10:: GUS* analysis*: The cellular specificity of *TPS10* was studied via promoter:: *GUS* analysis. A 2 kb upstream fragment was cloned and fused to drive *GUS* encoding gene. (A) The vector construct, consisting of *pTPS10:: GUS* module and DsRed module, was transformed to *M. truncatula* via *A. rhizogenes* mediated hairy root transformation. (B) The positive transformed roots were treated with *A. euteiches* for 2 h, 24 h and control were not treated. After treatment, roots were stained by X-Gluc substrate, embedded in PEG1500 and sectioned into 10-micron thick sections. (B) The root fragments, (C) root tips and (D) cross-sections are shown. The black bars represent 100 μm in B, C and 50 μm in D.

II.2.2.5 Localization of TPS10 protein

Terpenoids are either derived from the mevalonate pathway, which is active in the cytosol or from the plastidial 2-C-methyl-D-erythritol-4-phosphate (MEP) pathway (Aharoni et al., 2005). Terpenes like monoterpenes, diterpenes, and tetraterpenes are biosynthesized in the plastids,

whereas, biosynthesis of terpenes like sesquiterpenes, homoterpenes, and triterpenes takes place in the cytosol. To study the subcellular localization of *TPS10*, the coding sequence of *TPS10* (without the stop codon) was fused to *m-cherry* on the C-terminal and driven under the control of a CaMV 35S promoter. This construct was transiently expressed in *Nicotiana benthamiana* protoplasts and localization was studied using confocal microscopy. TPS10 was found to be localized in cytosol surrounding the chloroplast (Fig.II.10), which is expected from a class A terpene synthase family protein. Although *TPS10* localization is clearly demonstrated to be in the cytosol, a western blot analysis from the transformed protoplasts would further confirm these results.
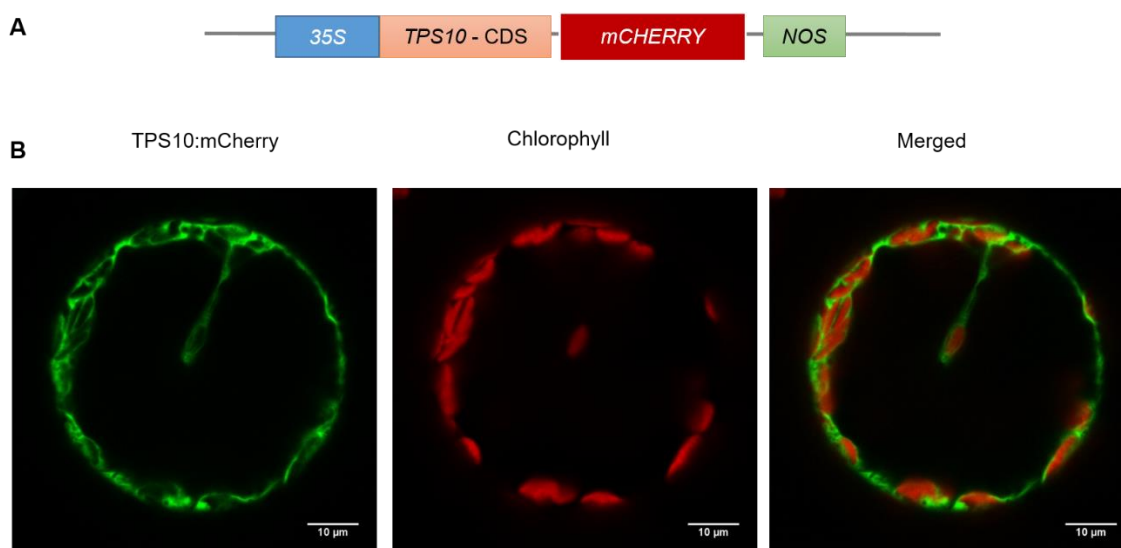
Fig.II.10: Subcellular localization of TPS10 protein in *N. benthamiana* protoplasts: (A) Schematic of the construct used for *TPS10* localization. The construct was transiently expressed in *N. benthamiana* protoplasts and the fluorescence images were taken using a confocal laser scanning microscope. (B) TPS10 in the cytosol is shown with the green fluorescence surrounded by red fluorescent chlorophyll in the merged image. The bars represent 10 μm.

II.2.2.6 Molecular characterization of *MtTPS10*

As the MtTPS10 belongs to the sesquiterpene catalyzing class A family, product identification of MtTPS10 was an important step towards characterization of the enzyme encoded by this gene. For this, *Saccharomyces cerevisiae* was used as the heterologous host for protein production and the construction of yeast level 1 and level M expression vectors were performed using Golden gate system (Engler et al., 2008). Plasmids containing the coding sequences of *farnesyl pyrophosphate synthase* (*FPPS*) and a truncated version of *hmg-CoA reductase* (*3-hydroxy-3-methyl-glutaryl-coenzyme A reductase*, *tHMGCR*) from *N.*

benthamiana were kindly provided by Prof. Alain Tissier and Dr. Sylvestre Marillonnet, respectively. The expression vector backbone, comprised of the plant coding sequences *FPPS, tHMGCR* and *TPS10* under distinct galactose inducible promoters, the origin of replication for *E. coli* and *S. cerevisiae*, *E. coli* antibiotic selection marker and yeast *URA3* (orotidine-5'-phosphate decarboxylase, an essential enzyme in pyrimidine biosynthesis in *S. cerevisiae*) selection marker. As a negative control, a construct containing only *FPPS* and *tHMGCR* was used. Both the constructs were transformed in yeast and the positive yeast clones were selected on Synthetic Drop-out medium without uracil. After galactose induction, the accumulating products were extracted from the medium using solvents like hexane or pentane and injected into GC-MS for product identification. The products were identified by comparing the MS spectra of peaks with the in-built library spectra and the most similar compound match was chosen. The TPS10 produced a blend of sesquiterpenes and sesquiterpene alcohols, of which 11 were sesquiterpenes and 6 were sesquiterpene alcohols (Fig.II.11; m/z of all the compounds are provided in Appendix Fig.VII.2.6). Interestingly, TPS10 also catalyzed the formation of a major product which could not be identified by MS spectra comparison, and the closest match with an 80 % similarity was alpha-bisabolol. Therefore, structure elucidation of this major product using NMR was required. NMR measurements usually require a minimum amount of 1 mg purified compound thereby, various tests were conducted for the production of the major product in higher concentration. The first test was to try a different yeast strain, here a yeast strain from OrganoBalance (kindly provided by Dr. Swanhild Lohse, IPB) was tested. This strain has a truncated version of *HMGCR* integrated into its genome, hence, higher levels of precursor molecules are available for higher end product formation. The peak abundance of the major product was comparatively higher than that produced by Invitrogen yeast strain (Fig.II.12).
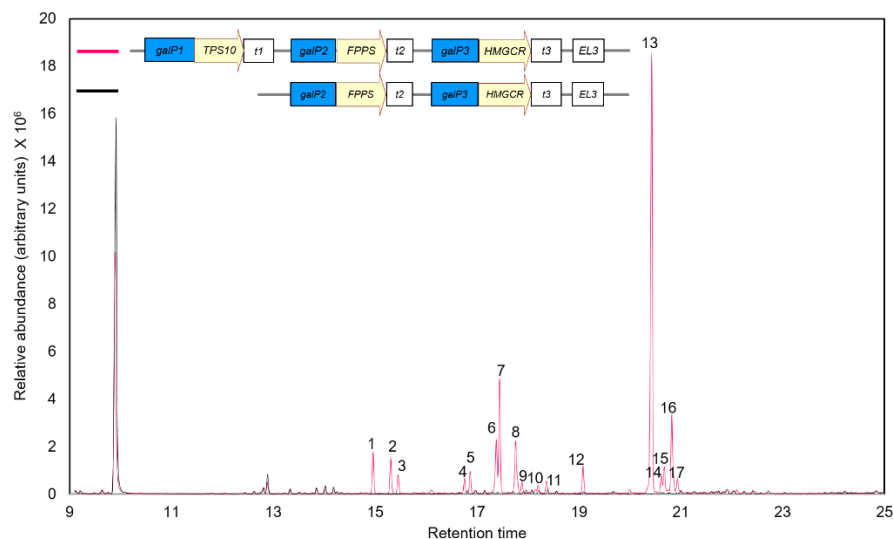
Fig.II.11: Product profile of TPS10 identified after heterologous expression in Invitrogen strain: *TPS10* was expressed together with *farnesyl pyrophosphate synthase* (*FPPS*) and a truncated *hmg - CoA reductase* (*3-hydroxy-3-methyl-glutaryl-coenzyme A reductase, tHMGCR*) and the resulting products were analyzed using GC-MS. The product profile composed of several sesquiterpenes and sesquiterpene alcohols and were annotated by comparison of MS spectra: (1) α-Longipinene, (2) Ylangene, (3) Longicyclene, (4) Farnesene, (5) α-Himachalene, (6) Himachalene, (7) Alloaromadendrene, (8) β-Himachalene, (9) Bisabolene, (10) Bisabolene,(11) Longibomeal, (12) Humalene-1,6-dien-3-ol, (13) major product, (14) Allohimachalol, (15) Shyobunol, (16) α-Bisabolol, (17) Shyobunol.
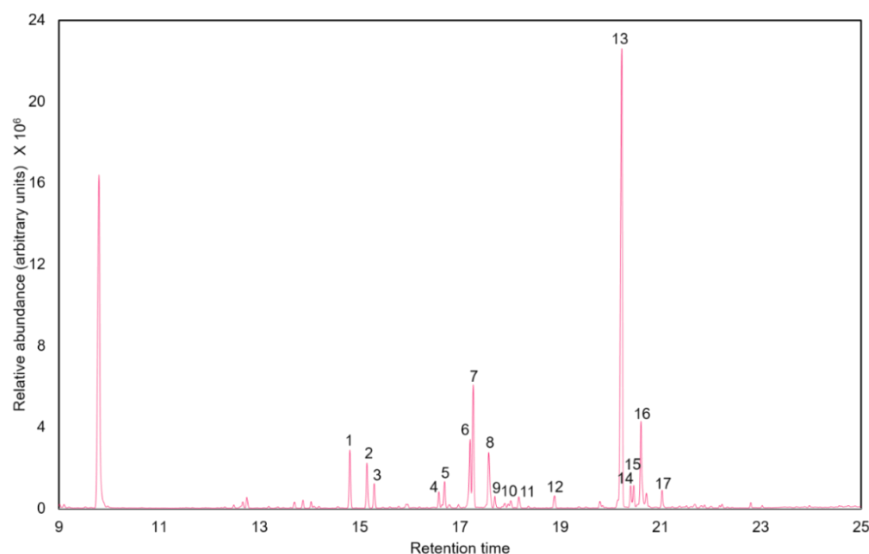
Fig.II.12: Product profile of TPS10 after expression in Organobalance yeast strain

The next task was to purify the major product from the minor products (Fig.II.11 and 12, peak 13). For this, the column chromatography technique was used, which separates complex mixtures based on their adsorption capacity and interaction between the mobile phase and the stationary phase. Silica (SiO_2) was used as the stationary phase and the compounds were eluted using a gradient of hexane and ethyl acetate ranging from 99 % hexane up to 80 % hexane + 10 % ethyl acetate. All elutes including the flow through and wash steps were measured in GC-MS. The GC-MS chromatogram reveals that the major peak could be separated from other minor peaks and was eluted at 90 % and 85 %, however, the peak abundance drastically reduced during this process (Fig.II.13).
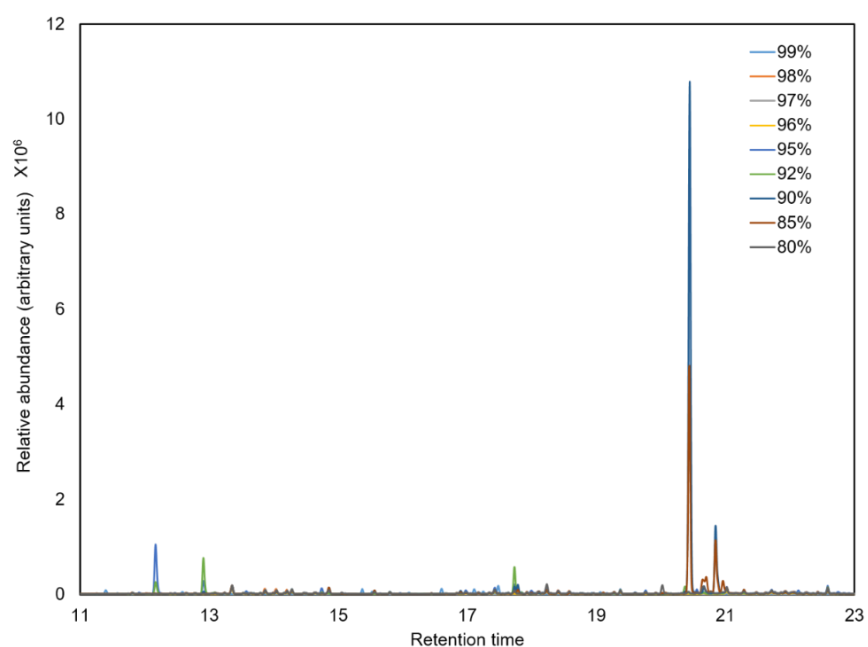
Fig.II.13: Chromatogram data depicting elutes obtained via column chromatography: The separation of the major product from other peaks was tested using column chromatography. Different percentage of elution solvents were used, elutes were collected and measured using GC-MS. The major product could be separated at 90% and 85%, but the abundance of the peak decreased during this process.

Due to the decrease in major peak's abundance during the chromatographic process, peak separation by LC-MS was decided. One major obstacle was that the solvent used for product extraction from yeast and GC-MS measurement was a hydrophobic solvent, whereas in LC-MS usually hydrophilic solvents, such as methanol are used. Therefore, after product extraction, the hydrophobic solvent needs to be evaporated and should be re-dissolved in methanol. This evaporation step also led to a decrease in major product's abundance. Therefore, an ideal extraction solvent was needed that extracts the products efficiently and

evaporates sooner, not affecting the peak's abundance. Different solvents were tested for higher product extraction and low loss during the evaporation process. The three different solvents tested were – dodecane, hexane, and pentane. Hexane and pentane solvent were used to extract the end products from yeast cultures, whereas, dodecane was added during galactose induction process for entrapping the products formed. This dodecane layer was later extracted with hexane or pentane and used for GC-MS measurement. A volume of 100 μl from the extracts of different solvents was used for the measurement. The chromatogram (Fig.II.14) demonstrates that pentane and hexane can extract the major product peak in higher abundance, whereas, the dodecane extract contained a high abundance of dodecane impurities and low amount of products were extracted.
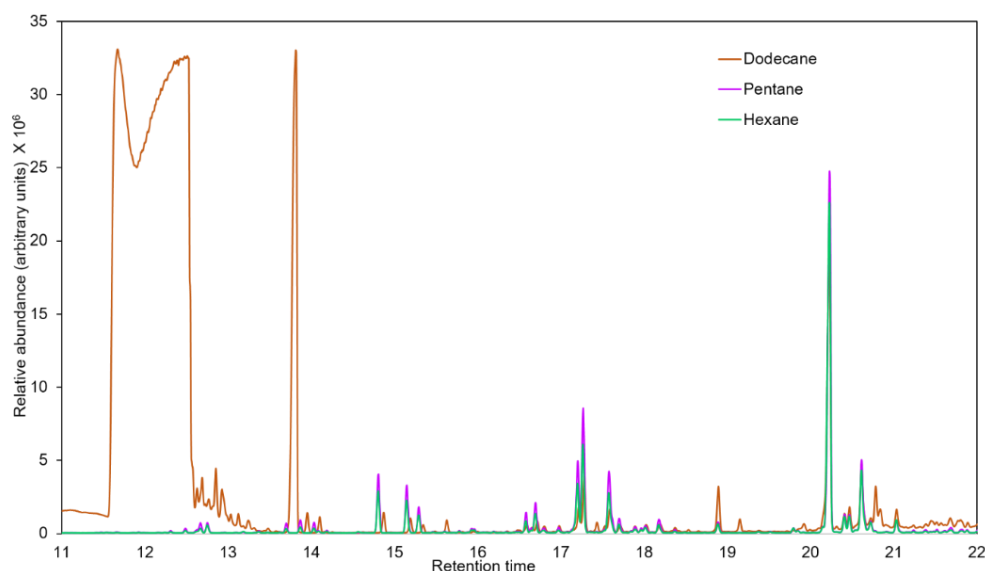
Fig.II.14: Test with different solvents for product extraction from yeast: Three different solvents, namely dodecane, hexane, and pentane were tested for product extraction in high concentration. The chromatogram data points from all measurements were exported to excel and a scatter plot was made with the data points. Pentane (pink) and hexane (green) extracted the products to an equivalent abundance, whereas dodecane (brown) extracted more of the impurities.

Therefore, for further extractions, either hexane or pentane was used. Next, in order to investigate the loss in peak abundance due to the evaporation process, an experiment was performed. Here, 100 μl yeast extract with hexane or pentane was injected in GC-MS and the remaining 1.9 ml was evaporated using rotavap. To this dried extract, 1.9 ml fresh solvent was added and again 100 μl was used for GC-MS measurement. The chromatogram obtained before and after evaporation were compared for each solvent. This revealed pentane as an ideal solvent because the major peak intensity was not affected before and after evaporation

(Fig.II.15.B), whereas, with hexane as the solvent, the peak's abundance was almost reduced to half after evaporation (Fig.II.15.A). In order to have concentrated product for NMR measurement, silica tubes were also used as adsorbent material. These silica tubes are able to adsorb compounds on their surface, thereby forcing the yeast cells to secrete more of the compounds in the medium for easier extraction. Overall, TPS10 products were extracted in high concentration using Organobalance yeast strain, silica tubes as adsorbents and pentane as the extraction solvent. After extraction, the extract was dried using rotavap, re-dissolved in methanol and the major peak was separated from other products using LC-MS (performed by Anja Ehrlich, IPB).
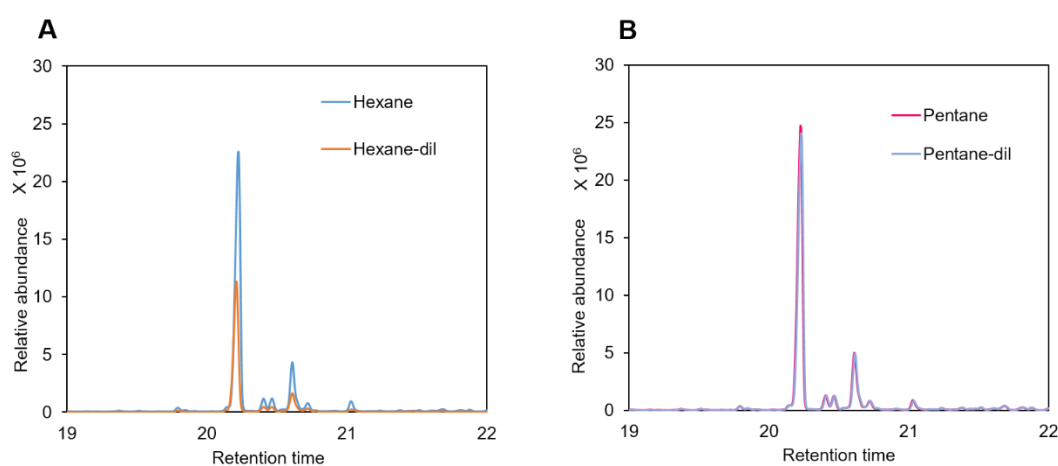
Fig.II.15: Evaporation effect tested with hexane and pentane as the extraction solvent: Chromatogram showing the relative peak abundance of the major product before and after evaporation, 100 µl from a total of 2 ml extract was used for GC-MS (denoted by hexane (blue) and pentane (pink)), the remaining 1.9 ml was evaporated, re-dissolved in fresh solvent and 100 µl again used for GC-MS (denoted by hexane-dil (brown) and pentane-dil (blue)). (A) Chromatogram showing evaporation effect when hexane used as a solvent for product extraction. (B) Data depicting evaporation effect when pentane used as a solvent. Evaporation of pentane solvent did not have any effect on the peak abundance.

Many fractions containing the major product were obtained from LC-MS and these methanolic fractions were extracted using pentane and measured in GC-MS for the determination of peak purity. The fractions containing a good abundance of the major peak were combined and the methanol solvent was completely evaporated. The dried extract was used for structure elucidation of the major peak using NMR (performed by Dr. Andrea Porzel, IPB) and the data showed that the major product of TPS10 corresponds to himachalol and not to alpha-bisabolol which was the predicted match according to NIST library search (Fig.II.16).

For biological assays, accurate concentrations of the compounds are important, therefore, a second trial of TPS10 product extraction was performed for use in bioassay experiments against *A. euteiches*. The same extraction protocol, used for NMR, was followed, but before evaporation, the extracted products were divided into two equal volumes. One volume was re-dissolved in pentane after evaporation, for determining the concentration of major peak using standard curve. The second half was re-dissolved in methanol for bioassay experiments. As TPS10 catalyzed various minor products and a major product formation, concentration of only the major product 'himachalol' was determined using the standard curve method. The curve was plotted using trans-farnesol as the standard compound and its concentration ranged from 10 µM to 100 µM. Three serial dilutions of TPS10 products from yeast were used, 1:10, 1:100 and 1:1000. For each concentration of trans-farnesol and TPS10 product dilutions, three replicates were measured in GC-MS. The data points of relative peak abundance were exported to Excel and a scatter plot of concentration versus peak abundance was plotted (Fig.II.17). The relative peak intensity of TPS10 product dilutions 1:10 and 1:100 could not be extrapolated on the standard curve, as the values were bigger compared to the highest concentration of farnesol used (100 µM), however dilution 1:1000 could be extrapolated on the standard curve and was comparable to trans-farnesol with 60 mM concentration.

Himachalol
CAS 1891-45-8
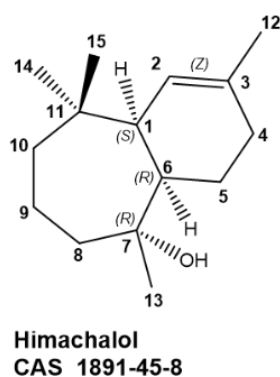
Fig.II.16: Structure elucidation of the major product using NMR: The purified extract of the major peak was used for compound identification using NMR by Dr. Andrea Porzel (IPB, Halle)
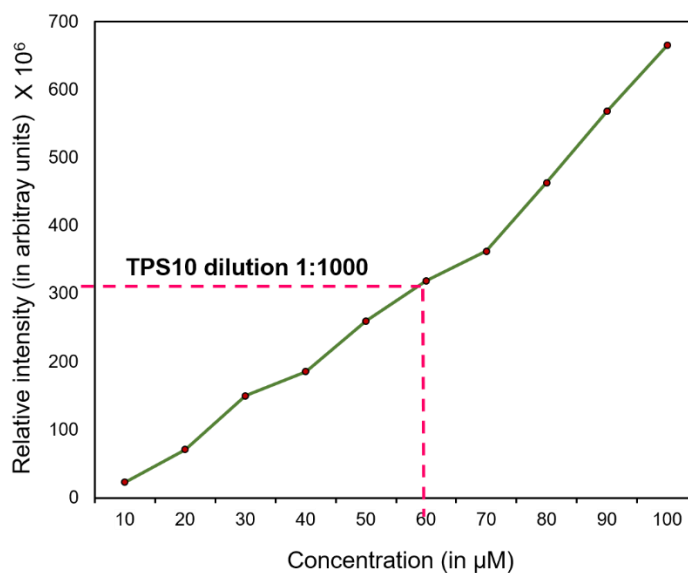
Fig.II.17: Standard curve for determining concentration: A standard curve using trans-farnesol was made using GC-MS measurements ranging from 10 μM to 100 μM. Three different dilutions of yeast extract were made, only the major product peak abundance was considered for plotting the data points. A dilution of 1:1000 was extra-plotted on the standard curve and the concentration was determined to be 60 mM.

II.2.2.7 Functional characterization of *MtTPS10*

Now that *TPS10* had been proved to be an oomycete inducible gene, the next quest is to study its function against *A. euteiches*. The functional role of *TPS10* was identified using classical approaches of knock-down and overexpression studies. For knock-down approach, *Tnt1* insertion mutants were searched in the Samuel Noble foundation database which houses a large collection of *M. truncatula* insertions. The genomic sequence of *TPS10* was blasted in the Noble foundation web database against either *Tnt1* high confidence FSTs (flanking sequence tags) or low confidence FSTs. The resulted lines were compared based on their highest similarity to *TPS10* sequence. One insertion line, NF10408-low 18 showed 100 % similarity of 223 bp fragment behind the *Tnt1* insertion, in the sixth intron. The seeds of NF10408-18 were ordered from the foundation and were genotyped in a previous study (Ph.D. thesis Dorothée Klemann, 2016).

A

ATG   TGA

NF10408-low 18

B

F1   Mutant
                              (TPS10/tps10)

F2   Homozygous   Homozygous
         mutant   Heteroygous   background (WT)
       (*tps10/tps10*)   (TPS10/tps10)   (TPS10/TPS10)
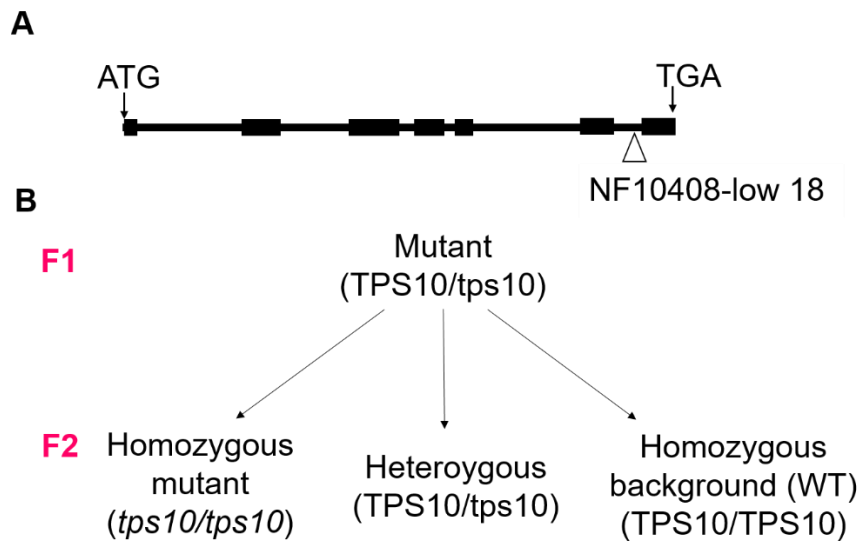
Fig.II.18: Schematic of *Tnt1* insertion in *TPS10* gene: (A) Pictorial representation of *TPS10* exon-intron assembly. Black boxes represent exon and the lines between them represent introns. The start codon ATG and the stop codon, TGA are shown and the triangle shows the *Tnt1* insertion in the gene. (B) The selfing scheme of the heterozygous *Tnt1* line is shown.

The line NF10408-18 was obtained in a heterozygous state and after one round of selfing, homozygous mutant, heterozygous mutant, and homozygous background line were obtained. An important feature of these *Tnt1* insertions is that these lines contain on an average 25 random *Tnt1* insertions in different locations of the genome (Tadege et al., 2008). Therefore, for the comparison of *tps10* mutant, homozygous TPS10/TPS10 obtained in an F2 generation will be treated as the wild-type and is denoted as background (BG), this line theoretically should possess all the background mutations in the genome like in *tps10* mutant but not in the *TPS10* gene.

The first step towards characterization of *tps10* mutant was the quantification of *TPS10* transcript levels after 2 h of *A. euteiches* treatment. One-week-old seedlings of *tps10* and BG line were treated with *A. euteiches* zoospores for 2 h and the control seedlings were treated with swamp water. The qPCR quantification showed only a basal level of *TPS10* transcript induction in mock-treated as well as in *tps10*. Interestingly, *A. euteiches* treated *tps10* had comparable transcript levels like mock treated BG and the transcript levels in mock-treated *tps10* were below the detection levels, suggesting that the *tps10* after 2 hours *A. euteiches* treatment behaves as BG treated with swamp water (Fig.II.19). However, in BG line, the *TPS10* transcript levels were drastically induced after *A. euteiches* treatment (Fig.II.19). This illustrates that the *Tnt1* insertion NF10408-low 18 line has a loss-of-function in *TPS10* gene.
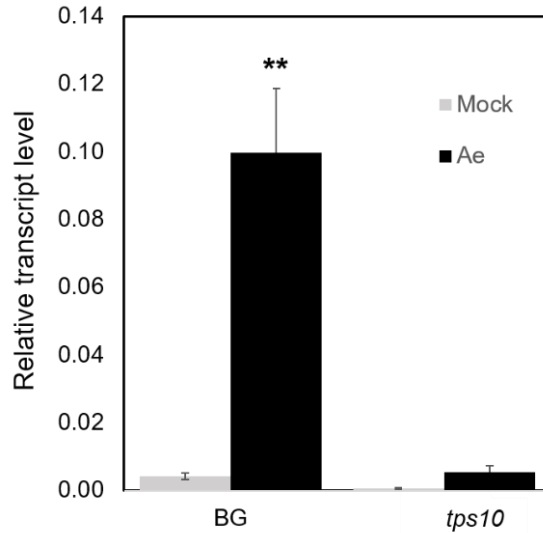
Fig.II.19: *TPS10* **accumulation in BG (wild-type) and** *tps10* **mutant**: One-week-old seedlings were treated for 2 h with *A. euteiches* zoospores and *TPS10* transcript accumulation was quantified using qPCR and normalized against *MtHIS3like*. The data shown is with 3 replicates, error bars represent standard error (SE), and significance was tested between mock treated and *A. euteiches* treated seedlings of the respective line, statistics was performed using one-factorial ANOVA followed by Tukey HSD, ** = p ≤ 0.01.

II.2.2.8 The role of *TPS10* in plant's response to *A. euteiches*

The functional role of *TPS10* in plants during *A. euteiches* infection was studied using the identified *tps10* mutant and the BG lines. Many terpene synthases are known to produce volatile products either as a direct defense or an indirect response to pathogens. Therefore, to analyze whether *TPS10* is also involved in the formation of volatile products to counter *A. euteiches*, the *tps10* mutant and wild-type plants were grown in lecaton substrate for six weeks. After six weeks, the plants were carefully separated from the substrate and depending on the root architecture, 2-4 Sorbstar sticks were inserted in the roots and the roots were either infected with *A. euteiches* zoospores or mock treated with swamp water for 12 h (Fig.II.20). These Sorbstar sticks adsorb plant emitted volatiles on their surface, which can be desorbed and measured in a GC-MS. After 12 h, these sticks were collected and stored in GC vials until the final measurement, while the root material was harvested and stored at -80 °C. The Sorbstar sticks were measured using thermodesorption GC-MS and the data was analyzed by comparing the chromatograms of *A. euteiches* treated BG and *tps10* plants as well as mock-treated BG and *tps10* mutant plants. As the *TPS10* products were already identified via heterologous yeast expression (Fig.II.11), thereby, the MS spectrum was filtered for sesquiterpene specific m/z of 119 and 204. As expected, the GC-MS profile from mock-

treated plants did not show any peak corresponding to sesquiterpenes, whereas, in the chromatogram of *A. euteiches* treated BG plants, few sesquiterpenes were detected. The detected sesquiterpenes were found missing in the *tps10* mutant volatile collection (Fig.II.21, peaks 1-8).

Infection with Ae for 12 hours
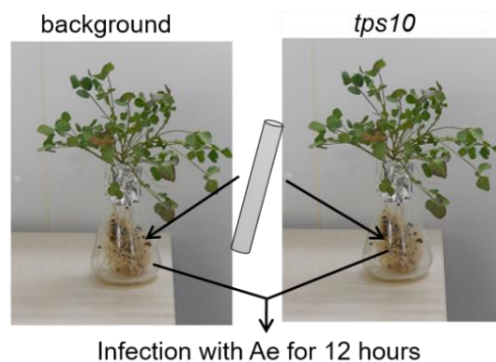
Fig.II. 20. Volatile collection from *tps10* and BG line: Six-week-old plants were used for volatile emission experiment, where Sorbstar sticks were inserted in the roots and the roots were infected with either *A. euteiches* (Ae) zoospores or mock treated for 12 h. The volatiles adsorbed on the sticks were then measured using GC-MS.
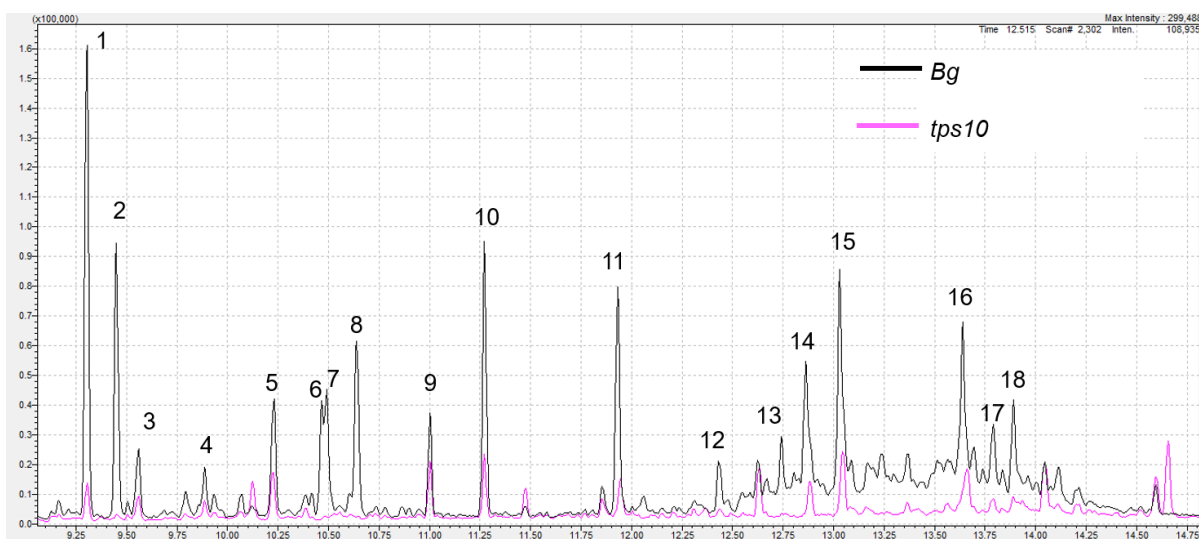
Fig.II.21: Comparative chromatogram of a BG and *tps10* volatile profile: Six-week-old BG and *tps10* mutant plants were used for volatile emission. Sorbstar sticks were inserted in roots and infected with *A. euteiches* zoospores for 12 hours and the sticks were then measured using GC-MS. The peaks correspond to 1) Longipinene, (2) Ylangene, (3) Longicyclene, (4) Longifolene, (5) Allohimachalol, (6) 7-epi-cis-Sesquisabinene hydrate, (7) Alloaromadendrene, (8) Himachalene, (9) Nerolidol, (10) Fokienol, (11) Longibomeal, (12) Cholest-8-en-3.beta.-ol, acetate, (13) Thunbergol, (14) Nerolidyl propionate, (15) Heptasiloxane, (16) Cyclodecasiloxane, (17) 1-Heptatriacotanol, (18) 1-Heptatriacotanol. Peaks 1-8 are sesquiterpenes and were identified in Fig.II.11.

The peaks 1-8 from the volatile collection were also identified from yeast expressing TPS10 products (Fig.II.11). Therefore, these products should correspond to TPS10. Some other peaks were also found to be missing in mutant plants (9-15), but these products were not observed in TPS10 yeast product profile and were not classified as TPS10 products. This suggests that few TPS10 products are volatile under natural conditions and are released as a response to *A. euteiches* treatment. Interestingly, the major product of *TPS10* (himachalol) was not found in volatile emission, which hints toward its further modification *in planta*.

In order to investigate the putative enzymes that might modify the major product of *TPS10 in planta*, several genes were picked from the transcriptomics data (Tab.II.1). Transcripts encoding transferases and cytochrome P450 family proteins (CYP450) were selected from commonly upregulated genes after *A. euteiches* treatment of seedlings and adult plants (Tab.II.1). All the selected transcripts were first validated using qPCR and only three out of the ten selected genes were found to be significantly upregulated after *A. euteiches* treatment, among them one UDP-glucosyltransferase (*Medtr2g098430*) and two CYP450 enzymes (*Medtr5g007550* and *Medtr8g104080*) (Fig.II.22).

Tab.II.1 selected candidate from the transcriptomics

S. No.	Gene_Id	Putative function	Dataset
1	Medtr3g084520	UDP-glucuronosyl/UDP-glucosyltransferase	Seedling transcriptomics
2	Medtr8g083290	UDP-glucuronosyl/UDP-glucosyltransferase	Seedling transcriptomics
3	Medtr5g090610	UDP-glucose glucosyltransferase	Seedling transcriptomics
4	Medtr2g034480	Glucan endo-1,3-beta-glucosidase	Adult plant transcriptomics
5	Medtr2g098430	UDP-glucosyltransferase family protein	Adult plant transcriptomics
6	Medtr8g087425	Glutathione S-transferase	Adult plant transcriptomics
7	Medtr5g007550	Cytochrome P450 family 71	Common in seedling and adult transcriptomics
9	Medtr8g104080	Cytochrome P450 family 71 protein	Common in seedling and adult transcriptomics
9	Medtr8g104100	Cytochrome P450 family 71 protein	Common in seedling and adult transcriptomics
10	Medtr5g016440	Cytochrome P450 family	Common in seedling and adult transcriptomics
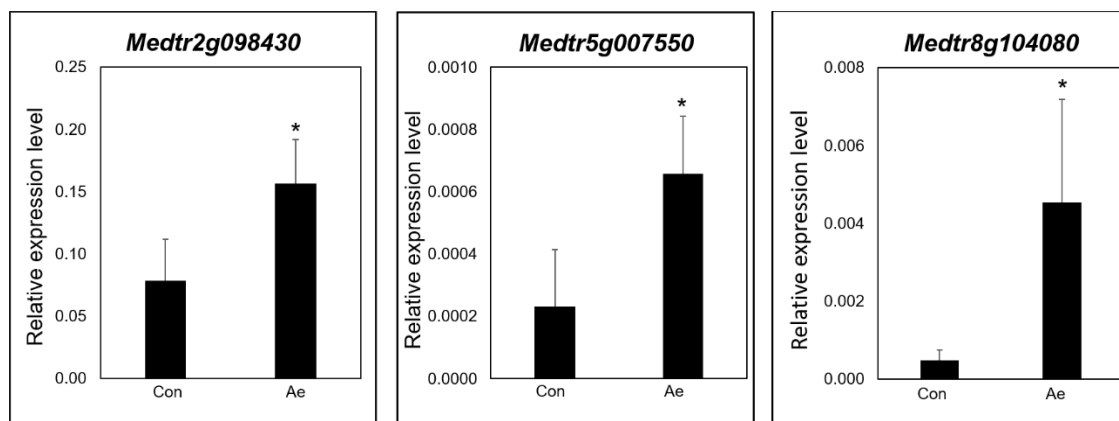
Fig.II.22: qPCR validation of potential TPS10 product modifying enzymes: six-week-old plant roots treated and non-treated with *A. euteiches* were used for the quantification. The transcript levels were normalized against *MtHIS3like*, The data shown is with 3 replicates, error bars represent standard error (SE), and significance was tested between non-infected (con) and infected roots (Ae) using one-factorial ANOVA followed by Tukey HSD, * = $p \leq 0.05$.

To test if the validated candidates modify the TPS10 major product, the coding sequence of these candidates were cloned under galactose inducible promoters and expressed in yeast together with *TPS10*, *FPPS* and *tHMGCR* and *Arabidopsis* reductase (*ATR* in case of CYP P450s; work done by Dr. Sunayana Rathi). The products formed were extracted from the yeast culture using hexane and measured in GC-MS. The GC-MS chromatogram data revealed that the selected candidates were not able to modify TPS10 products (data not shown).

Next, in order to study the role of these volatile products during *A. euteiches* infection and to examine the response of *tps10* mutant to *A. euteiches* infection, one-week-old *tps10* and BG plants were infected with *A. euteiches* and analyzed four weeks later. The *A. euteiches* susceptibility of *tps10* and BG plants were quantified using two parameters, root and shoot fresh weight and *A. euteiches* biomass in infected roots. In general, the *A. euteiches* susceptible plants have characteristic features, like, brownish, water-soaked roots and are stunted in growth. The root and shoot biomass of *tps10* mutant drastically decreased after *A. euteiches* infection compared to non-infected *tps10* plants, whereas, the infected BG plants did not show any significant reduction in growth compared to non-infected plants (Fig.II.23.A, B). The root and shoot biomass of *tps10* almost reduced to half, compared to the non-infected *tps10*.
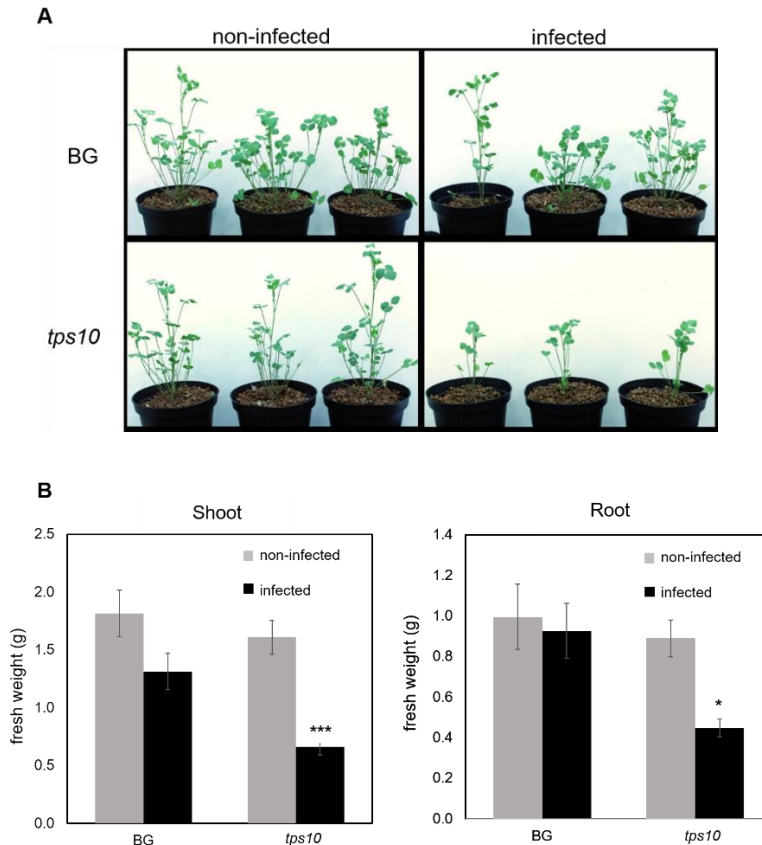
Fig.II.23: Phenotypic analysis of *tps10* mutant and the BG plants: (A) Three representatives of four weeks old *tps10* and BG plants without and with *A. euteiches* infection are shown. (B) The fresh weight of roots and shoots of mutant and background plants were measured, statistical significance was tested between non-infected and infected plants of the respective line, the analysis was performed using ANOVA, n=18-20, *= p ≤0.05, ***= p ≤0.001.

The stunted growth of *tps10* plants might hint towards their *A. euteiches* susceptibility. To test this, *A. euteiches* biomass was quantified from the roots of infected *tps10* and BG plants using qPCR. The qPCR data demonstrates that indeed the *tps10* mutant shows significantly enhanced amount of *A. euteiches 5.8s rRNA*, which corresponds to *A. euteiches* biomass in the roots, compared to infected BG plants (Fig.II.24.B). In addition, the transcript level of *TPS10* was also quantified in these plants (Fig.II.24.A). As expected, the *TPS10* transcripts levels were significantly reduced in *tps10* mutant plants, compared to infected BG plants. However, it is noteworthy, that due to the long infection period with *A. euteiches*, the transcript levels of *TPS10* in infected BG plants were lower compared to the 2 h treated BG plants (Fig.II.19). *TPS10* transcript level in *tps10* mutant was also different than 2 h treated *tps10* (Fig.II.19), but still, these increased levels can be considered as the new basal levels at later

stages of *A. euteiches* infection. This implies that a non-functional *TPS10* in the mutant plants renders them susceptible to *A. euteiches* infection.
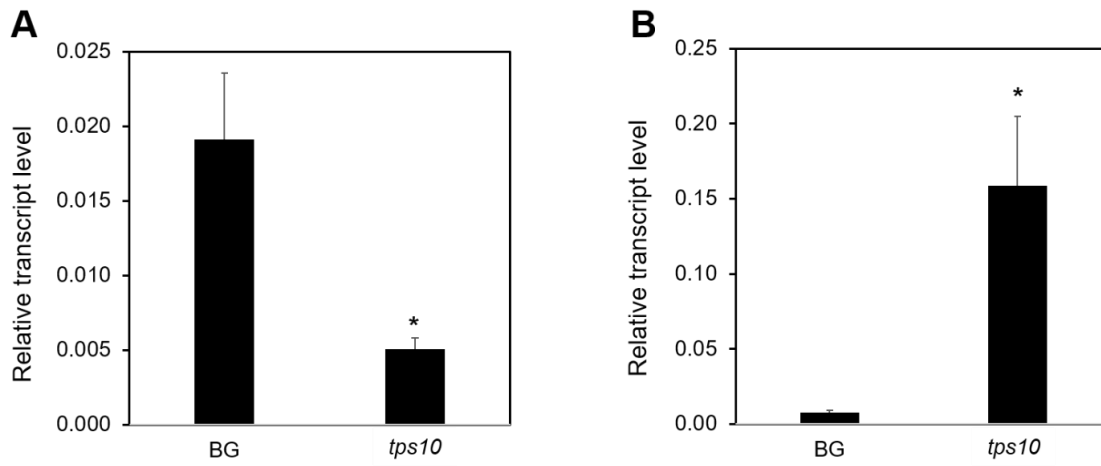
Fig.II.24: Quantification of *TPS10* and *A. euteiches 5.8s rRNA* transcripts in *tps10* and BG plants: Four weeks old *A. euteiches* infected roots of *tps10* and BG were used for the quantification of (A) *TPS10* and (B) *A. euteiches 5.8s rRNA*. The transcript accumulation was normalized against *MtHIS3like* and statistical significance was tested between infected *tps10* and BG plants, statistics was performed using one-factorial ANOVA, Tukey HSD test, *= $p \leq 0.05$, n= 3, error bars represent standard error (SE).

II.2.2.9 Confirmatory approaches for the identification of *TPS10* role in plant defense against *A. euteiches*

To further validate that the susceptibility of *tps10* mutant plants to *A. euteiches* infection is due to a non-functional *TPS10*, confirmatory approaches were required as the *Tnt1* insertion line have other random insertions in the genome. To address this, two different approaches were undertaken: i) overexpression and rescue of *tps10* mutant plants, ii) targeted knock-down of *TPS10* using amiRNA. A hypothesis was proposed that by overexpressing the coding sequence of *TPS10* under a native promoter, the susceptibility of *tps10* mutant plants could be rescued and might show a similar phenotype like BG plants after infection, whereas, via amiRNA targeting *TPS10* approach, plants could be made more susceptible to *A. euteiches*, like that of *tps10* mutant (Fig.II.25)
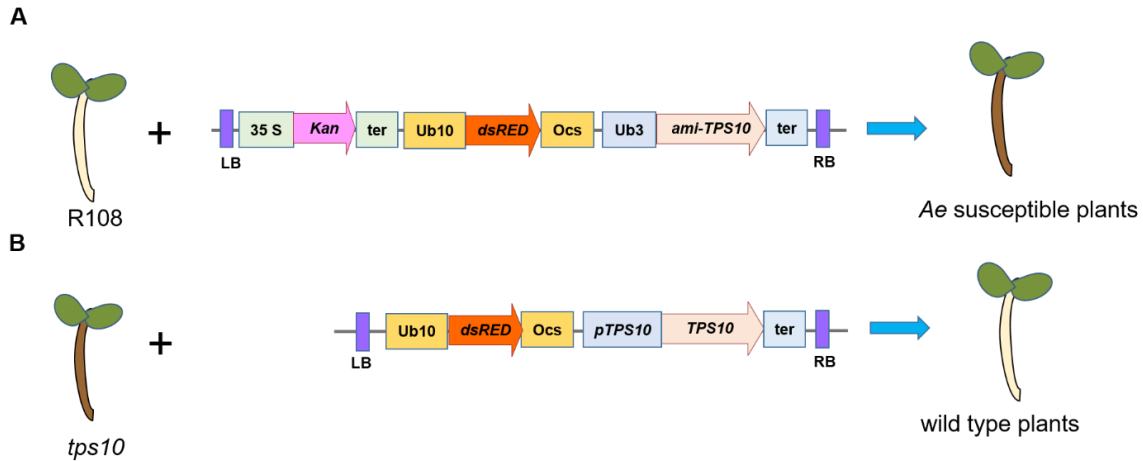
Fig.II.25. Illustration of the proposed hypothesis: (A) Generation of *A. euteiches* susceptible plants using amiRNA targeting silencing of *TPS10*. (B) Rescue of the *A. euteiches* susceptible phenotype of *tps10* mutant by complementing with *TPS10* coding sequence under a native promoter. The vector constructs for both the approaches also contained a DsRed module for the selection of positive transformants.

II.2.2.10 Complementation of *tps10* mutant

For the complementation approach, a construct containing coding sequence of *TPS10* under a 2 kb native promoter (*pTPS10:: TPS10*) and a negative control construct consisting of *pTPS10:: GUS* construct were used. Both the constructs were transformed in *tps10* mutant roots via *A. rhizogenes* mediated hairy root transformation, the transformed roots were selected by the red fluorescence encoded by the DsRed module and the plants were infected with *A. euteiches.* After four weeks of infection, *TPS10* transcript levels and the *A. euteiches* biomass were quantified from the transformants using qPCR. *tps10* mutant transformed with *pTPS10:: GUS* showed lower *TPS10* transcript levels and higher *A. euteiches 5.8s rRNA* expression. Moreover, *tps10* transformed with *pTPS10:: TPS10* could also not rescue the *A. euteiches* susceptibility of *tps10* mutant plants (Fig.II.26.A, B). However, one plant (Fig.II.26; *TPS*-2) showed higher *TPS10* transcript accumulation, compared to *pTPS10:: GUS* plants, but this high expression did not influence the *A. euteiches* infection in this plant. The other two *pTPS10:: TPS10* expressing plants (TPS-1 and TPS-3) showed lower *TPS10* transcript accumulation and also lower *A. euteiches 5.8s rRNA* levels. Such variability in *tps10* mutant expressing *pTPS10:: TPS10* could be attributed to either late infection stages and/or transient expression system. Additionally, the roots of *tps10* mutants were difficult to transform and the efficiency of transformed roots were very low.

A

B
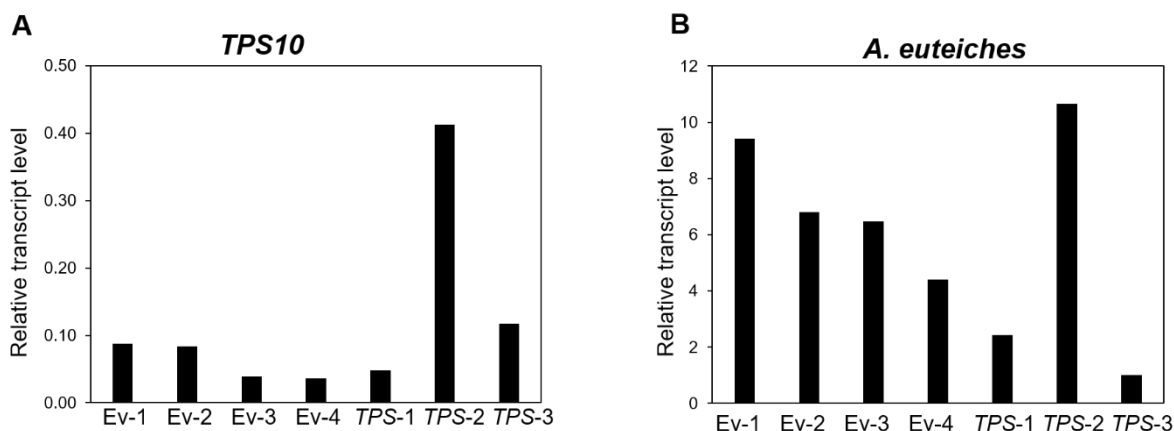
Fig.II.26: qPCR quantification of *TPS10* and *A. euteiches 5.8s rRNA*: *tps10* mutant seedlings were transformed via hairy root transformation and after four weeks of *A. euteiches* infection, (A) *TPS10* and (B) *A. euteiches 5.8s rRNA* expression were quantified from three empty vector (Ev) lines (*pTPS10::GUS*) and three complementation (*TPS*) line (*pTPS10::TPS10*). The transcript accumulation were normalized against *Actin2*.

The *TPS10* was showed to catalyze the biosynthesis of many volatile sesquiterpenes *in planta* after *A. euteiches* infection. Therefore, another approach for analyzing the *tps10* transformed with *pTPS10:: TPS10* was to collect the volatiles from the transformed plants after *A. euteiches* infection. For this, the transformed plants were grown in lecaton substrate. After 3-4 weeks, plants were separated from the substrate and sorbstar sticks were inserted in the roots and the roots were infected with *A. euteiches* zoospores for 12 h. The adsorbed volatiles were measured using thermodesorption GC-MS and the data was analyzed by comparing the chromatogram of *tps10* mutants transformed with either *pTPS10:: TPS10* or *pTPS10:: GUS*. The MS spectrum was filtered for sesquiterpene specific m/z of 119 and 204 and the peaks were identified by comparing the MS spectra to the standard NIST library. The GC-MS chromatogram revealed peaks mostly belonging to various additives of siloxane, probably coming from the Sorbstar sticks. Many trials were repeated, but no complementation could be achieved using *pTPS10:: TPS10*.
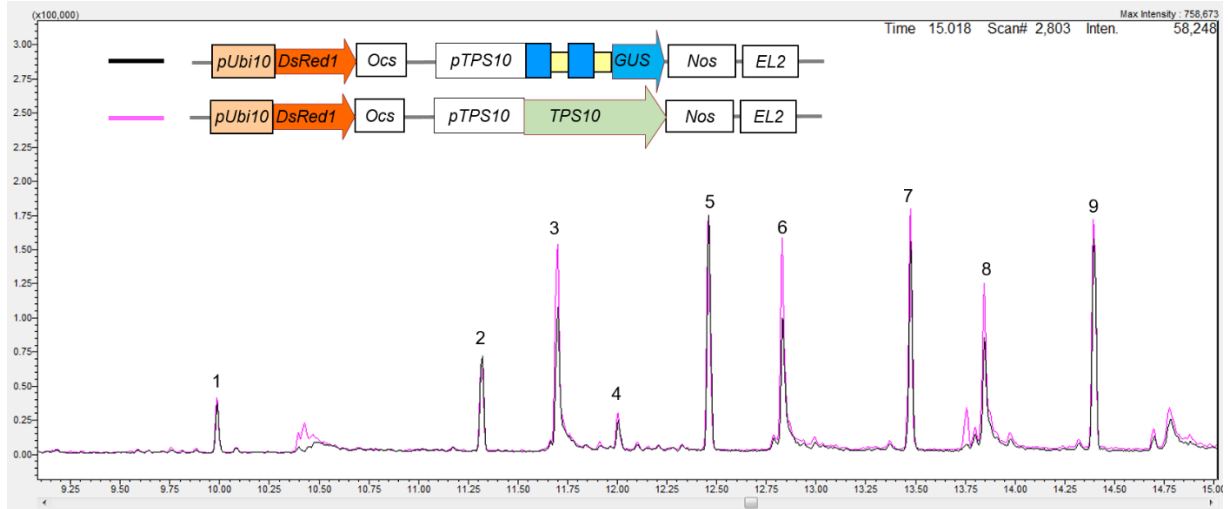
Fig.II.27: Chromatogram data of empty vector and complemented lines: Volatiles were collected from empty vector (black chromatogram, *pTPS10:: GUS*) plants and the complemented (pink chromatogram, *pTPS10:: TPS10*) plants. The data shown here is only from one replicate, but 3 or more replicates were compared and analyzed and all showed the same chromatogram pattern.

A hypothesis was postulated that an anti-sense RNA might be transcribed from the *Tnt1* promoter, which might lead to repression of the *TPS10* sense transcript from *pTPS10:: TPS10* construct. To test this hypothesis, RNA was isolated from *tps10* mutant, BG and R108 plants, treated with either *A. euteiches* or mock for 2 h. The cDNA was synthesized from the potential anti-sense transcript, close to *Tnt1* insertion using a gene-specific primer, cDNA-*Tnt1*. A small region of 153 bp was amplified from the synthesized cDNA using forward and reverse primers. As control reactions, cDNA was synthesized without reverse transcriptase and with random primers. The PCR showed faint bands in the case of cDNA synthesized from cDNA-*Tnt1*, negative reverse transcriptase and water control, whereas, cDNA synthesized with the random primer showed stronger bands in the *A. euteiches* treated samples (Fig.II.28). It should be noted that a prominent band was also visible in case of *tps10* mutant infected with *A. euteiches*. This can be explained as transcription might have taken place from the exons upstream of *Tnt1*, but this transcription is not translated into protein, as sesquiterpenes were found missing in *tps10* mutant, compared to BG.
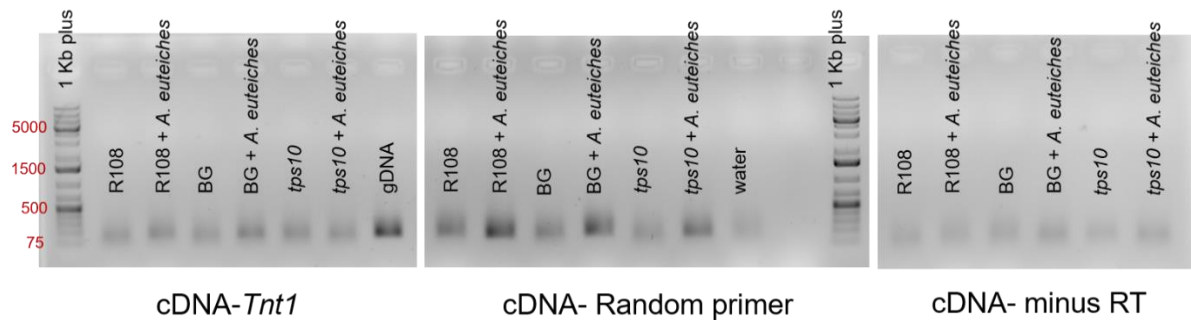
Fig.II.28 Analysis of NAT mediated silencing: cDNA was synthesized from *tps10*, BG and R108 plants using cDNA-Tnt1 primer, random primer and without reverse transcriptase. PCR with cDNA-*Tnt1* samples showed only weak and faint bands, whereas stronger bands were observed in cDNA synthesized using random primer and basal bands in negative reverse transcriptase. As positive and negative control, genomic DNA and water were used. The ladder size (in bp) are shown in red.

II.2.2.11 amiRNA targeting silencing of *TPS10*

An artificial miRNA (amiRNA) approach was used to downregulate the *TPS10* transcripts. For the construction of amiRNA construct, an endogenous *M. truncatula* miRNA backbone, miR159b (kindly provided by Prof. Dr. Franziska Krajinski-Barth, University of Leipzig) was used. Cloning of *TPS10* sense and antisense primers were performed according to Devers et al. (2013) and the sequence targeting *TPS10* were obtained from WMD3 web designer with a setting of 1 target and 0 accepted off targets. The endogenous sense and antisense sequences of miR159b were replaced using overlapping PCR, according to Devers et al. (2013). Briefly, PCRs were performed using the following combination of primers: primer I and primer A (Product A), primer II and primer II (Product B), primer B and primer V (Product C). The resulting products from these three PCRs were used as the final template and a PCR was performed using Primer A and Primer B (Fig.II.29). The final PCR product was A-tailed and ligated into pCR-TOPO 2.1 vector and transformed in *E. coli* cells. The positive bacterial colonies were confirmed by colony PCR, restriction digestion and sequencing. The modified miRNA backbone targeting *TPS10* and the plant entry vector (p9RFP_UBQ3 Expr; kindly provided by Prof. Dr. Franziska Krajinski-Barth, University of Leipzig) were restriction digested by *MluI* and *SpeI* and ligated using T4 DNA ligase (Fig.II.30). The ligated product was transformed in *E. coli* and the positive clones were identified using colony PCR and sequencing. As the entry vector did not have any visual selection marker for the identification of positive clones, a large number of colonies had to be screened and a number of ligation trials were repeated.
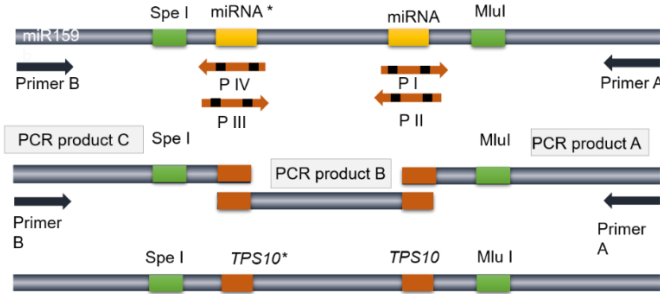
Fig.II.29: Schematic of overlapping PCR (modified after Warthmann et al., 2008): *M. truncatula* miRNA backbone-miR159 was used as the template for overlapping PCR, according to Devers et al. (2013).
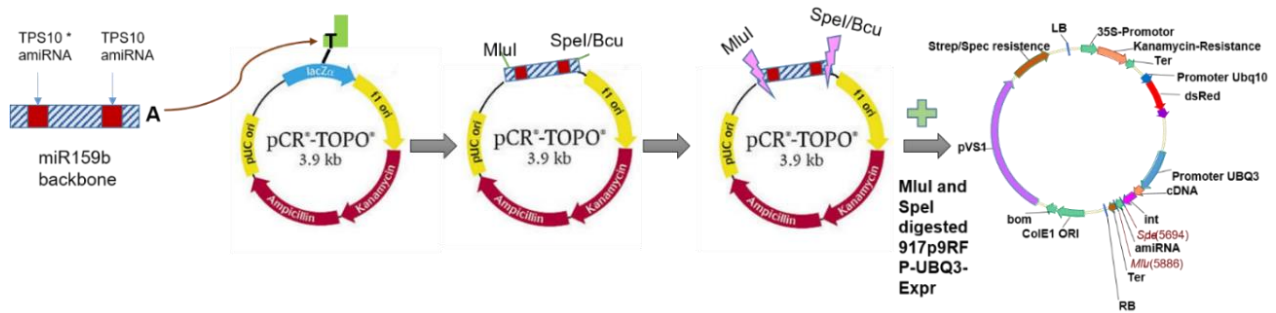
Fig.II.30: Schematic for ligation of A-tailed PCR product and pCR2.1 TOPO and subsequent cloning into plant compatible vector

After many trials of colony selection, the final plasmid containing the desired amiRNA precursor molecule was confirmed via restriction digestion and sequencing. The final construct and the empty vector were transformed in roots of cultivar R108 via root transformation. As *TPS10* is an early pathogen-responsive gene and due to the transient transformation approach, many time points after *A. euteiches* infection were tested. After few trials, one week of *A. euteiches* infection was considered a good time point, as the effect of *TPS10* knockdown on plant's susceptibility to *A. euteiches* was observed. The transformed plants were infected with *A. euteiches* and after one-week *A. euteiches* marker gene and *TPS10* transcript levels were quantified using qPCR (Fig.II.31). The final experiment resulted in four empty vector plants and four knock-down plants, denoted by ami-*tps10*. The qPCR quantification data showed that the empty vector plants had variable expression of *TPS10* but on an average higher expression and these plants harbored less *A. euteiches* biomass, compared to *ami-tps10* plants. In contrast, the four ami-*tps10* plants showed a lower *TPS10*

expression and harbored higher *A. euteiches* biomass. This suggests that our hypothesis 'knockdown of *TPS10* leads to *A. euteiches* susceptible plants' holds true.
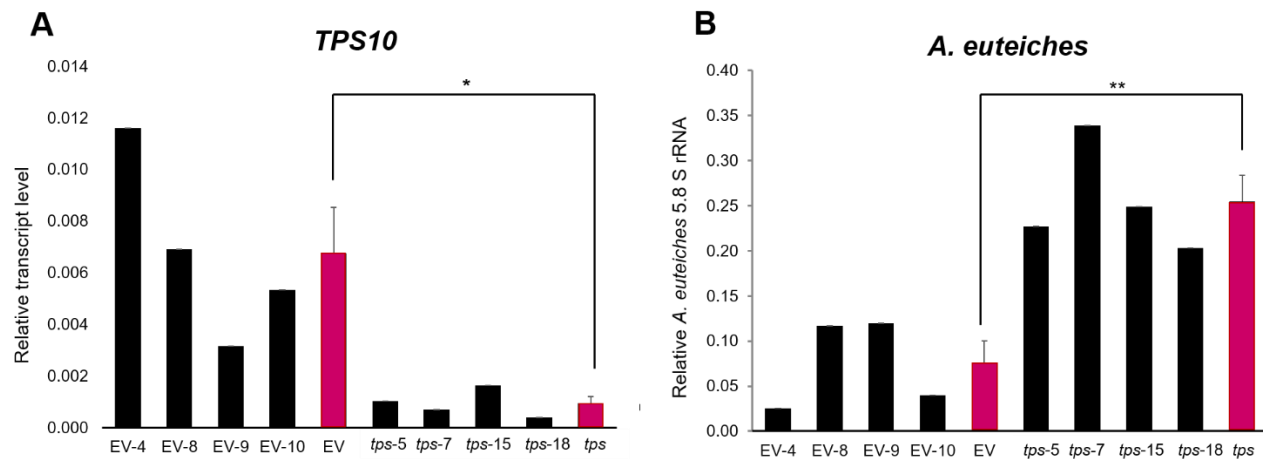
Fig.II.31: qPCR quantification of *TPS10* and *A. euteiches 5.8s rRNA* expression level: The expression level of (A) *TPS10* and (B) *A. euteiches 5.8s rRNA* was quantified in four empty vector (EV) and in ami-*tps10* plants each; transcript levels were normalized against *Actin2*. Pink bar represents mean of the four plants, and the statistical test was done using one-factorial ANOVA followed by Tukey HSD test. *= $p \leq 0.05$, ** = $p \leq 0.01$, significance was tested between average EV and ami-*tps10* plants.

To investigate whether the knock-down of *TPS10* could be correlated to the expression level of the mature miRNA, a stem-loop RT-PCR was also performed for the detection and amplification of mature miRNA. The stem-loop RT-PCR technique developed by Chen et al. (2005), involves two steps: reverse transcription and real-time PCR. A stem-loop reverse primer (SLP) (sequence kindly provided by Dr. Emmanuel Devers, ETH, Zurich) was selected such that it forms a hair-pin and 5-8 nucleotide at the 3' end were made complementary to the mature miRNA molecule. The stem-loop reverse primer hybridizes to the miRNA and is reverse transcribed to cDNA. For a normal PCR, the product length should be bigger than the sum of forward and reverse primers and as the mature miRNA is only ~21 nucleotide in length, the SLP not only helps elongate the miRNA length but also due to the presence of hairpin-loop can reverse transcribe the miRNA. After the reverse transcription, the products were quantified using a forward primer that comprises of 12-15 nucleotide of the mature miRNA and a universal reverse primer that binds to the hair-pin loop of SLP (Fig.II.32). The mature miRNA was successfully quantified using stem-loop RT-PCR (Fig.II.33). Although, the expression level of mature miRNA could not be perfectly co-related with the downregulation

of *TPS10* transcript. For instance, *tps10*-7 and *tps10*-18 have a similar expression of mature miRNA, but the *TPS10* knock-down is more efficient in the *tps10*-18 plant compared to *tps10*-7. However, these two lines showed the lowest *TPS10* expression compared to other lines. Overall, this variation can again be attributed to the transient root transformation system and more conclusive results could be drawn using stable hairy root cultures.

```
Fwd primer GACGGCCTTGATAGGTGAATGT

   GACGGCC        TTGATAGGTGAATGT                      GGTC

                  |||||||||||||||                   G      C

   miRNA159b    5'- TTGATAGGTGAATGTACGCTT  GTCGTATCCAGTGCA      G

                          ||||| |||||||||||||||        A

   Stem-loop RT primer      3'  GCGAA CAGCATAGGTCACG        G

                                                    C      G

                                                       TTAT
```

Fig.II.32: Pictorial representation of stem-loop primer consisting of 5 bp complementarity to the mature miRNA and the forward primer used for the miRNA amplification also have complementarity with mature miRNA. The universal reverse primer (not shown) have complementarity to the stem-loop primer.
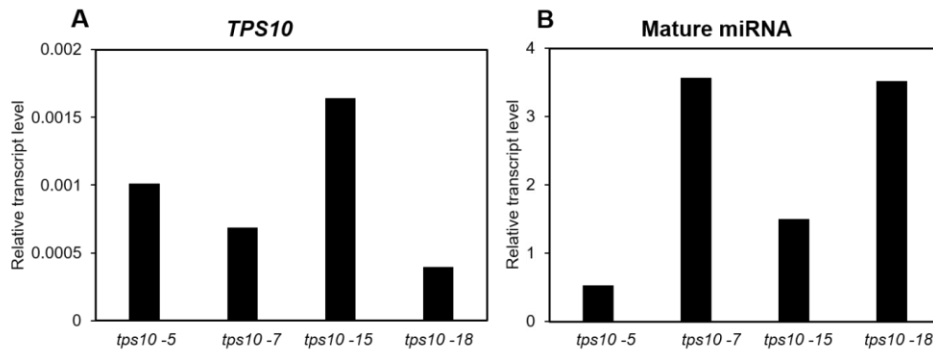
Fig.II.33: Quantification of *TPS10* transcript and mature miRNA targeting *TPS10* in ami-*tps10* plants: ami-*tps10* plants infected with *A. euteiches* for 1 week were used for the quantification of (A) *TPS10* transcript and (B) mature miRNA, the transcripts of *TPS10* and the mature miRNA were normalized against *Actin2* and the housekeeping miRNA *U6*, respectively.

II.2.2.12 Bioassay

The results described above proved that the knock-down of *TPS10* leads to highly *A. euteiches* susceptible plants, the next quest is whether TPS10 products, produced in yeast

might have some direct inhibitory effect on *A. euteiches* growth. For this, *A. euteiches* growth inhibition assays were investigated in terms of two parameters, mycelial growth, and the zoospore germination.

For mycelial inhibition assay, different concentrations of TPS10 products were added to the edge of CMA plates containing *A. euteiches* mycelial pieces. In control plates, yeast extract of empty vector and pure solvent (pentane) were added. When the mycelium was fully grown in the control plates, the plates were photographed and the mycelial area was measured using Fiji software. The data showed that at a concentration of ~ 3000 nmol and 2000 nmol, the mycelial growth was significantly inhibited near and around the product application (Fig.II.34), while with lower amounts of products, no effects were observed. The empty vector extract and the solvent only plate showed full mycelium growth.
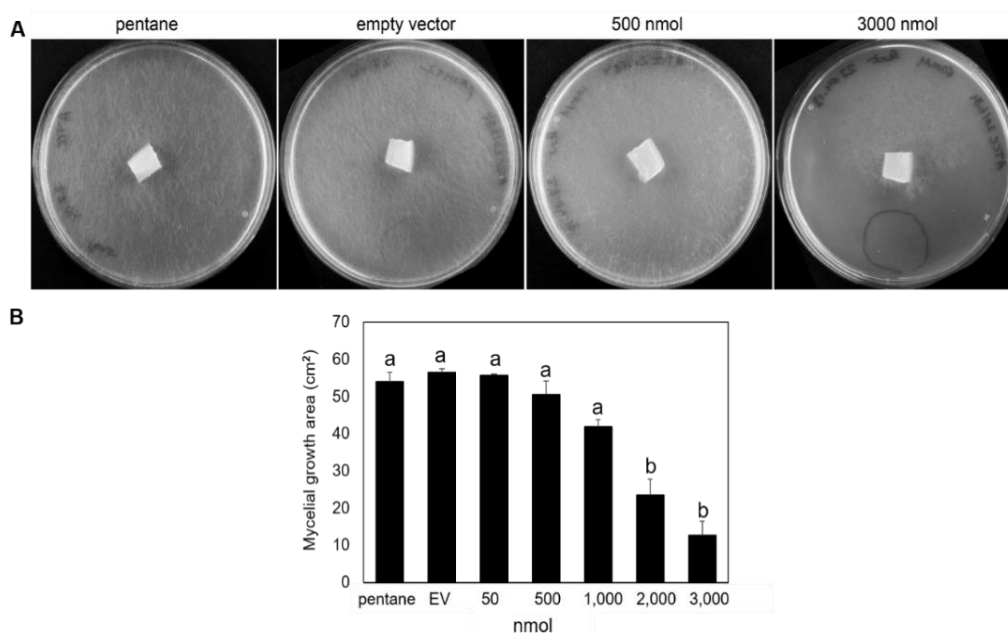
Fig.II.34. Mycelium growth inhibition assay: (A) The yeast extracted TPS10 products were applied to the CMA plates containing *A. euteiches* mycelial agar piece. The concentration of ~ 3000 nmol showed growth inhibition compared to empty vector extract and solvent only. (B) Histogram depicting various concentrations used and their effect on mycelial growth. The data shown are mean of three or more replicates, statistical significance was tested between all treatments; one-factorial ANOVA, Tukey HSD test, *= $p \leq 0.05$, $n \geq 3$.

For zoospore germination assay, TPS10 products from yeast were diluted with swamp water to various concentrations. The diluted yeast extract from empty vector control and zoospores diluted only with the swamp water (0 μM) were used as controls.100 μl (around 7000

zoospores) of *A. euteiches* zoospore solution was mixed with the diluted TPS10 products in a 1:1 ratio and incubated for 1 hour in dark at room temperature. After the incubation period, 100 µl was plated onto CMA plates and the zoospore germination was checked microscopically after 24 h. In empty vector extract and swamp water dilution, a good rate of zoospore germination was observed, whereas, zoospores incubated with TPS10 products were affected to varying degree depending on the product concentration. At a concentration of 250 µM, few zoospores germinated, whereas, at a concentration of 500 µM, none of the zoospores germinated (Fig.II.35). This shows that TPS10 products inhibit *A. euteiches* mycelium growth and zoospores germination at the µmolar range, with this data it is to conclude that TPS10 products are involved in the direct defense of *M. truncatula* root infection by *A. euteiches*.
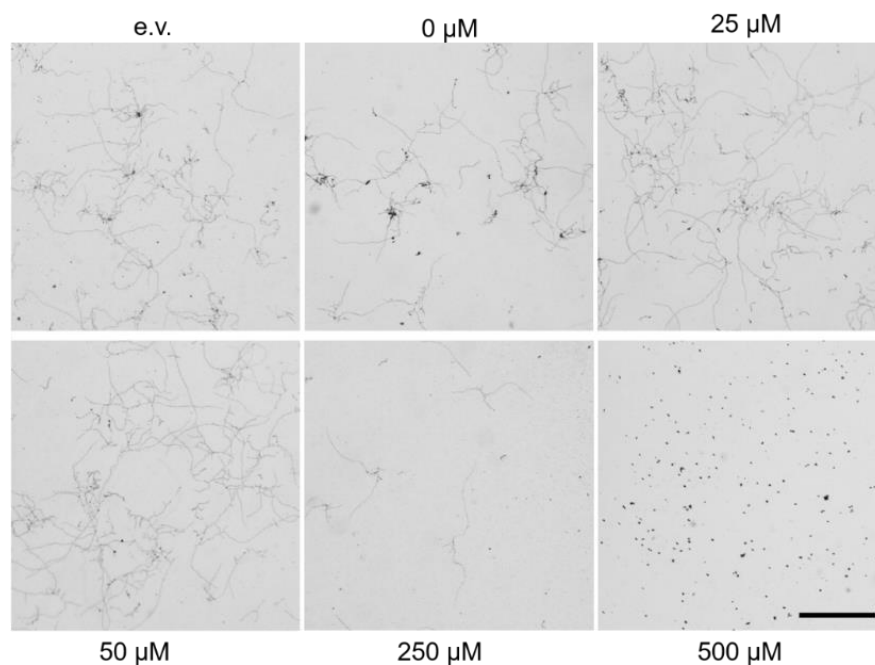
Fig.II.35: Zoospore germination assay: The zoospore germination assay was tested with various TPS10 product concentrations together with empty vector control extracts and swamp water diluted zoospores. The data shown here are from one out of three replicates. Bar represents 1 mm.

III. Discussion

Plants have been dealing with both pathogenic and beneficial organisms, since their first arrival on land. On one hand, plants form symbiotic associations with many beneficial organisms, such as mycorrhizal fungi, rhizobia, and plant growth-promoting bacteria. On the other hand, plants have developed defense mechanisms to ward off the potential pathogens and eventually protect themselves from harmful organisms. This study focused on the early pathogen-specific responses of the host plant. The early interaction periods are defined as the time point before a pathogen completes the invasion of a host plant, usually within 24 hours after pathogen and plant contact (Shen et al., 2017). Many previous studies have investigated the host plant response to microbes at late time points, ranging from 24 hours to several weeks (Giovannetti et al., 2015; Badis et al., 2015). However, this study was aimed to identify very early time points, even before the microbe penetrates the root. Transcriptome profiling analyses were performed from the roots of six-day-old seedlings and six-week-old adult plants treated and non-treated for two hours with *A. euteiches* zoospores.

III.1 Comparative transcriptomic approach between seedling and adult plants

A comparative approach was applied to the transcriptomic datasets of seedlings and adult plants. The comparison revealed a higher number of differentially regulated genes in seedling roots compared to roots of adult plants (Fig.II.1). The high number of induced genes in seedlings can be attributed to various reasons: (i) the development stage of the plant, since it has been demonstrated that the growth stage of the plant affects interaction with the microbial community (Smalla et al., 2001; Berg and Smalla, 2008); (ii) in seedling stage, *A. euteiches* zoospores were applied directly to a single root on the plate and the zoospore contact to host root was prominent, whereas, in adult plants, the zoospores suspension was applied to a fully developed root system growing in an aeroponic system. It might be that fewer zoospores per root were applied to adult plants compared to the seedlings. Moreover, in nature, young seedlings are more prone to *A. euteiches* infection, which might explain their strong response to the zoospores at an early time point (Hughes et al., 2013). In addition, seedlings might be in a more decisive mode of growth or defense.

The overlapping genes between seedling and adult stage were studied in more detail, as these might hint towards early root responses that are independent on the plant development stage. Among the overlapping genes, the class of terpene synthases was quite interesting, as no terpene synthases have been characterized against *A. euteiches* infection so far. However, previous studies have also shown upregulation of secondary metabolism class after 1 day

and 6-day *A. euteiches* infection (Badis et al., 2015; Djébali et al., 2009, 2011). Djébali et al. (2009, 2011) demonstrated that the synthesis of lignin via phenylpropanoid pathway plays a major role in *A. euteiches* resistance in A17, whereas Badis et al. (2015) showed the upregulation of flavonoid pathway genes in partial resistant line and also an accumulation of flavonoids in the resistant line. Badis et al. (2015) further illustrated the antimicrobial action of 2'-O-methylisoliquiritigenin (a flavonoid metabolite) against *A. euteiches* zoospore germination. It is to be noted, that phenylpropanoid and flavonoid pathways were upregulated at late *A. euteiches* infection stages of 1 and 6 days, where mycelium penetrates the rhizodermis and central cylinder, whereas, this study identified terpene synthases after early *A. euteiches* contact. It can be speculated that terpene products might be employed by plants in early stages, whereas, compounds derived from flavonoid and phenylpropanoid pathway are involved in the late stages of *A. euteiches* infection. The common regulated terpene synthase class contained two terpene synthase genes: *MtTPS6* and *MtTPS10*. *In silico* analysis of *MtTPS6* (Fig.II.3) revealed that this is a root-specific and *A. euteiches* responsive gene. It is speculated that *MtTPS10* and *MtTPS6* might be working in a synergistic manner against *A. euteiches* infection. Although, this speculation needs to be further tested, starting with the characterization of *MtTPS6* in *A. euteiches* treated plants.

Another interesting gene identified from the adult plants transcriptomics was a *WRKY1b* transcription factor that was upregulated after *A. euteiches* treatment. In general, WRKY transcription factors are known to be involved in the regulation of many plant physiological processes, abiotic stresses and biosynthesis of secondary metabolites (Zhang et al., 2018; Xu et al., 2004; Ma et al., 2009). Many studies have shown that biosynthesis of secondary metabolites can be controlled by WRKY transcription factors. For instance, Xu et al. (2004) showed that *Gossypium arboreum* WRKY1 (*GaWRKY1*) positively regulates the sesquiterpene synthase (δ-cadinene synthase), which is involved in the biosynthesis of sesquiterpene phytoalexins. *Artemisia annua* WRKY1 (*AaWRKY1*) had been shown to regulate the Amorpha-4,11-diene synthase, which is involved in the biosynthesis of artemisinin (Ma et al., 2009). WRKY family members contain a conserved DNA-binding region, the WRKY domain, which comprises of highly conserved WRKYGQK peptide sequence and a zinc finger motif ($CX_{4-7}CX_{22-23}HXH/C$) (Pandey and Somssich, 2009). The WRKY domain recognizes and binds to the W-box (C/TTGACT/C) present in the promoter of the defense-related genes and induce their expression (Pandey and Somssich, 2009; Chen and Chen, 2002; Yu et al., 2001; Phukan et al., 2016). *In silico* analysis of *MtTPS10* 2 kb

promoter region revealed three W-box binding sites (Appendix, Fig.VII.2.3). Additionally, the protein sequence alignment of MtWRKY1b with already published WRKYs like, AtWRKY18 of *A. thaliana* (Chen and Chen, 2002), PcWRKY4 of *Petroselinum crispum* (Cormack et al., 2002), Wizz of *N. tabacum* (Hara et al. 2000) and AaWRKY1 of *Artemisia annua* (Ma et al., 2009) was performed (Appendix, Fig.VII.2.1). The MtWRKY1b did not share much similarity to any of the WRKYs tested, which can be attributed to different evolution of these plant species. Despite the low similarity, the WRKY motif was conserved in all the tested plant species (WRKYGQK). The expression data of *MtWRKY1b* was also analyzed using MtGEA web database and Medicago eFP browser. The outcome of expression data analysis was very similar to that of *MtTPS6*. *MtWRKY1b* was induced after 1 day of *A. euteiches* treatment, but the induction was not enormous as this of *MtTPS6* (Fig.II.2). The predicted lower expression of *MtWRKY1b* (from MtGEA webpage), in comparison to *MtTPS6* can be attributed to the late infection time point of 1 day. As a transcription factor that might be involved in the regulation of *MtTPS10*, MtWRKY1b should be induced at an early time point after pathogenic contact, like 2 h time point used for this study, or even earlier. Additionally, the root specific expression (predicted by eFP browser) of *MtWRKY1b* also supports the idea of *MtWRKY1b* regulating *MtTPS10* activation.

However, for the characterization of these genes, qPCR validation will be an important step. To better understand the role of *MtWRKY1b* and *MtTPS6* in *A. euteiches* infection, a time course experiment ranging from 0 min to 1-2 weeks after *A. euteiches* treatment might give a deeper insight. Further expression of MtTPS6 products in yeast and testing these products on *A. euteiches* growth will provide valuable information to the existing *M. truncatula- A. euteiches* plant pathosystem. Additionally, the binding of MtWRKY1b transcription factor to *MtTPS10* promoter could be tested via yeast one-hybrid assay or a transactivation assay. This would prove the regulatory role of MtWRKY1b. Furthermore, the effect of gene knock-down of *MtTPS6*, *MtWRKY1b* could also be studied using *Tnt1* insertion lines from the Noble Foundation as well independent knock-down approach, such as amiRNA or CRISPR-Cas9.

III.2 *MtTPS10* is a root specific early oomycete responsive gene

M. truncatula genome has 23 terpene synthase members, four of them have been functionally characterized. Three of them - *MtTPS1*, *MtTPS3,* and *MtTPS5* - belong to the sesquiterpene-producing family (Arimura et al., 2008), whereas *MtTPS4* belongs to monoterpene producing family (Parker et al., 2014). These four TPS enzymes were characterized either after wounding or herbivore attack (Gomez et al., 2005), depicting their direct role in the

biosynthesis of defense-terpenes against herbivores. Our transcriptomic data revealed induction of a putative sesquiterpene synthase, *MtTPS10*, after 2 hours of *A. euteiches* treatment (Fig.II.1 and II.2). Interestingly, the four *TPS* genes characterized in *M. truncatula* were also induced after early contact with the herbivore, ranging from 30 minutes to 24 hours, similar to *MtTPS10* induction. *MtTPS10* is one among the 19 TPS members that have not been characterized yet. *TPS10* transcripts were induced after early contact with *A. euteiches* (Fig.II.6) and the transcript accumulation decreased at the late time points, whereas no induction was observed in the mock-treated plants. The rapid increase after pathogen contact and the subsequent decrease in *MtTPS10* transcript accumulation just after 6 hours suggest a tight regulation of this gene in the plant system.

The *MtTPS10* transcripts were induced exclusively after pathogenic oomycete contact (Fig.II.7). The *TPS10* transcripts levels were neither induced by contact with beneficial fungi (*R. irregularis*) nor with pathogenic fungi (*C. trifolii*), abiotic stresses such as NaCl and wounding and MeJA treatment. The sole induction of *MtTPS10* by two pathogenic oomycetes (*A. euteiches* and *P. palmivora*) can be attributed to their unique cell wall components, which might act as a trigger for *MtTPS10* induction. A detailed cell wall analysis of two major oomycete orders classifies the cell wall into three types: i) type I- devoid of N-acetylglucosamine (GlcNAc) and contains glucouronic acid and mannose, ii) type II - contains ~ 5 % GlcNAc and cross-linked residues between cellulose and 1,3–ß- glucans, iii) type III - contains > 5 % GlcNAc and 1,6–linked GlcNAc residues (Mélida et al., 2013). The cell wall of *A. euteiches* belongs to type III and that of *Phytophthora* (*P. infestans* and *P. parasitica*) to type I (Mélida et al., 2013). The *Aphanomyces* cell wall consists of 1,6-linked GlcNAc in the alkali-soluble fraction (ASF) and alkali insoluble fraction (AIF), a feature that is unusual and has never been reported from any eukaryotic microbe (Mélida et al., 2013). Additionally, the labeling experiments with fluorescein isothiocyanate (FITC) also showed an abundance of GlcNAc or chitooligosaccharide exposed on the surface of *A. euteiches* hyphae (Rey et al., 2013). However, the involvement of GlcNAc as the inducer of *MtTPS10* can be nullified as the *Phytophthora* species are not known to have GlcNAc in their cell wall.

The lack of GlcNAc in the AIF isolated from the walls of these oomycete species is counterbalanced by a higher glucose content. In particular, AIF from *P. infestans* and *P. parasitica* consisted of 99 % glucose, of which 50 % was 1,4-linked and probably arose from cellulose. Among the Saprolegniales species, AIF from only *A. euteiches* consisted of a similar proportion of cellulose (46 %). The lower cellulose content in these species is counterbalanced

by a higher proportion of glucans with 1,3- and 1,3,6-linked glucosyl residues (Fig.III.1; Mélida et al., 2013). The common glucans in *A. euteiches* and *Phytophthora* species might hint towards the cell wall component responsible for the induction of *MtTPS10*. Moreover, the branched glucan-chitosaccharide from *A. euteiches* cell wall fraction induced defense gene expression and nuclear Ca^{2+} oscillations in *M. truncatula* root epidermis (Nars et al., 2013). The GlcNAc and cell wall glucose polymers (ß-1,3;1,6-glucans or chitin), which are active sources of oligoglucosides or chitooligosaccharide, are reported to act as MAMPs in plant systems (Silipo et al., 2010; Boller and Felix, 2009).
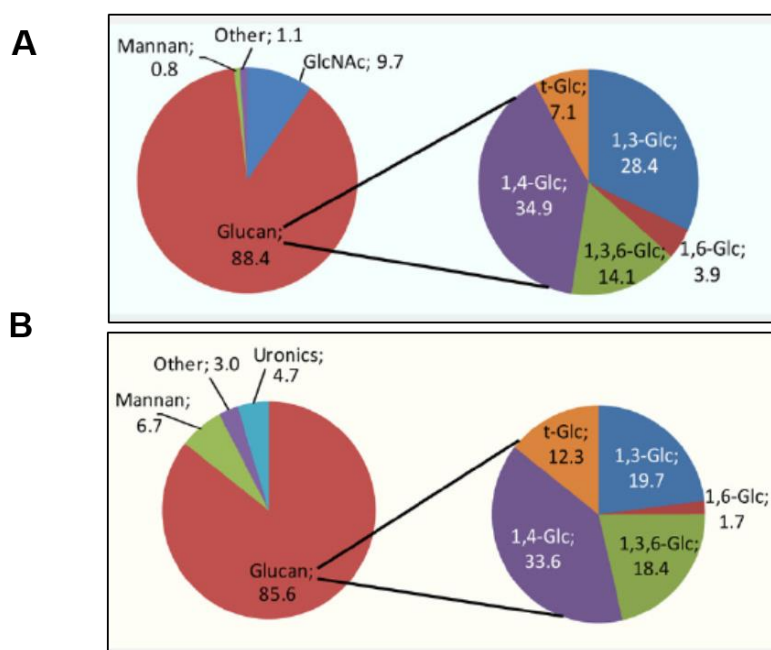
Fig.III.1 The typical carbohydrate composition of two oomycetes: (A) *Aphanomyces euteiches* and (B) *Phytophthora infestans* cell wall. (modified after Mélida et al., 2013).

It will be interesting for further studies to elucidate the cell wall component or the oomycete specific trigger that is responsible for the induction of *MtTPS10*. Many cell wall-specific PAMPs are reported in the literature, such as a well-studied PAMP from *Phytophthora sojae*, which is a heptaglucan and consists of ß-1,6 linked glucosyl residues, and actively elicits phytoalexin accumulation in soybean (Cheong and Hahn, 1991). Oomycete pathogens release the glucan PAMPs by the action of endoglucanases (Okinaka et al., 1995). For instance, *P. sojae* releases glucan elicitors by the action of its own ß-1,3-endoglucanases, as plants are not known to produce this enzyme (Waldmüller et al., 1992). A similar kind of enzyme – a ß-1,6-endoglucanase, has been reported to be produced by *A. euteiches* during the saprophytic

growth. This enzyme is hypothesized to be involved in the release of chitosaccharide elicitors during plant interaction (Nars et al., 2013).

These cell wall-specific PAMPs are recognized by plants via receptors, among them LysM-domain receptors are reported to recognize GlcNAc residues from microbes and symbionts. One such LysM receptor in *M. truncatula* is NFP (receptor for Nod factor) and the *nfp* mutants are reportedly more susceptible to *A. euteiches* infection compared to the wild type, suggesting its role in pathogenic as well as symbiotic pathway (Rey et al., 2013). To test whether an *A. euteiches* cell wall-specific component is perceived by NFP, it would be interesting to study the induction of *MtTPS10* by *A. euteiches* in *nfp* mutants.

This study identified *MtTPS10* as a root-specific gene (Fig.II.8). Until now, no terpene synthase has been characterized from roots of *M. truncatula*. This contrasts to *Arabidopsis*, in which two root specific terpene synthases have been characterized, a diterpene synthase (Vaughan et al., 2013) and a monoterpene synthase (Chen et al., 2004). In addition, one sesquiterpene synthase encoding an epi-aristolochene synthase has been characterized from *N. attenuata* roots (Bohlmann et al., 2002).

The GUS staining of roots infected for 2 h or 24 h was observed in almost all the cell layers, indicating that these lipophilic products of *TPS10* could readily diffuse and released into the environment. A basal level of staining was also observed in non-infected roots (Fig.II.9), which could be explained either by the transient root transformation system or by the strong responsive nature of the promoter. The rapid spread of GUS staining to all the cells could also function as systemic signaling in the plants. A similar pattern of GUS expression was reported in *Arabidopsis* using a transgenic line expressing *At3g2580/At3g2580:: GUS*. These tandem genes encode a root localized monoterpene synthase that produces 1,8-cineole as its principle product and the volatile nature of this compound was considered the reason for the overall staining pattern of promoter:: *GUS* fusion transformants (Chen et al., 2004).

III.3 TPS10 is a multiproduct sesquiterpene synthase

The TPS10 products were expressed heterologously in yeast, *Saccharomyces cerevisiae.* Yeast is a single cell eukaryotic organism and shares similar molecular, genetic and biochemical characteristics with higher eukaryotes, such as plants. Additionally, yeast is able to perform posttranslational modification of foreign proteins through similar mechanisms, as found in plants. The TPS10 products were extracted from the yeast culture using non-polar solvents like hexane or pentane. The products were synthesized inside the yeast cell and

some amounts were secreted into the culture medium. Large-scale product extraction from yeast cells can be a tedious and time-consuming process. Therefore, for an easier extraction process, silica tubes were added to the culture. These silica tubes adsorb products secreted into the medium, thereby to maintain equilibrium, cells secrete more products into the culture.

In yeast, TPS10 catalyzed the formation of 17 sesquiterpenes and sesquiterpene alcohols, with himachalol (identified by NMR) as the major product (Fig.II.11). Therefore, TPS10 can be regarded as a multiproduct terpene synthase. Other terpene synthases identified from *M. truncatula* catalyze the formation of a single product, such as MtTPS1 (ß-caryophyllene) and MtTPS3 ((*E*)–nerolidol and geranyllinalool with FDP and GGDP as substrate, respectively). This contrasts to the closest homolog of MtTPS10, MtTPS5, which catalyzes the formation of 15 sesquiterpenoid products. MtTPS5 forms even 27 different products with cubebol as the major product, in the presence of Mg^{2+} (Arimura et al., 2008; Garms et al., 2010). Some other examples of multiproduct terpene synthases are δ-selinene synthase and γ-humulene synthase from *Abies grandis*, which produce 34 and 52 different sesquiterpenes, respectively. This is the highest number produced by any terpene synthases until to date (Steele et al., 1998). The large skeletal terpene diversity of TPS10 could be attributed to the characteristic ability of terpene synthases to form multiple products using a single substrate (Degenhardt et al., 2009). According to Degenhardt et al. (2009), multiproduct terpene synthases (half of the characterized monoterpene and sesquiterpene synthase) are capable of producing also significant amounts of additional products (at least 10 % of the total) along with the major product. The most definitive proof of a single terpene synthase producing multiple products comes from the heterologous expression of terpene synthase genes. For example, one of the first cloned terpene synthase, (+)-sabinene synthase from *Salvia officinalis* produces 63 % sabinene, 21 % gamma terpene, 7 % terpinolene, 6.5 % limonene and 2.5 % myrcene (Wise et al., 1998). These additional products were also found from the essential oil of the plant (Wise et al., 1998). Based on the reaction mechanism and the products formed, TPS superfamilies are subdivided into two classes: class I and class II. Class I consists of a monoterpene, sesquiterpene, and diterpene synthases, whereas class II comprises of diterpene and triterpene synthases (Chen et al., 2011). A unique feature of class I terpene synthases is the stochastic nature of bond rearrangements that lead to the formation of the unusual carbocation intermediate and this is how a single TPS gives rise to multiple products (Chen et al., 2011; Steele et al., 1998; Christianson et al., 2006).

An *in silico* analyses of TPS10 protein sequence demonstrated the presence of conserved motifs (Appendix, Fig.VII.2.2), such as a highly conserved aspartate-rich region, DDxxDD, known to be involved in binding divalent metal ions which further interacts with the diphosphate moiety of the substrate (Degenhardt et al., 2009). The TPS10 also contains a second aspartate region DDIASNEFE, which is a modified version of the less conserved consensus sequence (L,V)(V,L,A)-(N,D)D(L,I,V)x(S,T)xxxE. This region is termed as NSE/DTE motif and binds the trinuclear magnesium cluster together with the DDxxDD motif. Different terpene synthases employ various ways for the generation of multiple products. For instance, the γ -humulene synthase of *A. grandis* contains two DDxxDD motifs on the opposite side of the active site cleft. This suggests that substrate binding may take place in two different conformations leading to the formation of two different sets of products (Steele et al., 1998; Degenhardt et al., 2009). The NSE/DTE motif, which replaces the second DDxxDD motif in many terpene synthases (including TPS10), can also enhance the formation of multiple products (Degenhardt et al., 2009). Additionally, the larger carbon skeleton and the presence of double bonds in FDP greatly increase the structural diversity of the sesquiterpene products formed using FDP as the substrate (Degenhardt et al., 2009).

III.4 *TPS10 Tnt-1* insertion plants are susceptible to *A. euteiches*

For the functional characterization of TPS10, a reverse genetics approach was followed using *Tnt1* insertion line. *Tnt1* is a member of the class I viral retrotransposon that moves into new locations in a genome by a 'copy and paste' mechanism (Kumar and Bennetzen, 1999). These retrotransposons use an mRNA intermediate to copy themselves and insert into new chromosomal locations after reverse transcription (Tadege et al., 2008; Wessler, 2006). The mutations generated by retrotransposons are stable, as no excision during replicative transposition is involved (Tadege et al., 2008). The *Medicago truncatula* mutant database harbors around 21,000 lines containing around 520,000 random insertions within the genome. *Tnt1* insertion in *TPS10* was identified by a BLAST search from the Noble foundation database. The line NF10408-low 18 was identified in previous work and contained a *Tnt1* insertion in the 6th intron (Fig.II.18), this insertion led to the knock-down of TPS10 at the transcript level and some of the volatile products were also found missing in the *tps10* mutant (Fig.II.19, 21). The two-hour treatment with *A. euteiches* resulted in the induction of transcript level in BG plants, compared to the mock-treated plants, whereas, basal transcript level was observed in *tps10* mutant plants (Fig II.19). However, this basal transcript level increased to some extent at the later stages of infection (Fig.II.24.A), which shows that there might be some

leaky expression from the gene at later time points. This leaky expression, however, could not rescue the susceptibility of mutant plants to *A. euteiches* (Fig.II.23, 24.A). It is known that *A. euteiches* infection leads to reduced growth and function of the roots, and at later stages could also spread to the shoots and stems (Hughes et al., 2013). Our dataset also showed that the *tps10* mutant plants are reduced in root and shoot biomass and harbored significantly enhanced amount of *A. euteiches* biomass compared to BG plants (Fig.II.23.B).

The higher susceptibility of *tps10* mutants can be attributed to the inability of the mutant to synthesize volatiles against *A. euteiches* infection (Fig.II.21). Some of the compounds from the volatile blend of BG plants were also identified from the heterologous yeast expression (Fig.II.2; peaks 1-8). Interestingly, the major product and other hydroxylated products were missing from the plant volatile blend, which might be further modified *in planta*. The lack of hydroxylated products from the plant volatile blend was previously reported by Arimura et al. (2008) and was explained by their subsequent modification *in planta*. The modification reaction such as hydroxylation, acetylation, methylation, and glycosylation plays an important role in the large variety and complexity of the plant secondary metabolites (Vogt and Jones, 2000). For the identification of the putative modifying enzyme of TPS10 products, three enzymes were validated from the transcriptomics: one UDP-glucosyltransferase, UGT (*Medtr2g098430*) and two CYP450 (*Medtr5g007550* and *Medtr8g104080*) (Fig.II.22). The UGTs are known to transfer nucleotide-diphosphate-activated sugars to low molecular weight substrates (Vogt and Jones, 2000). These additions by UGTs increase the stability and solubility of many secondary metabolites and subsequently modify their bioactivity (Lim and Bowles, 2004). Langlois-Meurinne et al. (2005) reported two UGTs from *Arabidopsis* that might play a role in defense response against *P. syringae*. In *Arabidopsis*, 27 UGTs have been shown to glycosylate a diversity of monoterpenes, sesquiterpenes and diterpenes like geraniol, linalool, terpineol and citronellol (Caputi et al., 2008). Aharoni et al. (2003) reported that the overexpression of a strawberry terpene synthase-FaNES1 in *Arabidopsis* leads to the production of a linalool derivative, owing to the presence of an endogenous *Arabidopsis* hydroxylase. CYP450s oxidize various terpenoids ultimately leading to their diversification (Keeling and Bohlmann, 2006). These haem-containing proteins cleave atmospheric oxygen reductively using NADPH or NADH while oxidizing the substrate (Schuler and Werck-Reichhart, 2003). Boachon et al. (2015) demonstrated that CYP76C1 from *Arabidopsis* is involved in linalool metabolism and production of oxidized derivatives in the flowers, which affect the behavior of flower-visiting insects. Another CYP450 from *Arabidopsis* (CYP701A3)

is reported to be involved in three step oxidations of ent-kaurene to kaurenoic acid (Helliwell et al., 1998, 1999).

The selected enzymes did not modify the TPS10 products, which can be attributed to these enzymes being highly substrate and regio/stereospecific (Boachon et al., 2015). Moreover, further mining of the transcriptomics data and co-expression analysis with *TPS10* might hint towards the potential *TPS10* modifying enzymes. Another approach could be an untargeted metabolomics with *tps10* mutant and the BG plant, with and without *A. euteiches*. Such a metabolomics approach might provide with the prospective modified TPS10 major product.

III.5 Complementation of *tps10* mutants

An attempt to rescue the susceptibility of *tps10* mutants by expressing the coding sequence of *TPS10* under the control of the native promoter (Fig.II.26) was not successful. This failed attempt could be explained by two hypothesizes:

i) Natural anti-sense transcript (NAT) mediated silencing of the *TPS10* transcript –NATs are non-protein coding fully processed mRNAs that are transcribed from the opposite strand of protein-coding sense transcripts (Werner and Swan, 2010; Beiter et al., 2009). The sense and the corresponding anti-sense transcripts share complementary exons and can form RNA-RNA hybrids which are subsequently degraded via the RNA interference pathway (Werner and Swan, 2010). It is reported that the expression of an anti-sense transcript leads to epigenetic repression of the related transcript (Zinad et al., 2017). For instance, complementary RNA hybrid formation in *Arabidopsis* triggers a strong RNAi response and formation of siRNAs from the hybrid sequence (Baulcombe, 2004). Additionally, *Tnt1* is reported to be induced during pathogen related stresses, due to the presence of a defense inducible promoter in its long terminal repeat (LTR) (Hernández-Pinzón et al., 2012; Grandbastien et al., 2005; Beguiristain et al., 2001). Similar events might be occurring in *tps10* mutants when transformed with *TPS10* coding sequence under its native promoter (Fig.III.2). Overall, it is speculated that *A. euteiches* treatment might induce the *Tnt1* retrotransposon promoter that further induces the formation of an antisense transcript from the *TPS10* gene and the *A. euteiches* inducible promoter might form a sense transcript from the transient *TPS10*. The sense and antisense being complementary can form double-stranded hybrids, which might be degraded by the RNAi pathway, eventually leading to a failed complementation attempt.
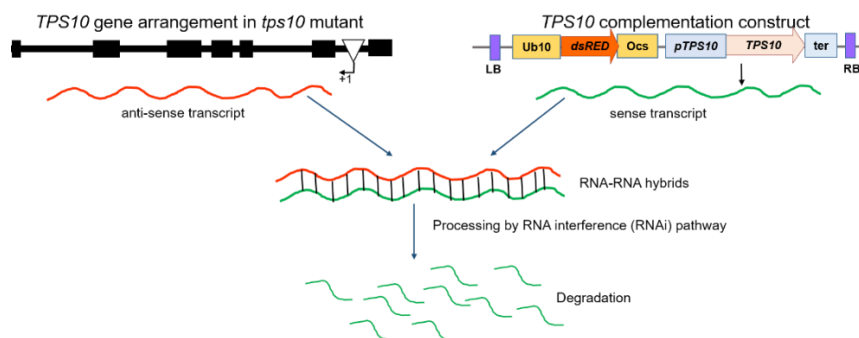
Fig.III.2 Hypothetical schematic for failed complementation approach: *A. euteiches* treatment might activate *Tnt1* promoter and *TPS10* promoter, which leads to the formation of sense and anti-sense transcript, respectively. The sense and anti-sense forms RNA-RNA hybrid, which is degraded via the RNAi pathway.

ii) Lack of regulatory elements in the coding sequence – A *Tnt1* insertion in the intron of *TPS10* sequence rendered the mutant plants susceptible to *A. euteiches*. This suggests that the regulatory *cis*-elements play an important role in proper functioning of this gene. The absence of these regulatory elements in the cloned CDS might explain the unsuccessful attempt at *tps10* mutant complementation. However, one plant showed higher accumulation of *TPS10* transcripts (Fig.II.26), but it did not influence the *A. euteiches* infection. Therefore, for future work, a 4000 base pair genomic sequence (without UTRs) of *TPS10* was cloned under the control of its native promoter. As the *tps10* mutants had a leaky expression at later infection stages, a c-myc-tag was also included in the final construct for differentiating between endogenous plant protein and transient protein levels (Fig.III.3) via Western blot technique. For further complementation approaches, this construct might give a positive outcome. Either the same construct or another construct with a *CaMV* 35S promoter driving *TPS10* genomic sequence could also be used as the overexpression cassette in the BG plants or plants of the lines R108 or A17. Such transiently transformed plants should show increased resistance to *A. euteiches* infection.

Fig III.3 Vector construct with genomic *TPS10* sequence under 2 Kb native promoter, a DsRed module for selecting the transformants and c-myc tag.

III.6 Targeted downregulation of *TPS10* via amiRNA

Both prokaryotes and eukaryotes share a common feature of establishing and maintaining basic cellular functions using various classes of small RNAs (Ossowski et al., 2008). Two

classes of small RNAs, which are widely studied are – small interfering RNAs (siRNAs) and microRNAs (miRNAs) (Schwab et al., 2006). These small RNAs are components of RNA-induced silencing complex (RISC), which uses them to recognize complementary motifs in target nucleic acid (Bartel, 2004; Filipowicz et al., 2005; Schwab et al., 2006). siRNAs and miRNAs are typically ~19-24 nucleotides in length (Schwab et al., 2006). Both these classes differ in their biosynthesis, on one hand, miRNA originates from longer, single-stranded transcripts containing imperfect foldbacks, leading to the accumulation of the only miRNA via Dicer-mediated processing (Ossowski et al., 2008), this reduces the off-target probability. On the other hand, precursors of siRNAs form perfectly complementary double-stranded (dsRNA) molecules that might originate as intermediates of viral replication or through the action of RNA dependent RNA polymerases on single-stranded plant RNAs. The diced siRNA products derived from the long complementary precursors can correspond to many portions of the precursors (Ossowski et al., 2008). This increases the probability of potential off-targets, as a large number of siRNAs diced from the silencing construct may target any gene that shares perfect or near perfect complementarity to these siRNAs (Warthmann et al., 2008). This is why an artificial miRNA (amiRNA) methodology was used in this study for targeting the transcripts of *MtTPS10* transcripts. This technique exploits the endogenous miRNA precursors for the generation of a single specific miRNA targeting the GOI. For the selection of an endogenous precursor molecule, few criteria are important, such as, the endogenous miRNA backbone must have a non-canonical loop-to-base processing, with the first cleavage step occurring in the top region of the precursor independent of the miRNA sequence (Bologna et al., 2009; Devers et al., 2013). Additionally, a physical separation of the first cleavage position and the miRNA sequence provides flexibility for the manipulation of amiRNA sequences (Bologna et al., 2009, Devers et al., 2013). Many endogenous miRNA precursor molecules have been employed for successful gene downregulation, such as MIR528 from *Oryza sativa*, which was used as precursor miRNA to silence three genes separately in rice (Warthmann et al., 2008). Another example comes from *Chlamydomonas reinhardtii*, in which cre-MIR1157 was used as a precursor to silence three different genes (Molnar et al., 2009). *A. thaliana* miR319 as the backbone has also been reported to downregulate expression of flottilin gene in *M. truncatula* roots (Haney et al., 2010). However, for this study, an endogenous *M. truncatula* miRNA backbone (mtr-miR159b) was used as the precursor for an efficient downregulation. This backbone was identified through miRNA degradome data from *M. truncatula* roots (Devers et al., 2011). The amiRNA sequences targeting *TPS10* were generated using the WMD3 web miRNA designer. The output from the WMD3 consisted of

many amiRNAs, of which the first two sequences, designated as *TPS10*-a and *TPS10*-b were selected for this study. *TPS10*-a and *TPS10*-b were selected based on their hybridization energies from the binding of miRNA to the intended target site of -39.01 and -34.42 kcal/mol, respectively. The endogenous miRNA and miRNA* (passenger strand; opposite arm of the miRNA) were replaced with amiRNA and amiRNA* using overlap PCR strategy (Fig.II.30) and after cloning into a suitable plant compatible vector, were transformed via *A. rhizogenes* mediated root transformation. The transformed plants after *A. euteiches* infection were analyzed using qPCR. The transformation trial with *TPS10*-a was not successful, as the *TPS10* transcripts were not downregulated, whereas trials with *TPS10*-b were successful and were further used for this study. The hairy root transformation is a transient approach and all the transformation events are independent of each other. This can explain the varying levels of transcript downregulation in the ami-*tps10* mutant plants (Fig.II.32.A). However, the *TPS10* transcript downregulation led to higher susceptibility of these plants, demonstrating the direct involvement of *TPS10* against *A. euteiches* (Fig.II.31.B). The empty vector plants also showed varying levels of *TPS10* transcript, but overall had lower susceptibility to *A. euteiches* (Fig.II.31.A). The knock-down experiments using amiRNA were repeated at least five times, in order to have a consistent and significant dataset. The variation due to independent transformation events could be reduced by establishing a stable hairy root cultures, where a single transformed root segment proliferates into hairy roots. With that, the variability in the knock-down should be low. Moreover, hairy root cultures can be maintained over years by sub-culturing onto a new medium.

III.7 Defensive role of TPS10 products

Higher plants are capable of coping against pests and pathogens by the production of low molecular weight secondary metabolites, having anti-microbial activity and are synthesized *de novo* after stress treatments (Ahuja et al., 2011). Such compounds are termed 'phytoalexins' and include various classes of metabolites, like isoflavonoids, terpenoids, polyacetylenes and dihydrophenanthrenes (Grisebach and Ebel, 1978). In plants, there exists another class of antimicrobial compounds, termed as 'phytoanticipins' that are low molecular weight compounds present in plants before any challenge by micro-organisms and are produced after infection solely from preexisting constituents (VanEtten et al.,1994). The phytoanticipins are sequestered as preformed compounds in vacuoles or other organelles and are released after pathogenic attack through hydrolyzing enzymatic activity (González-Lamothe et al., 2009), whereas, production of phytoalexins involves transcriptional and

translational activity, proper trafficking and secretion of these antimicrobial compounds at the site of infection (González-Lamothe et al., 2009).

This study identified TPS10 products as putative phytoalexins against *A. euteiches*, which was measured in terms of inhibition of mycelial growth and zoospore germination (Fig.II.34, 35). *A. euteiches* mycelium was inhibited up to 50 % after addition of 3 μmol. The degree of inhibition depended, however, on the position where TPS10 products were applied. This can be attributed to either the volatile nature of the products and/or the concentration gradient of the applied products. In the case of zoospore germination, 75 % of zoospores did not germinate at a concentration of 250 μM, whereas at a concentration of 500 μM, zoospore germination was completely inhibited. Here, the concentration gradient of products did not play any role, as the zoospore and products were mixed before plating. The concentration of TPS10 products were determined only in terms of the major product himachalol (Fig.II.17). It is reported that himachalol and himachalene isolated from the Himalayan cedar wood oil (Cedrus deodara) have insecticidal activity against pulse beetle (*Callosobruchus analis* F.) and the housefly (*Musca domestica* L.) (Singh and Agarwal, 1988). Many literature studies demonstrate the role of terpene natural products as toxins, growth inhibitors, and deterrents to micro-organisms and animals (Gerschenzon and Dudareva, 2007). For example, the milkweed *Asclepias curassavica* contains cardenolides in its latex canals and poisons the lepidopteran larvae, *Trichoplusia ni* by inhibiting the Na^+/K^+ - ATPases (Dussourd et al., 2000). Other commercial examples of toxic plant terpenes are artemisinin and taxol. Artemisinin is derived from the plant *Artemisia annua* and is one of the most widely used anti-malarial drug. This sesquiterpene lactone is capable of killing all asexual stages of *Plasmodium falciparum*, by inhibiting the $Ca^{2+}/ATPase$ of the sarcoendoplasmic reticulum (Jordan et al., 2004; Krishna et al., 2006). The anti-cancer drug taxol, isolated from yew trees, binds to tubulin of tumor cells, which interferes with microtubule dynamics and arrests mitosis (Jordan and Wilson, 2004). Although this study did not focus on the mode of action of TPS10 products, it will be interesting for future studies.

TPS10 produced multiple products in yeast expression system and *in planta*. This multiproduct ability can be attributed to the uniqueness of terpene synthases and is also thought of as a direct way to enhance terpene function (Gershenzon and Dudareva, 2007). Many hypotheses are postulated for the role of terpene mixtures in plant defense. As plants face challenges from a wide range of enemies, a diverse combination of terpenes may help to achieve simultaneous protection against numerous predators, parasites and competitors

and these mixtures have been reported to impede the ability of enemies to evolve resistance (Gershenzon and Dudareva, 2007; Pimentel and Bellotti, 1976). This hypothesis has, however, not been examined for terpenes, but research on transgenic *Bt* broccoli shows that the lepidopteran herbivore feeding on broccoli carrying two different *Bt* toxins developed resistance slower than the ones feeding on broccoli with only one *Bt* toxin (Zhao et al., 2003). The individual components of the terpene defense mixture can act synergistically to provide greater toxicity than the equivalent amount of a single component (Gershenzon and Dudareva, 2007). Additionally, the mixture of terpenes may be toxic to enemies for a longer period of time than single compounds, as a result of effects at the sensory level (Phillips and Croteau, 1999; Gershenzon and Dudareva, 2007). Moreover, mixtures containing compounds with different physical properties might allow longer persistence of defenses (Gershenzon and Dudareva, 2007). An example of such synergism occurs in conifer resins, which is a mixture of monoterpene olefins with anti-herbivore and anti-pathogen activity and diterpene acids having toxic and deterrent properties. When the resin ducts of conifers are attacked by herbivores or pathogens, the more volatile monoterpenes act as solvents enabling the rapid flow of the less volatile diterpenes out of the resin ducts (Phillips and Croteau, 1999; Gershenzon and Dudareva, 2007).

In addition to synergism, the components of the defense mixture may show 'contingency', meaning that the compounds are not classical synergists but might have similar biological activity (Challis et al., 2003). For example, via molecular modeling, it was shown that the sesquiterpenes isolated from *Landolphia dulcis* interact with the same macromolecular target, but in a slightly different manner (Staerk et al., 2004). For further studies, it will be interesting to examine whether TPS6 and TPS10 act in a synergistic or contingent manner, as the encoding genes of both of them were induced after early interaction of roots with *A. euteiches*.

III.8 Model with the current understanding

As a sum of results of this study, a hypothetical model can be postulated in combination with already published data (Fig.III.4). This model hypothesizes that the induction of *TPS10* after early contact with *A. euteiches* zoospores might occur due to the binding of an unknown cell wall-specific oomycete ligand to an unknown plant receptor. As the *TPS10* transcript levels were only induced after early interaction with oomycetes, the unknown plant receptor might recognize common cell wall features of the two oomycetes used. The ligand-receptor binding might further induce downstream signaling that might activate the WRKY transcription factor. The activated WRKY might then bind to the *TPS10* promoter and/or *TPS6* promoter and

eventually drive their transcription. TPS6 is annotated as a monoterpene synthase, and an interesting observation is that no monoterpenes were identified from the volatile bouquet of *tps10* mutant and BG plants, suggesting that the TPS6 products either might be non-volatile or may be metabolized further *in planta*. TPS10 products being lipophilic might either diffuse through the cells or require a transporter. For instance, *Petunia hybrida* flowers emit benzenoid and phenylpropanoid volatiles and the passage of these volatiles is dependent on an ABC transporter (*PhABCG1*) (Adebesin et al., 2017). The TPS10 products then inhibit the growth of *A. euteiches* in the rhizosphere. Further analysis of transcriptomic data might reveal other signaling components and genes influencing *A. euteiches* infection. Interestingly, a transcriptomic approach using *tps10* and BG plants might also give an insight on the genes functioning upstream of *TPS10* and genes involved in further metabolism of TPS10 major product, himachalol. This study showed that TPS10 products have an inhibitory influence on *A. euteiches* mycelium and zoospore germination, but the volatile products might also have a different function under natural conditions. Plants can communicate with neighboring species via volatile cues. Therefore, it can be hypothesized that TPS10 products might also be involved as warning signals for the neighboring plants and the neighboring plants after perceiving these products might transform them into a more effective attack against *A. euteiches*. For example, Sugimoto et al. (2014) showed that (*Z*)-3-hexenol emitted as a response of herbivore damage can be perceived by neighboring conspecific plants and subsequently converted to a glycoside. This glycoside suppresses the growth and survival rates of cutworm. The TPS10 products might also be involved in plant signaling in terms of distal or systemic signaling for activation of plant defense responses. This can be tested by analyzing the root sections at the site of *A. euteiches* inoculation and the adjacent segments or by applying split-root systems. TPS10 products might also be involved in tritrophic interactions, where the volatile products might be induced by *A. euteiches* and released to attract natural enemies of the pathogen. These hypothesis for putative functions of TPS10 needs to be further tested and proven.
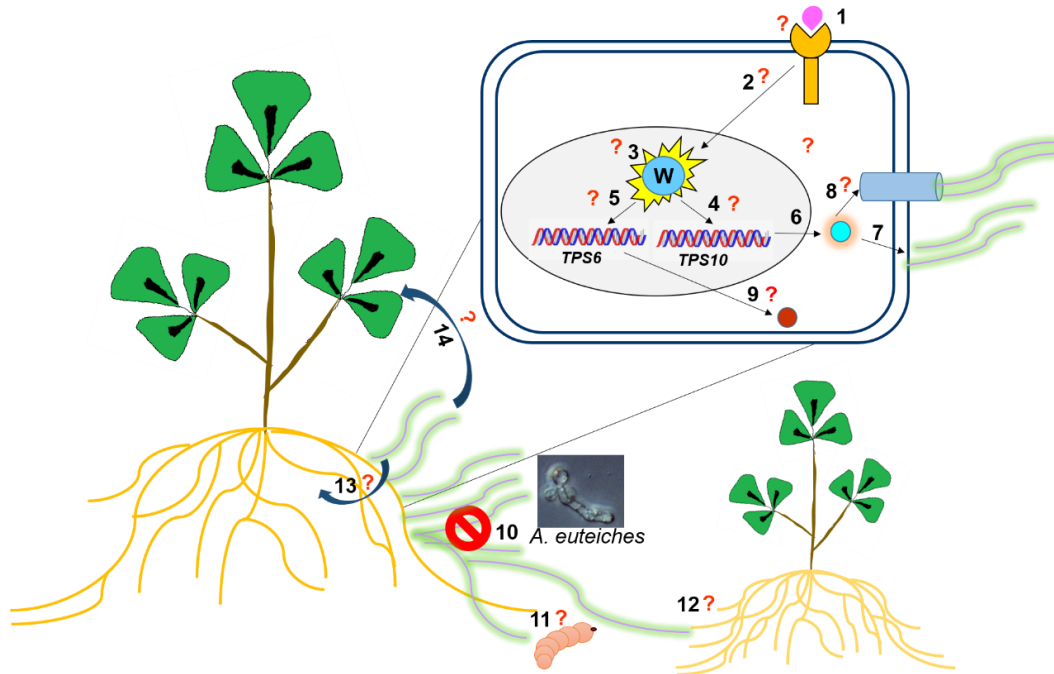
Fig.III.4. Pictorial representation of the hypothetical model: After an early encounter with *A. euteiches*, (1) the oomycete specific ligand might bind a plant receptor and (2) activates downstream PAMP signaling, (3) this further activates WRKY (W) transcription factor. (4) The activated WRKY might induce the expression of *TPS10* and/or (5) *TPS6*. (6,9) The *TPS10* and/or *TPS6* transcripts are translated in the cytosol, (7) where the enzyme catalyzes the product formation using cytosolic FDP (in case of TPS10; chloroplastic substrate for TPS6) and releases volatiles that either might diffuse out through the cell or (8) might require a transporter. (10) The released volatiles act as a defense response against the pathogen; (11) these volatiles might initiate tri-trophic interaction by attracting enemies of the attacking pathogen, (12) or might also act as warning signals for the neighboring plants. As the volatiles emitted by plants have a limited travel range, (13) they also might function as signaling molecules for local defense response or (14) distal response.

IV. Summary

Plants are sessile organisms and encounter a wide variety of microbes both above ground and below ground. Some microbial interactions can be beneficial for the plants, whereas some microbes cause diseases in plants. Plants have evolved to survive with both kinds of microbes in the natural environment. Below-ground plant-microbe interactions have recently come in the limelight, as their studies would be beneficial for agricultural purposes, especially in the present era of dramatic climate change.

This study identified a gene encoding a terpene synthase (*TPS10*) via transcriptomics from two different plant developmental stages, six-day-old seedlings and six-week-old adult plants, infected with *A. euteiches* for two hours. We characterized *TPS10* in terms of its molecular, functional and biological role against *A. euteiches*. Here, we showed that *TPS10* is an oomycete specific gene and is not induced by any of the tested beneficial or pathogenic fungi. *TPS10* has a root-specific expression after *A. euteiches* infection and encodes a sesquiterpene synthase, which catalyzes the formation of a mixture of sesquiterpenes and sesquiterpene alcohols, with the major product himachalol. This mixture of products inhibits *A. euteiches* mycelial growth and zoospore germination, both tested under laboratory conditions. Further understanding of the role of TPS10 *in planta* came from the analysis of *Tnt1* mutants and amiRNA targeting *TPS10*. The volatile bouquet collected from *Tnt1* mutants and wild-type plants demonstrated that *tps10-Tnt1* plants do not emit sesquiterpenes after infection with *A. euteiches*, which makes these plants more susceptible to the pathogen. Additionally, himachalol was absent from the volatile blend collected from *A. euteiches* treated BG plants, which might be further modified *in planta.* The amiRNA approach yielded similar results, plants with knock-down *TPS10* showed higher susceptibility to *A. euteiches*, compared to the empty vector transformed plants. With the identification and characterization of *MtTPS10*, we added valuable information to the current *Medicago-Aphanomyces* plant-pathosystem studies.

V. Materials and methods

V.1 Chemicals and supplies

Chemicals were obtained from companies like Merck, Sigma Aldrich, Carl Roth, and Roche. Enzymes and kits were obtained from companies like Macherey Nagel, Thermo Scientific, New Englands Biolabs, Promega, Fermentas, Bio&Sell, Qiagen, and Invitrogen. Positive bacterial clones were selected using the following antibiotics:

Tab.V.1: Used Antibiotics

Antibiotic	Stock Concentration	Final Concentration
Carbenicillin	50 mg/ml	50 µg/ml
Kanamycin	50 mg/ml	50 µg/ml
Streptomycin	50 mg/ml	50 µg/ml
Spectinomycin	100 mg/ml	100 µg/ml
Acetosyringone	100mM	1mM/ml
X-Gal	50 mg/ml (in DMSO)	50 µg/ml

V.2 Organisms

Organisms were grown using suitable media at appropriate growth conditions, followed by transformation procedures wherever applicable.

V.2.1 *Escherichia coli* (*E. coli*)

For cloning purposes and plasmid multiplication, *E. coli* (DH10B, Invitrogen) was used.

Genotype: F– endA1 deoR+ recA1 galE15 galK16 nupG rpsL Δ(lac)X74 φ80lacZΔM15 araD139 Δ(ara,leu)7697 mcrA Δ(mrr-hsdRMS-mcrBC) StrR λ–

V.2.1.1 Growth media and conditions

E. coli were cultured either in Luria Bertani (LB, Tab.V.3) agar or LB broth medium at 37 °C for a duration of 16 h. When grown in liquid medium, culture tubes were maintained at 37 °C with continuous shaking at 200 rpm.

V.2.1.2 Preparation of chemically competent *E. coli* cells

Competent *E. coli* cells were prepared using chemicals (Tab.V.2).

A frozen aliquot of *E. coli* cells was streaked on an LB plate without antibiotic and grown for 16 h at 37 °C. Then a single colony was used for inoculating 4 ml LB medium and grown overnight at 37 °C with shaking. 2 ml culture was then used for inoculating fresh 200 ml LB medium and shaken for 3-4 h until an OD_{600} of 0.6 was reached. The culture was ice-cooled for 10 min and divided into four parts for centrifugation. All centrifugation steps were performed at 4 °C and 3220 g for 10 min. After the first round of centrifugation, each aliquot of pelleted cells was re-suspended in 20 ml cold transformation buffer 1 (TFB 1, Tab.V.2), followed by a centrifugation step. The resulted pelleted cells were further re-suspended in 2 ml cold TFB 2 (Tab.V.2) and 50 µl cells were aliquoted in 1.5 ml Eppendorf tubes. The cells were shock frozen in liquid nitrogen before further storage at -80 °C.

Tab.V.2: Components of TFB 1 and TFB 2

Transformation buffer 1		Transformation buffer 2	
Substances	Amount for 500 ml	Substances	Amount for 500 ml
30 mM CH₃COOK	1.475 g	100 mM MOPS	2.095 g
10 mM CaCl₂	0.735 g	75 mM CaCl₂	1.1 g
50 mM MnCl₂	4.95 g	10 mM RbCl	0.12 g
100 mM RbCl	6.05 g	15 % Glycerol	75 ml
15 % Glycerol	75 ml		
pH adjusted to 5.8 (with 1 M acetic acid), filter sterilized and stored at 4 °C.		pH adjusted to 6.5 (with 1 M KOH), filter sterilized and stored at 4 °C.	

V.2.1.3 Transformation of *E. coli*

The prepared chemically competent cells were used for transformation of DNA fragments and plasmids. An aliquot of chemically competent cells was thawed on ice for 2-3 min and 100-200 ng of plasmid DNA or 15 µl ligation mix was added to the cells and incubated for 30 min on the ice. The cells were then heat shocked for 90 s at 42 °C and then cooled on ice for 2 min. The cells were revived for 1 h in SOC (Super Optimal Broth with Catabolite Repression-Tab.V.3) medium and incubated at 37 °C with continuous shaking at 350 rpm. After revival, they were plated on LB agar plates containing suitable antibiotics and X-Gal (5-Bromo-4-Chloro-3-Indolyl β-D-Galactopyranoside) for blue-white selection of constructs containing

LacZ marker gene. Positive colonies were tested using colony PCR and restriction digestion of isolated plasmid DNA. The glycerol stock of positives colonies were prepared by mixing 300 µl of 50 % sterile glycerol and 700 µl of overnight grown *E. coli* culture, snap frozen in liquid nitrogen and stored at -80 °C.

Tab.V.3: Components of bacterial growth medium

Luria bertani (LB) medium		SOC medium	
Substances	Amount	Substances	Amount for 1 L
Tryptone	1 % (w/v)	Tryptone	20 g
Yeast extract	0.5 % (w/v)	Yeast extract	5 g
NaCl	0.5 % (w/v)	NaCl	0.5 g
Agar*	1.5 % (w/v)	ddH$_2$O	1 L
ddH2O up to a desired volume		pH adjusted to 7.0, 100 ml aliquots were autoclaved and 1.8 ml sterile glucose and 0.5 ml sterile MgCl$_2$ per 100 ml were added.	

V.2.2 *Agrobacterium rhizogenes* (*A. rhizogenes*)

A. rhizogenes strain, ARqua1 (Quandt et al., 1993) was used for the generation of hairy roots.

Genotype: Onc[+], Streptomycin[+], biotype II (Keane et al., 1970).

Transgenic hairy roots induced by this bacterium resembles wild-type roots in morphology, therefore, can be subsequently used for root architectural and root microbe interaction studies.

V.2.2.1 Growth media and conditions

A. rhizogenes cells were cultured in LB medium with suitable antibiotics and grown at 28 °C for 48 h. For root transformation of *M. truncatula*, the bacteria was grown on yeast-tryptone medium (Tab.V.4) with 2 mM CaCl$_2$.

Tab.V.4: Components of yeast tryptone media

Substances	Amount
Tryptone	0.5 % (w/v)
Yeast extract	0.3 % (w/v)
Microagar*	1.5 % (w/v)
ddH$_2$O	Up to the desired volume

pH adjusted to 7.0, autoclaved and 2 mM CaCl$_2$ was added. * - was added for solid medium.

V.2.2.2 Preparation of electro-competent *A. rhizogenes* cells.

A glycerol stock of ARqua1 electro-competent cells was streaked on LB agar without antibiotic and grown for 48 h at 28 °C. A single colony was then used for inoculating 4 ml LB medium and grown overnight at 28 °C with continuous shaking at 250 rpm. 2 ml culture was then used for inoculating 200 ml LB medium and shaken at 28 °C for 3-4 h until an OD$_{600}$ of 0.6 was reached. The culture was then ice-cooled for 10 min, divided into four parts and centrifuged for 10 min at 3220 g, 4 °C. The pelleted cells were washed and re-suspended in 40 ml ice-cold sterile ddH$_2$O on the ice, followed by centrifugation and washed again with 20 ml sterile ddH$_2$O. The cells were then re-suspended in 10 ml ice-cold 10 % glycerol followed by centrifugation. The cells were again re-suspended in 1 ml ice-cold 10 % glycerol and aliquots of 50 µl were made, shock frozen and stored at - 80 °C.

V.2.2.3 Transformation of *A. rhizogenes*

A. rhizogenes competent cells were transformed using electroporation. An aliquot of electro-competent cells was thawed on ice for few mins and 200-500 ng of plasmid DNA was added to the thawed cells. The resulting mixture was then added to a pre-chilled cuvette (VWR cuvette with 2 mm gap) and inserted into the cuvette arm of electroporator (Micropulser Electroporator, BioRad Laboratories GmbH, Munich, Germany). A pulse of 2.2 kV for approximately 5 ms was applied to cells, 1 ml LB was then added for the revival and shaken in 2 ml Eppendorf tubes at 28 °C for 2-4 h. After revival in LB, cells were plated on LB agar with appropriate antibiotics and grown for 48 h at 28 °C. Glycerol stock was made from positive colonies in the same way as for *E. coli*.

V.2.3 *Saccharomyces cerevisiae* (*S. cerevisiae*)

For heterologous expression of plant proteins, *S. cerevisiae* was used as host organism.

V.2.3.1 Strains

INV*Sc1*: is a fast-growing diploid strain for expression. This strain was used for product identification of MtTPS10.

Genotype: *MATa his3D1 leu2 trp1-289 ura3-52 MA*T *his3D1 leu2 trp1-289 ura3-52*

OB-AB001: is a strain kindly provided by OrganoBalance GmbH, Berlin. This strain was used for large scale production of MtTPS10 products.

Genotype: *MATα his3-11,15 leu2-3,112 ura3-52 MAL3 SUC2 GAL tHMH his⁻leu⁻ura⁻*

V.2.3.2 Growth media and conditions

S. cerevisiae was cultured in YPD medium and grown at 30 °C with shaking at 250 rpm. The transformed yeast cells were selected by plating on Synthetic Drop-Out medium (Tab.V.5).

Tab.V.5: Components of yeast growth medium

Synthetic Drop-out medium		YPD medium	
Substances	Amount for 1 L	Substances	Amount for 1 L
Synthetic Drop-Out medium Supplements without Uracil	0.8-1 g	Tryptone	20 g
Yeast Nitrogen Base without aminoacids	6.7 g	Yeast Extract	10 g
Microagar*	20 g	Microagar*	20 g
ddH$_2$O	920 ml	ddH$_2$O	920 ml
Autoclaved for 15 min and 2 % (v/v) filter sterilized glucose was added. * - was added for solid medium.		Autoclaved for 15 min and 2 % (v/v) filter sterilized glucose or galactose was added. * - was added for solid medium.	

V.2.3.3 Preparation of chemically competent *S. cerevisiae* cells

For good transformation efficiency, competent cells were prepared using monovalent cation lithium acetate method (LiAc) attributed to its chaotropic effect.

A glycerol stock of yeast cells was streaked on YPD plate without antibiotic and grown for 2 days at 30 °C. A single colony was then used to inoculate 20 ml YPD medium and grown overnight with shaking at 30 °C. The primary culture with an OD$_{600}$ of 4.5 was then used to

inoculate 250 ml YPD medium and grown for 3-4 h until an OD_{600} of 0.9 was reached. The culture was centrifuged at 3220 g for 5 min at 4 °C in a GSA rotor. The pelleted cells were re-suspended in 50 ml sterile ddH_2O followed by centrifugation and re-suspended in 1 ml transformation buffer (Tab.V.6). For long-term storage, 15 % glycerol was added and aliquots of 50 µl were made. The aliquoted yeast cells were slowly frozen overnight in a Styrofoam box at –80 °C and later stored at –80 °C.

V.2.3.4 Transformation of *S. cerevisiae*

Lithium acetate (LiAc)-PEG method was used for yeast transformation. A 10 µl aliquot of salmon sperm DNA was made single stranded by heating at 95 °C for 10 min, briefly centrifuged and kept on ice for few mins. To this single-stranded DNA solution, 0.1 µg plasmid DNA and 50 µl of prepared competent cells were added and mixed. Next, 600 µl plating buffer (Tab.V.6) and 10 µl DMSO were added, mixed and incubated with vigorous shaking at 30 °C for 45 min. The cells were then heat shocked for 15 min at 42 °C and incubated at room temperature for 20-30 min. After a brief spin, the supernatant was removed and the cells were washed with 400 µl sterile ddH_2O. The re-suspended cells were plated out on Synthetic Drop-out medium without Uracil and incubated at 30 °C for 48 h.

Tab.V.6: Components of yeast transformation buffer and plating buffer

Transformation buffer		Plating buffer	
Substances	Amount for 100 ml	Substances	Amount for 100 ml
10 X Lithium Acetate	10 ml	10 X Lithium Acetate	10 ml
10 X TE, pH 7.5	5 ml	10 X TE, pH 7.5	10 ml
ddH_2O	Up to 100 ml	50 % PEG -3350	80 ml
Filter sterilized and stored at room temp.		Filter sterilized and stored at room temp.	

V.2.3.4 Small scale product extraction from yeast

For TPS10 product identification, positively transformed colonies from a well-grown plate were inoculated in 5 ml YPD growth medium containing 2 % glucose and grown for 24 h with shaking at 30 °C. The cultures were centrifuged and the pelleted cells were re-suspended in fresh 5 ml YPD growth medium containing 2 % galactose in order to induce product formation. After 24 h of cultivation at 30 °C, cultures were extracted with 2 ml hexane or pentane and later measured using GC-MS.

V.2.3.5 Large Scale product extraction from yeast

Large-scale extraction of products was performed for the identification of TPS10 major product and for bioassay experiments. Positively transformed colonies were cultured in 5 ml

YPD containing 2 % glucose at 30 °C with shaking. After 24 h, the cultures were centrifuged and the pelleted cells from four culture tubes were used for inoculating fresh 250 ml YPD containing 2 % glucose in a 1 L Erlenmeyer flask and grown for 24 h at 30 °C with shaking. After 24 h, the cultures were again centrifuged and the pelleted cells were re-suspended in 250 ml YPD containing 2 % galactose in a 1 L Erlenmeyer flask and grown again for 24 h at 30 °C with shaking. Additionally, 20 silicon tubes (Rotilabo Silicon tubes, Carl Roth GmbH, Germany) of approximately 1-2 cm in length were added for product adsorption. After 24 h, cultures and silica tubes were extracted separately using 100 ml and 50 ml pentane, respectively. The extracts were then dried to full dryness using rotatory evaporator and re-dissolved in appropriate solvent either for NMR or for bioassay experiments.

V.2.4 *Colletotrichum trifolii* (*C. trifolii*)

C. trifolii race 2 was kindly provided by Prof. Dr. Natalia Requena, Karlsruhe Institute of Technology, Karlsruhe, Germany.

C. trifolii mycelial piece was sub-cultured on oat meal agar (OMA, Tab.V.7) plates. The plates were sealed using leucopore tape and grown at 23 °C in dark under UV light for sporulation (incubator chamber in Prof. Holger Deising's lab).

Tab.V.7: Components of OMA

Substances	Amount for 1 L
Grinded Oat Meal (Bauckhof,Zartblatt,Demeter)	50 g
Agar-Agar, Kobe I (Carl Roth, GmbH)	12 g
ddH$_2$O	1 L

Autoclaved for 45 min at 121 °C.

After 14 days of growth, spores were washed from the OMA plates using 0.02 % Tween20 and collected in a 1.5 ml Eppendorf tube. Spores were then counted in a hemocytometer and 10^5 spores were used for infecting the plants. For glycerol stock preparation, spores from OMA plates were streaked and mixed with 1.5 ml 40 % glycerol and incubated in ice for 1 h and stored in – 80 °C.

V.2.5 *Rhizophagus irregularis* (*R. irregularis*)

For mycorrhizal experiments, the DAOM197198 strain was used, kindly provided by Prof. Dr. Natalia Requena, Karlsruhe Institute of Technology, Karlsruhe, Germany.

V.2.5.1 Growth media and conditions

R. irregularis has to be cultivated together with the host plant. This can be achieved either by invitro dual-compartment system or cultivation in a green house with the host plant.

V.2.5.2 Monoaxenic sterile culture: DAOM197198 was cultured in a dual compartment system at 28 °C in dark. A Plant compartment (Pc) containing *A. rhizogenes* transformed *Daucus carota* hairy roots were cultured on M-medium containing sucrose and inoculated with *R. irregularis* spores. Fungal hyphae were allowed to grow from Pc to Fungal Compartment (Fc), where they proliferated and formed spores. This compartment was filled with M-medium without sucrose and after 6-10 months spores were collected from the Fc by dissolving agar pieces in 0.01 M citrate buffer (0.1 M citric acid solution, 0.1 M sodium citrate, pH 6) overnight at room temperature with slow shaking in dark. Next day, citrate buffer was removed and spores were washed 2-3 times with ddH$_2$O. An equal amount of spores were used for plant inoculation.

V.2.5.3 Non-sterile culture in pots: Washed spores of DAOM197198 and sterilized *Allium porrum* (cultivar Elefant, Erfurter Samen und Pflanzenzucht GmbH) seeds were placed in 21 cm pots filled with lecaton (2-5 mm size, Original Lamstedt Ton; Fibo ExClay, Lamsted, Germany). The spores and seeds were covered with approximately 2 cm layer of lecaton and cultivated for 6-10 months. When the pots were enriched with spores after 6 months, a 1: 4 dilution was used for mycorrhizal experiments.

V.2.6 *Aphanomyces euteiches* (*A. euteiches*)

V.2.6.1 Strains: Ae1a (obtained from INRA Rennes, France), ATCC201684, a pea isolate from Denmark and AeRB84, a more aggressive strain from France were kindly provided by Prof. Christophe Jacquet, Paul Sabatier University, Toulouse, France.

V.2.6.2 Growth of mycelium and production of zoospores

A. euteiches strain ATCC201684 was used for all infection studies (unless stated). The strain was routinely sub-cultured on 1.7 % (w/v) corn meal agar (CMA, Sigma Aldrich, Germany) in the dark at 24 °C. For zoospore production, 1 cm^2 mycelial piece from the edge of a fully-grown CMA plate (10-15 day old) was transferred to a sterile plastic pot (with lid) containing a

1:3 mixture of yeast tryptone medium (0.3% w/v yeast extract, 0.5 % w/v tryptone) and swamp water in dark at 24°C. After 3 days of mycelial growth, old medium was decanted, and the mycelial mats were washed 2-3 times with sterile tap water and incubated overnight in swamp water for zoospore release. The zoospores were counted using a hemocytometer and appropriate volumes containing 10^5 zoospores and 3000 zoospores were directly applied to the roots of adult plants and seedlings on plates, respectively.

V.2.7 *Medicago truncatula* (*M. truncatula*)

V.2.7.1 Lines used: SARDI core collection lines were kindly provided by Jean-Marie Prosperi, INRA Montpellier- 163, 174, 544, 736, 734, 530, 651, 368, 555, 154, 543, 239, 648, 542, 550, 49, 552, 337, 245, 321, 545, 557, 263, 198, 310, 144, 290, 549, 213, A17, R108. *Tnt1* insertion lines were ordered from 'Noble Research Institute', USA.

V.2.7.2 Sterilization and germination of *M. truncatula* seeds

M. truncatula seeds were scarified using concentrated sulphuric acid for 5 min followed by intensive washing with ddH$_2$O and placed on 0.7 % (w/v) water agar plates (high rise petri-plates) under sterile conditions. Then, 1 ml ddH$_2$O was added to the lid of the plates, sealed with parafilm and kept inverted in dark for 3-4 days at 4 °C in order to break dormancy. After the cold storage, the seeds were incubated differently depending on the final transfer either to the pots or to the plates. For pot transfer, the plates were kept for one day in the dark at room temperature and few hs in light (25 °C) before the transfer to pots. For use in root transformation, plate assay, and aeroponics, seeds were stored at 12 °C for two more days in the dark.

V.2.7.3 Sterile culture of *M. truncatula*

The germinated seeds were placed in square plates filled 2/3 either with M-medium (Appendix Tab.VII.1.1.i) for seedling assays or with fahreus medium (Harrison Lab Modifications; Appendix Tab.VII.1.1.iii) for hairy root transformation. The plates were further cultivated in a growth cabinet under light period of 16 h at 26 °C and dark period of 8 h at 20 °C and 40 % humidity.

V.2.7.4 Non-sterile cultivation in lecaton

Single germinated seedlings were potted in moistened 13 cm pots filled with lecaton (Original Lamstedt Ton; Fibo ExClay) and fertilized the same day with 10 ml long-ashton (LA, Tab.V.8) fertilizer. Plants were covered with a lid for 1 week in order to maintain humidity and placed in

phytochamber under light period of 16 h at 26 °C and dark period of 8 h at 20 °C and 40 % humidity. The plants were watered 3 times a week and fertilized once per week.

Tab.V.8: LA composition

Macroelements

Substances	Amount for 1 L
KNO_3	4.04 g
$Ca(NO)_3.4H_2O$	9.44 g
$NaH_2PO_4.H_2O$	1.84 g
$MgSO_4.7H_2O$	7.53 g

Microelement A

Substances	Amount for 1 L
$MnSO_4.4H_2O$	2.23 g
$CuSO_4.5H_2O$	0.25 g
$ZnSO_4.5H_2O$	0.29 g
H_2BO_3	3.10 g
NaCl	5.90 g

Microelement B

Substance	Amount for 1 L
$NH_4)_6Mo_7O_{24}.4H_2O$	0.88 g

For 1 L LA 100 % PO_4 fertilizer, 10 ml microelement A, 1 ml microelement B, 0.22 g Fe-EDTA and above listed macro elements were added. For 20 % PO_4, 0.37 g of $NaH_2PO_4.H_2O$ was used.

V.2.7.5 Cultivation in aeroponic system

For early root-microbial studies, well grown and substrate free plants were grown in an aeroponic system. Aeroponic system is a system where plants are grown suspended in a semi-closed environment and nutrient medium is sprayed to the dangling roots, while the shoot part extends above. As the aeroponic is conducted in the air with droplets of nutrient and water, plants can make use of plentiful of oxygen, water, and nutrients. The composition of nutrient medium can be easily monitored and modified. As the plants were grown in the same chamber, variability between individual plants can be avoided. The aeroponic system used consisted of a large plastic container of dimensions 67 x 50 x 67 cm with a perforated polystyrene lid (12 holes of 36.6 mm diameter each) on the top and a mist generator, connected to a pump, at the bottom for spraying nutrient solution to the roots (Fig.V.1). The container was filled with 50 L MSR medium (Appendix Tab.VII.1.1.ii) without vitamins and sucrose and the pH was maintained to 6.5 before the seedling transfer. Overnight water-soaked, and washed Rockwool plugs were inserted in the lid of the aeroponic system and 6-day old seedlings were inserted in the Rockwool. The nutrient solution was sprayed for 30 min per hour with a break of 15 min in between and a night break of 4 h was given with the

help of an automatic timer. The nutrient solution was regularly monitored for pH and foreign contaminants.
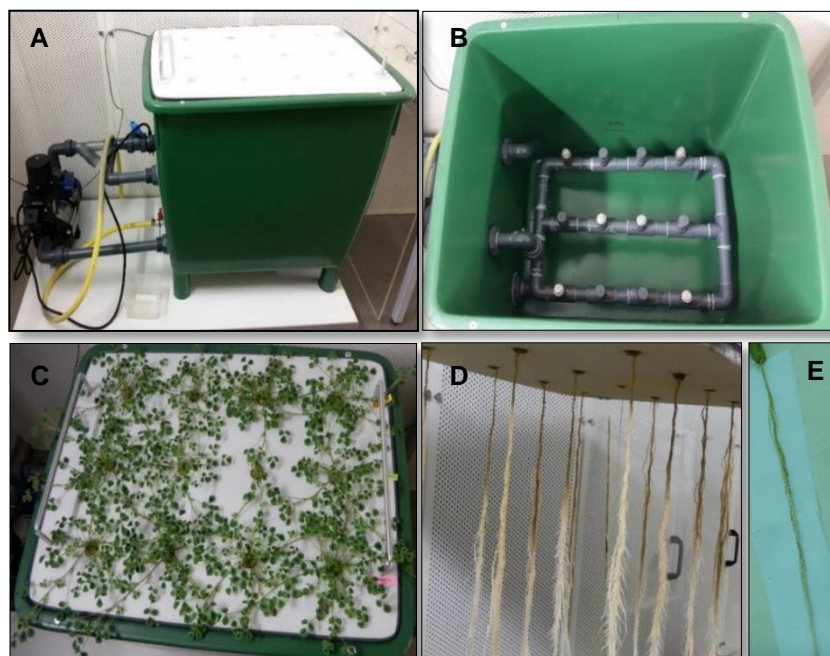
Fig.V.1: *M. truncatula* cultivation in an aeroponic system: (A) Aeroponic chamber with a perforated Styrofoam lid connected to a pump for sprinkling nutrient medium. (B) 12 sprinkles attached to the bottom of the aeroponic chamber. (C) Six-week-old *M. truncatula* A17 plants. (D and E) The root system of well-grown plants.

V.2.7.6 *M. truncatula* axenic root transformation

M. truncatula hairy roots were generated via *A. rhizogenes* mediated root transformation. The generated hairy roots are well adapted for root-microbe and root architecture studies. Additionally, hairy root cultures can be propagated for a longer time.

Vector constructs containing disarmed T-DNA region carrying the GOI with left and right borders, plant and bacterial antibiotic marker, fluorescent visualization marker (DsRed) and origin of replication (Appendix Fig.VII.4) was transformed in ARqua1 and grown in LB agar containing kanamycin and streptomycin for 48 h. Positive colonies were cultured in LB medium with antibiotics for another 24 h and 200 µl was plated out on YT agar containing 2 mM CaCl$_2$, antibiotics, and 200 µl acetosyringone (1 mM/ml). Meanwhile, *M. truncatula* seeds were also sterilized and germinated on 0.7 % water agar plate. The plates were kept inverted at 4 °C for 4 days and 12 °C for 1-2 days in the dark. When the seedlings were around 1 cm long and *A. rhizogenes* was fully grown, root transformation was performed (Fig.V.2). The germinated seedlings were placed in a water-filled petri plate to avoid desiccation and the

seed coat was removed. The root tip (approx. 3 mm) was cut using a sharp scalpel, scraped on the Agrobacterium lawn and placed on 2/3 filled fahreus medium square plates.
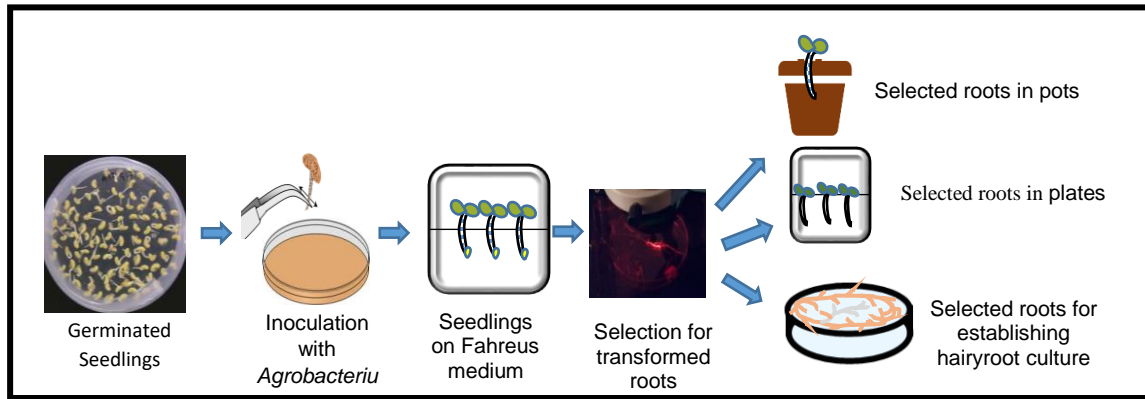
Fig.V.2: Schematic Representation of *M. truncatula* hairy root transformation

The roots were laid over the agar such that shoot part was in the agar free zone and had enough space to grow. Seven seedlings were placed in a plate and 1 ml sterile tap water was pipetted on top of agar to avoid meristem drying and the plates were sealed with leucopore tape to allow gas exchange. The plates were covered with an aluminum foil to maintain a dark environment for roots, incubated at an angle of 45° for 4 days and then vertically for 1 week in a climate chamber with 16 h light phase of 20 °C and 8 h dark phase at 17 °C. The plates were further cultivated for 3-4 weeks in a climate chamber with 16 h light phase of 24 °C and 8 h dark phase at 20 °C. After 2 weeks, 5 ml of sterile tap water was pipetted into the plates to avoid drying and maintain humidity. After 4-5 weeks of growth, roots were screened for transformation using red fluorescence emitted by constitutively expressing DsRed module under a stereo microscope (Leica MZIII-Fluorescence microscope). Non-transformed roots were carefully removed and the selected transformed plants were transferred to pots filled with lecaton. After 1 week in lecaton, roots were screened again for transformation and transgenic plants were transferred again to lecaton pots. The transgenic plants were then further grown for 1 week followed by infection with *A. euteiches*. Plants were fertilized with LA fertilizer once per week and watered 3 times a week. While harvesting, the roots were carefully taken out of lecaton, washed in ddH$_2$O and dried with paper towels. About 2 cm center piece of roots were stored in 50 % ethanol for staining purposes and the rest was snap frozen in liquid nitrogen and later stored in -80 °C until RNA extraction.

V.3 Molecular biology methods

V.3.1 Classical cloning

amiRNA targeting *TPS10* was cloned using classical cloning method into a plant compatible vector. amiRNA sequences targeting *TPS10* were designed using webmicroRNA designer (http://wmd3.weigelworld.org/cgi-bin/webapp.cgi) and these sequences (Appendix Tab.VII.4) were integrated into an endogenous *M. truncatula* microRNA backbone miR159b (Devers et al., 2013; kindly provided by Prof. Dr. Franziska Krajinski-Barth, University of Leipzig) using overlapping PCR. Overlapping PCR was performed according to Devers et al. (2013) using high fidelity AccuPrime™ *Pfx* Supermix (Life Technologies, GmbH). The resulting PCR product was gel purified using Montage Gel Extraction Kit (Merck Millipore, Merck KGaA, Darmstadt, Germany), followed by A-tailing of the PCR product for TA ligation in pCR 2.1 TOPO TA vector, since the high-fidelity polymerases do not add A-tail to the 3' end which is necessary for TA ligation. The A-tailed PCR product and vector were ligated overnight using Promega T4 DNA ligase at 16 °C. The ligated products were transformed in *E. coli* and the positive clones were confirmed using restriction digestion and sequencing (Eurofins Genomics, Germany). The confirmed clones and plant transformation vector (p9RFP_Ub3_Expr; kindly provided by Prof. Dr. Franziska Krajinski-Barth, University of Leipzig) were restrictions digested with *MluI* and *SpeI* (*BcuI*) fast digest enzymes and the digested products were gel purified, ligated and transformed in *E. coli*. The positive colonies were confirmed by colony PCR (Bio&Sell Taq Polymerase) and sequenced before proceeding to root transformation.

V.3.2 Golden gate modular cloning

Classical cloning method requires several cloning and transformation steps and therefore is a time-consuming method. On the other hand, Golden gate modular cloning (MoClo System) developed by Dr. Sylvestre Marillonnet (Engler et al., 2008) can assemble many DNA fragments in a single step with high efficiency. Golden gate system exploits the ability of type IIs restriction endonucleases that cut outside of their recognition site sequence, allowing DNA fragments flanked by compatible restriction sites and overhangs to be digested and ligated easily. Since the ligated products lack the original type IIs restriction site it will not be re-digested in a second restriction ligation reaction. Four base pairs are usually placed distal to the cleavage site such that recognition sites are removed after digestion and only 4 base pair overhang remains, these overhangs are helpful in assembling multiple DNA fragments in a specific unidirectional manner. Pre-existing type IIs restriction sites in DNA fragment were

removed via a point mutation such that amino acid remains the same. All vector constructs used in this study are listed in Appendix Tab.VII.1.3.

V.3.2.1 Construction of plant transformation vectors

Golden gate MoClo system was used for the construction of level -1, level 1 and level 2 plant transformation vector. Their backbones contained *E. coli* origin of replication (ori), *E. coli* selection marker (kanamycin in level -1 and level 2, carbenicillin in level 1), and a *LacZ* module flanked by *BsaI* (level -1 and 1) or *BsaI* and *BpiI* (level 2) restriction sites to select for the insertion. The final plant transformation vector contained a suitable promoter driving gene of interest or coding sequence module and a terminator, this module was placed close to the right border (RB) and plant selection marker (DsRed) module close to the left border (LB). An example of a plant transformation vector construct is provided in Appendix Fig.VII.2.4.

V.3.2.2 Construction of yeast expression vectors

Golden gate MoClo system was also used for the construction of level 1 and level M yeast expression system. Their backbones contained *E. coli* origin of replication (ori), *S. cerevisiae* origin of replication (2μ), *E. coli* antibiotic selection marker (carbenicillin in level 1, spectinomycin in level 2), *S. cerevisiae* URA3 selection marker and a *LacZ* module flanked by *BsaI* (level 1) or *BsaI* and *BpiI* (level M) restriction sites to select for the insertion. In order to assemble six different level 1 modules, level 1 plasmids were restriction digested with *BpiI* creating 4 bp specific overhang for the construction of level M vectors. An example of a plant transformation vector construct is provided in Appendix Fig.VII.2.5.

V.3.3 Polymerase chain reaction (PCR)

PCR is an *invitro* DNA amplification method based on the ability of DNA polymerase to synthesize new strand complementary to the template. A normal PCR cycle involves three basic steps: denaturation of template DNA fragment, annealing of complementary primers and elongation of DNA strand. The PCR reaction was performed in a thermocycler with heated lid (C1000 Touch™ Thermal Cycler, BioRad Laboratories GmbH, Germany). All oligonucleotides were synthesized by Eurofins Genomics and are listed in Appendix Tab.VII.2. Different DNA polymerases were used depending on the downstream requirement of the PCR product. The non-proofreading Bio & Sell Taq polymerase was used for colony PCR, genotyping *Tnt1* insertion lines and detection of genomic DNA in RNA samples. The proofreading polymerases KOD and AccuPrime™ Pfx Supermix were used for cloning

purposes. All PCR reactions were performed according to manufacturer's guidelines (Tab.V.9, 10).

Tab.V.9: PCR using different polymerases

Accuprime™ Pfx Supermix		KOD hot start polymerase		Bio&Sell Taq polymerase	
Components	Amount	Components	Amount	Components	Amount
Accuprime™ *Pfx* Supermix	22.5 µl	10 X Buffer	5 µl	10 X Reaction Buffer	1 µl
Forward Primer (5 µM)	1 µl	25 mM MgSO4	3 µl	Lösung S (10X)	1 µl
Reverse Primer (5 µM)	1 µl	dNTPs (2 mM each)	5 µl	dNTPs	0.5 µl
Template DNA	10 pg-200 ng	Forward primer (10 µM)	1.5 µl	Forward primer (10 µM)	1 µl
		Reverse primer (10 µM)	1.5 µl	Reverse primer (10 µM)	1 µl
		Template DNA	10 ng	Template DNA	10 ng
		KOD Hot Start DNA Polymerase (1 U/µl)	1 µl	$MgCl_2$ (25 mM)	1 µl
		ddH$_2$O	Up to 50 µl	Taq Polymerase (5 U/µl)	0.5 µl
				ddH2O	Up to 10µl

Tab.V.10: Schematic PCR Program of used polymerases

No.	Steps	KOD hot start polymerase	Accuprime™ *Pfx* Supermix	Bio&Sell Taq polymerase
1.	Polymerase Activation	95 °C for 2 min	95 °C for 5 min	95 °C for 2 min
2.	Denaturation	95 °C for 20 secs	95 °C for 15 secs	95 °C for 30 secs
3.	Annealing	Lowest primer Tm °C for 20 secs	55-65 °C for 30 secs	55-65 °C for 30 secs
4.	Extension	70 °C for 20 secs/Kb	68 °C for 1 min/Kb	72 °C for 1 min/Kb
		Repeat Cycle 2-4 for 30-40 cycles.		
5.	Final Extension			72 °C for 5 min
6.	Hold time	12 °C for infinite time		

V.3.4 Agarose gel electrophoresis

Analysis of PCR products, restriction digested plasmid DNA and RNA integrity were performed using gel electrophoresis. Depending on the expected size of DNA fragment either 1 or 2 % (w/v) agarose gel (Bio&Sell, Germany) in 1x TAE (50X TAE: 2M TRIS base, 1M $C_2H_4O_2$, 50 mM Na_2EDTA pH 8.5) was used. Fragment sizes were determined using DNA ladders such as O´Gene Ruler 1 kb plus (Thermo Scientific, Germany) and Hyperladder V (Bioline GmbH, Germany). For visualization of nucleic acids, 0.75 µl of undiluted SERVA DNA StainG (SERVA GmbH, Heidelberg, Germany) per 50 ml 1x TAE was used. After electrophoresis, gels were analyzed using a gel documentation system (FUSION FX7, Vilber Lourmet, Eberhardzell, Germany). Depending on the purity of PCR products, either PCR purification or gel extraction were performed using kits like Nucleospin® Gel and PCR CleanUp (Macherey Nagel, Germany) and Montage Gel Extraction Kit (Meck Millipore) according to manufacturer's instruction. The DNA fragments were excised from the gel using a UV spotlighter NU-72 (Faust, Schaffhausen, Switzerland).

V.3.5 Isolation of genomic DNA

For genomic DNA isolation, 100 mg of frozen plant material was grounded in liquid nitrogen by mortar and pestle and they were further reduced to a fine powder form using Retsch Beadmill (Retsch MM 400) and a steel bead of 7 mm at a frequency of 30 Hz for 1 min. Genomic DNA from frozen fine powder was extracted using NucleoSpin® Plant II kit (Macherey Nagel, Germany) according to manufacturer's guidelines and the concentration of

DNA was measured using NanoDrop1000 (peQLabBiotechnologie GmbH, Erlangen, Germany) and stored at -20 °C.

V.3.6 Isolation of plasmid DNA (miniprep)

A liquid culture (5 ml) of bacteria was grown according to suitable culture conditions of bacterial species used. Plasmid DNA was then isolated using NucleoSpin® Plasmid EasyPure Kit (Macherey Nagel, Germany) according to manufacturer's instructions, the concentration was measured using Nanodrop and stored at -20 °C.

V.3.7 Plasmid midi prep isolation

Plasmid DNA from a 50 ml bacterial culture was isolated using Midiprep Kit (Macherey Nagel, Germany) according to manufacturer's guidelines. The concentration of eluted DNA was measured using Nanodrop and further concentrated using PEG DNA Precipitation method described below.

V.3.8 Precipitation of DNA

The plasmid DNA was mixed with PEG-solution (13 g PEG 4000, 67 mg $MgCl_2$, 25 ml 1.2 M Na-acetate pH 5.2 in a total volume of 50 ml) in the ratio of 1: 1 and incubated at room temperature for 20 min, followed by centrifugation for 20 min at 17000 g. The supernatant was carefully removed and the pellet was washed with 1 ml 70 % ethanol. The pellet was then dried at 37 °C and re-dissolved in 20 µl ddH_2O, concentration measured and stored at - 20 °C.

V.3.9 Isolation of RNA

RNA was isolated from 100 mg of frozen plant material, grounded in liquid nitrogen by mortar and pestle and further reduced to a fine powder form using Retsch Beadmill (Retsch MM 400) and a steel bead of 7 mm at a frequency of 30 Hz for 1 min. RNA isolation was performed using RNeasy plant minikit (Qiagen, Hilden, Germany) according to manufacturer's instructions followed by DNase digestion using Ambion DNA-*free*™ DNA Removal kit (Invitrogen, Thermo Scientific, Germany). RNA concentration was determined using NanoDrop1000 Spectrophotometer. RNA integrity and quality were analyzed either using agarose gel electrophoresis (1 % (w/v) agarose) or QIAxcel Advanced System (Qiagen, Hilden, Germany). RNA was stored at - 80 °C.

V.3.10 Isolation of RNA using TRIzol

For stem-loop qRT-PCR, total RNA was isolated using TRIzol method.

RNA was isolated from 100 mg of frozen plant material, grounded in liquid nitrogen by mortar and pestle and further reduced to a fine powder form using Retsch Beadmill (Retsch MM 400) and a steel bead of 7 mm at a frequency of 30 Hz for 1 min. 1 ml of TRIzol reagent (Tab.V.11) was then added to the frozen plant material, mixed well and incubated at room temperature for 5 min, followed by centrifugation for 15 min at 17000 g and 4 °C. The supernatant was carefully taken up and added to a new Eppendorf tube containing 200 µl chloroform, vortexed and incubated at room temperature for 5 min. For phase separation, the extract was centrifuged for 15 min at 17000 g and 4 °C. The aqueous layer was carefully taken up and mixed in a 1:1 ratio with isopropanol and 1 µl glycogen was also added. Glycogen acts as an inert carrier molecule for RNA. After centrifugation for 10 min at 17000 g and 4 °C, the supernatant was carefully removed and ice cold 70 % ethanol was added. After centrifugation for 5 min at 17000 g, the supernatant was completely removed and the pellet was air dried. The dried pellet was re-suspended in 40 µl RNase free water and RNA concentration was determined using NanoDrop1000 followed by DNase treatment using Ambion DNA-*free*™ DNA Removal kit. RNA integrity and quality were analyzed either by agarose gel electrophoresis (1 % (w/v) agarose) or QIAxcel Advanced System (Qiagen, Hilden, Germany). RNA was further stored at - 80 °C.

Tab.V.11: TRIzol components

Substances	Amount for 10 samples
Phenol RNA Grade	3.8 ml
4M Guanidium thiocyanate	2 ml
4M Ammonium thiocyanate	1 ml
Glycerin	500 µl
ddH$_2$O	Up to 10 ml
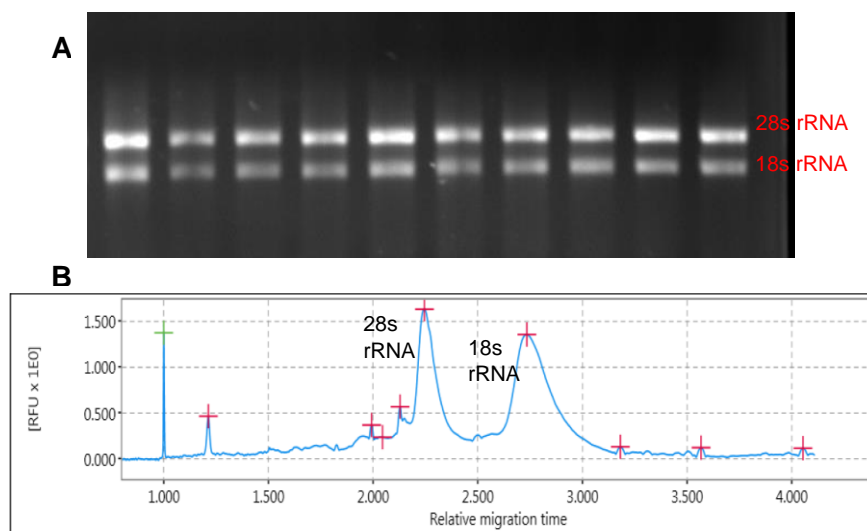
Fig.V.3: Analysis of RNA integrity. (A) RNA integrity analysis on gel. 28s rRNA and 18s rRNA bands are shown. B: RNA Integrity analyzed using QIAxcel advanced system. Good Quality RNA having two clear peaks of 28s rRNA and 18s rRNA are shown.

V.3.11 cDNA synthesis of mRNA

The isolated RNA was reverse transcribed to cDNA for qPCR analysis.

Prior to cDNA synthesis, DNase digested RNA was tested for residual genomic DNA via amplification of a 221 bp *Mt-His3-like* fragment using PCR. In case of complete DNase digestion, RNA was used for synthesizing complementary DNA (cDNA) using Protoscript® II First-strand cDNA synthesis kit. 0.5 µg-1 µg RNA was used as a template with 2 µl of Oligo(T)$_{23}$ in a total reaction mix of 8 µl. The secondary structure of RNA was denatured by heating at 65 °C for 5 min. After denaturation, samples were briefly centrifuged and kept on ice before addition of 10 µl Protoscript II Reaction Mix (2X) and 2 µl Protoscript II Enzyme Mix (10X). Total 20 µl cDNA synthesis reaction mix was incubated at 42 °C for one hour and the reaction was inactivated by incubating at 80 °C for 5 min. For further usage, cDNA was stored at -20 °C.

V.3.12 cDNA synthesis of miRNAs

For the detection of small miRNAs, another cDNA synthesis approach was undertaken. Small miRNAs (~21 bp) are difficult to detect due to their small size but with the help of miRNA specific stem-loop primer, these miRNAs were elongated as well as reverse transcribed to cDNA.

Small RNAs were reverse transcribed according to (Devers et al., 2011) using sequence-specific stem-loop primers and oligodT primer to allow simultaneous quantification of mRNAs and normalization against a housekeeping gene. Briefly, DNase treated 1 µg RNA was added

to a reaction mix containing 1 µl of 10 mM dNTPs, 1 µl per 2.5 µM specific stem-loop qRT primer, 1 µl of oligodT primer and ddH$_2$O up to a volume of 36.5 µl. This reaction mix was heated to 65 °C for 5 min in order to denature any secondary structures and chilled on the ice after a brief centrifugation. To this reaction mix, 10 µl of 5X reaction buffer, 2 µl of 0.1 mM DTT, 0.5 µl RiboLock and 1 µl of Revert Aid reverse transcriptase (Thermo Scientific, Germany) was added, followed by gentle mixing and brief centrifugation. Following the program was used for cDNA synthesis:

30 min at 16 °C → 1 h at 42 °C → 5 min at 85 °C → kept on 4 °C

cDNA was further stored at - 20 °C.

V.3.13 Quantitative polymerase chain reaction (qPCR)

Gene expression analysis was performed using qPCR. This method uses real-time fluorescence to measure DNA quantity at the end of each cycle. Thereby, the measured fluorescence is directly proportional to the amplified nucleic acid. If the target molecules are abundant, fluorescence will appear earlier during the PCR cycle and vice versa. The cycle at which first qPCR fluorescence signal can be detected over the background fluorescence is termed as quantitation cycle (Cq) or threshold cycle (Ct). Ct or Cq values can be used to determine relative target abundance between two or more samples. The qPCR was performed using an instrument from CFX ConnectReal-Time PCR System (Biorad Laboratories, Munich, Germany). 5x EvaGreen® qPCR Mix II (Bio & Sell, Germany) was used in combination with gene-specific primers whose binding specificity were confirmed by BLAST search. Data evaluation was done using Bio-Rad CFX Manager Software. Target genes were normalized to a reference gene and the relative expression value of target genes were then calculated using the formula: $2^{-\Delta Ct}$, where $\Delta Ct = Ct_{\text{Target gene}} - Ct_{\text{Reference gene}}$. The standard deviation between the biological replicates were also calculated and proper significance tests such as t-test or ANOVA were performed in R software. The following program was used: Initial denaturation at 95 °C for 15 min, 39 cycles of denaturation at 95 °C for 15 s, annealing, extension, and plate read at 60 °C for 30 s and 95 °C for 10 s. The melt curve and the plate read was performed from 65 °C to 95 °C, data points were collected every 0.5 °C with 5 s hold between them. The primers were synthesized by Eurofins genomics and are listed in Appendix Tab.VII.1.2

V.3.14 Microarray

In order to analyze early *M. truncatula* responsive genes to *A. euteiches* zoospores and *R. irregularis* spores, the whole transcriptomic analysis was performed using Affymetrix *Medicago* GeneChip array in an Affymetrix GeneAtlas system. Affymetrix GeneChip WT PLUS Reagent Kit was used for priming the entire length of both Poly (A) and non-Poly (A) mRNA to provide a complete and unbiased coverage of the transcriptome. The Medicago GeneChip array is a 49-format array composed of 11 pairs of 25 mer oligonucleotide, with each pair consisting of perfect match (PM) oligonucleotide and a mismatch (MM) control oligonucleotide containing a single nucleotide substitution at the thirteen-base position.

After 2 hours post-treatment (hpt) with zoospores or spores, root material was harvested and RNA was isolated as described before. 250 ng RNA was used to produce biotinylated sense strand cDNA, fragmented and hybridized to Medicago GeneChip array as per manufacturer's instructions. The GeneChip was washed, stained and scanned using the Gene Atlas system. Data was analyzed by Dr. Benedikt Athmer (IPB, Halle).

V.4 Microscopic Methods

V.4.1 Ink staining of AMF and oomycete structures

Harvested roots were treated with 10 % KOH at 70- 90 °C (depending on the root age) for 10 min. Roots were then washed three times with H_2O and incubated at room temperature for 10 min with 2 % acetic acid. After acetic acid removal, roots were stained with 5 % Sheaffer Skrip in 2 % acetic acid at 90 °C for 10 min. Stained roots were washed once with H_2O and stored at 4 °C until analysis was done.

For mycorrhizal colonization analysis, AMF structures were quantified according to Trouvelot et al. (1986). Briefly, 30-50 root segments were taken on a slide and mycorrhization was scored using different parameters. Observed parameters were calculated using Mycocalc software (Trouvelot et al., 1986).

V.4.2 Staining with WGA-Alexa fluor 488 conjugate

The roots were covered with 20 % KOH and boiled at 90 °C for 10 min. Then, KOH was removed and roots were rinsed thoroughly with ddH_2O, followed by addition of 0.1 M HCl and incubation at room temperature for 1-2 h. Then, HCl was removed and roots were again thoroughly washed with ddH_2O and also once with 1x phosphate buffer saline (135 mM NaCl, 3 mM KCl, 1.5 mM KH2PO4, 8 mM Na2HPO4, pH 7.4) solution before incubating the treated roots overnight with PBS-WGA staining solution (final concentration of WGA-AlexaFluor- 0.2

µg/ml). The stained structures were later analyzed using an epifluorescence microscope AxioImager (Zeiss GmbH, Jena, Thuringia, Germany) using the reflector module 09 (EX BP 450-490/BS FT510/EM LP515).

V.4.3 GUS staining for promoter activity

Glucouronidase (*GUS*) reporter assay is the most valuable tool for studying promoter activity, where *GUS* breaks down carbohydrate substrate into smaller fragments. This property can be utilized by fusing *GUS* to a promoter under study. Two different kinds of carbohydrate substrates are available for GUS, namely X-Gluc (5-Bromo-4-chloro-3-indolyl-β-D-glucuronide) which on cleavage and further oxidization gives a dense blue color and MUG (4-Methylumbelliferyl -D-glucuronide) which on cleavage gives a fluorescent product detectable by spectrophotometer.

Promoter activity was visualized using X-Gluc (Glycosynth, UK) as substrate. Transformed roots, *A. euteiches* infected or non-infected, were incubated with the staining solution (Tab.V.12) under vacuum infiltration for few minutes to allow penetration of staining solution into the roots and then incubated for 1-2 h at 37 °C. GUS stained roots were later embedded in PEG 1500, according to Tretner et al. (2008) and sectioned in 10 µm size using microtome. The stained root fragments and the sections were analyzed using a Stemi2000 (Zeiss) and an AxioImager (Zeiss), respectively.

Tab.V.12: GUS staining solution components

Components	Concentration	Final Concentration	Amount for 100 ml
NaH_2PO_4, pH 7	500 mM	100 mM	20 ml
Na_2EDTA, pH 7	250 mM	10 mM	4 ml
$K_3Fe(CN)_6$	50 mM	0.5 mM	1 ml
$K_4Fe(CN)_6$	50 mM	0.5 mM	1 ml
X-Gluc(104 mg in 2 ml DMSO)	100 mM	2 mM	2 ml
Triton X-100	10 %	0.1%	1 ml
ddH_2O			71 ml

V.4.4 Localization of TPS10 protein in protoplasts

The full-length coding sequence of *TPS10* without stop codon was fused to *mCherry* at the C-terminal under a CaMV *35S* promoter using Golden gate cloning (cloned by Dr. Dorothée Dreher; Ph.D. thesis Dorothée Klemann, 2016) and used for the localization studies.

V.4.4.1 Isolation of mesophyll protoplast

4-week-old, well developed *N. benthamiana* plants were used for protoplast isolation. The third and fourth leaves from the shoot tip were selected for isolation. The leaves were placed on a white paper, the midrib carefully removed and leaves were cut into 2 mm small pieces with a sharp scalpel. Freshly cut leaves were placed in an enzyme-filled petri plate and twice vacuum infiltrated (10 ml enzyme solution for two leaves). The infiltrated leaf pieces appeared dark, transparent and ideally should sink at the bottom of petri plate. The leaf pieces were further incubated for 30 min under the vacuum and for another four h in dark at room temperature. After four h, the enzyme solution should appear green. The petri plates were gently shaken by hand and slow shaking on a lab shaker was performed for 30 min in dark to release the protoplasts. 4.5 ml of protoplast suspension was filtered through a 100-micron nylon mesh into 15 ml culture tubes on ice and centrifuged for 1 min at 4 °C, 200g and supernatant was carefully removed. The pellet was re-suspended in 2-3 ml W5 solution, gently mixed, centrifuged and re-suspended again in 2-3 ml W5 solution. The protoplasts were allowed to gravity settle to the bottom of the tube by incubating for 40 min on ice. The supernatant was further removed, the pellet re-suspended in 2-3 ml MMG solution and incubated on ice for 40 min. The protoplasts were counted in a counting chamber and diluted to 100,000 protoplasts/ml. A detailed description of solutions used is supplied in Appendix Tab.VII.1.4.

V.4.4.2 Transformation of protoplast

5-10 µg plasmid DNA was used per 10000 protoplasts. 200 µl protoplast suspension was added to plasmid DNA in a 2 ml Eppendorf tube and gently mixed. To this mixture 220 µl (1.1 volume of protoplast suspension) PEG solution was added, carefully mixed and incubated at room temperature for 5-10 min. To it, 880 µl W5 (4.4 volume of protoplast suspension) was added and carefully mixed. Centrifugation for 1 min at 200 g and 4 °C was done. The supernatant was carefully removed (All PEG should be removed, else protoplasts might die). The transformed protoplasts were incubated overnight at room temperature. Next morning,

transformed protoplasts were analyzed by a confocal laser scanning microscope (LSM 780, Zeiss).

V.5 Metabolomics Methods

V.5.1 Gas Chromatography Mass Spectrometry (GC-MS)

The yeast extract was measured using GCMS QP2010 SE (Shimadzu, Japan) coupled to AOC 5000 sample injection system and QP2010 Ultra mass spectrometer with electron ionization. Chromatographic separation was performed on a RXI-5il MS capillary column (30 m x 0.25 mm, Shimadzu, Japan) using splitless injection system and an injection volume of 1 µl was used. The injection temperature rose from 50 °C to 250 °C and the flow rate of helium was 0.93 ml/min. The GC column oven temperature ramp was as follows: 50 °C for 1 min, 50 to 300 °C at a rate of 7 °C min^{-1}, 300 to 320 °C with a rate of 50 °C min^{-1} and 320 °C for 2 min at 70 eV. Mass spectrometry was performed in a full scan mode from 45 to 400 m/z. Data analysis was done using device-specific GCMS Postrun Analysis.

V.5.2 Thermo desorption GC-MS

The root volatiles emitted after *A. euteiches* treatment were adsorbed on silica tubes (Sorbstar, Restek, Germany) and later measured in thermo-desorption GC-MS (TD-20) coupled to GCMS QP2010 SE (Shimadzu, Japan), 48-Sample autosampler and QP2010 Ultra mass spectrometer with electron ionization. Here, the volatiles are first thermally desorbed from the tubes and passed through a cold trap to concentrate the volatile peaks before transferring it to GC-Column coupled to mass spectrometer. Chromatographic separation was performed on a RXI-5il MS capillary column (30m x 0.25mm, Shimadzu, Japan) using split Injection mode. The GC Column oven temperature ramp was as follows: 50 °C for 1 min, 50 to 300 °C at a rate of 15 °C min^{-1}, 300 to 320 °C at a rate of 20 °C min^{-1} and 320 °C for 2 min. Mass spectrometry was performed in a full scan mode from 35 to 500 m/z. Data analysis was done by device-specific GCMS Postrun Analysis.

V.5.3 High performance liquid chromatography (HPLC) for separation of major peak

The dried yeast extract was dissolved in 5 ml methanol and was subjected to HPLC- APCI-MS analysis (performed by Anja Ehrlich, NWC, IPB). The peaks were separated using a YMC-Pack column (150 x 10 mm ID 120 Å 5 µm ODS-A) and Agilent 1260 Infinity Quaternary Pump, including an autosampler and a fraction collector. For elution, the gradient of 30 % methanol for 15 minutes to 100 % methanol was used. The flow rate was maintained at 800 µl per min and the column temperature was maintained at 25 °C. An Agilent MSD Single 6120 Single Quadrupole mass spectrometer was used to detect the metabolites and was operated in

positive mode. The operation parameters for LC-APCI were as follows: ion spray voltage 3500 V, nebulizing gas 35 psig, drying gas temperature 250 °C and scanned for a mass range of 150-300 m/z.

VI. References

Adebesin, F., Widhalm, J.R., Boachon, B., Lefèvre, F., Pierman, B., Lynch, J.H., Alam, I., Junqueira, B., Benke, R., Ray, S., Porter, J.A., Yanagisawa, M., Wetzstein, H.Y., Morgan, J.A., Boutry, M., Schuurink, R.C., and Dudareva, N. (2017). Emission of volatile organic compounds from petunia flowers is facilitated by an ABC transporter. Science **356,** 1386.

Aderem, A., and Ulevitch, R.J. (2000). Toll-like receptors in the induction of the innate immune response. Nature **406,** 782-787.

Aharoni, A., Giri, A.P., Deuerlein, S., Griepink, F., de Kogel, W.J., Verstappen, F.W., Verhoeven, H.A., Jongsma, M.A., Schwab, W., and Bouwmeester, H.J. (2003). Terpenoid metabolism in wild-type and transgenic Arabidopsis plants. Plant Cell **15,** 2866-2884.

Ahuja, I., Kissen, R., and Bones, A.M. (2012). Phytoalexins in defense against pathogens. Trends Plant Sci **17,** 73-90.

Akiyama, K., Matsuzaki, K., and Hayashi, H. (2005). Plant sesquiterpenes induce hyphal branching in arbuscular mycorrhizal fungi. Nature **435,** 824-827.

Alexandratos, N., and Bruinsma, J. (2012a). World agriculture towards 2030/2050: the 2012 revision. Agricultural Development Economics Division, Food and Agriculture Organization of the United Nations, Rome. Italy. 1-147.

Alexandratos, N., and Bruinsma, J. (2012b). "World agriculture towards 2030/2050: the 2012 revision,"ESA Working Papers 288998, Food and Agriculture Organization of the United Nations, Agricultural Development Economics Division (ESA).

Ane, J.M., Zhu, H., and Frugoli, J. (2008). Recent Advances in Medicago truncatula Genomics. Int J Plant Genomics **2008,** 256597.

Arimura, G.-i., Ozawa, R., Nishioka, T., Boland, W., Koch, T., Kühnemann, F., and Takabayashi, J. (2002). Herbivore-induced volatiles induce the emission of ethylene in neighboring lima bean plants. Plant J. **29,** 87-98.

Arimura, G., Ozawa, R., Kugimiya, S., Takabayashi, J., and Bohlmann, J. (2004). Herbivore-induced defense response in a model legume. Two-spotted spider mites induce emission of (E)-beta-ocimene and transcript accumulation of (E)-beta-ocimene synthase in Lotus japonicus. Plant Physiol **135,** 1976-1983.

Axtell, M.J., and Staskawicz, B.J. (2003). Initiation of RPS2-specified disease resistance in Arabidopsis is coupled to the AvrRpt2-directed elimination of RIN4. Cell **112,** 369-377.

Badis, Y., Bonhomme, M., Lafitte, C., Huguet, S., Balzergue, S., Dumas, B., and Jacquet, C. (2015). Transcriptome analysis highlights preformed defences and signalling pathways controlled by the prAe1 quantitative trait locus (QTL), conferring partial resistance to Aphanomyces euteiches in Medicago truncatula. Mol Plant Pathol **16,** 973-986.

Baldauf, S.L., Roger, A.J., Wenk-Siefert, I., and Doolittle, W.F. (2000). A Kingdom-Level Phylogeny of Eukaryotes Based on Combined Protein Data. Science **290,** 972.

Baldwin, I.T. (2010). Plant volatiles. Curr Biol **20,** R392-397.

Barker, D.G., Bianchi, S., Blondon, F., Dattée, Y., Duc, G., Essad, S., Flament, P., Gallusci, P., Génier, G., Guy, P., Muel, X., Tourneur, J., Dénarié, J., and Huguet, T. (1990). Medicago truncatula, a model plant for studying the molecular genetics of theRhizobium-legume symbiosis. Plant Molecular Biology Reporter **8,** 40-49.

Bartel, D.P. (2004). MicroRNAs: genomics, biogenesis, mechanism, and function. Cell **116,** 281-297.

Baulcombe, D. (2004). RNA silencing in plants. Nature **431,** 356.

Bécard, G., and Fortin, J.A. (1988). Early events of vesicular–arbuscular mycorrhiza formation on Ri T-DNA transformed roots. New Phytologist **108,** 211-218.

Beguiristain, T., Grandbastien, M.-A., Puigdomènech, P., and Casacuberta, J.M. (2001). Three Tnt1 Subfamilies Show Different Stress-Associated Patterns of Expression in Tobacco. Consequences for Retrotransposon Control and Evolution in Plants. Plant Physiol **127,** 212.

Beiter, T., Reich, E., Williams, R.W., and Simon, P. (2009). Antisense transcription: a critical look in both directions. Cell Mol Life Sci **66,** 94-112.

Bent, A.F., and Mackey, D. (2007). Elicitors, effectors, and R genes: the new paradigm and a lifetime supply of questions. Annu Rev Phytopathol **45,** 399-436.

Berg, G., and Smalla, K. (2009). Plant species and soil type cooperatively shape the structure and function of microbial communities in the rhizosphere. FEMS Microbiol Ecol **68,** 1-13.

Birnbaum, K., Shasha, D.E., Wang, J.Y., Jung, J.W., Lambert, G.M., Galbraith, D.W., and Benfey, P.N. (2003). A gene expression map of the Arabidopsis root. Science **302,** 1956-1960.

Blazer, V.S., Lilley, J.H., Schill, W.B., Kiryu, Y., Densmore, C.L., Panyawachira, V., and Chinabut, S. (2002). Aphanomyces invadansin Atlantic Menhaden along the East Coast of the United States. Journal of Aquatic Animal Health **14,** 1-10.

Boachon, B., Junker, R.R., Miesch, L., Bassard, J.E., Hofer, R., Caillieaudeaux, R., Seidel, D.E., Lesot, A., Heinrich, C., Ginglinger, J.F., Allouche, L., Vincent, B., Wahyuni, D.S., Paetz, C., Beran, F., Miesch, M., Schneider, B., Leiss, K., and Werck-Reichhart, D. (2015). CYP76C1 (Cytochrome P450)-Mediated Linalool Metabolism and the Formation of Volatile and Soluble Linalool Oxides in Arabidopsis Flowers: A Strategy for Defense against Floral Antagonists. Plant Cell **27,** 2972-2990.

Bohlmann, J., Stauber, E.J., Krock, B., Oldham, N.J., Gershenzon, J., and Baldwin, I.T. (2002). Gene expression of 5-epi-aristolochene synthase and formation of capsidiol in roots of Nicotiana attenuata and N. sylvestris. Phytochemistry **60,** 109-116.

Boisson-Dernier, A., Chabaud, M., Garcia, F., Becard, G., Rosenberg, C., and Barker, D.G. (2001). Agrobacterium rhizogenes-transformed roots of Medicago truncatula for the study of nitrogen-fixing and endomycorrhizal symbiotic associations. Mol Plant Microbe Interact **14,** 695-700.

Boller, T., and Felix, G. (2009). A renaissance of elicitors: perception of microbe-associated molecular patterns and danger signals by pattern-recognition receptors. Annu Rev Plant Biol **60,** 379-406.

Bologna, N.G., Mateos, J.L., Bresso, E.G., and Palatnik, J.F. (2009). A loop-to-base processing mechanism underlies the biogenesis of plant microRNAs miR319 and miR159. EMBO J **28,** 3646-3656.

Bos, R., Koulman, A., Woerdenbag, H.J., Quax, W.J., and Pras, N. (2002). Volatile components from Anthriscus sylvestris (L.) Hoffm. Journal of chromatography. A **966,** 233-238.

Boyd, L.A., Ridout, C., O'Sullivan, D.M., Leach, J.E., and Leung, H. (2013). Plant-pathogen interactions: disease resistance in modern agriculture. Trends Genet **29,** 233-240.

Brady, S.M., Orlando, D.A., Lee, J.Y., Wang, J.Y., Koch, J., Dinneny, J.R., Mace, D., Ohler, U., and Benfey, P.N. (2007). A high-resolution root spatiotemporal map reveals dominant expression patterns. Science **318,** 801-806.

Brunner, F., Rosahl, S., Lee, J., Rudd, J.J., Geiler, C., Kauppinen, S., Rasmussen, G., Scheel, D., and Nürnberger, T. (2002). Pep-13, a plant defense-inducing pathogen-associated pattern from Phytophthora transglutaminases. EMBO J **21,** 6681-6688.

Caputi, L., Lim, E.K., and Bowles, D.J. (2008). Discovery of new biocatalysts for the glycosylation of terpenoid scaffolds. Chemistry **14,** 6656-6662.

Cerri, M.R., Frances, L., Kelner, A., Fournier, J., Middleton, P.H., Auriac, M.C., Mysore, K.S., Wen, J., Erard, M., Barker, D.G., Oldroyd, G.E., and de Carvalho-Niebel, F. (2016). The Symbiosis-Related ERN Transcription Factors Act in Concert to Coordinate Rhizobial Host Root Infection. Plant Physiol **171,** 1037-1054.

Challis, G.L., and Hopwood, D.A. (2003). Synergy and contingency as driving forces for the evolution of multiple secondary metabolite production by Streptomyces species. Proc Natl Acad Sci U S A **100,** 14555.

Chen, C., and Chen, Z. (2002). Potentiation of developmentally regulated plant defense response by AtWRKY18, a pathogen-induced Arabidopsis transcription factor. Plant Physiol **129,** 706-716.

Chen, F., Tholl, D., Bohlmann, J., and Pichersky, E. (2011). The family of terpene synthases in plants: a mid-size family of genes for specialized metabolism that is highly diversified throughout the kingdom. Plant J **66,** 212-229.

Chen, F., Tholl, D., D'Auria, J.C., Farooq, A., Pichersky, E., and Gershenzon, J. (2003). Biosynthesis and emission of terpenoid volatiles from Arabidopsis flowers. Plant Cell **15,** 481-494.

Chen, F., Ro, D.K., Petri, J., Gershenzon, J., Bohlmann, J., Pichersky, E., and Tholl, D. (2004). Characterization of a root-specific Arabidopsis terpene synthase responsible for the formation of the volatile monoterpene 1,8-cineole. Plant Physiol **135,** 1956-1966.

Cheong, J.J., and Hahn, M.G. (1991). A specific, high-affinity binding site for the hepta-beta-glucoside elicitor exists in soybean membranes. Plant Cell **3,** 137.

Chisholm, S.T., Coaker, G., Day, B., and Staskawicz, B.J. (2006). Host-microbe interactions: shaping the evolution of the plant immune response. Cell **124,** 803-814.

Christianson, D.W. (2006). Structural Biology and Chemistry of the Terpenoid Cyclases. Chemical Reviews **106,** 3412-3442.

Clavijo McCormick, A., Unsicker, S.B., and Gershenzon, J. (2012). The specificity of herbivore-induced plant volatiles in attracting herbivore enemies. Trends Plant Sci **17,** 303-310.

Colditz, F., Niehaus, K., and Krajinski, F. (2007). Silencing of PR-10-like proteins in Medicago truncatula results in an antagonistic induction of other PR proteins and in

an increased tolerance upon infection with the oomycete Aphanomyces euteiches. Planta **226,** 57-71.

Colditz, F., Braun, H.P., Jacquet, C., Niehaus, K., and Krajinski, F. (2005). Proteomic profiling unravels insights into the molecular background underlying increased Aphanomyces euteiches-tolerance of Medicago truncatula. Plant Mol Biol **59,** 387-406.

Colditz, F., Nyamsuren, O., Niehaus, K., Eubel, H., Braun, H.-P., and Krajinski, F. (2004). Proteomic approach: Identification of Medicago truncatula proteins induced in roots after infection with the pathogenic oomycete Aphanomyces euteiches. Plant Mol Biol **55,** 109-120.

Cook, D.R. (1999). Medicago truncatula--a model in the making! Curr Opin Plant Biol **2,** 301-304.

Cormack, R.S., Eulgem, T., Rushton, P.J., Kochner, P., Hahlbrock, K., and Somssich, I.E. (2002). Leucine zipper-containing WRKY proteins widen the spectrum of immediate early elicitor-induced WRKY transcription factors in parsley. Biochimica et biophysica acta **1576,** 92-100.

Croft, K.P.C., Juttner, F., and Slusarenko, A.J. (1993). Volatile Products of the Lipoxygenase Pathway Evolved from Phaseolus vulgaris (L.) Leaves Inoculated with Pseudomonas syringae pv phaseolicola. Plant Physiol **101,** 13.

Croteau, R., Ketchum, R.E., Long, R.M., Kaspera, R., and Wildung, M.R. (2006). Taxol biosynthesis and molecular genetics. Phytochem Rev **5,** 75-97.

Cunnac, S., Occhialini, A., Barberis, P., Boucher, C., and Genin, S. (2004). Inventory and functional analysis of the large Hrp regulon in Ralstonia solanacearum: identification of novel effector proteins translocated to plant host cells through the type III secretion system. Mol Microbiol **53,** 115-128.

De Moraes, C.M., Lewis, W.J., Paré, P.W., Alborn, H.T., and Tumlinson, J.H. (1998). Herbivore-infested plants selectively attract parasitoids. Nature **393,** 570.

Degenhardt, J. (2009). Indirect defense responses to herbivory in grasses. Plant Physiol **149,** 96-102.

Degenhardt, J., Kollner, T.G., and Gershenzon, J. (2009). Monoterpene and sesquiterpene synthases and the origin of terpene skeletal diversity in plants. Phytochemistry **70,** 1621-1637.

Deslandes, L., Olivier, J., Peeters, N., Feng, D.X., Khounlotham, M., Boucher, C., Somssich, I., Genin, S., and Marco, Y. (2003). Physical interaction between RRS1-

R, a protein conferring resistance to bacterial wilt, and PopP2, a type III effector targeted to the plant nucleus. Proc Natl Acad Sci U S A **100,** 8024-8029.

Devers, E.A., Branscheid, A., May, P., and Krajinski, F. (2011). Stars and symbiosis: microRNA- and microRNA*-mediated transcript cleavage involved in arbuscular mycorrhizal symbiosis. Plant Physiol **156,** 1990-2010.

Devers, E.A., Teply, J., Reinert, A., Gaude, N., and Krajinski, F. (2013). An endogenous artificial microRNA system for unraveling the function of root endosymbioses related genes in Medicago truncatula. BMC Plant Biology **13,** 82.

Dixon, R.A., Achnine, L., Kota, P., Liu, C.J., Reddy, M.S., and Wang, L. (2002). The phenylpropanoid pathway and plant defence-a genomics perspective. Mol Plant Pathol **3,** 371-390.

Djebali, N., Jauneau, A., Ameline-Torregrosa, C., Chardon, F., Jaulneau, V., Mathe, C., Bottin, A., Cazaux, M., Pilet-Nayel, M.L., Baranger, A., Aouani, M.E., Esquerre-Tugaye, M.T., Dumas, B., Huguet, T., and Jacquet, C. (2009). Partial resistance of Medicago truncatula to Aphanomyces euteiches is associated with protection of the root stele and is controlled by a major QTL rich in proteasome-related genes. Mol Plant Microbe Interact **22,** 1043-1055.

Djébali, N., Mhadhbi, H., Lafitte, C., Dumas, B., Esquerré-Tugayé, M.-T., Aouani, M.E., and Jacquet, C. (2011). Hydrogen peroxide scavenging mechanisms are components of Medicago truncatula partial resistance to Aphanomyces euteiches. European Journal of Plant Pathology **131,** 559-571.

Dodds, P.N., Lawrence, G.J., Catanzariti, A.M., Teh, T., Wang, C.I., Ayliffe, M.A., Kobe, B., and Ellis, J.G. (2006). Direct protein interaction underlies gene-for-gene specificity and coevolution of the flax resistance genes and flax rust avirulence genes. Proc Natl Acad Sci U S A **103,** 8888-8893.

Donnelly, M.A., and Steiner, T.S. (2002). Two nonadjacent regions in enteroaggregative Escherichia coli flagellin are required for activation of toll-like receptor 5. J Biol Chem **277,** 40456-40461.

Dudareva, N., Pichersky, E., and Gershenzon, J. (2004). Biochemistry of plant volatiles. Plant Physiol **135,** 1893-1902.

Dudareva, N., Negre, F., Nagegowda, D.A., and Orlova, I. (2006). Plant Volatiles: Recent Advances and Future Perspectives. Critical Reviews in Plant Sciences **25,** 417-440.

Dussourd, D.E. (2003). Chemical Stimulants of Leaf-Trenching by Cabbage Loopers: Natural Products, Neurotransmitters, Insecticides, and Drugs. J Chem Ecol **29,** 2023-2047.

Eckstein-Ludwig, U., Webb, R.J., van Goethem, I.D.A., East, J.M., Lee, A.G., Kimura, M., O'Neill, P.M., Bray, P.G., Ward, S.A., and Krishna, S. (2003). Artemisinins target the SERCA of Plasmodium falciparum. Nature **424,** 957.

Endre, G., Kereszt, A., Kevei, Z., Mihacea, S., Kaló, P., and Kiss, G.B. (2002). A receptor kinase gene regulating symbiotic nodule development. Nature **417,** 962.

Engelberth, J., Alborn, H.T., Schmelz, E.A., and Tumlinson, J.H. (2004). Airborne signals prime plants against insect herbivore attack. Proc Natl Acad Sci U S A **101,** 1781-1785.

Engler, C., Kandzia, R., and Marillonnet, S. (2008). A One Pot, One Step, Precision Cloning Method with High Throughput Capability. PLoS One **3,** e3647.

Farmer, E.E. (2001). Surface-to-air signals. Nature **411,** 854.

Felix, G., Duran, J.D., Volko, S., and Boller, T. (1999). Plants have a sensitive perception system for the most conserved domain of bacterial flagellin. Plant J **18,** 265-276.

Fesel, P.H., and Zuccaro, A. (2016). β-glucan: Crucial component of the fungal cell wall and elusive MAMP in plants. Fungal Genetics and Biology **90,** 53-60.

Filipowicz, W. (2005). RNAi: the nuts and bolts of the RISC machine. Cell **122,** 17-20.

Fisher, M.C., Henk, D.A., Briggs, C.J., Brownstein, J.S., Madoff, L.C., McCraw, S.L., and Gurr, S.J. (2012). Emerging fungal threats to animal, plant and ecosystem health. Nature **484,** 186-194.

Fridman, E., Wang, J., Iijima, Y., Froehlich, J.E., Gang, D.R., Ohlrogge, J., and Pichersky, E. (2005). Metabolic, genomic, and biochemical analyses of glandular trichomes from the wild tomato species Lycopersicon hirsutum identify a key enzyme in the biosynthesis of methylketones. Plant Cell **17,** 1252-1267.

Frost, C.J., Appel, H.M., Carlson, J.E., De Moraes, C.M., Mescher, M.C., and Schultz, J.C. (2007). Within-plant signalling via volatiles overcomes vascular constraints on systemic signalling and primes responses against herbivores. Ecol Lett **10,** 490-498.

Fry, W.E., Grunwald, N.J. (2010). Introduction to Oomycetes. The Plant Health Instructor. DOI:10.1094/PHI-I-2010-1207-01.

Available:http://www.apsnet.org/edcenter/intropp/PathogenGroups/Pages/IntroOomycetes.aspx

Gang, D.R. (2005). Evolution of flavors and scents. Annu Rev Plant Biol **56,** 301-325.

Gang, D.R., Beuerle, T., Ullmann, P., Werck-Reichhart, D., and Pichersky, E. (2002). Differential production of meta hydroxylated phenylpropanoids in sweet basil peltate glandular trichomes and leaves is controlled by the activities of specific acyltransferases and hydroxylases. Plant Physiol **130,** 1536-1544.

Garms, S., Kollner, T.G., and Boland, W. (2010). A multiproduct terpene synthase from Medicago truncatula generates cadalane sesquiterpenes via two different mechanisms. J Org Chem **75,** 5590-5600.

Gassmann, A.J., and Hare, J.D. (2005). Indirect cost of a defensive trait: variation in trichome type affects the natural enemies of herbivorous insects on Datura wrightii. Oecologia **144,** 62-71.

Gaulin, E., Jacquet, C., Bottin, A., and Dumas, B. (2007). Root rot disease of legumes caused by Aphanomyces euteiches. Mol Plant Pathol **8,** 539-548.

Gaulin, E., Madoui, M.A., Bottin, A., Jacquet, C., Mathe, C., Couloux, A., Wincker, P., and Dumas, B. (2008). Transcriptome of Aphanomyces euteiches: new oomycete putative pathogenicity factors and metabolic pathways. PLoS One **3,** e1723.

Gaulin, E., Pel, M.J.C., Camborde, L., San-Clemente, H., Courbier, S., Dupouy, M.-A., Lengellé, J., Veyssiere, M., Le Ru, A., Grandjean, F., Cordaux, R., Moumen, B., Gilbert, C., Cano, L.M., Aury, J.-M., Guy, J., Wincker, P., Bouchez, O., Klopp, C., and Dumas, B. (2018). Genomics analysis of Aphanomyces spp. identifies a new class of oomycete effector associated with host adaptation. BMC Biology **16,** 43.

Gehrig, H., Schussler, A., and Kluge, M. (1996). Geosiphon pyriforme, a fungus forming endocytobiosis with Nostoc (cyanobacteria), is an ancestral member of the Glomales: evidence by SSU rRNA analysis. Journal of molecular evolution **43,** 71-81.

Genre, A., Chabaud, M., Timmers, T., Bonfante, P., and Barker, D.G. (2005). Arbuscular mycorrhizal fungi elicit a novel intracellular apparatus in Medicago truncatula root epidermal cells before infection. Plant Cell **17,** 3489-3499.

Gershenzon, J., and Dudareva, N. (2007). The function of terpene natural products in the natural world. Nat Chem Biol **3,** 408-414.

Gershenzon, J., McCaskill, D., Rajaonarivony, J.I., Mihaliak, C., Karp, F., and Croteau, R. (1992). Isolation of secretory cells from plant glandular trichomes and their use in biosynthetic studies of monoterpenes and other gland products. Analytical biochemistry **200,** 130-138.

Giovannetti, M., Mari, A., Novero, M., and Bonfante, P. (2015). Early Lotus japonicus root transcriptomic responses to symbiotic and pathogenic fungal exudates. Front Plant Sci **6,** 480.

Girardin, S.E., Sansonetti, P.J., and Philpott, D.J. (2002). Intracellular vs extracellular recognition of pathogens--common concepts in mammals and flies. Trends in microbiology **10,** 193-199.

Glazebrook, J. (2005). Contrasting mechanisms of defense against biotrophic and necrotrophic pathogens. Annu Rev Phytopathol **43,** 205-227.

Gobbato, E., Wang, E., Higgins, G., Bano, S.A., Henry, C., Schultze, M., and Oldroyd, G.E. (2013). RAM1 and RAM2 function and expression during arbuscular mycorrhizal symbiosis and Aphanomyces euteiches colonization. Plant Signal Behav **8** (10):e26049.

Gobbato, E., Marsh, J.F., Vernie, T., Wang, E., Maillet, F., Kim, J., Miller, J.B., Sun, J., Bano, S.A., Ratet, P., Mysore, K.S., Denarie, J., Schultze, M., and Oldroyd, G.E. (2012). A GRAS-type transcription factor with a specific function in mycorrhizal signaling. Curr Biol **22,** 2236-2241.

Godfray, H.C.J., Beddington, J.R., Crute, I.R., Haddad, L., Lawrence, D., Muir, J.F., Pretty, J., Robinson, S., Thomas, S.M., and Toulmin, C. (2010). Food Security: The Challenge of Feeding 9 Billion People. Science **327,** 812-818.

Gohre, V., and Robatzek, S. (2008). Breaking the barriers: microbial effector molecules subvert plant immunity. Annu Rev Phytopathol **46,** 189-215.

Gomez-Gomez, L., and Boller, T. (2000). FLS2: an LRR receptor-like kinase involved in the perception of the bacterial elicitor flagellin in Arabidopsis. Molecular cell **5,** 1003-1011.

Gomez, S.K., Cox, M.M., Bede, J.C., Inoue, K., Alborn, H.T., Tumlinson, J.H., and Korth, K.L. (2005). Lepidopteran herbivory and oral factors induce transcripts encoding novel terpene synthases in Medicago truncatula. Arch Insect Biochem Physiol **58,** 114-127.

Gonzalez-Lamothe, R., Mitchell, G., Gattuso, M., Diarra, M.S., Malouin, F., and Bouarab, K. (2009). Plant antimicrobial agents and their effects on plant and human pathogens. Int J Mol Sci **10,** 3400-3419.

Graham, P.H., and Vance, C.P. (2003). Legumes: importance and constraints to greater use. Plant Physiol **131,** 872-877.

Grandbastien, M.A., Audeon, C., Bonnivard, E., Casacuberta, J.M., Chalhoub, B., Costa, A.P., Le, Q.H., Melayah, D., Petit, M., Poncet, C., Tam, S.M., Van Sluys, M.A., and

Mhiri, C. (2005). Stress activation and genomic impact of Tnt1 retrotransposons in Solanaceae. Cytogenet Genome Res **110,** 229-241.

Grisebach, H., and Ebel, J. (1978). Phytoalexins, Chemical Defense Substances of Higher Plants? Angewandte Chemie International Edition in English **17,** 635-647.

Hamilton-Kemp, T.R., McCracken, C.T., Jr., Loughrin, J.H., Andersen, R.A., and Hildebrand, D.F. (1992). Effects of some natural volatile compounds on the pathogenic fungiAlternaria alternata and Botrytis cinerea. J Chem Ecol **18,** 1083-1091.

Hammer, K.A., Carson, C.F., and Riley, T.V. (2003). Antifungal activity of the components of Melaleuca alternifolia (tea tree) oil. Journal of Applied Microbiology **95,** 853-860.

Haney, C.H., and Long, S.R. (2010). Plant flotillins are required for infection by nitrogen-fixing bacteria. Proc Natl Acad Sci U S A **107,** 478-483.

Hara, K., Yagi, M., Kusano, T., and Sano, H. (2000). Rapid systemic accumulation of transcripts encoding a tobacco WRKY transcription factor upon wounding. Mol Gen Genet **263,** 30-37.

Heiden, A.C., Kobel, K., Langebartels, C., Schuh-Thomas, G., and Wildt, J. (2003). Emissions of Oxygenated Volatile Organic Compounds from Plants Part I: Emissions from Lipoxygenase Activity. Journal of Atmospheric Chemistry **45,** 143-172.

Heil, M. (2009). Damaged-self recognition in plant herbivore defence. Trends Plant Sci **14,** 356-363.

Heil, M., and Silva Bueno, J.C. (2007). Within-plant signaling by volatiles leads to induction and priming of an indirect plant defense in nature. Proc Natl Acad Sci U S A **104,** 5467-5472.

Heil, M., and Karban, R. (2010). Explaining evolution of plant communication by airborne signals. Trends Ecol Evol **25,** 137-144.

Helliwell, C.A., Poole, A., James Peacock, W., and Dennis, E.S. (1999). Arabidopsis ent-Kaurene Oxidase Catalyzes Three Steps of Gibberellin Biosynthesis. Plant Physiol **119,** 507.

Helliwell, C.A., Sheldon, C.C., Olive, M.R., Walker, A.R., Zeevaart, J.A.D., Peacock, W.J., and Dennis, E.S. (1998). Cloning of the Arabidopsis ent-Kaurene Oxidase Gene GA3 Proc Natl Acad Sci U S A **95,** 9019.

Hernandez-Pinzon, I., Cifuentes, M., Henaff, E., Santiago, N., Espinas, M.L., and Casacuberta, J.M. (2012). The Tnt1 retrotransposon escapes silencing in tobacco, its natural host. PLoS One **7,** e33816.

Hirsch, S., Kim, J., Munoz, A., Heckmann, A.B., Downie, J.A., and Oldroyd, G.E. (2009). GRAS proteins form a DNA binding complex to induce gene expression during nodulation signaling in Medicago truncatula. Plant Cell **21,** 545-557.

Hoffmann, B., Trinh, T.H., Leung, J., Kondorosi, A., and Kondorosi, E. (1997). A New Medicago truncatula Line with Superior in Vitro Regeneration, Transformation, and Symbiotic Properties Isolated Through Cell Culture Selection. Mol Plant Microbe Interact **10(3),** 307-315.

Huang, M., Sanchez-Moreiras, A.M., Abel, C., Sohrabi, R., Lee, S., Gershenzon, J., and Tholl, D. (2012). The major volatile organic compound emitted from Arabidopsis thaliana flowers, the sesquiterpene (E)-beta-caryophyllene, is a defense against a bacterial pathogen. New Phytologist **193,** 997-1008.

Huckelhoven, R. (2007). Cell wall-associated mechanisms of disease resistance and susceptibility. Annu Rev Phytopathol **45,** 101-127.

Hughes, T., Teresa, J., and Grau, C. (2014). Aphanomyces root rot (common root rot) of legumes**,** https://www.apsnet.org/edcenter/intropp/lessons/fungi/Oomycetes/Pages/Aphanomyces.aspx.

Igiehon, N.O., and Babalola, O.O. (2018). Below-ground-above-ground Plant-microbial Interactions: Focusing on Soybean, Rhizobacteria and Mycorrhizal Fungi. Open Microbiol J **12,** 261-279.

Irmisch, S., Jiang, Y., Chen, F., Gershenzon, J., and Köllner, T.G. (2014). Terpene synthases and their contribution to herbivore-induced volatile emission in western balsam poplar (Populus trichocarpa). BMC Plant Biology **14,** 270.

Ji, W., Xu, P., Li, Z., Lu, J., Liu, L., Zhan, Y., Chen, Y., Hille, B., Xu, T., and Chen, L. (2008). Functional stoichiometry of the unitary calcium-release-activated calcium channel. Proc Natl Acad Sci U S A **105,** 13668-13673.

Jia, Q., Li, G., Köllner, T.G., Fu, J., Chen, X., Xiong, W., Crandall-Stotler, B.J., Bowman, J.L., Weston, D.J., Zhang, Y., Chen, L., Xie, Y., Li, F.-W., Rothfels, C.J., Larsson, A., Graham, S.W., Stevenson, D.W., Wong, G.K.-S., Gershenzon, J., and Chen, F. (2016). Microbial-type terpene synthase genes occur widely in nonseed land plants, but not in seed plants. Proc Natl Acad Sci U S A **113,** 12328-12333.

Jones, F.R., and Drechsler, C. (1927). Root rot of peas in the United States caused by Aphanomyces euteiches. Journal of Agricultural Research. 30:293-325.

Jones, J.D., and Dangl, J.L. (2006). The plant immune system. Nature **444,** 323-329.

Jones, K.E., Patel, N.G., Levy, M.A., Storeygard, A., Balk, D., Gittleman, J.L., and Daszak, P. (2008). Global trends in emerging infectious diseases. Nature **451,** 990-993.

Jordan, M.A., and Wilson, L. (2004). Microtubules as a target for anticancer drugs. Nature reviews. Cancer **4,** 253-265.

Karban, R. (2007). Experimental clipping of sagebrush inhibits seed germination of neighbours. Ecol Lett **10,** 791-797.

Keane, P.J., Kerr, A., and New, P.B. (1970). Crown gall of stone fruit. II. Identification and nomenclature of Agrobacterium isolates. Australian Journal of Biological Sciences **23,** 585-595.

Keeling, C.I., and Bohlmann, J. (2006). Genes, enzymes and chemicals of terpenoid diversity in the constitutive and induced defence of conifers against insects and pathogens. New Phytologist **170,** 657-675.

Keeling, C.I., Weisshaar, S., Ralph, S.G., Jancsik, S., Hamberger, B., Dullat, H.K., and Bohlmann, J. (2011). Transcriptome mining, functional characterization, and phylogeny of a large terpene synthase gene family in spruce (Picea spp.). BMC Plant Biol **11,** 43.

Kennedy, G.G. (2003). Tomato, pests, parasitoids, and predators: tritrophic interactions involving the genus Lycopersicon. Annu Rev Entomol **48,** 51-72.

Kessler, A., and Baldwin, I.T. (2001). Defensive function of herbivore-induced plant volatile emissions in nature. Science **291,** 2141-2144.

Kessler, A., and Baldwin, I.T. (2002). Plant responses to insect herbivory: the emerging molecular analysis. Annu Rev Plant Biol **53,** 299-328.

Kessler, A., Halitschke, R., Diezel, C., and Baldwin, I.T. (2006). Priming of plant defense responses in nature by airborne signaling between Artemisia tridentata and Nicotiana attenuata. Oecologia **148,** 280-292.

Kevei, Z., Lougnon, G., Mergaert, P., Horvath, G.V., Kereszt, A., Jayaraman, D., Zaman, N., Marcel, F., Regulski, K., Kiss, G.B., Kondorosi, A., Endre, G., Kondorosi, E., and Ane, J.M. (2007). 3-hydroxy-3-methylglutaryl coenzyme a reductase 1 interacts with NORK and is crucial for nodulation in Medicago truncatula. Plant Cell **19,** 3974-3989.

Koeck, M., Hardham, A.R., and Dodds, P.N. (2011). The role of effectors of biotrophic and hemibiotrophic fungi in infection. Cell Microbiol **13,** 1849-1857.

Koske, R.E. (1981). Multiple germination by spores of Gigaspora gigantea. Transactions of the British Mycological Society **76,** 328-330.

Kost, C., and Heil, M. (2006). Herbivore-induced plant volatiles induce an indirect defence in neighbouring plants. Journal of Ecology **94,** 619-628.

Kovacevic, N., Pavlovic, M., Menkovic, N., Tzakou, O., and Couladis, M. (2002). Composition of the essential oil from roots and rhizomes of Valeriana pancicii Halácsy & Bald. Flavour and Fragrance Journal **17,** 355-357.

Krishna, S., Woodrow, C.J., Staines, H.M., Haynes, R.K., and Mercereau-Puijalon, O. (2006). Re-evaluation of how artemisinins work in light of emerging evidence of in vitro resistance. Trends in molecular medicine **12,** 200-205.

Kroumova, A.B., and Wagner, G.J. (2003). Different elongation pathways in the biosynthesis of acyl groups of trichome exudate sugar esters from various solanaceous plants. Planta **216,** 1013-1021.

Kumar, A., and Bennetzen, J.L. (1999). Plant retrotransposons. Annual review of genetics **33,** 479-532.

Kunze, G., Zipfel, C., Robatzek, S., Niehaus, K., Boller, T., and Felix, G. (2004). The N terminus of bacterial elongation factor Tu elicits innate immunity in Arabidopsis plants. Plant Cell **16,** 3496-3507.

Langenheim, J.H. (1994). Higher plant terpenoids: A phytocentric overview of their ecological roles. J Chem Ecol **20,** 1223-1280.

Langlois-Meurinne, M., Gachon, C.M., and Saindrenan, P. (2005). Pathogen-responsive expression of glycosyltransferase genes UGT73B3 and UGT73B5 is necessary for resistance to Pseudomonas syringae pv tomato in Arabidopsis. Plant Physiol **139,** 1890-1901.

Levenfors, J.P., Wikström, M., Persson, L., and Gerhardson, B. (2003). Pathogenicity of Aphanomyces spp. from Different Leguminous Crops in Sweden. European Journal of Plant Pathology **109,** 535-543.

Li, A.X., and Steffens, J.C. (2000). An acyltransferase catalyzing the formation of diacylglucose is a serine carboxypeptidase-like protein. Proc Natl Acad Sci U S A **97,** 6902-6907.

Lim, E.K., and Bowles, D.J. (2004). A class of plant glycosyltransferases involved in cellular homeostasis. EMBO J **23,** 2915-2922.

Lindeberg, M., Cartinhour, S., Myers, C.R., Schechter, L.M., Schneider, D.J., and Collmer, A. (2006). Closing the circle on the discovery of genes encoding Hrp regulon members and type III secretion system effectors in the genomes of three model Pseudomonas syringae strains. Mol Plant Microbe Interact **19,** 1151-1158.

Lo Presti, L., Lanver, D., Schweizer, G., Tanaka, S., Liang, L., Tollot, M., Zuccaro, A., Reissmann, S., and Kahmann, R. (2015a). Fungal effectors and plant susceptibility. Annu Rev Plant Biol **66,** 513-545.

Ma, D., Pu, G., Lei, C., Ma, L., Wang, H., Guo, Y., Chen, J., Du, Z., Wang, H., Li, G., Ye, H., and Liu, B. (2009). Isolation and characterization of AaWRKY1, an Artemisia annua transcription factor that regulates the amorpha-4,11-diene synthase gene, a key gene of artemisinin biosynthesis. Plant Cell Physiol **50,** 2146-2161.

Mackey, D., Holt, B.F., 3rd, Wiig, A., and Dangl, J.L. (2002). RIN4 interacts with Pseudomonas syringae type III effector molecules and is required for RPM1-mediated resistance in Arabidopsis. Cell **108,** 743-754.

Maillet, F., Poinsot, V., Andre, O., Puech-Pages, V., Haouy, A., Gueunier, M., Cromer, L., Giraudet, D., Formey, D., Niebel, A., Martinez, E.A., Driguez, H., Becard, G., and Denarie, J. (2011). Fungal lipochitooligosaccharide symbiotic signals in arbuscular mycorrhiza. Nature **469,** 58-63.

Marsh, J.F., Rakocevic, A., Mitra, R.M., Brocard, L., Sun, J., Eschstruth, A., Long, S.R., Schultze, M., Ratet, P., and Oldroyd, G.E. (2007). Medicago truncatula NIN is essential for rhizobial-independent nodule organogenesis induced by autoactive calcium/calmodulin-dependent protein kinase. Plant Physiol **144,** 324-335.

Martin, D.M. (2003). Induction of Volatile Terpene Biosynthesis and Diurnal Emission by Methyl Jasmonate in Foliage of Norway Spruce. Plant Physiol **132,** 1586-1599.

Mauch, F., Mauch-Mani, B., and Boller, T. (1988). Antifungal Hydrolases in Pea Tissue : II. Inhibition of Fungal Growth by Combinations of Chitinase and beta-1,3-Glucanase. Plant Physiol **88,** 936-942.

Medzhitov, R., and Janeway, C.A., Jr. (2002). Decoding the patterns of self and nonself by the innate immune system. Science **296,** 298-300.

Mélida, H., Sandoval-Sierra, J.V., Diéguez-Uribeondo, J., and Bulone, V. (2013). Analyses of extracellular carbohydrates in oomycetes unveil the existence of three different cell wall types. Eukaryotic cell **12,** 194-203.

Mewalal, R., Rai, D.K., Kainer, D., Chen, F., Kulheim, C., Peter, G.F., and Tuskan, G.A. (2017). Plant-Derived Terpenes: A Feedstock for Specialty Biofuels. Trends Biotechnol **35,** 227-240.

Miedes, E., Vanholme, R., Boerjan, W., and Molina, A. (2014). The role of the secondary cell wall in plant resistance to pathogens. Front Plant Sci **5,** 358.

Miller, J.B., Pratap, A., Miyahara, A., Zhou, L., Bornemann, S., Morris, R.J., and Oldroyd, G.E. (2013). Calcium/Calmodulin-dependent protein kinase is negatively and positively regulated by calcium, providing a mechanism for decoding calcium responses during symbiosis signaling. Plant Cell **25,** 5053-5066.

Mithofer, A., and Boland, W. (2012). Plant defense against herbivores: chemical aspects. Annu Rev Plant Biol **63,** 431-450.

Molnar, A., Bassett, A., Thuenemann, E., Schwach, F., Karkare, S., Ossowski, S., Weigel, D., and Baulcombe, D. (2009). Highly specific gene silencing by artificial microRNAs in the unicellular alga Chlamydomonas reinhardtii. Plant J **58,** 165-174.

Muhlemann, J.K., Klempien, A., and Dudareva, N. (2014). Floral volatiles: from biosynthesis to function. Plant Cell Environ **37,** 1936-1949.

Mumm, R., and Dicke, M. (2010). Variation in natural plant products and the attraction of bodyguards involved in indirect plant defenseThe present review is one in the special series of reviews on animal–plant interactions. Canadian Journal of Zoology **88,** 628-667.

Nakamura, S., and Hatanaka, A. (2002). Green-Leaf-Derived C6-Aroma Compounds with Potent Antibacterial Action That Act on Both Gram-Negative and Gram-Positive Bacteria. Journal of Agricultural and Food Chemistry **50,** 7639-7644.

Naoumkina, M.A., Zhao, Q., Gallego-Giraldo, L., Dai, X., Zhao, P.X., and Dixon, R.A. (2010). Genome-wide analysis of phenylpropanoid defence pathways. Mol Plant Pathol **11,** 829-846.

Nars, A., Lafitte, C., Chabaud, M., Drouillard, S., Melida, H., Danoun, S., Le Costaouec, T., Rey, T., Benedetti, J., Bulone, V., Barker, D.G., Bono, J.J., Dumas, B., Jacquet, C., Heux, L., Fliegmann, J., and Bottin, A. (2013). Aphanomyces euteiches cell wall fractions containing novel glucan-chitosaccharides induce defense genes and nuclear calcium oscillations in the plant host Medicago truncatula. PLoS One **8,** e75039.

Ning, Y., Liu, W., and Wang, G.L. (2017). Balancing Immunity and Yield in Crop Plants. Trends Plant Sci **22,** 1069-1079.

Nolan, K.E., Rose, R.J., and Gorst, J.R. (1989). Regeneration of Medicago truncatula from tissue culture: increased somatic embryogenesis using explants from regenerated plants. Plant Cell Reports **8,** 278-281.

Nurnberger, T., Brunner, F., Kemmerling, B., and Piater, L. (2004). Innate immunity in plants and animals: striking similarities and obvious differences. Immunological reviews **198,** 249-266.

Oerke, E.C. (2005). Crop losses to pests. The Journal of Agricultural Science **144,** 31-43.

Okinaka, Y., Mimori, K., Takeo, K., Kitamura, S., Takeuchi, Y., Yamaoka, N., and Yoshikawa, M. (1995). A structural model for the mechanisms of elicitor release from fungal cell walls by plant beta-1,3-endoglucanase. Plant Physiol **109,** 839-845.

Oldroyd, G.E. (2013). Speak, friend, and enter: signalling systems that promote beneficial symbiotic associations in plants. Nat Rev Microbiol **11,** 252-263.

Orians, C. (2005). Herbivores, vascular pathways, and systemic induction: facts and artifacts. J Chem Ecol **31,** 2231-2242.

Ossowski, S., Schwab, R., and Weigel, D. (2008). Gene silencing in plants using artificial microRNAs and other small RNAs. Plant J **53,** 674-690.

Pandey, S.P., and Somssich, I.E. (2009). The role of WRKY transcription factors in plant immunity. Plant Physiol **150,** 1648-1655.

Parker, M.T., Zhong, Y., Dai, X., Wang, S., and Zhao, P. (2014). Comparative genomic and transcriptomic analysis of terpene synthases in Arabidopsis and Medicago. IET Syst Biol **8,** 146-153.

Parniske, M. (2005). Plant-fungal associations: cue for the branching connection. Nature **435,** 750-751.

Parniske, M. (2008). Arbuscular mycorrhiza: the mother of plant root endosymbioses. Nat Rev Microbiol **6,** 763-775.

Phillips, M.A., and Croteau, R.B. (1999). Resin-based defenses in conifers. Trends Plant Sci **4,** 184-190.

Phukan, U.J., Jeena, G.S., and Shukla, R.K. (2016). WRKY Transcription Factors: Molecular Regulation and Stress Responses in Plants. Front Plant Sci **7,** 760.

Pichersky, E., Noel, J.P., and Dudareva, N. (2006). Biosynthesis of plant volatiles: nature's diversity and ingenuity. Science (New York, N.Y.) **311,** 808-811.

Pickett, J.A., and Khan, Z.R. (2016). Plant volatile-mediated signalling and its application in agriculture: successes and challenges. New Phytologist **212,** 856-870.

Pierik, R., Ballare, C.L., and Dicke, M. (2014). Ecology of plant volatiles: taking a plant community perspective. Plant Cell Environ **37,** 1845-1853.

Pieterse, C.M., Leon-Reyes, A., Van der Ent, S., and Van Wees, S.C. (2009). Networking by small-molecule hormones in plant immunity. Nat Chem Biol **5,** 308-316.

Pimentel, D., and Bellotti, A.C. (1976). Parasite-Host Population Systems and Genetic Stability. The American Naturalist **110,** 877-888.

Pina-Vaz, C., Goncalves Rodrigues, A., Pinto, E., Costa-de-Oliveira, S., Tavares, C., Salgueiro, L., Cavaleiro, C., Goncalves, M.J., and Martinez-de-Oliveira, J. (2004). Antifungal activity of Thymus oils and their major compounds. Journal of the European Academy of Dermatology and Venereology : JEADV **18,** 73-78.

Pinstrup-Andersen, P. (2001). The Future World Food Situation and the Role of Plant Diseases. The Plant Health Instructor. 10.1094/PHI-I-2001-0425-01.

Pollier, J., Moses, T., and Goossens, A. (2011). Combinatorial biosynthesis in plants: a (p)review on its potential and future exploitation. Nat Prod Rep **28,** 1897-1916.

Quandt, H.J. (1993). Transgenic root nodules of Vicia hirsuta: a fast and efficient system for the study of gene expression in indeterminate-type nodules. Mol Plant Microbe Interact, 6. 699. 10.1094/MPMI-6-699.

Radutoiu, S., Madsen, L.H., Madsen, E.B., Jurkiewicz, A., Fukai, E., Quistgaard, E.M.H., Albrektsen, A.S., James, E.K., Thirup, S., and Stougaard, J. (2007). LysM domains mediate lipochitin-oligosaccharide recognition and Nfr genes extend the symbiotic host range. EMBO J **26,** 3923-3935.

Rasmann, S., Köllner, T.G., Degenhardt, J., Hiltpold, I., Toepfer, S., Kuhlmann, U., Gershenzon, J., and Turlings, T.C.J. (2005). Recruitment of entomopathogenic nematodes by insect-damaged maize roots. Nature **434,** 732.

Rey, T., Nars, A., Bonhomme, M., Bottin, A., Huguet, S., Balzergue, S., Jardinaud, M.F., Bono, J.J., Cullimore, J., Dumas, B., Gough, C., and Jacquet, C. (2013). NFP, a LysM protein controlling Nod factor perception, also intervenes in Medicago truncatula resistance to pathogens. New Phytologist **198,** 875-886.

Rodriguez-Saona, C.R., Rodriguez-Saona, L.E., and Frost, C.J. (2009). Herbivore-induced volatiles in the perennial shrub, Vaccinium corymbosum, and their role in inter-branch signaling. J Chem Ecol **35,** 163-175.

Rose, R.J. (2008). Medicago truncatula as a model for understanding plant interactions with other organisms, plant development and stress biology: past, present and future. Functional Plant Biology **35,** 253-264.

Rose, R.J., Nolan, K.E., and Bicego, L. (1999). The Development of the Highly Regenerable Seed Line Jemalong 2HA for Transformation of Medicago truncatula — Implications for Regenerability via Somatic Embryogenesis. Journal of Plant Physiology **155,** 788-791.

Runyon, J.B., Mescher, M.C., and De Moraes, C.M. (2006). Volatile chemical cues guide host location and host selection by parasitic plants. Science **313,** 1964-1967.

Ruther, J., and Kleier, S. (2005). Plant-plant signaling: ethylene synergizes volatile emission in Zea mays induced by exposure to (Z)-3-hexen-1-ol. J Chem Ecol **31,** 2217-2222.

Samac, D.A., and Graham, M.A. (2007). Recent advances in legume-microbe interactions: recognition, defense response, and symbiosis from a genomic perspective. Plant Physiol **144,** 582-587.

Scala, A., Allmann, S., Mirabella, R., Haring, M.A., and Schuurink, R.C. (2013). Green leaf volatiles: a plant's multifunctional weapon against herbivores and pathogens. Int J Mol Sci **14,** 17781-17811.

Schilmiller, A.L., Last, R.L., and Pichersky, E. (2008). Harnessing plant trichome biochemistry for the production of useful compounds. Plant J **54,** 702-711.

Schilmiller, A.L., Miner, D.P., Larson, M., McDowell, E., Gang, D.R., Wilkerson, C., and Last, R.L. (2010). Studies of a biochemical factory: tomato trichome deep expressed sequence tag sequencing and proteomics. Plant Physiol **153,** 1212-1223.

Schnee, C., Kollner, T.G., Held, M., Turlings, T.C., Gershenzon, J., and Degenhardt, J. (2006). The products of a single maize sesquiterpene synthase form a volatile defense signal that attracts natural enemies of maize herbivores. Proc Natl Acad Sci U S A **103,** 1129-1134.

Schuler, M.A., and Werck-Reichhart, D. (2003). Functional genomics of P450s. Annu Rev Plant Biol **54,** 629-667.

Schultz, C.J., Kochian, L.V. & Harrison, M.J. (2010). Genetic variation for root architecture, nutrient uptake and mycorrhizal colonisation in Medicago truncatula accessions. Plant Soil **336**: 113-128

Schwab, R., Ossowski, S., Riester, M., Warthmann, N., and Weigel, D. (2006). Highly specific gene silencing by artificial microRNAs in Arabidopsis. Plant Cell **18,** 1121-1133.

Shen, Y., Liu, N., Li, C., Wang, X., Xu, X., Chen, W., Xing, G., and Zheng, W. (2017). The early response during the interaction of fungal phytopathogen and host plant. Open Biol **7**.

Silipo, A., Erbs, G., Shinya, T., Dow, J.M., Parrilli, M., Lanzetta, R., Shibuya, N., Newman, M.A., and Molinaro, A. (2010). Glyco-conjugates as elicitors or suppressors of plant innate immunity. Glycobiology **20,** 406-419.

Singh, D., and Agarwal, S.K. (1988). Himachalol andbeta-himachalene: Insecticidal principles of himalayan cedarwood oil. J Chem Ecol **14,** 1145-1151.

Smalla, K., Wieland, G., Buchner, A., Zock, A., Parzy, J., Kaiser, S., Roskot, N., Heuer, H., and Berg, G. (2001). Bulk and Rhizosphere Soil Bacterial Communities Studied by Denaturing Gradient Gel Electrophoresis: Plant-Dependent Enrichment and Seasonal Shifts Revealed. Applied and Environmental Microbiology **67,** 4742-4751.

Smil, V. (1999). Nitrogen in crop production: An account of global flows. Global Biogeochemical Cycles **13,** 647-662.

Spatafora, J.W., Chang, Y., Benny, G.L., Lazarus, K., Smith, M.E., Berbee, M.L., Bonito, G., Corradi, N., Grigoriev, I., Gryganskyi, A., James, T.Y., O'Donnell, K., Roberson, R.W., Taylor, T.N., Uehling, J., Vilgalys, R., White, M.M., and Stajich, J.E. (2016). A phylum-level phylogenetic classification of zygomycete fungi based on genome-scale data. Mycologia **108,** 1028-1046.

Staerk, D., Skole, B., Jorgensen, F.S., Budnik, B.A., Ekpe, P., and Jaroszewski, J.W. (2004). Isolation of a library of aromadendranes from Landolphia dulcis and its characterization using the VolSurf approach. Journal of natural products **67,** 799-805.

Steeghs, M., Bais, H.P., de Gouw, J., Goldan, P., Kuster, W., Northway, M., Fall, R., and Vivanco, J.M. (2004). Proton-transfer-reaction mass spectrometry as a new tool for real time analysis of root-secreted volatile organic compounds in Arabidopsis. Plant Physiol **135,** 47-58.

Steele, C.L., Katoh, S., Bohlmann, J., and Croteau, R. (1998). Regulation of Oleoresinosis in Grand Fir (Abies grandis). Differential transcriptional control of monoterpene, sesquiterpene, and diterpene synthase genes in response to wounding. Plant Physiol vol. **116**,4 (1998): 1497-504.

Stracke, S., Kistner, C., Yoshida, S., Mulder, L., Sato, S., Kaneko, T., Tabata, S., Sandal, N., Stougaard, J., Szczyglowski, K., and Parniske, M. (2002). A plant receptor-like kinase required for both bacterial and fungal symbiosis. Nature **417,** 959-962.

Sugimoto, K., Matsui, K., Iijima, Y., Akakabe, Y., Muramoto, S., Ozawa, R., Uefune, M., Sasaki, R., Alamgir, K.M., Akitake, S., Nobuke, T., Galis, I., Aoki, K., Shibata, D., and Takabayashi, J. (2014). Intake and transformation to a glycoside of (Z)-3-hexenol from infested neighbors reveals a mode of plant odor reception and defense. Proc Natl Acad Sci U S A **111** (19) 7144-7149.

Sugiyama, A., and Yazaki, K. (2012). Root Exudates of Legume Plants and Their Involvement in Interactions with Soil Microbes. In: Vivanco J., Baluška F. (eds) Secretions and Exudates in Biological Systems. Signaling and Communication in Plants, vol 12. Springer, Berlin, Heidelberg. pp. 27-48.

Tadege, M., Ratet, P., and Mysore, K.S. (2005). Insertional mutagenesis: a Swiss Army knife for functional genomics of Medicago truncatula. Trends Plant Sci **10,** 229-235.

Tadege, M., Wen, J., He, J., Tu, H., Kwak, Y., Eschstruth, A., Cayrel, A., Endre, G., Zhao, P.X., Chabaud, M., Ratet, P., and Mysore, K.S. (2008). Large-scale insertional mutagenesis using the Tnt1 retrotransposon in the model legume Medicago truncatula. Plant J **54,** 335-347.

Takabayashi, J., and Dicke, M. (1996). Plant-carnivore mutualism through herbivore-induced carnivore attractants. Trends in Plant Sci **1,** 109-113.

Tanaka, Y., Sasaki, N., and Ohmiya, A. (2008). Biosynthesis of plant pigments: anthocyanins, betalains and carotenoids. Plant J **54,** 733-749.

Tang, H., Krishnakumar, V., Bidwell, S., Rosen, B., Chan, A., Zhou, S., Gentzbittel, L., Childs, K.L., Yandell, M., Gundlach, H., Mayer, K.F.X., Schwartz, D.C., and Town, C.D. (2014). An improved genome release (version Mt4.0) for the model legume Medicago truncatula. BMC Genomics **15,** 312.

Thakore, Y. (2006). The biopesticide market for global agricultural use. Industrial Biotechnology **2,** 194-208.

Theis, N., and Lerdau, M. (2003). The Evolution of Function in Plant Secondary Metabolites. International Journal of Plant Sciences **164,** S93-S102.

Thines, M., and Kamoun, S. (2010). Oomycete-plant coevolution: recent advances and future prospects. Curr Opin Plant Biol **13,** 427-433.

Tholl, D. (2015). Biosynthesis and biological functions of terpenoids in plants. Advances in Biochemical Engineering/Biotechnology **148,** 63-106.

Tholl, D., and Lee, S. (2011). Terpene Specialized Metabolism in Arabidopsis thaliana. The Arabidopsis book **9,** e0143-e0143.

Thomas, M.R., Rose, R.J., and Nolan, K.E. (1992). Genetic transformation of Medicago truncatula using Agrobacterium with genetically modified Ri and disarmed Ti plasmids. Plant Cell Reports **11,** 113-117.

Tisserant, E., Malbreil, M., Kuo, A., Kohler, A., Symeonidi, A., Balestrini, R., Charron, P., Duensing, N., Frei dit Frey, N., Gianinazzi-Pearson, V., Gilbert, L.B., Handa, Y., Herr, J.R., Hijri, M., Koul, R., Kawaguchi, M., Krajinski, F., Lammers, P.J., Masclaux, F.G., Murat, C., Morin, E., Ndikumana, S., Pagni, M., Petitpierre, D., Requena, N., Rosikiewicz, P., Riley, R., Saito, K., San Clemente, H., Shapiro, H., van Tuinen, D., Becard, G., Bonfante, P., Paszkowski, U., Shachar-Hill, Y.Y., Tuskan, G.A., Young, J.P., Sanders, I.R., Henrissat, B., Rensing, S.A., Grigoriev, I.V., Corradi, N., Roux, C., and Martin, F. (2013). Genome of an arbuscular mycorrhizal fungus provides insight into the oldest plant symbiosis. Proc Natl Acad Sci U S A **110,** 20117-20122.

Torres, M.A., Jones, J.D., and Dangl, J.L. (2006). Reactive oxygen species signaling in response to pathogens. Plant Physiol **141,** 373-378.

Torto, T.A., Li, S., Styer, A., Huitema, E., Testa, A., Gow, N.A., van West, P., and Kamoun, S. (2003). EST mining and functional expression assays identify extracellular effector proteins from the plant pathogen Phytophthora. Genome research **13,** 1675-1685.

Tretner, C., Huth, U., and Hause, B. (2008). Mechanostimulation of Medicago truncatula leads to enhanced levels of jasmonic acid. J Exp Bot **59,** 2847-2856.

Turlings, T.C., Tumlinson, J.H., and Lewis, W.J. (1990). Exploitation of herbivore-induced plant odors by host-seeking parasitic wasps. Science **250,** 1251-1253.

Turlings, T.C.J., and Benrey, B. (1998). Effects of plant metabolites on the behavior and development of parasitic wasps. Écoscience **5,** 321-333.

Turlings, T.C.J., Lengwiler, U.B., Bernasconi, M.L., and Wechsler, D. (1998). Timing of induced volatile emissions in maize seedlings. Planta **207,** 146-152.

Van Den Boom, C.E.M., Van Beek, T.A., Posthumus, M.A., De Groot, A., and Dicke, M. (2004). Qualitative and Quantitative Variation Among Volatile Profiles Induced by Tetranychus urticae Feeding on Plants from Various Families. J Chem Ecol **30,** 69-89.

Van der Biezen, E.A., and Jones, J.D. (1998). Plant disease-resistance proteins and the gene-for-gene concept. Trends in biochemical sci **23,** 454-456.

VanEtten, H.D., Mansfield, J.W., Bailey, J.A., and Farmer, E.E. (1994). Two Classes of Plant Antibiotics: Phytoalexins versus "Phytoanticipins". Plant cell **6,** 1191-1192.

Vaughan, M.M., Wang, Q., Webster, F.X., Kiemle, D., Hong, Y.J., Tantillo, D.J., Coates, R.M., Wray, A.T., Askew, W., O'Donnell, C., Tokuhisa, J.G., and Tholl, D. (2013). Formation of the unusual semivolatile diterpene rhizathalene by the Arabidopsis class I terpene synthase TPS08 in the root stele is involved in defense against belowground herbivory. Plant Cell **25,** 1108-1125.

Venkateshwaran, M., Jayaraman, D., Chabaud, M., Genre, A., Balloon, A.J., Maeda, J., Forshey, K., den Os, D., Kwiecien, N.W., Coon, J.J., Barker, D.G., and Ané, J.-M. (2015). A role for the mevalonate pathway in early plant symbiotic signaling. Proc Natl Acad Sci U S A. **112,** 9781.

Vogt, T., and Jones, P. (2000). Glycosyltransferases in plant natural product synthesis: characterization of a supergene family. Trends Plant Sci **5,** 380-386.

Voirin, B., Bayet, C., and Colson, M. (1993). Demonstration that flavone aglycones accumulate in the peltate glands of Mentha x piperita leaves. Phytochemistry **34,** 85-87.

Waldmuller, T., Cosio, E.G., Grisebach, H., and Ebel, J. (1992). Release of highly elicitor-active glucans by germinating zoospores of Phytophthora megasperma f. sp. glycinea. Planta **188,** 498-505.

Wang, E., Schornack, S., Marsh, J.F., Gobbato, E., Schwessinger, B., Eastmond, P., Schultze, M., Kamoun, S., and Oldroyd, G.E. (2012). A common signaling process that promotes mycorrhizal and oomycete colonization of plants. Curr Biol **22,** 2242-2246.

Warthmann, N., Chen, H., Ossowski, S., Weigel, D., and Herve, P. (2008). Highly specific gene silencing by artificial miRNAs in rice. PLoS One **3,** e1829.

Werner, A., and Swan, D. (2010). What are natural antisense transcripts good for? Biochem Soc Trans **38,** 1144-1149.

Wessler, S.R. (2006). Transposable elements and the evolution of eukaryotic genomes. Proc Natl Acad Sci U S A **103,** 17600-17601.

Whipps, J.M. (2001). Microbial interactions and biocontrol in the rhizosphere. J Exp Bot **52,** 487-511.

Wicker, E., Hullé, M., and Rouxel, F. (2001). Pathogenic characteristics of isolates of Aphanomyces euteiches from pea in France. Plant Pathology **50,** 433-442.

Wise, M.L., Savage, T.J., Katahira, E., and Croteau, R. (1998). Monoterpene synthases from common sage (Salvia officinalis). cDNA isolation, characterization, and functional

expression of (+)-sabinene synthase, 1,8-cineole synthase, and (+)-bornyl diphosphate synthase. J Biol Chem **273,** 14891-14899.

Xu, Y.H., Wang, J.W., Wang, S., Wang, J.Y., and Chen, X.Y. (2004). Characterization of GaWRKY1, a cotton transcription factor that regulates the sesquiterpene synthase gene (+)-delta-cadinene synthase-A. Plant Physiol **135,** 507-515.

Yano, K., Yoshida, S., Muller, J., Singh, S., Banba, M., Vickers, K., Markmann, K., White, C., Schuller, B., Sato, S., Asamizu, E., Tabata, S., Murooka, Y., Perry, J., Wang, T.L., Kawaguchi, M., Imaizumi-Anraku, H., Hayashi, M., and Parniske, M. (2008). CYCLOPS, a mediator of symbiotic intracellular accommodation. Proc Natl Acad Sci U S A **105,** 20540-20545.

Yu, D., Chen, C., and Chen, Z. (2001). Evidence for an important role of WRKY DNA binding proteins in the regulation of NPR1 gene expression. Plant Cell **13,** 1527-1540.

Zhang, J., Yang, Y., Zheng, K., Xie, M., Feng, K., Jawdy, S.S., Gunter, L.E., Ranjan, P., Singan, V.R., Engle, N., Lindquist, E., Barry, K., Schmutz, J., Zhao, N., Tschaplinski, T.J., LeBoldus, J., Tuskan, G.A., Chen, J.G., and Muchero, W. (2018). Genome-wide association studies and expression-based quantitative trait loci analyses reveal roles of HCT2 in caffeoylquinic acid biosynthesis and its regulation by defense-responsive transcription factors in Populus. New Phytologist **220,** 502-516.

Zhao, J.Z., Cao, J., Li, Y., Collins, H.L., Roush, R.T., Earle, E.D., and Shelton, A.M. (2003). Transgenic plants expressing two Bacillus thuringiensis toxins delay insect resistance evolution. Nat Biotechnol **21,** 1493-1497.

Zinad, H.S., Natasya, I., and Werner, A. (2017). Natural Antisense Transcripts at the Interface between Host Genome and Mobile Genetic Elements. Front Microbiol **8,** 2292.

Zipfel, C. (2009). Early molecular events in PAMP-triggered immunity. Curr Opin Plant Biol **12,** 414-420.

Zipfel, C., and Felix, G. (2005). Plants and animals: a different taste for microbes? Curr Opin Plant Biol **8,** 353-360.

Zipfel, C., Robatzek, S., Navarro, L., Oakeley, E.J., Jones, J.D., Felix, G., and Boller, T. (2004). Bacterial disease resistance in Arabidopsis through flagellin perception. Nature **428,** 764-767.

VII. Appendix

VII.1 Tables

Tab.VII.1.1 Different plant growth medium used:

i. M-medium

Macro elements 20X	Stock Solution in 500 ml	Final Concentration mM
$MgSO_{4.7}H_2O$	7.31 gram	3.0
KNO_3	0.8 gram	0.79
KCl	0.65 gram	0.87
$Ca(NO_3)_2.4H_2O$	2.88 gram	1.22
Microelements 100 X		**µM**
KH_2PO_4	240 milligram	35.0
Na Fe EDTA	400 milligram	21.7
KI	37.5 milligram	4.5
$MnCl_2.4H_2O$	300 milligram	30.3
$ZnSO_4.7H_2O$	132.5 milligram	9.2
H_3BO_3	75 milligram	24.0
$CuSO_4.5H_2O$	6.5 milligram	0.5
$Na_2MoO_4.2H_2O$	120µl of solution 10mg/10ml	0.01
Vitamins 100X		**µM**
Glycine	150 milligram	40
Thiamin HCl	5 milligram	0.3
Pyridoxine HCl	5 milligram	0.5
Nicotinic Acid	25 milligram	4
Myo-inositol	2.5 gram	277
Sucrose		10 gram/L
Phytagel or Plant Agar		3 or 4 gram/L
pH		5.5

For 1 L M-Medium: 50 ml Macro-element (20 X), 10 ml Microelement t(100 X), 10 ml Vitamin solution (100 X) was used. Volume was adjusted with ddH_2O and pH adjusted to 5.5, autoclaved and used for experiments. (Bécard and Fortin 1988)

ii. MSR medium

Solution 1:Macro elements(for 1 L)	Amount (in gram)	Final Concentration µM
$MgSO_4._7H_2O$	73.9	2998
KNO_3	7.6	752
KCl	6.5	878
KH_2PO_4	0.41	30
Solution 2: Calcium Nitrate (1L)		
$Ca(NO_3)_2.4H_2O$	35.9	1521
Solution 3: Vitamins (500ml)		
Calcium panthotenate	0.09	1.88
Biotin	0.0001	0.004
Nicotinic Acid	0.1	8.12
Pyridoxine	0.09	5.32
Thiamine	0.1	2.96
Cyanocobalamine	0.04	0.25
Solution 4: NaFeEDTA(500ml)		
NaFeEDTA	0.16	
Solution 5: Microelements(500 ml)		
$MnSO_4.4H_2O$(100ml)	1.225	54.92
$ZnSO_4.7H_2O$(100ml)	0.14	4.869
H_3BO_3(100ml)	0.925	149.6
$CuSO_4.5H_2O$(100ml)	1.1	44
$Na_2MoO_4.2H_2O$(100ml)	0.12	4.96
$(NH_4)_6Mo_7O_{24}.4H_2O$	1.7	13.75

For 1 L M-Medium: 10 ml Solution 1, 10ml Solution 2, 5 ml Solution 3, 5 ml Solution 4, 1 ml Solution 5 and 4 gram of Plant Agar was used. Volume was adjusted with ddH_2O and pH adjusted to 6.5, autoclaved and used for experiments.

iii. Modified Fahreus medium (according to Boisson-Dernier et al., 2001)

Macro elements	Stock Solution	For 1 L mix	Final Concentration
$MgSO_4$	0.5 M	1 ml	0.5 mM
KH_2PO_4	0.7 M	29 µl	20 µM
NaH_2PO_4	0.4 M	25 µl	10 µM
$C_6H_5FeO_7$	20 mM	1 ml	20 µM
NH_4NO_3	1 M	1 ml	1 mM
$CaCl_2$ (after autoclave)	0.9 M	1 ml	0.9 mM
Microelements			
$MnCl_2$	1 mg/ml	33 µl	33 µg/l
$CuSO_4$	1mg/ml	33 µl	33 µg/l
$ZnCl_2$	1 mg/ml	7 µl	7 µg/l
H_3BO_3	1 mg/ml	100 µl	100 µg/l
Na_2MoO_4	1 mg/ml	33 µl	33 µg/l
Gelrite			11 g/L
200mg MES was added as buffer, pH adjusted to 7.4 and autoclaved. 25 mg/L Kanamycin was added for transgenic root selection.			

Tab.VII.1.2 Primers used for various purposes

Primer name	Sequence
Primers used for identification of *Tnt1* insertion in *TPS10*	
Tnt1 rev	GCTACCTCGTACTTTACTCC
TPS10-qPCR_F	CTCTAGGGAAGCTTCAGTTC
TPS10-qPCR_R	CTGTTGGCCTAAGACATTGC
Primers used for the identification of positive amiRNA clones via colony PCR	
ami921_Fwd	GTTCGTTTCGTCAATCCAGC
ami921_Rev	GAAACGACAATCTGATCGGG

Primer name	Sequence
Primers used for amiRNA cloning	
TPS10_I_miR	gtTTGATAGGTGAATGTACGCTTaaattggacacgcgtct
TPS10_II_miR	ttAAGCGTACATTCACCTATCAAacaaaaagatcaaggc
TPS10_III_miR	ttAAGCGTACATAGACCTATCACtctaaaaggaggtgatag
TPS10_IV_miR	gaGTGATAGGTCTATGTACGCTTaattaggttactagt
TPS10 _miR_A	CTGCAAGGCGATTAAGTTGGGTAAC
TPS10 _miR_B	GCGGATAACAATTTCACACAG
Primers used for cloning *TPS10* promoter	
Pro_TPS10_1	ttggtctcaacatggagcaccaaaatgcttacgtggcg
Pro_TPS10_2	ttggtctcaacaaGTAGGCTAATAGACTGATGATAACTAC
Pro_TPS10_3	ttggtctcaacatctacgcctgggagtttagataacattg
Pro_TPS10_4	ttggtctcaacaaCATTCTTCAAATTAATCAAAGGTGTTATAATAAGTGGCTC
Primers used for Stem-loop RT-PCR	
U6 Stemloop_RT	GTCGTATCCAGTGCAGGGTCCGAGGTATTCGCACTGGATACGACAAAATTTG
qRT U6_Fwd	CACGCATAAATCGAGAAATGGTC
TPS_stemloop_RT	GTCGTATCCAGTGCAGGGTCCGAGGTATTCGCACTGGATACGACAAGCG
TPS10_Stemloop_Fwd	GACGGCCTTGATAGGTGAATGT
Universal_qRT_Rev	CCAGTGCAGGGTCCGAGGT

Primer name	Sequence
Primers used for cloning *TPS10* genomic DNA	
TPS10-gen_1	ttggtctcaACATaatggctcccaaatctgacttgc
TPS10-gen_2	tt ggtctc a GTCTTTAAAAATAATTATTTCTCCATTTTGAACATAATTCTTATG
TPS10-gen_3	ttggtctcaagacaacctttgctctcttgctgtgc
TPS10-gen_4	ttggtctcaACAACATAAGATTACTTGATGACTGGTATAAAGAG
TPS10-gen_5	ttggtctcaacattatgtttaatacaattattagaaaaaaattattatatgcattgatatattgtaaatagttttat acagtcatctaatcaaatctcaccatagg
TPS10-gen_6	ttggtctcaACAACATCCTATCTCTTGCAAAAGGG
TPS10-gen_7	ttggtctcaACATgatggtggaaggtagtttttgg
TPS10-gen_8	ttggtctcaACAAATGCATAAAATAACATATCAGCCAACATGACC
TPS10-gen_9	ttggtctcaACATgcattgttttatggatatgttttgtcatgtatatttc
TPS10-gen_10	ttggtctcaACAACGAACGAATCAAACCACCACC
Primers used for identification of antisense- transcription from *Tnt1*	
cDNA_Tnt1	CAAGCTTATATGACTGAGGC
qRT_Fwd	GAAGAGTACATTCACCTATCAACAG
qRT_Rev	CCTGCCAATAACAATAGCAGC
Primers used for qPCR analysis	
*Mt-PT4*_Fwd	ACAAATTTGATAGGATTCTTTTGCACGT
*Mt-PT4*_Rev	TCACATCTTCTCAGTTCTTGAGTC
*Ri-ß-tubulin*_Fwd	CCAACTTATGGCGATCTCAACA
*Ri-ß-tubulin*_Rev	AAGACGTGGAAAAGGCACCA
*Ae_5.8s rRNA*_Fwd	TGTCTAGGCTCGCACATCGA
*Ae_5.8s rRNA*_Rev	AGTGCAATATGCGTTCAACGTTT
*His3-like*_Fwd	CTTTGCTTGGTGCTGTTTAGATGG
*His3-like*_Rev	ATTCCAAAGGCGGCTGCATA
*TPS10*_qRT_Fwd	CTCTAGGGAAGCTTCAGTTC

TPS10_qRT_Rev	CTGTTGGCCTAAGACATTGC
*Medtr2g098430_*Fwd	GGTTATGGGTGAGAGTAGTG
*Medtr2g098430_*Rev	CTCACGATCATTCAGTGTAG
*Medtr5g007550_*Fwd	TGTTAGACTCGTTGCTCGCT
*Medtr5g007550_*Rev	GAAAGGAAGGGACCGGAGAG
*Medtr8g104080_*Fwd	GCTGTGAGTTTGGGTGAGGT
*Medtr8g104080_*Rev	ACTACACCCCAGCACCATTT
*Actin2_*Fwd	ACTCACACCGTCACCAGAATCC
*Actin2_*Rev	TCAATGTGCCTGCCATGTATGT

Tab.VII.1.3 List of vector constructs made using golden gate modular cloning

Construct name	Destination vector	Construct description
pAGH55	pICH75055	CaMV *35 S*+ *tHMGCR*+ Nos Ter
pAGH56	pICH47732	Gal-promoter + *TPS10* + Ter
pAGH57	pICH47742	Gal-promoter + *FPS1*+ Ter
pAGH58	pICH47751	Gal-promoter + *tHMGCR* + Ter
pAGH59	pAGT564	*TPS10* + *FPS1*+ *tHMGCR* +Ter
pAGH92	pAGHT564	*FPS1* + *tHMGCR* + Ter
pAGH272	pAGM1311	*TPS10* promoter Fragment 1
pAGH273	pAGM1311	*TPS10* promoter Fragment 2
pAGH274	pICH41295	*TPS10* complete promoter
pAGH275	pICH47742	Promoter *TPS10* + *GUS with introns*+ Ter
pAGH292	pICH47742	Promoter *TPS10* + *TPS CDS*+ Ter
pAGH293	pAGM4673	DsRed + Promoter *TPS10* + *GUS* with introns+ Ter
pAGH294	pAGM4673	DsRed + Promoter *TPS10* + *TPS CDS*+ Ter
pAGH515	pAGM1311	*TPS10* genomic fragment 1
pAGH516	pAGM1311	*TPS10* genomic fragment 2
pAGH517	pAGM1311	*TPS10* genomic fragment 3
pAGH518	pAGM1311	*TPS10* genomic fragment 4
pAGH519	pAGM1287	*TPS10* genomic complete
pAGH520	pICH47742	*TPS10* Promoter + *TPS10* genomic + 4X Myc + Ter
pAGH521	pAGM4673	DsRed + *TPS10 Promoter* + *TPS10 genomic* + 4X Myc + Ter

Tab.VII.1.4 Buffers used for protoplast isolation and transformation (provided by Hagen Stellmach)

W5								
component	stock conc.	final conc.	50 ml	100 ml	200 ml	400 ml	500 ml	
NaCl	5 M	154 mM	1,54	3,08	6,16	12,32	15,4	ml
CaCl$_2$	1 M	125 mM	6,25	12,5	25	50	62,5	ml
KCl	0,1 M	5 mM	2,5	5	10	20	25	ml
MES pH 5.7	0,2 M	2 mM	0,5	1	2	4	5	ml
H$_2$O			39,21	78,42	156,84	313,68	392,1	ml
WI								
component	stock conc.	final conc.	5 ml	10 ml	15 ml	20 ml	30 ml	40 ml
mannitol	0,8 M	0,5 mM	3,15	6,3	9,45	12,6	18,9	25,2	ml
KCl	0,1 M	20 mM	1	2	3	4	6	8	ml
MES pH 5.7	0,2 M	4 mM	0,1	0,2	0,3	0,4	0,6	0,8	ml
H$_2$O			0,75	1,5	2,25	3	4,5	6	ml
MMG								
component	stock conc.	final conc.	5 ml	10 ml	15 ml	20 ml	30 ml	40 ml
mannitol	0,8 M	0,4 M	2,5	5	7,5	10	15	20	ml
MgCl$_2$	0,15 M	15 mM	0,5	1	1,5	2	3	4	ml
MES pH 5.7	0,2 M	4 mM	0,1	0,2	0,3	0,4	0,6	0,8	ml
H$_2$O			1,9	3,8	5,7	7,6	11,4	15,2	ml
PEG								
component	stock conc.	final conc.	5 ml	10 ml	15 ml	20 ml	30 ml	40 ml
mannitol	0,8 M	0,2 M	1,25	2,5	3,75	5	7,5	10	ml
CaCl$_2$	1 M	0,1 M	0,5	1	1,5	2	3	4	ml
PEG	solid	40 %	2	4	6	8	12	16	g
H$_2$O			1,5	3	4,5	6	9	12	ml
enzyme soln.								
component	stock conc.	final conc.	5 ml	10 ml	15 ml	20 ml	30 ml	40 ml
mannitol	0,8 M	0,4 M	2,5	5	7,5	10	15	20	ml
KCl	0,1 M	20 mM	1	2	3	4	6	8	ml
MES pH 5.7	0,2 M	20 mM	0,5	1	1,5	2	3	4	ml
H$_2$O			0,95	1,9	2,85	3,8	5,7	7,6	ml
cellulase R10		1,50%	75	150	225	300	450	600	mg
macerozyme R10		0,40%	20	40	60	80	120	160	mg
CaCl$_2$	1 M	10 mM	50	100	150	200	300	400	µl
BSA	0,1 g/ml	1 mg/ml	50	100	150	200	300	400	µl

VII.2 Figures
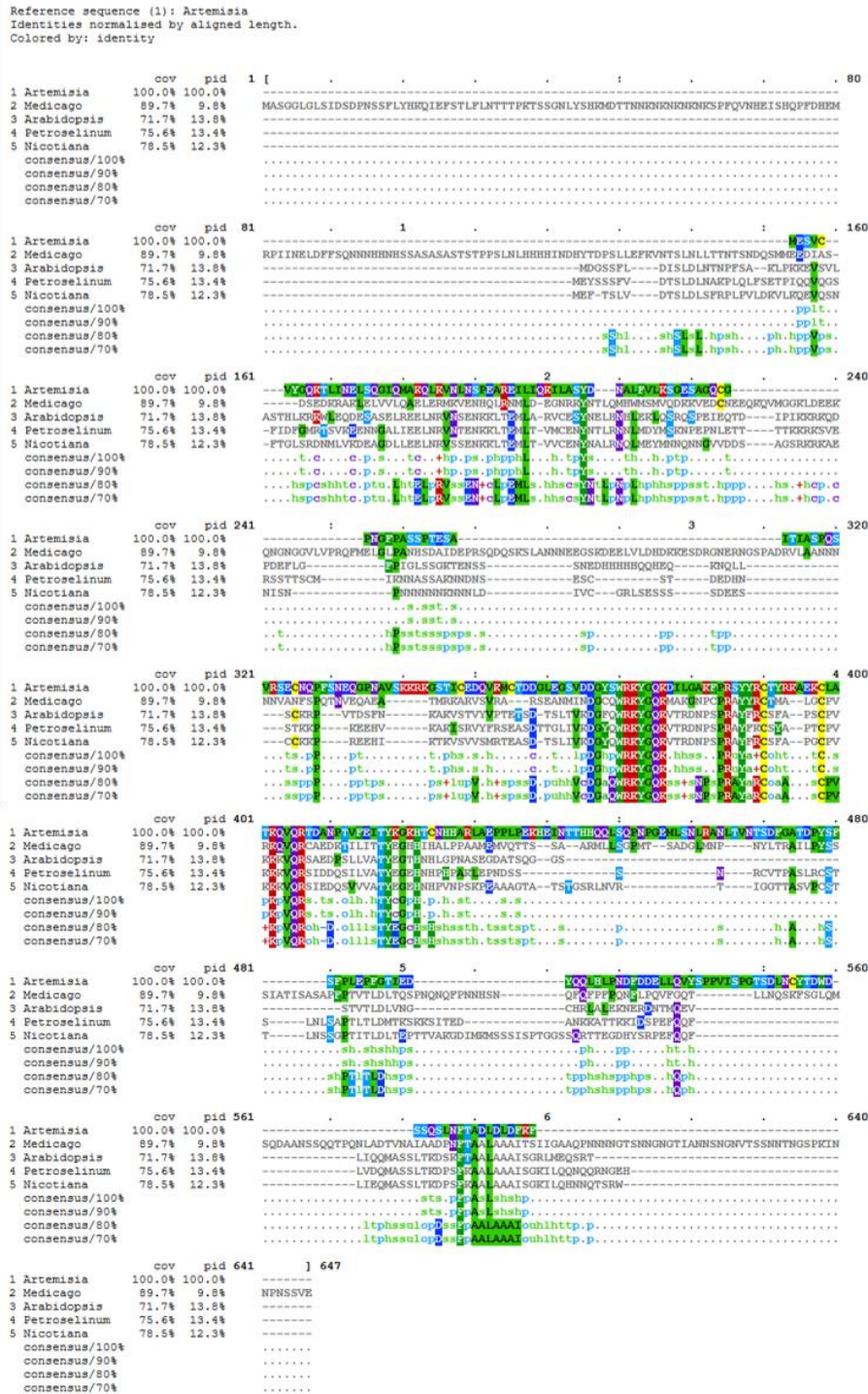
Fig.VII.2.1 Alignment of M. truncatula WRKY1 with other WRKYs. The amino acid sequence of MtWRKY1 was aligned with WRKYs from *Arabidopsis*, Artemisia, Nicotiana and Petroselinum using Clustal Omega (https://www.ebi.ac.uk/Tools/msa/clustalo/) and the color shading was performed using MView function provided by EMBL-EBI website.

Fig.VII.2.2 Domain analysis of TPS10: The amino acid sequence of TPS10 was analyzed for domains using NCBI conserved domain search.
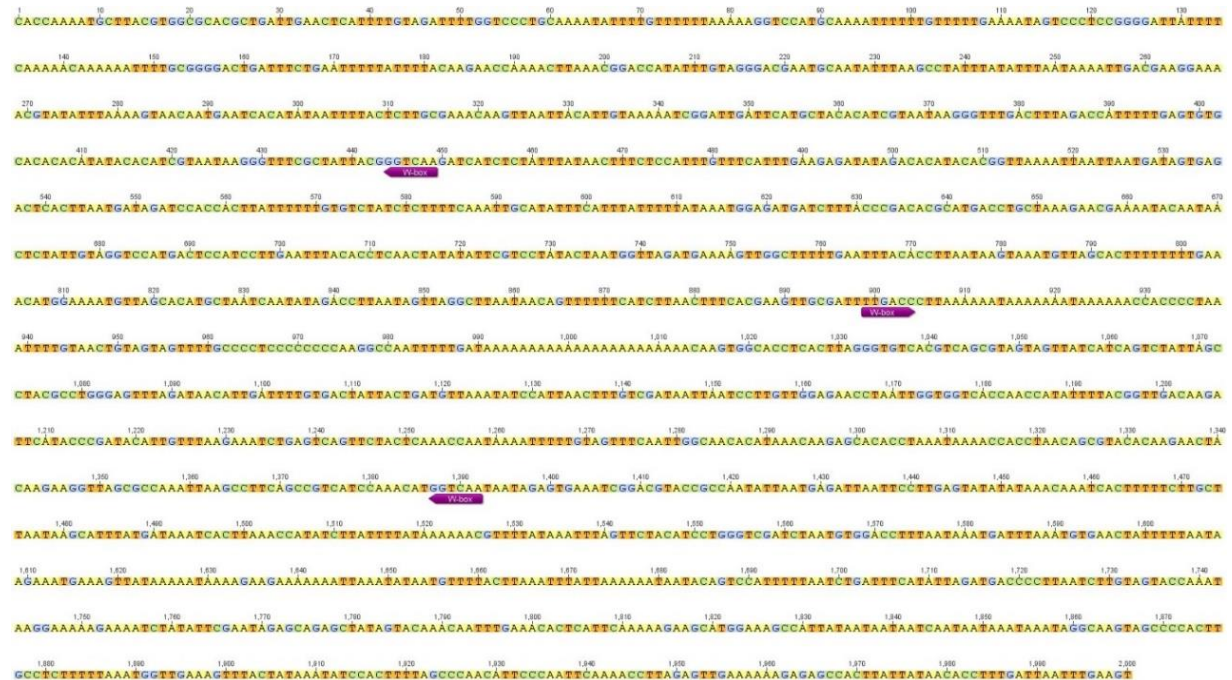
Fig.VII.2.3 Promoter analysis of *MtTPS10*: The 2 Kb promoter fragment was analyzed for cis-acting elements, enhancers and repressors using freely available online tool PlantCare (PlantCARE, a database of plant cis-acting regulatory elements and a portal to tools for in silico analysis of promoter sequences. Lescot M, Déhais P, Thijs G, Marchal K, Moreau Y, Van de Peer Y, Rouzé P, Rombauts S. Nucleic Acids Res. 2002 Jan 1;30(1):325-7.) and WRKY binding sites (W box; purple solid arrows) were annotated using Geneious software.
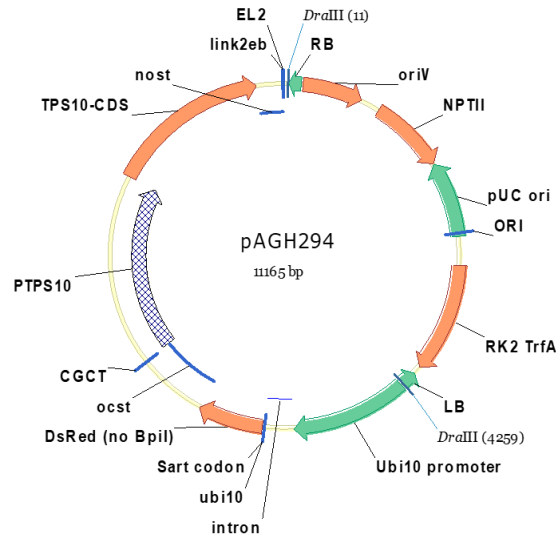
Fig.VII.2.4. An example of vector construct transiently transformed in *M. truncatula* roots*:* Vector constructs to be transformed in *M. truncatula* roots contain a DsRed module under its own ubiquitin promoter and a terminator, *E. coli* origin of replication, kanamycin marker and the main module, in this case, *Pro:TPS10+Ter* is cloned close to the right border and the DsRed selection marker close to the left border.
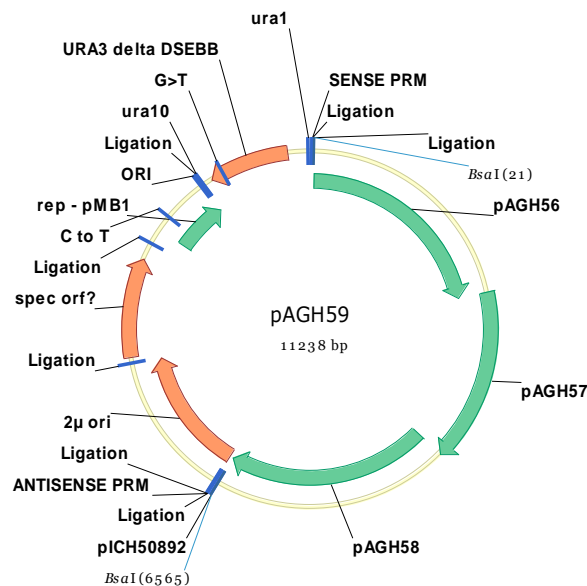
Fig.VII.2.5. An example of vector construct transformed in yeast: Vector constructs to be transformed in yeast contains *E. coli* origin of replication, yeast origin of replication, URA3 selection marker and plant coding sequences under galactose inducible promoters.

Fig.VII.2.6 m/z of TPS10 products: The most similar compound spectrum (top) and the measured spectra (bottom). Y- axis denoted the relative m/z abundance and x-axis denotes the retention time.

α- longipinene
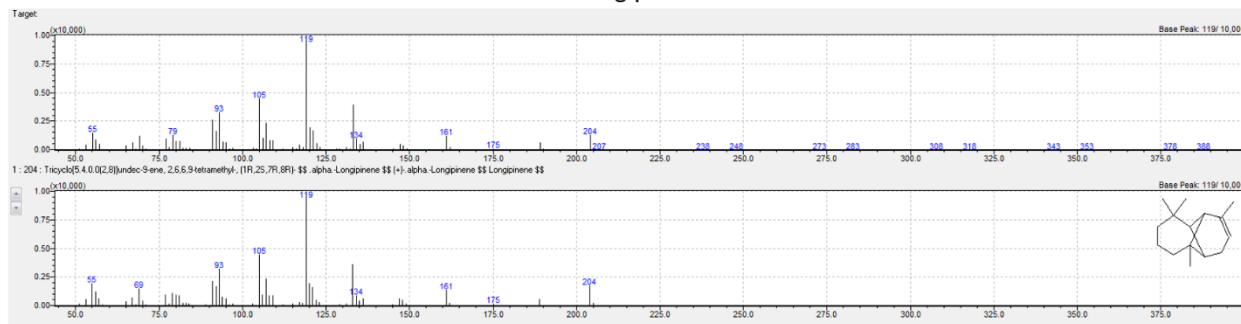
Ylangene
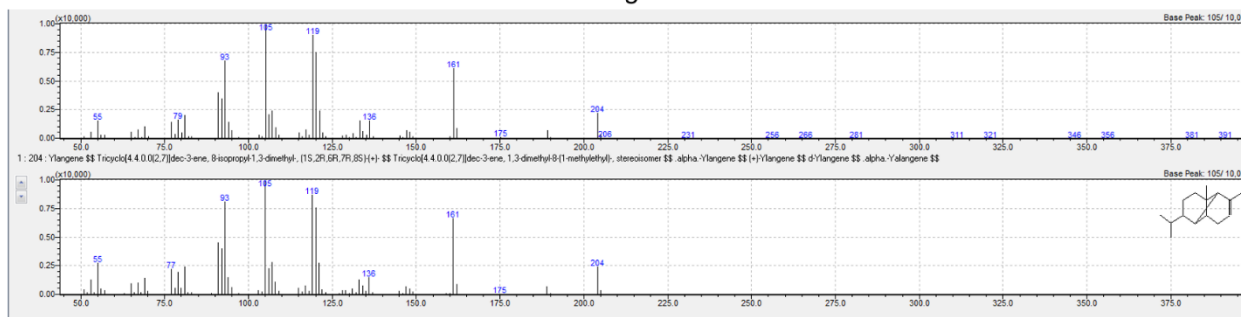
Longicyclene
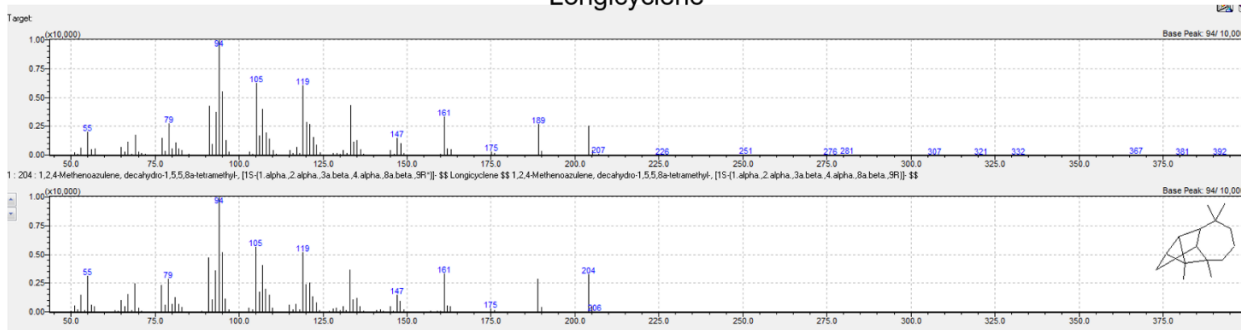
Farnesene

Alloaromadendrene

1 : 204 : Longipinene<beta-> $$ Tricyclo[5.4.0.02,8]undecane, 2,6,6-trimethyl-9-methylene-

ß- himachalene

1 : 204 : 1H-Benzocycloheptene, 2,4a,5,6,7,8-hexahydro-3,5,5,9-tetramethyl-, (R)- $$ .beta.-Himachalene $$ 1H-Benzocycloheptene, 2,4a.beta.,5,6,7,8-hexahydro-3,5,5,9-tetramethyl-, (+)- $$ (+)-.beta.-Himachalene $$ 3,5,5,9-Tetramethyl-2,4a,5,6,7,8-hexahydro-1H-benzo[a]cycloheptene-, (R)- $$ 1H-Benzocycloheptene, 2,4a,5,6,7,8-hexahydro-3,

Humalene-1,6-dien-3-ol

1 : 222 : Humulane-1,6-dien-3-ol $$ 3,7,7,10-Tetramethyl-2,8-cycloundecadien-1-ol # $$

bisabolol

Allohimachalol
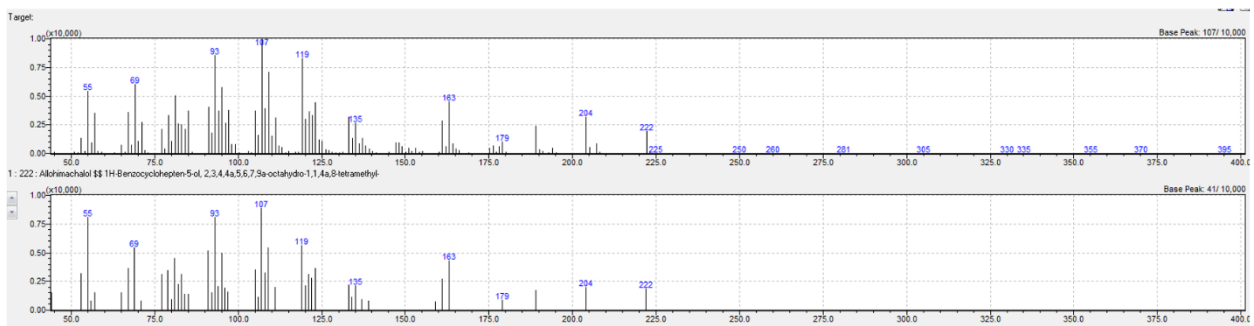
Shyobunol
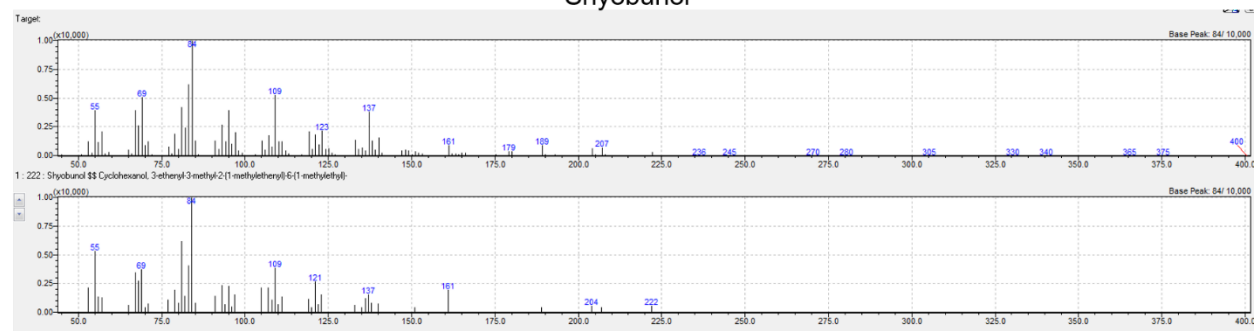
VII.3 Is there genetic variation in mycorrhization of *Medicago truncatula*?

Is there genetic variation in mycorrhization of *Medicago truncatula*?

Dorothée Dreher[*], Heena Yadav[*], Sindy Zander and Bettina Hause

Department of Cell and Metabolic Biology, Leibniz Institute of Plant Biochemistry, Halle, Germany
[*] These authors contributed equally to this work.

ABSTRACT

Differences in the plant's response among ecotypes or accessions are often used to identify molecular markers for the respective process. In order to analyze genetic diversity of *Medicago truncatula* in respect to interaction with the arbuscular mycorrhizal (AM) fungus *Rhizophagus irregularis*, mycorrhizal colonization was evaluated in 32 lines of the nested core collection representing the genetic diversity of the SARDI collection. All studied lines and the reference line Jemalong A17 were inoculated with *R. irregularis* and the mycorrhization rate was determined at three time points after inoculation. There were, however, no reliable and consistent differences in mycorrhization rates among all lines. To circumvent possible overlay of potential differences by use of the highly effective inoculum, native sandy soil was used in an independent experiment. Here, significant differences in mycorrhization rates among few of the lines were detectable, but the overall high variability in the mycorrhization rate hindered clear conclusions. To narrow down the number of lines to be tested in more detail, root system architecture (RSA) of *in vitro*-grown seedlings of all lines under two different phosphate (Pi) supply condition was determined in terms of primary root length and number of lateral roots. Under high Pi supply (100 μM), only minor differences were observed, whereas in response to Pi-limitation (3 μM) several lines exhibited a drastically changed number of lateral roots. Five lines showing the highest alterations or deviations in RSA were selected and inoculated with *R. irregularis* using two different Pi-fertilization regimes with either 13 mM or 3 mM Pi. Mycorrhization rate of these lines was checked in detail by molecular markers, such as transcript levels of *RiTubulin* and *MtPT4*. Under high phosphate supply, the ecotypes L000368 and L000555 exhibited slightly increased fungal colonization and more functional arbuscules, respectively. To address the question, whether capability for mycorrhizal colonization might be correlated to general invasion by microorganisms, selected lines were checked for infection by the root rot causing pathogen, *Aphanoymces euteiches*. The mycorrhizal colonization phenotype, however, did not correlate with the resistance phenotype upon infection with two strains of *A. euteiches* as L000368 showed partial resistance and L000555 exhibited high susceptibility as determined by quantification of *A. euteiches* rRNA within infected roots. Although there is genetic diversity in respect to pathogen infection, genetic diversity in mycorrhizal colonization of *M. truncatula* is rather low and it will be rather difficult to use it as a trait to access genetic markers.

INTRODUCTION

The arbuscular mycorrhiza (AM) represents a unique interaction between two eukaryotes, an obligate biotrophic fungus and its host plant, leading to an improved fitness of both interacting partners (*Bonfante & Genre, 2008*). AM fungi play an enormous role in terrestrial ecosystems due to their ubiquitous occurrence and their widespread interaction with plants. AM fungi, e.g., the species *Rhizophagus irregularis* (DAOM197198), belong to the kingdom of fungi and are classified to the subphylum *Glomeromycotina* within the phylum Mucoromycota (*Spatafora et al., 2016*).

The association between plant roots and AM fungi has proven to be an evolutionary successful strategy, since more than 80% of all terrestrial plant species live in symbiosis with AM fungi (*Schüssler, Schwarzott & Walker, 2001*). The host plant supplies the fungus with photoassimilates, which are metabolized to glycogen or lipids as energy storage (*Bago, Pfeffer & Shachar-Hill, 2000*). In turn, the AM fungus assists its host plant in acquisition of mineral nutrients and water (*Govindarajulu et al., 2005*; *Parniske, 2008*). Phosphate is one of the limiting nutrients for plant growth owing to its inaccessible form which has poor solubility and very slow diffusion. Roots affect the Pi concentration of the soil solution by active phosphate uptake, hence creating a Pi depletion zone around the root (*Hinsinger et al., 2005*). The extraradical fungal mycelium widely expands the Pi-depletion zone and due to the minor hyphal diameter, smaller soil pores can be exploited by a larger absorbing surface. Hence the symbiosis with AM fungi displays a powerful mechanism for plants to increase Pi availability.

The family of Fabaceae represents the third largest family of higher plants including more than 20,000 species and 700 genera (*Doyle & Luckow, 2003*). Due to their suitability for plant genomics, two species of this family, *Medicago truncatula* (*Rose, 2008*) and *Lotus japonicus* (*Handberg & Stougaard, 1992*) have been established as model plants mainly in order to get insights into agronomical important legume-microbe interactions. Key attributes of *M. truncatula* include its small, diploid genome consisting of two-times eight chromosomes with about 500 Mbp, its self-fertile nature and its rapid generation time. The genome of *M. truncatula* was sequenced capturing 94% of all *M. truncatula* genes (*Tang et al., 2014*; *Young et al., 2011*). Moreover, numerous ecotypes of *M. truncatula* have been collected throughout the Mediterranean Basin, and the considerable phenotypic variation for features such as growth habit, flowering time, trichome formation, and disease resistance represents an important resource to examine the genetic basis of legume functions (*Bonhomme et al., 2014*; *Kang et al., 2015*; *Stanton-Geddes et al., 2013*).

Previously, most studies in respect to interaction of *M. truncatula* with AM fungi have focused on single reference lines or a limited number of populations. The *M. truncatula* ecotype collection used in the present work is based on a survey about the genetic diversity in a collection of 346 inbred lines spanning the bulk of diversity that has been collected throughout the species range to date (*Ellwood et al., 2006*). Thirteen microsatellite markers were used to assign genetic relationships and select a nested core collection of 32 inbred lines, representing the genetic diversity of the complete collection (*Ronfort et al., 2006*). This collection has already been used successfully to identify key regulatory genes,

136

PeerJ

which are involved in the resistance of *M. truncatula* to the root pathogen *Aphanomyces euteiches* (*Badis et al., 2015*; *Bonhomme et al., 2014*). *A. euteiches* belongs to the kingdom of Chromalveolata and the class of Oomycota and causes the root rot disease in legumes. Primary disease symptoms in infected roots are water-soaked, softened brown lesions followed by significant reductions of root mass. Secondary symptoms like chlorosis, necrosis and wilting of the foliage might follow (*Hughes, Teresa & Grau, 2014*).

Besides the search for resistant ecotypes followed by proper breeding strategies, an alternative to reduce damage caused by soil-born plant pathogens could be the application of AM fungi as they have been shown to induce resistance towards root pathogens, as e.g., *A. euteiches* (*Azcón-Aguilar & Barea, 1996*; *Hilou et al., 2014*; *Whipps, 2004*). Additionally, the interaction of plants with AM fungi results in further beneficial effects, such as increased uptake of nutrients like phosphate, nitrogen (ammonium and nitrate), zinc, copper and potassium (*Cavagnaro, 2008*), and can lead to an increase in plant growth rate and total plant biomass (*Harrison, 1999*; *Parniske, 2008*). Moreover, AM can improve the tolerance of the plant to certain abiotic stresses, including drought, salt, and heavy metals (*Kamel et al., 2017*). Therefore, identification of traits causing a well-established mycorrhiza might help to improve the overall plant fitness.

The aim of this work was, therefore, to evaluate the SARDI core collection of *M. truncatula* ecotypes, collected in different parts of the world (*Ronfort et al., 2006*), regarding their symbiotic interaction with *R. irregularis*. The colonization rate of all ecotypes was evaluated, either using highly active inoculum or native sandy soil. To narrow down the number of ecotypes in order to have a closer look to slight differences in their mycorrhization, ecotypes were selected according to differences in the root system architecture (RSA) of seedlings. RSA describes the spatial arrangement of roots in the soil or growth media, is often quantified in terms of length of the primary root and number of lateral roots (*Chevalier et al., 2003*) and is known to be influenced by the availability and distribution of nutrients in the soil (*Thaler & Pagès, 1998*). On the one hand, RSA is altered by phosphate, which can affect the primary root length and number of lateral roots (*Gruber et al., 2013*; *Kellermeier et al., 2014*), on the other hand, colonization of roots by AM fungi is dependent on RSA, but also influences RSA (*Gutjahr & Paszkowski, 2013*; *Hodge et al., 2009*). Moreover, the relation between AM and RSA became obvious by the fact that plant phosphate transporter genes expressed specifically in arbuscule-containing cells play also a role in regulating relevant developmental programs, like root branching (*Volpe et al., 2016*). Using two regimes of Pi fertilization, the lines most deviating in RSA were selected and again analyzed in more detail for the interaction with *R. irregularis*, but also regarding their susceptibility towards the root pathogen *A. euteiches*.

MATERIAL & METHODS

Plant material and growth conditions

Plant materials used in this study included the set of nested core collection of *Medicago truncatula* (L.) Gaertn. consisting of 32 lines (*Ronfort et al., 2006*) and var. Jemalong A17 (Table S1). Seeds were treated with concentrated sulphuric acid for 5 min followed by

137

PeerJ

intensive washing with distilled water. Seeds were subsequently placed on sterile glass petri dishes with filter paper and stored for three days at 4 °C in the dark. Germination was performed in the dark at RT for one day and in light at RT for another day. Seedlings were transferred into pots (one seedling per pot with a diameter of 13 cm) filled with 600 ml expanded clay of 2–5 mm particle size (Original Lamstedt Ton; Fibo ExClay, Lamsted, Germany). For inoculation with *Rhizophagus irregularis*, expanded clay was mixed with inoculum (see below), for infection with *Aphanomyces euteiches* pure expanded clay was used. Growth of plants in soil containing lower spore density and higher AM fungi diversity was performed in native soil from Großbbeeren (Germany). This sandy soil contained 1.3% organic matter, 4% of clay in the soil dry weight, and 15 mg extractable P/g soil and had a pH of 7.6.

All lines were grown in a phytochamber with a 16 h/8 h cycle (22 °C/18 °C) at 220 µmol photons m^{-2} s^{-1}. Plants were watered with deionized water three times per week and fertilized weekly with 10 ml 10× Long Ashton solution (*Hewitt, 1966*) containing either 20% (corresponding to 3 mM) or 100% (corresponding to 13 mM) phosphate.

Inoculation with *Rhizophagus irregularis*, plant harvest, and determination of mycorrhization rate

R. irregularis (Schenk and Smith, isolate 49; *Maier et al., 1995*) was enriched in propagules by co-cultivation with leek (*Allium porrum*, cv. Elefant) in expanded clay as described previously (*Schaarschmidt et al., 2007*). Leek inoculum containing *R. irregularis* hyphae and spores was carefully mixed with clean expanded clay in a ratio of 2:8 (v/v) and used as highly active inoculum.

Plants of all lines inoculated with *R. irregularis* were harvested at 21, 35 and 50 days after inoculation. Plants grown in sandy soil were harvested at 35 days. Plants were quickly removed from the pot, roots carefully separated from the substrate, washed with distilled water and dried with a paper towel. For determination of mycorrhization rate using the Gridline intersection method (*Giovannetti & Mosse, 1980*), the whole root was used for subsequent staining. Selected lines were analyzed in independent experiments using the calculation method according to *Trouvelot, Kough & Gianinazzi-Pearson (1986)*. Here, an approximately 2 cm wide, centrally located section of every root system was used for staining and the remaining root material was snap frozen in liquid nitrogen and stored at −80 °C until isolation of RNA. Staining of all mycorrhizal samples was done with 5% (v/v) ink (Shaeffer Skrip jet black, Sheaffer Manufacturing, Madison, WI, USA) in 2% acetic acid as described before (*Vierheilig et al., 1998*). Fungal structures were assessed using a stereomicroscope.

Cultivation of plants for determination of root system architecture (RSA)

Seeds treated as described above were germinated on plates containing 0.7% plant agar (Duchefa Biochemie, Haarlem, North Holland, The Netherlands) at 12 °C in the dark for two days. In each case, seven seedlings were then transferred to plates containing Modified Strullu Romand Medium (*Declerck, Strullu & Fortin, 2005*) solidified with 0.4% (w/v) phytagel (Sigma-Aldrich, Munich, Germany) and either supplied with 100 µM phosphate

138

PeerJ

(high Pi) or 3 µM phosphate (low Pi). Plates were incubated vertically at 17−20 °C for seven days with a day/night cycle of 16 h/8 h. After taking photographs of all plates, length of primary roots and number of lateral roots were determined using the software 'Smart Root' (*Lobet, Pagès & Draye, 2011*). For each line and treatment at least three plates with seven seedlings each were evaluated.

Cultivation of *A. euteiches* and infection of plants

The cultivation and production of zoospores of *A. euteiches* (Drechs.) strain AERB84 (kindly provided by Dr. Anne Moussart, INRA France) and strain GB I1 (kindly provided by Dr. Phillip Franken, IGZ Germany) were performed as described before (*Hilou et al., 2014*). Both strains were cultivated on CMA-HST plates consisting of 17 g l^{-1} corn meal agar, 4 g l^{-1} yeast extract, 0.8 mg l^{-1} β-sitosterol, and 100 mg l^{-1} α-tocopherol acetate in 50 mM phosphate buffer (pH 6.8–7.0) in the dark at RT for 4–5 days. When the entire surface of the plate was occupied by the mycelium, 1 cm^2 pieces containing young hyphae were cut and transferred into new Petri dishes. After addition of a solution consisting of yeast extract tryptone (3.5 g l^{-1}) and autoclaved lake water in a ratio of 3:1 (v/v), plates were incubated at RT in the dark for 2 days. The newly formed mycelium was rinsed three times with autoclaved tap water for 45 min followed by overnight incubation to induce zoospores. Seedlings of *M. truncatula* cultivated on vertical plates as described above were infected by adding of 200,000 motile zoospores to each root. Three weeks after infection, phenotypic alterations were evaluated. *M. truncatula* plants grown in expanded clay for two weeks were infected at the stem base by the addition of about 1,000,000 motile zoospores of *A. euteiches* per plant. Control plants were mock-inoculated with an equal volume of autoclaved water. One day before infection, all pots were water saturated. Four weeks after infection, roots were harvested and snap-frozen in liquid nitrogen until isolation of RNA.

Staining of fungal structures with Wheat Germ Agglutinin (WGA)-AlexaFluor488

In order to stain fungal and oomycete structures within root tissue, Wheat Germ Agglutinin (WGA) conjugated to AlexaFluor488 (Life Technologies GmbH, Darmstadt, Hesse, Germany) was used enabling staining of cell wall components of fungi and oomycetes, such as *A. euteiches*. Freshly harvested roots were placed in 50% (v/v) ethanol for at least four hours followed by incubation in 20% KOH for 10 min at 90 °C. After washing with distilled water, roots were incubated in 0.1 M HCl for 2 h and then transferred into phosphate-buffered saline (135 mM NaCl, 3 mM KCl, 1.5 mM KH_2PO_4, 8 mM Na_2HPO_4, pH 7.4) containing 0.2 µg ml^{-1} WGA-AlexaFluor488 for at least 6 h. Stained roots were analyzed using an epifluorescence microscope AxioImager (Zeiss GmbH, Jena, Thuringia, Germany) using the reflector module 09 (EX BP 450-490/BS FT510/EM LP515). Photographs were taken by an AxioCam (Zeiss) and combined using Adobe Photoshop.

Monitoring of mycorrhization and *A. euteiches* infection by determination of transcript accumulation using qRT-PCR

Roots frozen in liquid nitrogen were homogenized using mortar and pestle. Total RNA was prepared using the Qiagen RNeasy PlantMiniKit (Qiagen, Hilden, North Rhine-Westphalia, Germany) according to the manufacturer's instruction, and followed by

139

PeerJ ————————————————————————

Organism	Gene		Sequence
M. truncatula	*Histone3-like* (Medtr4g097170.1)	fwd	5′-CTT TGC TTG GTG CTG TTT AGA TGG-3′
		rev	5′-ATT CCA AAG GCG GCT GCA TA-3′
M. truncatula	*MtPT4*	fwd	5′-ACA AAT TTG ATA GGA TTC TTT TGC ACG T-3′
		rev	5′-TCA CAT CTT CTC AGT TCT TGA GTC-3′
R. irregularis	*RiBTub* (AF394773)	fwd	5′-CCA ACT TAT GGC GAT CTC AAC A-3′
		rev	5′-AAG ACG TGG AAA AGG CAC CA-3′
A. euteiches	5.8S rRNA (AY683887)	fwd	5′-TGT CTA GGC TCG CAC ATC GA-3′
		rev	5′-AGT GCA ATA TGC GTT CAA CGT TT-3′

DNase digestion using Ambion RNase-free DNase (ThermoFisher Scientific, Schwerte, North Rhine-Westphalia, Germany). For real-time qRT-PCR analyses, 1 µg of total RNA was converted into cDNA with Moloney Murine Leukemia Virus Reverse Transcriptase, Point Mutant (Promega, Madison, WI, USA) using oligo(dT)20 primer. The obtained cDNA was diluted 20 times to serve as template for qRT-PCR.

Transcript levels of genes encoding *R. irregularis* β-tubulin (*RiBTub*), *M. truncatula* phosphate transporter4 (*MtPT4*) as well as *A. euteiches*-specific 5.8s rRNA levels were determined according to *Hilou et al. (2014)* using EvaGreen QPCR Mix II (Bio and Sell, Feucht, Bavaria, Germany) and primers listed in Table 1. The Ct-values of the target gene (TG) were normalized to the housekeeping gene *M. truncatula histone3-like* (*MtHIS3L*). The transcript accumulation of a gene from one sample was determined using the mean of three technical replicates. The resulting logarithmic values were converted using the formula $2^{-\Delta Ct}$.

Statistical analyses

If not otherwise indicated, three independent biological replicates were used for determination of mycorrhization rate and transcript levels. To identify significant differences statistical tests were conducted by Student's *t*-test for pairwise comparisons and one-way-ANOVA with Tukey's HSD test for multiple comparisons. Additionally, two-factorial ANOVA was applied to access interaction effects between the factors genotype and treatment for the data shown in Fig. 1. Standard deviation (SD) is used throughout to indicate variation from the mean.

RESULTS

Mycorrhization of core collection of *M. truncatula* accessions

The 32 accessions of the SARDI core collection and the reference line A17 were grown in expanded clay inoculated with *R. irregularis*, and fertilized with Long-Ashton fertilizer containing 3 mM (20%) phosphate instead of 13 mM, which correspond to 100% phosphate. Roots were harvested at three different time points (21, 35 and 50 days post infection [dpi]). Fungal structures in the roots were stained with ink and quantified using the Gridline Intersection method (Figs. 1A–1C). The overall mycorrhization rate increased over time in all accessions, but there were only slight differences in mycorrhization rate

140

PeerJ
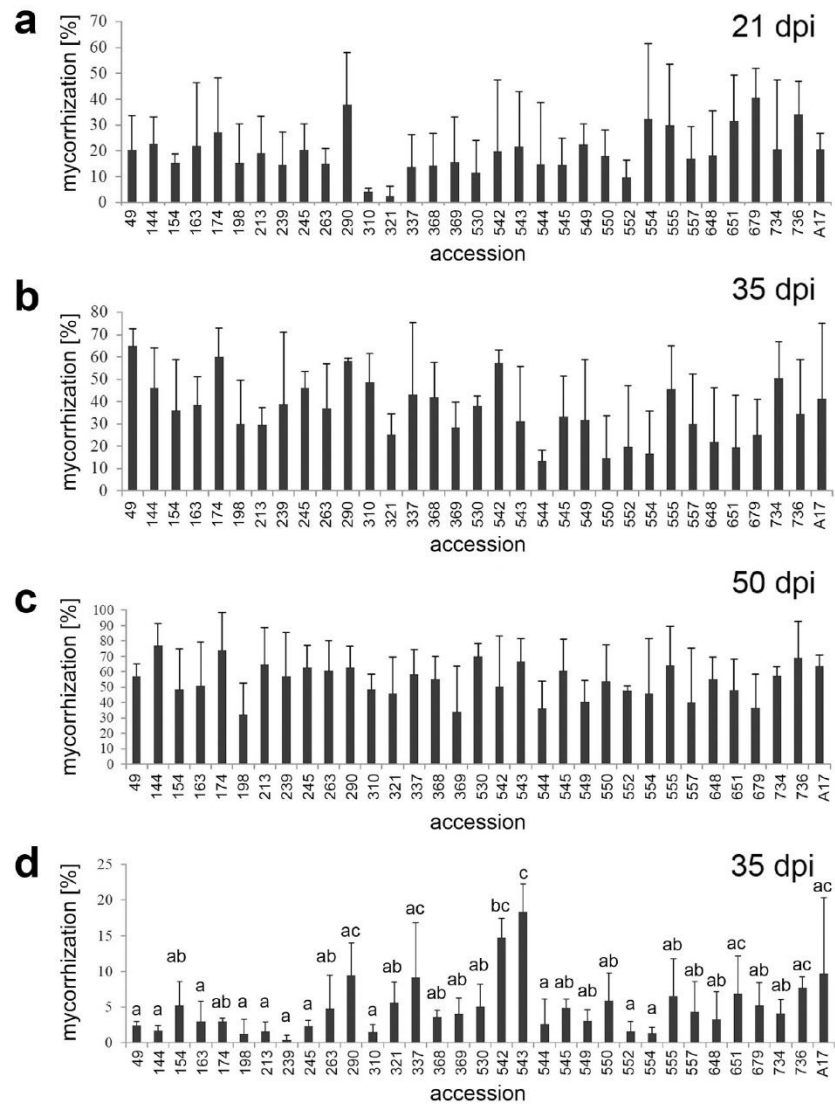
Figure 1 **Mycorrhization rates of the 32 accessions of the core collection and A17.** Plants of the 32 accessions of the core collection and the reference line A17 were inoculated with *R. irregularis* propagated on leek cultures (A, B, C) or were grown in native sandy soil (D). Mycorrhization rate was determined after the time periods indicated. Please note that all line numbers used in the text were abbreviated and contained the last three numerals of their original numbers only (see Table S1). Data are presented as means $\pm$SD ($n = 3$). There were no significant differences in (A, B, C); different letters in (D) indicate significant differences according to one-way-ANOVA with Tukey's HSD test, $p < 0.05$.

141

between the accessions at all harvest points. The largest differences were found at 21 dpi and ranged from 2.7% (line 321) to 40% (line 679) of root colonization. Comparisons between all lines by ANOVA revealed, however, that there were no significant differences in colonization rates at all three time points of inoculation. The overall development of shoot and root biomass within one accession compared to the other accessions was rather consistent at the different plant ages (not shown). To avoid possible overlay of differences by use of the highly effective inoculum, a native soil was used for an independent experiment (Fig. 1D). This soil had a much lower spore density and higher AM fungi diversity compared to the inoculum of trap cultures. The earliest time point with detectable colonization in this soil was detected at 35 dpi, since the process of mycorrhization was much slower compared to the *R. irregularis* inoculum. The colonization rate ranged from 0.4% to 18.3% (lines 239 and 543, respectively) and showed few significant differences among lines according to one-way ANOVA (Fig. 1D). To assess genotype, treatment and interaction effects, a two-factorial ANOVA was performed using data from all experiments, but no significant interaction effect was detected (Table S2). The high variance in mycorrhization rate of all 32 accessions under all conditions hampered to conclude on clear and reliable differences between the lines.

Length of primary roots and number of lateral roots in seedlings grown under phosphate-repleted and phosphate-depleted conditions

Since there were only minor differences in the mycorrhization rate and no correlation between mycorrhization rates and plant development, few accessions should be selected for a more detailed analysis. Due to the fact that Pi limitation is a driving force for mycorrhization in *M. truncatula* and at the same time affects the RSA, seedlings of all accessions of the core collection including A17 were grown on plates containing either 100 μM or 3 μM Pi for seven days. There were obvious differences in the RSA monitored in terms of primary root length and lateral root number (Fig. 2, Fig. S1). Under both Pi conditions, no line exhibited significant differences in root length and number of lateral roots compared to A17 according to Students *t*-test with Bonferroni correction. However, comparing root length of seedlings between both Pi conditions, length of primary root decreased significantly in line 163 and increased significantly in lines 321, 368 and 542 under Pi limitation in comparison to high Pi supply (Fig. 2A). There were, however, other lines differing in the number of lateral roots in response to Pi limitation, whereby again the lateral root number changed differently in the lines. Whereas the number in some lines increased, in others it decreased (Fig. 2B). Some lines developed less or no lateral roots under Pi limitation (e.g., 49, 239, 734), whereas others responded to the deficiency with an enhanced number of lateral roots (e.g., 213, 263, A17) or did not exhibit differences (e.g., 555, 736). From these lines showing significantly altered parameters, lines 163, 368 and 542 with changed primary root length under high Pi supply as well as line 213 with highest number of lateral roots under Pi limitation were selected as candidates to analyze its strength of interaction with the AM fungus in more detail. Additionally, line 555 was included, because this line did not change RSA upon Pi limitation and exhibited a stable, but very low number of lateral roots.

PeerJ
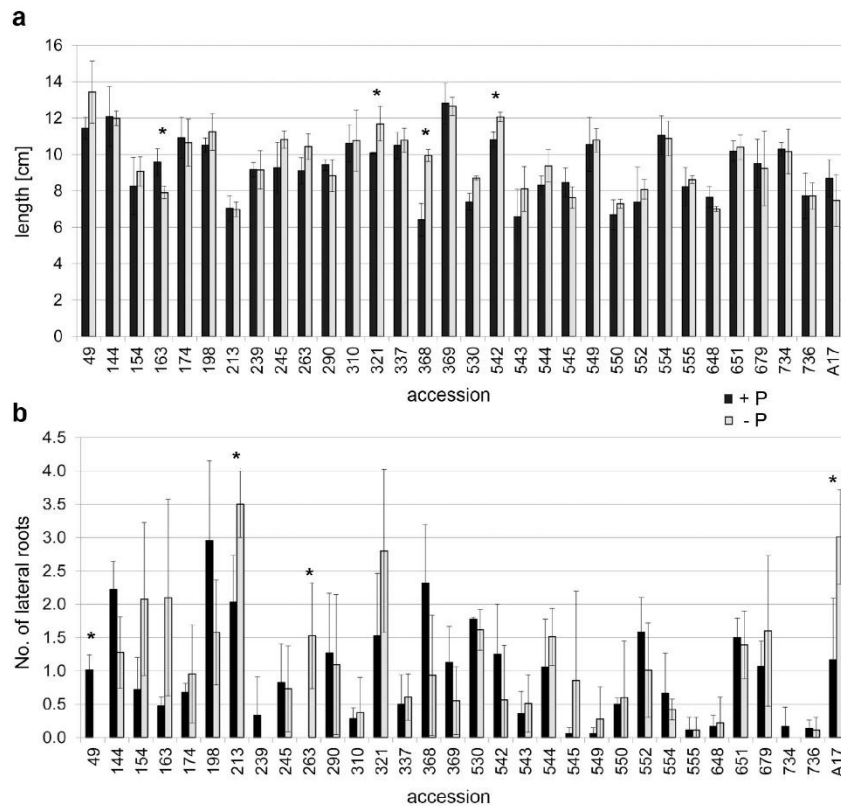
Figure 2 **Root architecture of seedlings.** Seedlings were cultivated on media with 100 μM (black bars) or 3 μM (gray bars) Pi for seven days. (A) Length of primary root, (B) number of lateral roots. Data are presented as means ± SD ($n = 3$ with seven plants each) and were compared between high/low Pi by the Student's t test; * $P \leq 0.05$.

Mycorrhization of selected accessions under two phosphate regimes

Seedlings of lines 163, 213, 368, 542, 555 and A17 were inoculated with *R. irregularis* and grown either under limited Pi supply (Long-Ashton fertilizer containing 20% phosphate corresponding to 3 mM Pi) or under full Pi supply (Long Ashton fertilizer containing 100% phosphate corresponding to 13 mM Pi) for two weeks. Mycorrhization parameters, such as frequency of mycorrhiza, intensity of mycorrhizal colonization and arbuscule abundance were determined (Figs. 3A and 3B). In comparison to fertilization with 100% Pi, fertilization with 20 % Pi resulted in higher mycorrhizal colonization in all accessions. However, in comparison to the reference line A17, the selected lines did not show differences in all the parameters determined, neither upon Pi limitation nor under full Pi supply. To check the functionality of the symbiosis in more detail, molecular markers, such as the transcript levels of a mycorrhizal fungal gene (*RiTUB*) and of a mycorrhiza-induced plant gene

143

3 mM phosphate

13 mM phosphate

163   213   368   542   555   A17
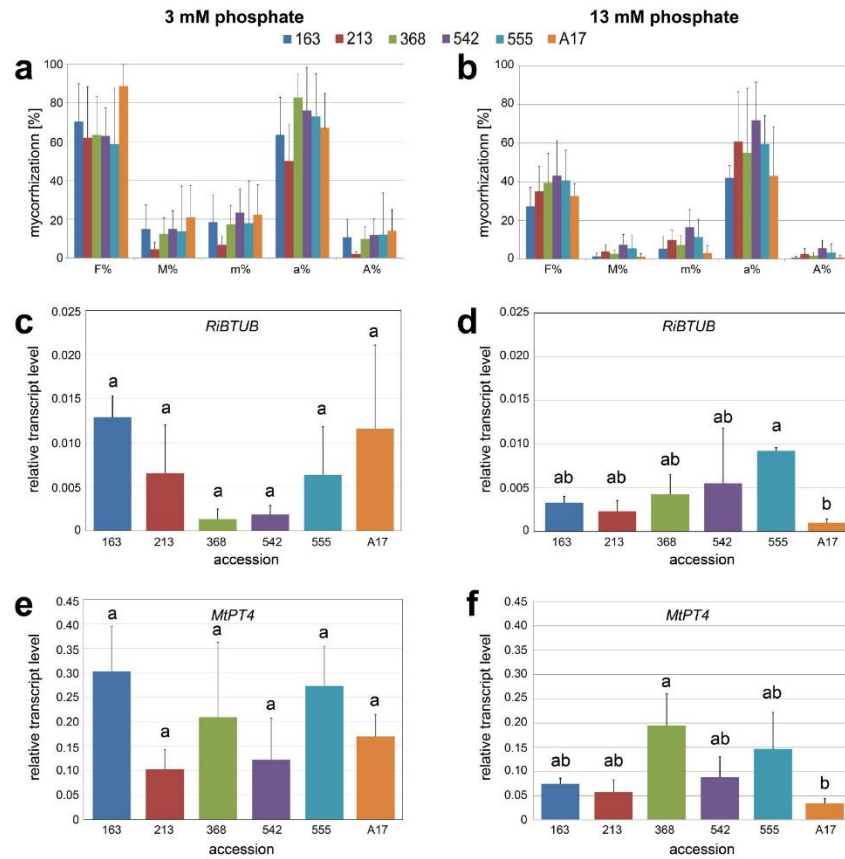
Figure 3 **Mycorrhization of selected accessions.** Accessions No. 163, 213, 368, 542, 555 and reference line A17 were grown in expanded clay, inoculated with *R. irregularis* for two weeks and fertilized either with reduced phosphate levels (20% corresponding to 3 mM Pi, A, C, E) or fully supplied with phosphate (100% corresponding to 13 mM Pi, B, D, F). (A, B) Mycorrhization rate quantified using the method described by *Trouvelot, Kough & Gianinazzi-Pearson (1986)*. F%, frequency of mycorrhiza in the root system; M%, intensity of the mycorrhizal colonization in the root system; m%, intensity of the mycorrhizal colonisation in the root fragments; a%, arbuscule abundance in mycorrhizal parts of root fragments; A%, arbuscule abundance in the root system. Data are presented as means + SD ($n = 5$). There were no significant differences between the ecotypes within each parameter analyzed (tested using one-way-ANOVA with Tukey's HSD test). (C, D) Mycorrhization determined by transcript level of *RiBTUB* in relation to *MtHIS3L*. Data are presented as means ± SD ($n = 3$). Different letters indicate significant differences (one-way-ANOVA with Tukey's HSD test, $p < 0.05$). (E, F) Functional arbuscules determined by transcript level of *MtPT4* in relation to *MtHIS3L*. Data are presented as means ± SD ($n = 3$). Different letters indicate significant differences (one-way-ANOVA with Tukey's HSD test, $p < 0.05$).

144

(*MtPT4*), were determined (Figs. 3C–3F). Upon fertilization with 20% Pi, transcript levels of both marker genes did not show significant differences among the accessions. Upon full Pi supply, however, two lines exhibited significant differences: line 555 showed higher transcript accumulation of *RiTUB* pointing to a higher colonization by *R. irregularis* in comparison to A17. Regarding the *MtPT4* transcripts, line 368 showed significantly higher levels than the reference line. This was accompanied by a high density of arbuscules, which were stained with fluorescently labeled WGA (Fig. S2).

Infection of selected lines with *A. euteiches*

To check whether the slightly altered mycorrhization phenotype of lines 368 and 555 might be linked to a higher susceptibility towards other soil-born microorganisms, one week old *in vitro* grown seedlings of all selected lines were infected with two strains of *A. euteiches* (Fig. S3). Both strains did not show differences in their infection capability. Roots of all lines appeared to turn brownish, but shoots of susceptible lines did not grow further and developed senescence-like symptoms (lines 163, 213, and 555). When plants were grown in expanded clay and infected with *A. euteiches* (strain GB I1), susceptible lines showed a significant reduction of biomass (Fig. 4A). Line 368 turned out to be highly tolerant towards *A. euteiches* and did not show an impaired fresh weight. Interestingly this was the line, which showed a higher arbuscule abundance determined by *MtPT4* transcript levels. To confirm the infection strength deduced from phenotypic observations, the amount of *A. euteiches* rRNA in infected roots was determined (Fig. 4B). *A. euteiches* rRNA was not detectable in non-infected roots, but in all infected roots. The levels, however, differed drastically—lines previously identified to be susceptible exhibited high levels of *A. euteiches* rRNA, whereas resistant or partially resistant lines showed only low levels of *A. euteiches* rRNA (*Bonhomme et al., 2014*; *Djébali et al., 2009*). This was also visible after staining of hyphae with fluorescently labeled WGA (Fig. S4), where roots of the susceptible lines were heavily stained and that of the partial resistant lines 368 and A17 showed only few labeled hyphae.

DISCUSSION

Interactions of plants with AM fungi provide several benefits for the plant, on the first place enhanced mineral nutrition (*Smith & Read, 2008*). Therefore, the ability, but also the extent of plants to interact with AM fungi might affect the general plant performance. Genetic diversity present in wild accessions of *M. truncatula* was used to identify putative differences in mycorrhization. The core collection used is part of the South Australian Research and Development Institute (SARDI) collection of *Medicago* spp, which is the largest in the Southern Hemisphere (*Skinner et al., 1999*). Large numbers of molecular markers make it feasible to identify key traits from mapping populations (*Ellwood et al., 2006*; *Ronfort et al., 2006*). In this study, however, no obvious and reliable differences in the mycorrhization rate of these accessions could be found over time. Inoculation with *R. irregularis* and determination of overall mycorrhization rate did not reveal significant differences between the accessions (Fig. 1). This is reminiscent of the data shown by *Schultz, Kochian & Harrison (2010)*, who analyzed eight lines of the SARDI *M. truncatula* collection

PeerJ
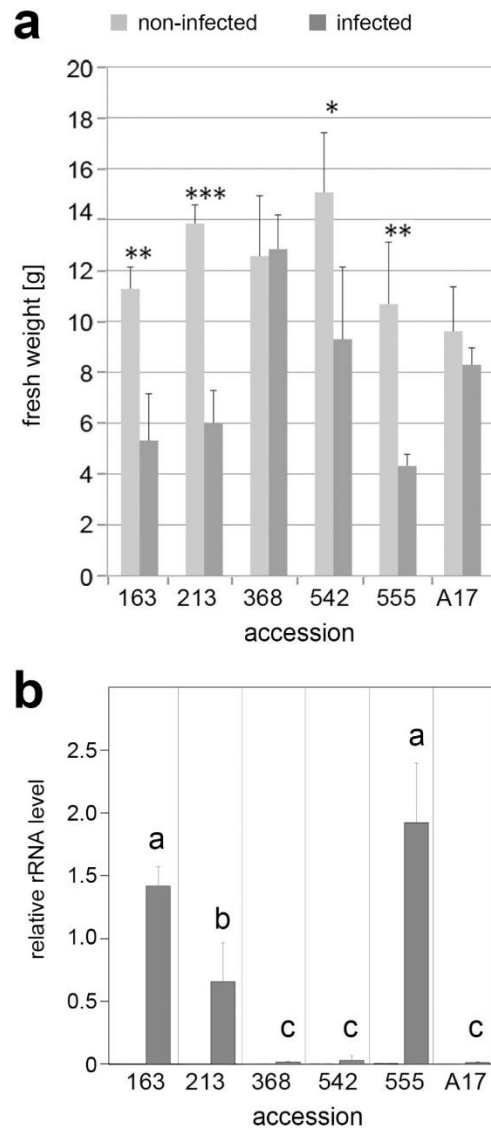
Figure 4 Infection of selected accessions with *A. euteiches*. Seedlings of accessions No. 163, 213, 368, 542, 555 and reference line A17 were grown in expanded clay for two weeks followed by infection with *A. euteiches* strain GB I1 for four weeks. (A) Biomass of plants without (light gray bars) and with (dark gray bars) infection. Data are presented as means $\pm$ SD ($n \geq 7$) and were compared between non-infected and infected plants by the Student's t test; *$P \leq 0.05$. (B) Infection by *A. euteiches* was determined by level of *A. euteiches* (Ae) rRNA in relation to *MtHIS3L* mRNA. Note the absence of Ae-rRNA in non-infected roots. Data are presented as means $\pm$ SD ($n = 3$). Different letters indicate significant differences between the infected plants (one-way-ANOVA with Tukey's HSD test, $p < 0.05$).

146

PeerJ

in a similar manner by inoculation with *R. irregularis*. They selected different lines of the collection than used in this work, yet two lines (530 referred to as F83005 and 736 referred to as DZA045 in *Schultz, Kochian & Harrison, 2010*) were overlapping to our studies. In both studies (*Schultz, Kochian & Harrison, 2010*), and the present study) it appeared that the process of root colonization by AM fungi is generally variable between individual plants, so that differences between lines are hard to identify. Here, a higher number of replicates would be necessary to improve the probability to find reliable differences between the accessions. Several other crop species, such as pearl millet, barley, maize, durum wheat and onion, showed a large variation between ecotypes regarding the ability for AM fungal symbiosis (*An et al., 2010*; *Baon, Smith & Alston, 1993*; *Galván et al., 2011*; *Kaeppler et al., 2000*; *Krishna et al., 1985*; *Singh et al., 2012*; *Smith, Grace & Smith, 2009*) or in the genetic variation in their capacity to profit from AM symbiosis (*Sawers et al., 2017*), whereas others, such as sorghum, did not show differences in mycorrhization of a large collection of ecotypes (*Leiser et al., 2016*). For the latter example, mycorrhization of various ecotypes showed rather variations in dependence on Pi-availability in the soil. Therefore, mycorrhization of *M. truncatula* accessions under two phosphate fertilization regimes was analyzed using molecular markers. To narrow down the number of accession, five of them were selected according to their RSA response towards full or limited Pi supply.

Under Pi limitation, plants alter their root morphology, topology, and distribution patterns influencing also their interaction with AM fungi (*Bouain, Doumas & Rouached, 2016*). Therefore, RSA was analyzed in terms of length of the primary root and number of lateral roots after growth of seedlings on agar plates either with 100 µM or 3 µM Pi. These two root parameters have been frequently used for determination of Pi deficiency response of various plants, since they are straightforward and easy to assess (*Chevalier et al., 2003*). Under high Pi supply, there were striking differences mainly in the number of lateral roots between all accessions of the core collection (Fig. 2B). There were accessions exhibiting several lateral roots, whereas others did not develop lateral roots within the time frame of the experiment. In response to Pi limitation, only few of the *Medicago* accessions showed significant alterations in length of primary roots, among them three lines exhibited an increase and one line a decrease in primary root length. In comparison to high Pi supply, the number of lateral roots was also changed only in few accessions, whereby three lines showed a significant increase in lateral root number. One line showed a significant decrease in the number of lateral roots, because it did not develop any lateral roots under Pi limitation. Pi deficiency has been shown to reduce the growth of primary roots and to enhance lateral root formation and the length and density of root hairs in many plant species (*Desnos, 2008*; *López-Bucio, Cruz-Ramírez & Herrera-Estrella, 2003*), among them *Arabidopsis thaliana* Col-0 (*Péret et al., 2014*). However, not all ecotypes of *A. thaliana* show these typical features. Out of 73 accessions nearly 25 % did not respond to Pi limitation by shorter primary roots (*Chevalier et al., 2003*). Moreover, Pi limitation has opposite effects in monocots showing promotion of primary root growth and inhibition of lateral root formation (*Li et al., 2012*; *Sun et al., 2014*). Other plant species, such as white lupine (*Lupinus albus*), are able to develop so-called cluster roots, which are covered by large numbers of dense root hairs (*Lambers et al., 2006*) and present another evolutionary

147

adaptation mechanism in response to Pi starvation. This points to a genetically determined root architectural response to low Pi conditions for better acquisition of Pi through root morphology and physiological adjustment, which cannot be generalized for all species (*Péret et al., 2014*).

Mycorrhization levels were determined in the five selected *Medicago* accessions using two different Pi fertilization regimes. Again, the differences in mycorrhization rate between the accessions were not significantly different, mainly due to the high variation between single plants of one ecotype. However, the dependence of mycorrhization rate on Pi supply was obvious. Under full Pi supply (13 mM Pi) frequency and intensity of mycorrhizal colonization were reduced in comparison to both parameters determined from plants grown under Pi limitation (3 mM Pi). It is well known that symbiosis establishment is promoted under Pi deficiency conditions and is limited under full Pi supply (*Andreo-Jimenez et al., 2015*). Even addition of Pi to mycorrhizal plants leads to a reduction of colonization preceded by rapid repression of symbiotic gene expression as shown for petunia (*Breuillin et al., 2010*). Under full Pi supply (limited mycorrhization), two accessions (lines 555 and 368) exhibited, however, slightly enhanced mycorrhization. Roots of line 555 harbored significantly more fungal material (determined by transcript accumulation of fungal housekeeping gene encoding β-tubulin) and line 368 harbored more active arbuscules as indicated by the significantly enhanced transcript levels of *MtPT4*. Transcript levels of *MtPT4* are indicative for the arbuscule abundance including their functionality, because it is directly linked to one key feature of the mycorrhizal symbiosis, namely the transport of phosphate (*Isayenkov, Fester & Hause, 2004*; *Javot et al., 2007*). Since the differences were detectable only upon full Pi supply, the question raised, whether these lines might be more susceptible also to other microorganism infecting roots. Both accessions behaved, however, differently in respect to infection with *A. euteiches*: Whereas line 555 was highly susceptible, line 368 was partially resistant. This was visible not only in a plate assay performed with two strains of *A. euteiches*, but also in adult plants grown and infected in pots. Next to the decrease in biomass of all susceptible lines, the amount *of A. euteiches* rRNA was increased in these roots showing unequivocally the different infection levels of the selected lines (Fig. 4). Differences in the colonization of roots by *A. euteiches* were additionally visible after WGA staining—the highly susceptible lines exhibited a rather dense hyphal network. Among the tested lines, line 368, 542 and A17 belong to the (partial) resistant accessions as demonstrated by *in vitro* inoculation assays previously published (*Bonhomme et al., 2014*; *Djébali et al., 2009*). This points to the fact that mycorrhization phenotype and pathogen susceptibility of *M. truncatula* are not correlated, neither positively nor negatively.

CONCLUSION

Interaction of plants with AM fungi is beneficial for plants not only for better supply with nutrients but also as bioprotective agent against root and foliar diseases (*Hilou et al., 2014*; *Jung et al., 2012*). Genetically diverse *Medicago* accessions with clearly different responses towards AM fungi would help to identify underlying genes regulating this symbiotic

association. Genetic diversity among the accessions of the SARDI collection in regard to resistance against *A. euteiches*, in drought-related traits and in morphological traits, such as plant height, trichome density and flowering time, have been successfully used to identify candidate genes by a Genome-Wide Association Study (GWAS) (*Bonhomme et al., 2014*; *Kang et al., 2015*; *Stanton-Geddes et al., 2013*). Thereby, the whole genome sequence and single nucleotide polymorphism (SNP) information for 288 inbred accessions provided by the HapMan project (http://www.medicagohapmap.org/) represent tremendous resources for GWAS. Although there are differences in mycorrhization among the tested accessions, the high standard variations will, however, hamper such an identification of candidate genes either by QTL analyses or GWAS. Here, a higher number of biological replicates or much more strongly contrasting phenotypes might be useful to identify genes that control basal processes in root development in response to environmental impacts. It is tempting to speculate that the differences in RSA and/or in plant's response to Pi limitation might be traits to be used for identification of regulatory genes.

ACKNOWLEDGEMENTS

ADDITIONAL INFORMATION AND DECLARATIONS

Funding

Grant Disclosures

Competing Interests

Bettina Hause is an Academic Editor for PeerJ. The other authors declare there are no competing interests.

Author Contributions

- Dorothée Dreher conceived and designed the experiments, performed the experiments, analyzed the data, wrote the paper, prepared figures and/or tables, reviewed drafts of the paper.
- Heena Yadav conceived and designed the experiments, performed the experiments, analyzed the data, prepared figures and/or tables, reviewed drafts of the paper.

PeerJ ———————————————————————————————

- Sindy Zander performed the experiments, reviewed drafts of the paper.
- Bettina Hause conceived and designed the experiments, analyzed the data, wrote the paper, prepared figures and/or tables, reviewed drafts of the paper.

Data Availability

The following information was supplied regarding data availability:
   The raw data have been uploaded as Supplemental Files.

Supplemental Information

Supplemental information for this article can be found online at http://dx.doi.org/10.7717/peerj.3713#supplemental-information.

REFERENCES

An G-H, Kobayashi S, Enoki H, Sonobe K, Muraki M, Karasawa T, Ezawa T. 2010. How does arbuscular mycorrhizal colonization vary with host plant genotype? An example based on maize (*Zea mays*) germplasms. *Plant Soil* **327**:441–453 DOI 10.1007/s11104-009-0073-3.

Andreo-Jimenez B, Ruyter-Spira C, Bouwmeester HJ, Lopez-Raez JA. 2015. Ecological relevance of strigolactones in nutrient uptake and other abiotic stresses, and in plant-microbe interactions below-ground. *Plant Soil* **394**:1–19 DOI 10.1007/s11104-015-2544-z.

Azcón-Aguilar C, Barea JM. 1996. Arbuscular mycorrhizas and biological control of soil-borne plant pathogens—an overview of the mechanisms involved. *Mycorrhiza* **6**:457–464 DOI 10.1007/s005720050147.

Badis Y, Bonhomme M, Lafitte C, Huguet S, Balzergue S, Dumas B, Jacquet C. 2015. Transcriptome analysis highlights preformed defences and signalling pathways controlled by the *prAe1* quantitative trait locus (QTL), conferring partial resistance to *Aphanomyces euteiches* in *Medicago truncatula*. *Molecular Plant Pathology* **16**:973–986 DOI 10.1111/mpp.12253.

Bago B, Pfeffer P, Shachar-Hill Y. 2000. Carbon metabolism and transport in arbuscular mycorrhiza. *Plant Physiology* **124**:949–957 DOI 10.1104/pp.124.3.949.

Baon J, Smith S, Alston A. 1993. Mycorrhizal responses of barley cultivars differing in P efficiency. *Plant Soil* **157**:97–105 DOI 10.1007/BF00038752.

Bonfante P, Genre A. 2008. Plants and arbuscular mycorrhizal fungi: an evolutionary-developmental perspective. *Trends in Plant Science* **13**:492–498 DOI 10.1016/j.tplants.2008.07.001.

Bonhomme M, André O, Badis Y, Ronfort J, Burgarella C, Chantret N, Prosperi J-M, Briskine R, Mudge J, Debéllé F, Navier H, Miteul H, Hajri A, Baranger A, Tiffin P, Dumas B, Pilet-Nayel M-L, Young ND, Jacquet C. 2014. High-density genome-wide association mapping implicates an F-box encoding gene in *Medicago truncatula* resistance to *Aphanomyces euteiches*. *New Phytologist* **201**:1328–1342 DOI 10.1111/nph.12611.

150

Bouain N, Doumas P, Rouached H. 2016. Recent advances in understanding the molecular mechanisms regulating the root system response to phosphate deficiency in Arabidopsis. *Current Genomics* **17**:308–304 DOI 10.2174/1389202917666160331201812.

Breuillin F, Schramm J, Hajirezaei M, Ahkami A, Favre P, Druege U, Hause B, Bucher M, Kretzschmar T, Bossolini E, Kuhlemeier C, Martinoia E, Franken P, Scholz U, Reinhardt D. 2010. Phosphate systemically inhibits development of arbuscular mycorrhiza in Petunia hybrida and represses genes involved in mycorrhizal functioning. *The Plant Journal* **64**:1002–1017 DOI 10.1111/j.1365-313X.2010.04385.x.

Cavagnaro TR. 2008. The role of arbuscular mycorrhizas in improving plant zinc nutrition under low soil zinc concentrations: a review. *Plant Soil* **304**:315–325 DOI 10.1007/s11104-008-9559-7.

Chevalier F, Pata M, Nacry P, Doumas P, Rossignol M. 2003. Effects of phosphate availability on the root system architecture: large-scale analysis of the natural variation between Arabidopsis accessions. *Plant, Cell and Environment* **26**:1839–1850 DOI 10.1046/j.1365-3040.2003.01100.x.

Declerck S, Strullu D, Fortin A. 2005. *In vitro culture of mycorrhizas. Soil biology series.* Berlin Heidelberg: Springer.

Desnos T. 2008. Root branching responses to phosphate and nitrate. *Current Opinion in Plant Biology* **11**:82–87 DOI 10.1016/j.pbi.2007.10.003.

Djébali N, Jauneau A, Ameline-Torregrosa C, Chardon F, Jaulneau V, Mathé C, Bottin A, Cazaux M, Pilet-Nayel M-L, Baranger A, Aouani ME, Esquerré-Tugayé M-T, Dumas B, Huguet T, Jacquet C. 2009. Partial resistance of *Medicago truncatula* to *Aphanomyces euteiches* is associated with protection of the root stele and is controlled by a major QTL rich in proteasome-related genes. *Molecular Plant-Microbe Interactions* **22**:1043–1055 DOI 10.1094/MPMI-22-9-1043.

Doyle JJ, Luckow MA. 2003. The rest of the iceberg. Legume diversity and evolution in a phylogenetic context. *Plant Physiology* **131**:900–910 DOI 10.1104/pp.102.018150.

Ellwood SR, D'Souza NK, Kamphuis LG, Burgess TI, Nair RM, Oliver RP. 2006. SSR analysis of the *Medicago truncatula* SARDI core collection reveals substantial diversity and unusual genotype dispersal throughout the Mediterranean basin. *Theoretical and Applied Genetics* **112**:977–983 DOI 10.1007/s00122-005-0202-1.

Galván GA, Kuyper TW, Burger K, Keizer LCP, Hoekstra RF, Kik C, Scholten OE. 2011. Genetic analysis of the interaction between *Allium* species and arbuscular mycorrhizal fungi. *Theoretical and Applied Genetics* **122**:947–960 DOI 10.1007/s00122-010-1501-8.

Giovannetti M, Mosse B. 1980. An evaluation of techniques for measuring vesicular arbuscular mycorrhizal infections in roots. *New Phytologist* **84**:489–500 DOI 10.1111/j.1469-8137.1980.tb04556.x.

Govindarajulu M, Pfeffer PE, Jin H, Abubaker J, Douds DD, Allen JW, Bucking H, Lammers PJ, Shachar-Hill Y. 2005. Nitrogen transfer in the arbuscular mycorrhizal symbiosis. *Nature* **435**:819–823 DOI 10.1038/nature03610.

151

Gruber BD, Giehl RFH, Friedel S, Von Wirén N. 2013. Plasticity of the Arabidopsis root system under nutrient deficiencies. *Plant Physiology* **163**:161–179 DOI 10.1104/pp.113.218453.

Gutjahr C, Paszkowski U. 2013. Multiple control levels of root system remodeling in arbuscular mycorrhizal symbiosis. *Frontiers in Plant Science* **4**:Article 204 DOI 10.3389/fpls.2013.00204.

Handberg K, Stougaard J. 1992. *Lotus japonicus*, an autogamous, diploid legume species for classical and molecular genetics. *The Plant Journal* **2**:487–496 DOI 10.1111/j.1365-313X.1992.00487.x.

Harrison M. 1999. Molecular and cellular apsects of the arbuscular mycorrhizal symbiosis. *Annual Review of Plant Physiology and Plant Molecular Biology* **50**:361–389 DOI 10.1146/annurev.arplant.50.1.361.

Hewitt E. 1966. *Sand and water culture methods used in the study of plant nutrition.* London: Commonwealth Agricultural Bureau, 430–434.

Hilou A, Zhang H, Franken P, Hause B. 2014. Do jasmonates play a role in arbuscular mycorrhiza-induced local bioprotection of *Medicago truncatula* against root rot disease caused by *Aphanomyces euteiches*? *Mycorrhiza* **24**:45–54 DOI 10.1007/s00572-013-0513-z.

Hinsinger P, Gobran GR, Gregory PJ, Wenzel WW. 2005. Rhizosphere geometry and heterogeneity arising from root-mediated physical and chemical processes. *New Phytologist* **168**:293–303 DOI 10.1111/j.1469-8137.2005.01512.x.

Hodge A, Berta G, Doussan C, Merchan F, Crespi M. 2009. Plant root growth, architecture and function. *Plant and Soil* **321**:153–187 DOI 10.1007/s11104-009-9929-9.

Hughes T, Teresa J, Grau C. 2014. Aphanomyces root rot (common root rot) of legumes. *Available at https://www.apsnet.org/edcenter/intropp/lessons/fungi/Oomycetes/Pages/Aphanomyces.aspx*.

Isayenkov S, Fester T, Hause B. 2004. Rapid determination of fungal colonization and arbuscule formation in roots of *Medicago truncatula* using real-time (RT) PCR. *Journal of Plant Physiology* **161**:1379–1383 DOI 10.1016/j.jplph.2004.04.012.

Javot H, Penmetsa RV, Terzaghi N, Cook DR, Harrison MJ. 2007. A *Medicago truncatula* phosphate transporter indispensable for the arbuscular mycorrhizal symbiosis. *Proceedings of the National Academy of Sciences of the United States of America* **104**:1720–1725 DOI 10.1073/pnas.0608136104.

Jung S, Martinez-Medina A, Lopez-Raez J, Pozo M. 2012. Mycorrhiza-induced resistance and priming of plant defenses. *Journal of Chemical Ecology* **38**:651–664 DOI 10.1007/s10886-012-0134-6.

Kaeppler S, Parke J, Mueller S, Senior L, Stuber C, Tracy W. 2000. Variation among maize inbred lines and detection of quantitative trait loci for growth at low phosphorus and responsiveness to arbuscular mycorrhizal fungi. *Crop Science* **40**:358–364 DOI 10.2135/cropsci2000.402358x.

Kamel L, Keller-Pearson M, Roux C, Ané J-M. 2017. Biology and evolution of arbuscular mycorrhizal symbiosis in the light of genomics. *New Phytologist* **213**:531–536 DOI 10.1111/nph.14263.

152

PeerJ

Kang Y, Sakiroglu M, Krom N, Stanton-Geddes J, Wang M, Lee Y-C, Young ND, Udvardi M. 2015. Genome-wide association of drought-related and biomass traits with HapMap SNPs in *Medicago truncatula*. *Plant, Cell and Environment* **38**:1997–2011 DOI 10.1111/pce.12520.

Kellermeier F, Armengaud P, Seditas TJ, Danku J, Salt DE, Amtmann A. 2014. Analysis of the root system architecture of Arabidopsis provides a quantitative readout of crosstalk between nutritional signals. *The Plant Cell* **26**:1480–1496 DOI 10.1105/tpc.113.122101.

Krishna K, Shetty K, Dart P, Andrews D. 1985. Genotype dependent variation in mycorrhizal colonization and response to inoculation of pearl millet. *Plant Soil* **86**:113–125 DOI 10.1007/BF02185031.

Lambers H, Shane MW, Cramer MD, Pearse SJ, Veneklaas EJ. 2006. Root structure and functioning for efficient acquisition of phosphorus: matching morphological and physiological traits. *Annals of Botany* **98**:693–713 DOI 10.1093/aob/mcl114.

Leiser WL, Olatoye MO, Rattunde HFW, Neumann G, Weltzien E, Haussmann BIG. 2016. No need to breed for enhanced colonization by arbuscular mycorrhizal fungi to improve low-P adaptation of West African sorghums. *Plant Soil* **401**:51–64 DOI 10.1007/s11104-015-2437-1.

Li Z, Xu C, Li K, Yan S, Qu X, Zhang J. 2012. Phosphate starvation of maize inhibits lateral root formation and alters gene expression in the lateral root primordium zone. *BMC Plant Biology* **12**:89 DOI 10.1186/1471-2229-12-89.

Lobet G, Pagès L, Draye X. 2011. A novel image-analysis toolbox enabling quantitative analysis of root system architecture. *Plant Physiology* **157**:29–39 DOI 10.1104/pp.111.179895.

López-Bucio J, Cruz-Ramírez, Herrera-Estrella L. 2003. The role of nutrient availability in regulating root architecture. *Current Opinion in Plant Biology* **6**:280–287 DOI 10.1016/S1369-5266(03)00035-9.

Maier W, Peipp H, Schmidt J, Wray V, Strack D. 1995. Levels of a terpenoid glycoside (blumenin) and cell wall-bound phenolics in cereal mycorrhizas. *Plant Physiology* **109**:465–470.

Parniske M. 2008. Arbuscular mycorrhiza: the mother of plant root endosymbioses. *Nature Reviews. Microbiology* **6**:763–775 DOI 10.1038/nrmicro1987.

Péret B, Desnos T, Jost R, Kanno S, Berkowitz O, Nussaume L. 2014. Root architecture responses: in search of phosphate. *Plant Physiology* **166**:1713–1723 DOI 10.1104/pp.114.244541.

Ronfort J, Bataillon T, Santoni S, Delalande M, David JL, Prosperi J-M. 2006. Microsatellite diversity and broad scale geographic structure in a model legume: building a set of nested core collection for studying naturally occurring variation in *Medicago truncatula*. *BMC Plant Biology* **6**:28 DOI 10.1186/1471-2229-6-28.

Rose R. 2008. *Medicago truncatula* as a model for understanding plant interactions with other organisms, plant development and stress biology: past, present and future. *Functional Plant Biology* **35**:253–264 DOI 10.1071/FP07297.

153

Sawers RJH, Svane SF, Quan C, Grønlund M, Wozniak B, Gebreselassie M-N, González-Muñoz E, Chávez Montes RA, Baxter I, Goudet J, Jakobsen I, Paszkowski U. 2017. Phosphorus acquisition efficiency in arbuscular mycorrhizal maize is correlated with the abundance of root-external hyphae and the accumulation of transcripts encoding PHT1 phosphate transporters. *New Phytologist* **214**:632–643 DOI 10.1111/nph.14403.

Schaarschmidt S, González M-C, Roitsch T, Strack D, Sonnewald U, Hause B. 2007. Regulation of arbuscular mycorrhization by carbon. The symbiotic interaction cannot be improved by increased carbon availability accomplished by root-specifically enhanced invertase activity. *Plant Physiology* **143**:1827–1840 DOI 10.1104/pp.107.096446.

Schultz C, Kochian L, Harrison M. 2010. Genetic variation for root architecture, nutrient uptake and mycorrhizal colonisation in *Medicago truncatula* accessions. *Plant Soil* **336**:113–128 DOI 10.1007/s11104-010-0453-8.

Schüssler A, Schwarzott D, Walker C. 2001. A new fungal phylum, the *Glomeromycota*: phylogeny and evolution. *Mycological Research* **105**:1413–1421 DOI 10.1017/S0953756201005196.

Singh A, Hamel C, DePauw R, Knox R. 2012. Genetic variability in arbuscular mycorrhizal fungi compatibility supports the selection of durum wheat genotypes for enhancing soil ecological services and cropping systems in Canada. *Canadian Journal of Microbiology* **58**:293–302 DOI 10.1139/w11-140.

Skinner DZ, Bauchan GR, Auricht G, Hughes S. 1999. A method for the efficient management and utilization of large germplasm collections. *Crop Science* **39**:1237–1242 DOI 10.2135/cropsci1999.0011183X003900040046x.

Smith FA, Grace EJ, Smith SE. 2009. More than a carbon economy: nutrient trade and ecological sustainability in facultative arbuscular mycorrhizal symbioses. *New Phytologist* **182**:347–358 DOI 10.1111/j.1469-8137.2008.02753.x.

Smith SE, Read DJ. 2008. *Mycorrhizal symbiosis*. Third edition. London: Academic Press.

Spatafora JW, Chang Y, Benny GL, Lazarus K, Smith ME, Berbee ML, Bonito G, Corradi N, Grigoriev I, Gryganskyi A, James TY, O'Donnell K, Roberson RW, Taylor TN, Uehling J, Vilgalys R, White MM, Stajich JE. 2016. A phylum-level phylogenetic classification of zygomycete fungi based on genome-scale data. *Mycologia* **108**:1028–1046 DOI 10.3852/16-042.

Stanton-Geddes J, Paape T, Epstein B, Briskine R, Yoder J, Mudge J, Bharti AK, Farmer AD, Zhou P, Denny R, May GD, Erlandson S, Yakub M, Sugawara M, Sadowsky MJ, Young ND, Tiffin P. 2013. Candidate genes and genetic architecture of symbiotic and agronomic traits revealed by whole-genome, sequence-based association genetics in *Medicago truncatula*. *PLOS ONE* **8**:e65688 DOI 10.1371/journal.pone.0065688.

Sun H, Tao J, Liu S, Huang S, Chen S, Xie X, Yoneyama K, Zhang Y, Xu G. 2014. Strigolactones are involved in phosphate- and nitrate-deficiency-induced root development and auxin transport in rice. *Journal of Experimental Botany* **65**:6735–6746 DOI 10.1093/jxb/eru029.

154

Tang H, Krishnakumar V, Bidwell S, Rosen B, Chan A, Zhou S, Gentzbittel L, Childs KL, Yandell M, Gundlach H, Mayer KF, Schwartz DC, Town CD. 2014. An improved genome release (version Mt4.0) for the model legume *Medicago truncatula*. *BMC Genomics* **15**:312 DOI 10.1186/1471-2164-15-312.

Thaler P, Pagès L. 1998. Modelling the influence of assimilate availability on root growth and architecture. *Plant and Soil* **201**:307–320 DOI 10.1023/a:1004380021699.

Trouvelot A, Kough J, Gianinazzi-Pearson V. 1986. Mesure du taux de mycorhization VA d'un système radiculaire. Recherche des méthodes d'estimation ayant une signification fonctionnelle. In: Gianinazzi-Pearson V, Gianinazzi S, eds. *The mycorrhizae: physiology and genetic.* Paris: INRA Presse, 217–221.

Vierheilig H, Coughlan AP, Wyss U, Piché Y. 1998. Ink and vinegar, a simple staining technique for arbuscular-mycorrhizal fungi. *Applied and Environmental Microbiology* **64**:5004–5007.

Volpe V, Giovannetti M, Sun X-G, Fiorilli V, Bonfante P. 2016. The phosphate transporters LjPT4 and MtPT4 mediate early root responses to phosphate status in non mycorrhizal roots. *Plant, Cell & Environment* **39**:660–671 DOI 10.1111/pce.12659.

Whipps JM. 2004. Prospects and limitations for mycorrhizas in biocontrol of root pathogens. *Canadian Journal of Botany* **82**:1198–1227 DOI 10.1139/b04-082.

Young ND, Debelle F, Oldroyd GED, Geurts R, Cannon SB, Udvardi MK, Benedito VA, Mayer KFX, Gouzy J, Schoof H, Van de Peer Y, Proost S, Cook DR, Meyers BC, Spannagl M, Cheung F, De Mita S, Krishnakumar V, Gundlach H, Zhou S, Mudge J, Bharti AK, Murray JD, Naoumkina MA, Rosen B, Silverstein KAT, Tang H, Rombauts S, Zhao PX, Zhou P, Barbe V, Bardou P, Bechner M, Bellec A, Berger A, Berges H, Bidwell S, Bisseling T, Choisne N, Couloux A, Denny R, Deshpande S, Dai X, Doyle JJ, Dudez A-M, Farmer AD, Fouteau S, Franken C, Gibelin C, Gish J, Goldstein S, Gonzalez AJ, Green PJ, Hallab A, Hartog M, Hua A, Humphray SJ, Jeong D-H, Jing Y, Jocker A, Kenton SM, Kim D-J, Klee K, Lai H, Lang C, Lin S, Macmil SL, Magdelenat G, Matthews L, McCorrison J, Monaghan EL, Mun J-H, Najar FZ, Nicholson C, Noirot C, O/'Bleness M, Paule CR, Poulain J, Prion F, Qin B, Qu C, Retzel EF, Riddle C, Sallet E, Samain S, Samson N, Sanders I, Saurat O, Scarpelli C, Schiex T, Segurens B, Severin AJ, Sherrier DJ, Shi R, Sims S, Singer SR, Sinharoy S, Sterck L, Viollet A, Wang B-B, Wang K, Wang M, Wang X, Warfsmann J, Weissenbach J, White DD, White JD, Wiley GB, Wincker P, Xing Y, Yang L, Yao Z, Ying F, Zhai J, Zhou L, Zuber A, Denarie J, Dixon RA, May GD, Schwartz DC, Rogers J, Quetier F, Town CD, Roe BA. 2011. The Medicago genome provides insight into the evolution of rhizobial symbioses. *Nature* **480**:520–524 DOI 10.1038/nature10625.

155

Supplemental data to

Is there Genetic Variation in Mycorrhization of *Medicago truncatula*?

Heena Yadav[#], Dorothée Dreher[#], Sindy Zander and Bettina Hause

Leibniz Institute of Plant Biochemistry, Department of Cell and Metabolic Biology, Weinberg 3,

D06120 Halle, Germany

Email corresponding author: bettina.hause@ipb-halle.de

Supplemental table

Table S1: List of the 33 accessions analyzed in this study

Hapmap ID	Line No*	Population of origin (accession)	Country of origin	Category
HM000 (HM101)	A17_Varma	A17	NA	Doug Cook UC Davis
HM001	L000163	SA22322	Syria	CC8
HM002	L000174	SA28064	Cyprus	CC8
HM003	L000544	ESP105-L	Spain	CC8
HM004	L000736	DZA045-6	Algeria	RILParent/CC8
HM005	L000734	DZA315-16	Algeria	RILParent/CC8
HM006	L000530	F83005-5	France	RILParent/CC8
HM007	L000651	Salses71B	France	CC8
HM008	L000368	DZA012-J	Algeria	CC8
HM009	L000555	GRC020-B	Greece	CC16
HM010	L000154	SA24714	Italy	CC16
HM011	L000543	DZA327-7	Algeria	CC16
HM012	L000239	SA26063	Morocco	CC16
HM013	L000648	Salses42B	France	CC16
HM014	L000542	DZA233-4	Algeria	CC16
HM015	L000550	F11013-3	France	CC16
HM016	L000049	SA09707	Tunisia	CC16
HM031	L000545	ESP158-A	Spain	CC32
HM032	L000549	F11005-E	France	CC32
HM033	L000552	F20047-A	France, Corsica	CC32
HM034	L000554	F20089-B	France, Corsica	CC32
HM035	L000679	F66017	France	CC32
HM036	L000337	GRC042-1	Greece	CC32
HM037	L000557	GRC064-B	Greece	CC32
HM038	L000369	PRT180-A	Portugal	CC32
HM039	L000263	SA03116	Israel	CC32
HM040	L000321	SA03780	Italy	CC32
HM041	L000198	SA09048	Libya	CC32
HM042	L000290	SA09119	Turkey	CC32
HM043	L000310	SA09944	Tunisia	CC32
HM044	L000245	SA14161	Jordan	CC32
HM045	L000144	SA14163	Jordan	CC32
HM046	L000213	SA27882	Morocco	CC32

*All line numbers used in the text were abbreviated and contained the last three numerals only.

Supplemental figures:
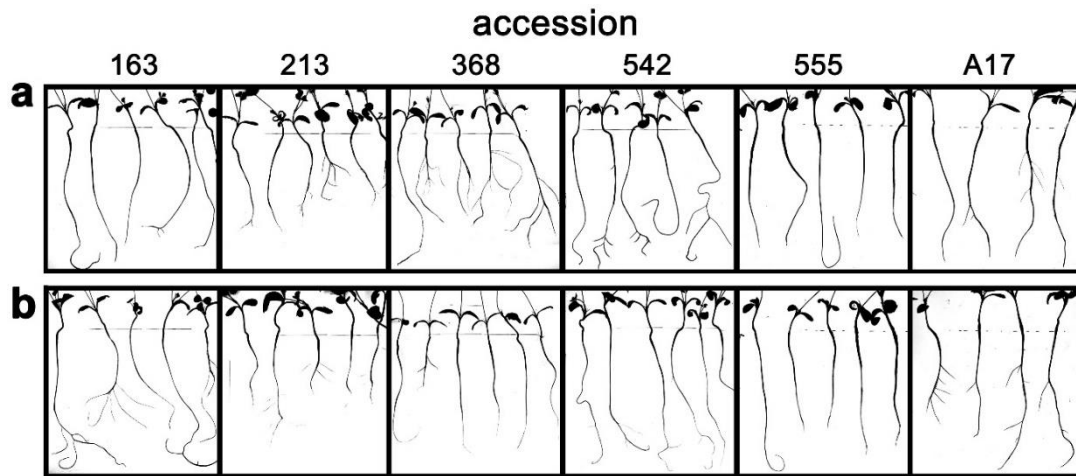
Figure S1: RSA of selected accessions grown on two phosphate concentrations. Seedlings were grown on plates containing either 13 mM Pi (a) or 3 µM Pi (b). Pictures were taken seven days after transfer of seedlings to plates.
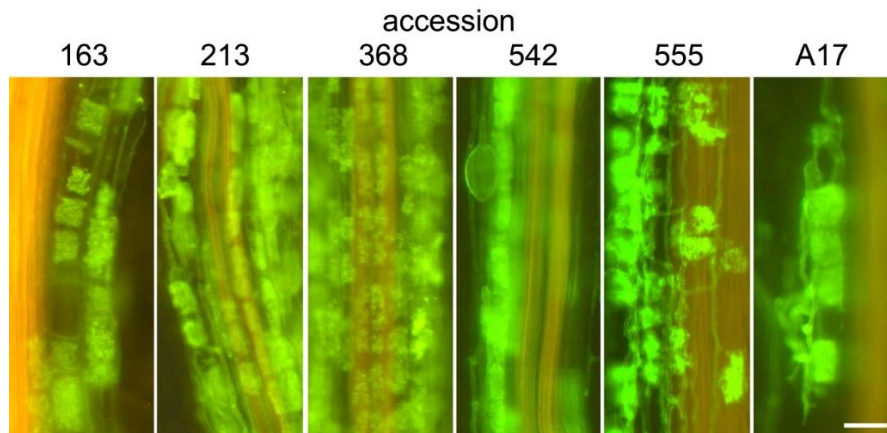
Figure S2: Arbuscule phenotype of selected accessions. Roots of plants inoculated with *R. irregularis* for two weeks under full Pi supply were stained with WGA-AlexaFluor488. Bar represents 50 µm for all micrographs.

accession

163　　　213　　　368　　　542　　　555　　　A17
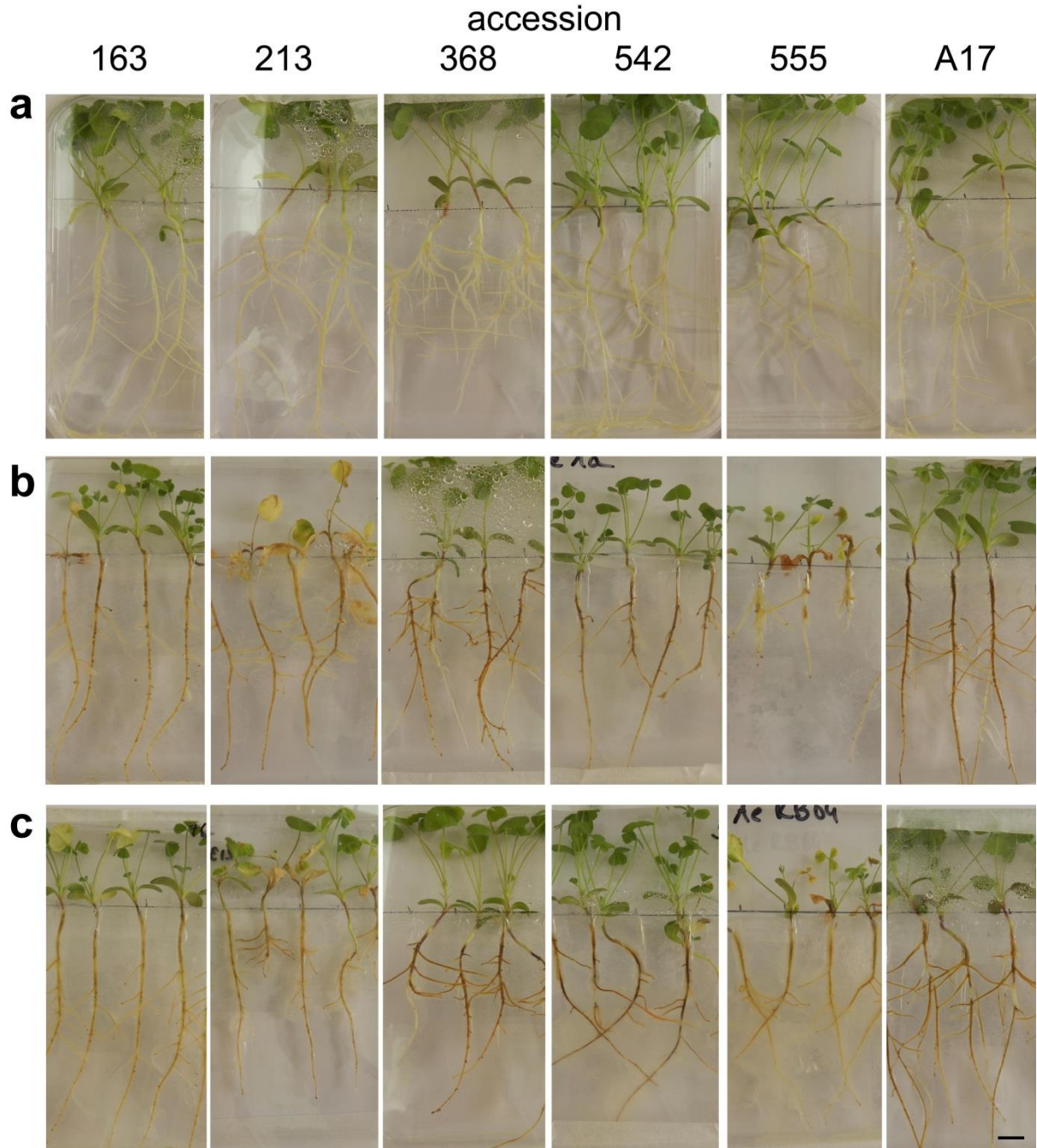
Figure S3: Phenotype of seedlings infected with two different strains of _A. euteiches._ Seedlings of selected

accessions were cultivated on vertical plates and infected either with _A. euteiches_ strain GB l1 (b) or strain AERB84

(c). Non-infected controls are given in (a). Bar represents 1 cm for all photographs.
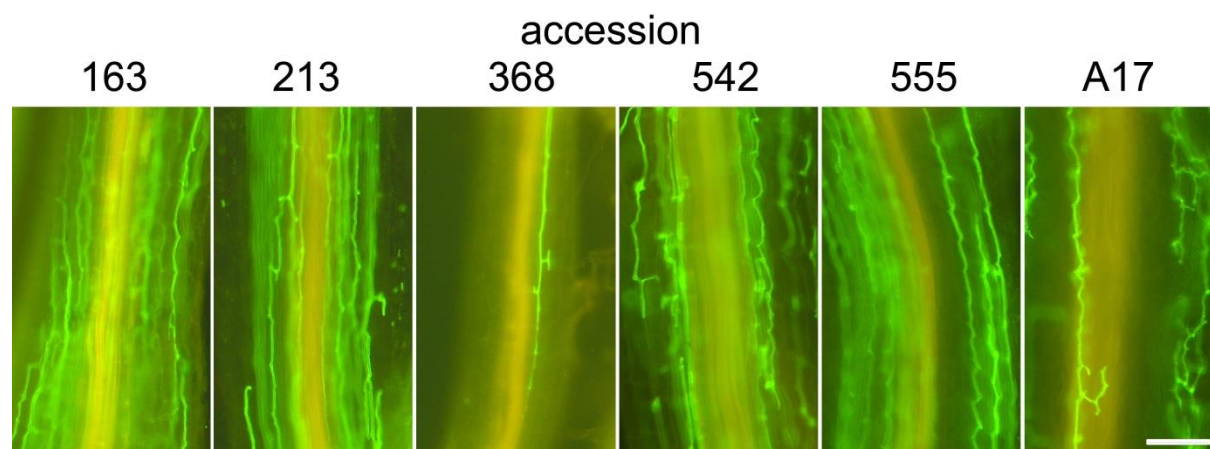
Figure S4: Hyphal growth of *A. euteiches* in roots of selected accessions. Roots of plants grown in expanded clay and infected with *A. euteiches* strain GB I1 for four weeks were stained with WGA-AlexaFluor488. Bar represents 100 µm for all micrographs.

of my group, who have always maintained a positive environment for working: **Dr. Yulong Li**, **Dr. Christine Hallmann**, **Chandan Chiniga Kemparaju**, **Henrikje Smits**, **Mandy Püffeld** and **Markus Gießmann**. I also want to thank the members of SZB department for the cheerful, friendly and positive work place, especially **Prof. Alain Tissier** (for the support and help for GC-MS and for valuable suggestions for the project) **Tom Schreiber** (for explaining the anti-sense PCR and for critics during the seminars, which always helped me to look at the project from a different angle), **Stephan Grunewald** (for training me in table-tennis and for being a good friend), **PD Dr. Gerd Balcke** (for explaining the metabolomics and helping in the identification of the putative modified TPS10 major product), **Dr. Sylvestre Marillonnet** (for the help with golden gate cloning) and all the other members of the **SZB department** for a friendly and positive work place. I sincerely thank all the people mentioned throughout the thesis, their help contributed for the development of the project.

I want to thank **Haider Sultani**, for the useful inputs and suggestions for bioassay experiments and for being a good friend. I also want to acknowledge the help from **Dr. Emmanuel Devers**, for the designing of miRNA primers, quantifying miRNA and for troubleshooting many of my cloning problems.

This work would not have been possible without the funding from **'Erasmus Mundus BRAVE' program** and the coordinators from India, Germany and Greece, especially MLU coordinator, **Prof. Dr. Sven E. Behrens,** who always helped in the smooth functioning of this program.

I also want to thank my **JNU friends**, who inspired me to apply for the scholarship and a very special thanks goes to my friends in Halle and in India, who have always given me the moral and emotional support throughout my studies, for always offering a helping hand to me whenever required. I thank them for sticking by my side, even when I was irritable and depressed.

Last but not least my parents, without them I would not have been here. They have always believed in me and supported in my every decision. How can I forget to mention my lovely sister and naughty brother for making my life lively whenever I felt low in life.

I thank the Almighty for surrounding me with so many good people, I could not have asked for more.

IX. Curriculum vitae

Name	Heena Yadav
Gender	Female
Date of birth	04.04.1990
Place of birth	Kota, Rajasthan
Nationality	Indian

Education

October 2014 – Till Date	Ph.D. candidate at Leibniz Institute of Plant Biochemistry (IPB), Halle, Germany. Thesis Title: Interactions of *Medicago truncatula* with soil-borne microbes- Role of *MtTPS10* in defense against *Aphanomyces euteiches.*
2012 – 2014	Master of Science in Life Science at Jawaharlal Nehru University (JNU), New Delhi, India. Thesis Title: Construction of *IFU5* deletion mutant in *Candida albicans.*
2009-2011	Bachelor of Science in Biotechnology at University of Kota, Rajasthan, India.

Scientific activities

Plant Biology Europe 2018, Copenhagen, Denmark (2018): Selected for oral presentation 'Role of a Sesquiterpene Synthase in defense of *Medicago truncatula* against *Aphanomyces euteiches*'

3rd Summer Academy in Plant Molecular Biology Heiligkreuztal, Germany (2017): Oral presentation 'Characterization of a pathogen induced Sesquiterpene Synthase in the roots of *Medicago truncatula'*

3rd Doctoral Researcher's Conference of GRK1798 'Signalling at the Plant Soil Interface' (2017): Oral Presentation- 'Sesquiterpenes produced in roots of *Medicago truncatula* play a role in defence mechanism against *Aphanomyces euteiches'*.

29th Conference Molecular Biology of Plants, Dabringhausen, Germany (2016): Poster Presentation- 'Sesquiterpenes produced in roots of *Medicago truncatula* play a role in defense mechanism against *Aphanomyces euteiches'*.

Utrecht Summer School, Netherlands (2015): Poster and Oral Presentation – 'Analysis of genetic variability of *Medicago truncatula* responsiveness to *Rhizophagus irregularis'*

X. List of publications

- **Yadav, H**., Dreher, D., Athmer, B., Porzel, A., Gavrin, A., Baldermann, S., Tissier, A.F., and Hause, B. (2019). Medicago TERPENE SYNTHASE 10 is involved in defense against an oomycete root pathogen. *Plant Physiology*.
  DOI: https://doi.org/10.1104/pp.19.00278

- Hause B and **Yadav H**, (2019); book chapter: Creation of chimeric plants – transformation of *Medicago truncatula* roots in 'The model legume *Medicago truncatula*'

- Dreher D[#], **Yadav H[#]**, Zander S, Hause B. (2017) Is there genetic variation in mycorrhization of *Medicago truncatula*? *PeerJ*
  DOI: https://doi.org/10.7717/peerj.3713

XI. Eidesstattliche Erklärung

Hiermit erkläre ich, dass ich die vorliegende wissenschaftliche Arbeit selbständig und ohne fremde Hilfe angefertigt habe. Ich erkläre, dass ich keine anderen als die von mir angegebenen Quellen und Hilfsmittel benutzt habe und die den Werken wörtlich und inhaltlich entnommenen Stellen als solche kenntlich gemacht habe. Ich versichere weiterhin, dass ich mich erstmals mit dieser Arbeit um die Erlangung des Doktorgrades bewerbe. Diese Arbeit wurde an keiner anderen Fakultät oder Universität zur Begutachtung eingereicht.

Heena Yadav

Halle (Saale)